Numéro National de Thèse : 2021LYSEN080

THESE DE DOCTORAT DE L'UNIVERSITE DE LYON

opérée par
l'Ecole Normale Supérieure de Lyon
en cotutelle avec
l'Université d'Edimbourg

Ecole Doctorale N° 340
Biologie Moléculaire, Intégrative et Cellulaire

Discipline : Science de la Vie

Soutenue publiquement le 10/12/2021, par :
Jeanne LOUE-MANIFEL

Comparative analysis of the function and regulation of the ZOU/ICE protein complex in *Arabidopsis thaliana* and *Marchantia polymorpha*

Analyse comparative de la fonction et de la régulation du complexe protéique ZOU/ICE chez *Arabidopsis thaliana* et *Marchantia polymorpha*

Devant le jury composé de :

MAGNANI, Enrico,	DR INRAE	INRAE Versailles	Rapporteur
RENAULT, Hugues	CR CNRS	Université de Strasbourg	Rapporteur
KIDNER, Catherine	Reader	University of Edinburgh	Examinatrice
DELATTRE, Marie	DR CNRS	ENS de Lyon	Examinatrice
MONNIAUX, Marie	CR CNRS	ENS de Lyon	Examinatrice
DEPEGE-FARGEIX, Nathalie	MC UCBL	ENS de Lyon	Coencadrante de thèse
GOODRICH, Justin,	Professor	University of Edinburgh	Codirecteur de thèse
INGRAM, Gwyneth	DR CNRS	ENS de Lyon	Directrice de thèse

Résumé

Chez les Angiospermes, le développement de la graine et l'accumulation des réserves imposent la mise en place d'une communication étroite entre l'embryon et l'albumen. Chez certaines Angiospermes, comme l'arabette des dames aussi appelée *Arabidopsis thaliana*, ce dialogue entre embryon et albumen est régulé par un complexe protéique composé de deux facteurs de transcription : ZHOUPI et INDUCER OF CBF EXPRESSION1 (ZOU/ICE). Plus précisément, ce complexe ZOU/ICE permet la dégradation de l'albumen et donc le bon développement de l'embryon et régule également la mise en place d'une interface complexe entre l'albumen et l'embryon composée d'une gaine extracuticulaire et de la cuticule embryonnaire. Dans une première partie, l'analyse de la régulation et de la fonction du complexe ZOU/ICE a permis de mettre en évidence une redondance fonctionnelle cryptique entre les gènes ICEs au cours du processus de développement de la graine mais aussi la régulation post traductionnelle de ces protéines ICEs, en particulier l'ubiquitination participant à leur dégradation par l'action de la protéine HOS1. Dans un deuxième temps, des approches de génétique, de biologie moléculaire et cellulaire chez la Bryophyte *Marchantia polymorpha*, dépourvue de graines et d'albumen, ont permis de mieux comprendre la fonction ancestrale du complexe ZOU/ICE. Ce complexe s'est révélé avoir un rôle clé d'une part dans le contrôle du développement des rhizoïdes, impliqués dans le transport de l'eau, et d'autre part dans la biogénèse de la cuticule. L'étude de la composition de la cuticule de *M. polymorpha*, et des cibles transcriptionnelles du complexe ZOU/ICE impliquées dans sa mise en place, ont permis d'émettre des hypothèses novatrices sur l'importance de la modification de la composition de la paroi, et la production des espèces réactives de l'oxygène dans la biogenèse de la cuticule des plantes.

Abstract

In angiosperms, the development of the seed and the accumulation of reserves require the establishment of close communication between the embryo and the endosperm. In *Arabidopsis thaliana*, this coordination is regulated by a protein complex made up of two transcription factors: ZHOUPI and INDUCER OF CBF EXPRESSION (ZOU/ICE). The ZOU/ICE complex controls the degradation of the endosperm and thus the optimal development of the embryo, and regulates the establishment of a complex interface between the endosperm and the embryo composed of an extracuticular sheath and of the embryonic cuticle. In a first part of my work, the analysis of the regulation and the function of the ZOU/ICE complex made it possible to highlight the regulation underlying a cryptic redundancy in seed development between the two ICE genes in *Arabidopsis thaliana*, as well as to explore the post-translational regulation of their proteins, in particular the potential role of ubiquitination in their degradation via the HOS1 protein. Secondly, genetic and molecular and cellular biology analyses in the bryophyte *Marchantia polymorpha*, which does not produce seeds, provided a better understanding of the ancestral function of the ZOU/ICE complex. Indeed, this study revealed two potential ancestral functions of this complex, firstly in the control of the development of pegged rhizoids involved in the transport of water and secondly in the biogenesis of the cuticle. The study of the composition of the cuticle of *Marchantia polymorpha*, and of the transcriptional targets of the ZOU/ICE complex involved in its establishment, made it possible to formulate innovative hypotheses about the importance of the modification of the composition of the wall, and the production of reactive oxygen species in plant cuticle biogenesis.

Acknowledgements

First of all, I would like to thanks Marie Delattre, Marie Monniaux, Catherine Kidner, Enrico Magnani and Hugues Renault for accepting to be members of my panel.

I would like to thank the members of my committee, Christophe Trehin, Steven Fry and Pierre-Marc Delaux who have supported, guided, encouraged and advised me during these four years. I would like to thanks all the people who have been involved in this project, either directly or indirectly: Samuel Knosp and Mathieu Erhardt from the IBMP institute in Strasbourg ; Moritz Nowack and Norbert Bollier from the VIB-UGhent Center ;Tomoo Shimada and Kenta Moriya from the University of Kyoto.

Gwyneth, Nathalie, Justin you allowed me to do my PhD on a great subject. Although I had a big discussion with myself about whether I wanted to do a PhD, I already had a very precise idea of what would be the PhD of my dream: a joint PhD on transcription factors! You allowed me to do it ! Before I start, I was also convinced that a good project is good but a good project with a very good supervision is definitely better. I am grateful for that !

Gwyneth, you are the first person I met and as you could discover very quickly, I REALLY WANTED to do my internship with you ! And even after the Covid, four years of PhD and the writing, I am still delighted of this choice!! Thank you for your daily enthusiasm and optimism at all time, for believing in me and giving me a second chance after BMIC.

Nathalie, you supervised me from the beginning but you did much more than that! I would have not done that without your precious advice and your good mood. Du coup je tenais à te remercier très très sincèrement pour tout et surtout te redire encore une fois que tu gères la fougère comme personne !

Justin, your Marchantias drove me crazy (in a good way!) ! I am grateful for your trust, your patience and your beautiful pictures you sent me which cheers me up ! It is a shame that circumstances did not allow me to physically come back working with you. I also would like to thank you (and Nathalie) for making me discover teaching.

Jérémy Just, a sincere thank you for your bioinformatics knowledge brought to this project (and for your amazing food and the perfect coloured match socks-shirt ahah!)!

Simone, thank you for your perseverance with the AFM and the indentor I'm sure that one day you will find out that Marchantia is the funkiest plant ever!

Edudu, your help with the qPCR has been very precious!! Thank you !!!!!!!

Sophy Boeuf, Audrey Creff, Yen-Ting Lu, Erica De Leau, thank you for sharing your technical knowledge with me. Sophy, I'm so sorry that all those experiments you did to help me were so frustrating ! I promise it wasn't on purpose!!! Thank you for your great help. My dear Erica,

Edinburgh would not have been the same without you (and Dick), you have been a great scientific and personal support to me in the lab but even more so outside the lab. I really enjoyed our “quality time” (as you say). DeeDee, I will always think of you when I eat stinging candy and see a permanent marker or nice coloured pens but more seriously, thank you for letting me bother you all the time with my silly questions !!!

Auré, thank you for making me discover your passion of teaching and the big world of the popularisation of science, I learnt a lot from you! Thank you for your trust with les RDV aux Jardins, interventions in school, Mission Pollinisation (thank you Alice too!) and the running sessions! I apologize for cancelling last minute !

Thank you Yoan for the nice bryophytic discussions and for the tea :D !

Ma p’tite Elsa you understood it from the beginning, Bryophytes are the best ;) It was really nice to share the office with you, thanks for your good mood and for all the junk food during the writting ! Carlos and Gwenno thank you for sharing your skills with ImageJ with me and the coffee! I also would like to thanks the thésards anonymes (Sana et Yannick), I won’t say more...

Thank you to the people that I have not mentioned from the “foyer”, Pint of Science, the RDP and IMPS, you all have contributed to my PhD and made me enjoyed it!

Roomiiiiie Katie !!! I don’t know if you will read these lines but I can’t not thank you. You’ve always been here with a sweet word when I came home late from the lab you were my release valve after a big day and the best roommate ever!

Le poulailler (ordre alphabétique!): Chopy, Garance, Hinda, Laurine, Léa, Lise, Léo, Nico, I owe you a big thank you for all the wonderful moments spent together that make the thesis goes more smoothly! On n’a pas fait que cancaner et manger ensemble on a aussi bossé et échangé scientifiquement (mais beaucoup cancaner quand même !) Merci pour votre soutien dans cette dure épreuve ! Extra merci à Lise pour son soutien et son aide avec Inkscape !

Maman, Coco, sans vous je n’en serais pas là, je n’aurais probablement pas fait de thèse… Merci d’avoir cru en moi et pour votre confiance dans le choix mes études même si ca voulait dire partir à l’autre bout du monde et lorsque je me suis tournée vers ce monde obscure qu’est la recherche. Je n’oublie pas le bon mangé et les tasses de thés pendant la rédaction !!!

Mon plus grand merci revient à Jérémie sans qui cette fin de thèse aurait été beaucoup beaucoup plus difficile qu’elle ne l’a été !!! Milles mercis d’avoir toujours été là pour m’écouter parler de mes PCR qui ne marchaient pas et de mes Marchantia qui étaient trop mimi, milles mercis pour ton soutien au quotidien tout simplement !

Thank you the PhD, thank you all, for making me evolve…!

Contents

INTRODUCTION 5

1 Land plant evolution and key innovations: from the green algae to the angiosperms 7

1.1 Description of the different groups of plants 7

1.2 Plant Life cycles: the rise of the sporophyte 8

1.3 Two land plant models and their life cycles: *Marchantia polymorpha* and *Arabidopsis thaliana* 9

1.3.1 What is a model plant? 9

1.3.2 M. polymorpha. 11

1.3.3 A. thaliana. 13

2 The move to land: key innovations 14

2.1 Life on land 14

2.2 Rhizoids: the 2 in 1 structure of liverworts, which combine the uptake of nutrients and water and their transport 16

2.2.1 Rhizoids, roots and vasculature: three important innovations 16

2.2.2 Similarities between rhizoids and root hairs 19

2.2.3 Pegged rhizoids also show similarity to xylem vessels 21

2.3 Plant cuticle, the waterproofing layer of the plant surface, is one of the first innovations of land plants 22

2.3.1 What is a plant cuticle? 22

2.3.1.1 The structure of the cuticle 22

2.3.1.2 The Composition of the cuticle 23

2.3.2 How to make a cuticle? 27

2.3.2.1 Cuticle biosynthesis within epidermal cells 27

2.3.2.2 Export of cuticle components from epidermal cells 32

2.3.2.3 Cuticle assembly at the epidermal surface 34

WAX DEPOSITION 36

2.3.3 How is the cuticle production controlled post germination? 37

2.3.4 The functions of the cuticle post germination 38
2.3.4.1 Limiting water loss 39
2.3.4.2 Protection against pathogens 40
2.3.4.3 Protection against UV radiation 41
2.3.4.4 Preventing adhesion and fusion of organs 41
2.4 Key innovations in seed plants 42
2.4.1 The seed 43
2.4.1.1 The transition to seeds: from the early seed-like structures to the seed 43
2.4.1.2 What is a seed? 44
2.4.2 Seed development in Angiosperms requires double fertilization. 48
2.4.2.1 Generalities in seed development 48
2.4.2.2 Seed Development in *Arabidopsis thaliana* 49
2.4.3 Coordination and regulation of the embryo/endosperm interface 53
2.4.3.1 The endosperm plays key roles in coordinating seed development 53
2.4.3.2 Embryonic surface formation necessitates cross talk between endosperm and embryo 58
2.4.3.3 ZOU/ICE1 form a key hub coordinating embryo surface formation and endosperm development 64
3 Aim of the thesis 68
CHAPTER 1: 69
DOES DECIPHERING ZOU/ICE COMPLEX REGULATION SHED LIGHT ON ZOU/ICE FUNCTION DURING SEED DEVELOPMENT? 69
Preamble 70
I) Negative regulation by HOS1 reveals cryptic genetic redundancy of ICE1 and ICE2 during seed development. 72
II – Further considerations 91
CHAPTER 2 95
ARE THE ZOU/ICE FUNCTIONS IN EMBRYONIC SURFACE FORMATION IN *ARABIDOPSIS THALIANA* CONSERVED IN *MARCHANTIA POLYMORPHA*? 95
I - ZOU/ICE function in cuticle biogenesis is ancient 98

II – Do MpICE proteins have other ZOU-dependant roles and ZOU-independent roles?.135

II.1 Gene expression patterns.....135

II.2 Roles in surface formation.....135

II. 3 Other potential roles of MpZOU and MpICE proteins (excluding roles in pegged rhizoid formation).....139

II.4 Material and Methods.....143

CHAPTER 3.....147

Is the ZOU/ICE function in endosperm cell elimination in *Arabidopsis thaliana* conserved in *Marchantia polymorpha*?.....147

I- The ZOU/ICE1 transcription factors control programmed cell death and formation of a novel water conducting tissue in the liverwort *Marchantia polymorpha*.....150

II- Further considerations.....171

GENERAL DISCUSSION AND PERSPECTIVES.....175

I The regulation of the activity of the ZOU/ICE complex: Conservation and divergence. .176

II The ZOU/ICE complex in the control of *M. polymorpha* gemma cuticle and *A. thaliana* embryonic cuticle formation.....178

III What is the link between pegged rhizoid formation, cuticle biogenesis and endosperm cell death?.....180

REFERENCES.....183

Abbreviations

2-MAG: 2-MONOACYLGLYECROL
A.thaliana, At : *Arabidopsis thaliana*
ABA: abscisic acid
ABC transporters: ATP (Adenosine Triphosphate)-binding cassette
ABCG: ATP-binding cassette subfamily G
ABRC: Arabidopsis Biological Ressource Center
ALE1: ABNORMAL LEAF SHAPE1
ANOVA test: ANalysis Of Variance test
AP2 : APETALA2
AP2M : ADAPTOR PROTEIN-2 MU-ADAPTIN
ATML1: ARABIDOPSIS THALIANA MERISTEM LAYER1
BAHD acyltransferase: BEAT, AHCT, HCBT and DAT acyltransferase
BCIP: 5-Bromo-4-Chloro-3-indolyl-phosphate
BDG: BODYGUARD
BETL: BASAL ENDOSPERM TRANSFER LAYER
BFN1: BIFUNCTIONAL NUCLEASE1
bHLH: basic helix-loop-helix
BLAST: Basic Local Alignment Search Tool
BSA: Bovine Serum Albumin
Cas9: CRISPR-associated protein 9
CBF: C-REPEAT/DRE BINDING FACTOR
cDNA: complementary DNA
CDS: Coding DNA Sequence
CE: Chalazal endosperm
CER: ECERIFERUM
CIF: CASPARIAN STRIP INTEGRITY FACTOR
CoA: Coenzyme A
Col-0: Columbia-0
COP1: CONSTITUTIVE PHOTOMORPHOGENIC1
CRISPR: Clustered Regularly Interspaced short palindromic repeats
CUS1: CUTIN SYNTHASE1
DAMPS: Damage Associated Molecular patterns
DCF: DEFICIENT IN CUTIN FERULATE
DCR: DEFECTIVE IN CUTICULAR RIDGES
DIC: Differential Interference Contrast
DMP: DOMAIN MEMBRANE PROTEINS
DNA: Deoxyribonucleic acid
dPCD: developmental Programmed Cell Death
EAS: Endosperm Adjacent to the Scutellum
ECH: ECHIDNA
ECR: enoylCoA reductase
EDTA: Ethylenediaminetetraacetic acid
EF1: ELONGATION FACTOR1
EIF4: EUKARYOTIC INITIATION FACTOR4
EMS: Ethyl metane sulfonate
ER: Endoplasmic Reticulum
ESR: Embryo Surrounding Region
Evo-Devo: Evolution and Development
FAA: Formaldehyde Alcohol Acetic Acid
FA-CoA: Fatty acyl CoA
FAE complex: Fatty Acid Elongation complex
FDH: FIDDLEHEAD
FRH1: FEW RHIZOIDS1

GC: Gas Chromatography

GDSL: Glycine Aspartic acid Serine Leucine

GFP: Green Fluorescent Protein

GNL: GNOM-LIKE

GPAT: GLYCEROL 3-PHOSPHATE ACYLTRANSFERASE

GRI: GRIM REAPER

GSO: GASSHO

GUS: β-glucuronidase

H202: hydrogen peroxide

HCD: beta-hydroxyacyl-CoA dehydratase

HCl: Hydrochloric acid

HDG1: HOMEODOMAIN GLABROUS1

HD-ZIP-IV: homeodomain-leucine zipper IV

HOS1: HIGH EXPRESSION OF OSMOTICALLY RESPONSIVE GENES1

ICE1 or ICE2: INDUCER OF CBF EXPRESSION 1 or 2

ICE1-D: Gain of function mutant of ICE1

KCR: beta-ketoacyl-CoA reductase

KCS: beta-ketoacyl-CoA synthase

KRAAM motif: Lysine Arginine Alanine Alanine Methionine motif

KRS: KERBEROS

LACS: Long Chain Acyl-Coa synthetase

LRL: Lotus Japonicus ROOTHAIRLESS LIKE

LTP: Lipid Transfer Protein

LTPG: glycosylphosphatidylinositol-anchored LTP

LW: Lysine Tryptophan

LWHA: Lysine Tryptophan Histidine Alanine

M, mM, µM: Molar, milimolar, micromolar

M. polymorpha, Mp: Marchantia polymorpha

MAH1: MID-CHAIN ALKANE HYDROXYLASE1

ME: micropylar endosperm

Mm, µm: milimeters, micrometers

MMC: Single maternal cell

MpACT: ACTIN 7

MpAPT: ADENINE PHOSPHORIBOSYL TRANSFERASE

MPK: MITOGEN ACTIVATED PROTEIN KINASE

MS: Murashige and Skoog

Mya: Million year ago

NAC domain: NAM, ATAF and CUC domain

NASC: Notthingham Arabidopsis Stock Center

NBT: nitroblue tetrazolium

NLS: Nuclear Localization Sequence

nm: nanometer

NMR: Nuclear Magnetic Resonnance Spectroscopy

OCL11: OUTER CELL LAYER11

OST1: OPEN-STOMATA1

P. patens, Pp : Physcomitrella patens

PAS2: PASTICCINO2

PASPA3: PUTATIVE ASPARTATIC PROTEINASE A3

PBS: phosphate-buffered saline

PCW: polysaccharide cell wall

PDF2: PROTODERMAL FACTOR 2

PE : peripherical endosperm

PEC1 : PERMEABLE CUTICULE 1

PEM : PIPES, EGTA, Magnesium

PM : Plasma membrane

Q-PCR : Quantitative Polymerase Chain Reaction

r.p.m: revolution per minute of rotor

RAM: Root Apical Meristem

REDOX: Oxidation reduction

RGP3: REVERSIBLY GLYCOSYLATED POLYPEPTIDE3

RHD6: ROOT HAIR DEFETIVE6

RNA: Ribonucleic acid

ROS: Reactive Oxygen Species

RSL1 and RSL2: RHD SIX-LIKE1 and 2

SAM: Shoot Apical Meristem

SCRM: SCREAM, the other name for ICE proteins

SEM: Scanning Electron Microscope

sgRNA: single guide RNA

SHN: SHINE

SPCH: SPEECHLESS

STIG1: STIGMA-SPECIFIC PROTEIN1

SUC5: SUCROSE TRANSPORTER5

Tak-1 or Tak-2: Takaragaike-1 or 2

T-DNA: Transfer

TEM: Transmission Electron Microscope

TF: transcription factors

TWS1: TWISTED SEED1

UV: Ultraviolet

v/v: volume for volume

VLC: Very Long Chain

VLCFA: Very Long Chain Fatty Acyl CoA

VND: VASCULAR-RELATED NAC-DOMAIN

w/v: weight for volume

WS: WAX SYNTHASE

WSD1: WAX ESTER SYNTHASE/DIACYGLYCEROL ACYLTRANSFERASE1

XET: Xyloglucan Endotransglycosylase

Y2H: Yeast-Two Hybrid

Z. mays, Zm : Zea mays

ZOU: ZHOUPI

General preamble

My thesis is divided in four main parts: Introduction, Chapter 1, Chapter 2, Chapter 3.

The first part is an introduction divided in two sections: the first one presents briefly the two model plants used during this thesis *Arabidopsis thaliana* and *Marchantia polymorpha* and the second focuses more specifically on three innovations acquired during the evolution of plants on land: the rhizoids, the cuticle and the seed.

Then three chapters of results and discussion are presented, one on *A. thaliana* and two on *M. polymorpha*. My contribution is defined at the beginning of each Chapter.

A general bibliography is presented at the end of the thesis.

INTRODUCTION

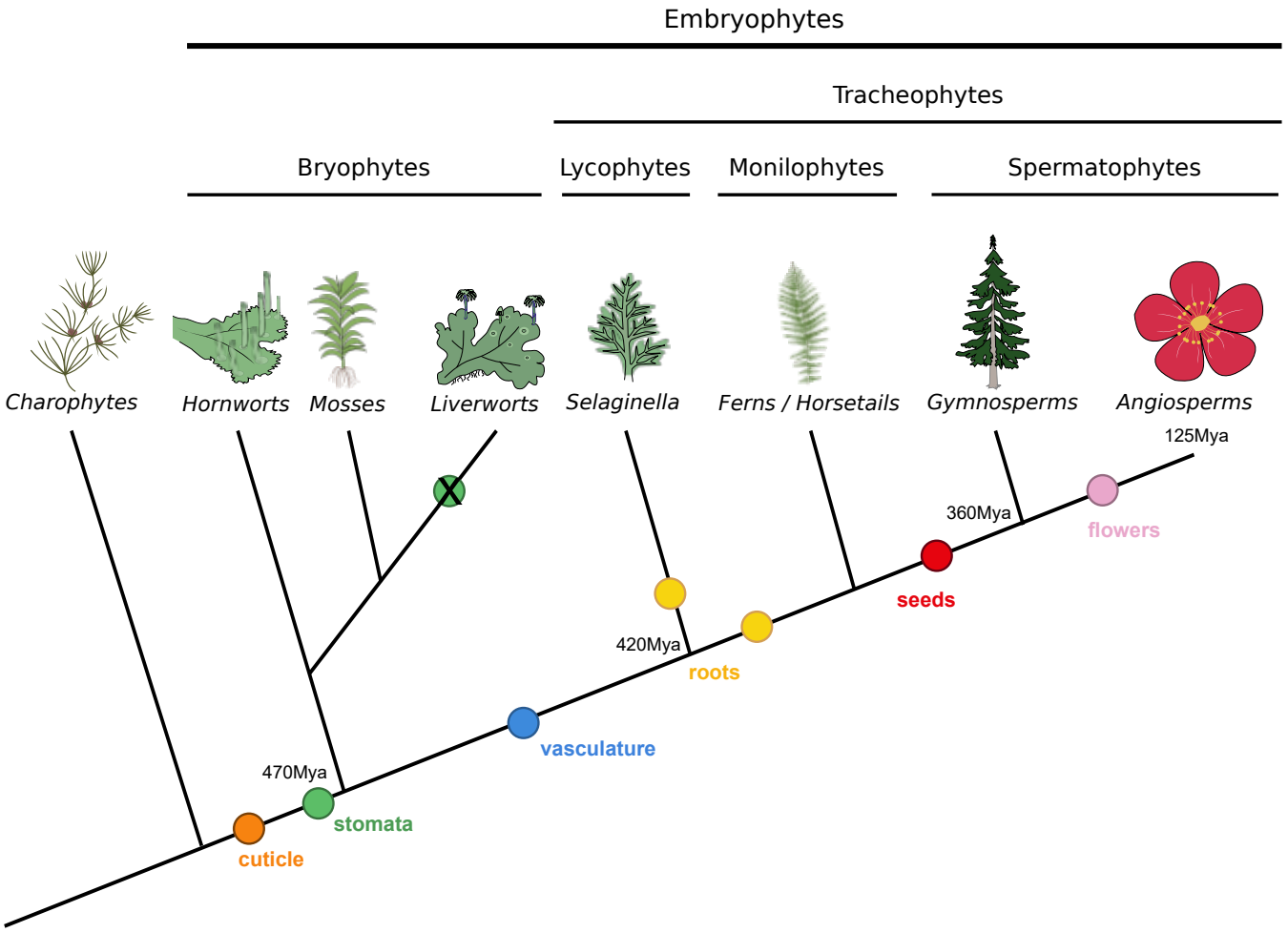

Figure 1 : Key innovations in land plant evolution.
Phylogenetic relationships between the major groups of land plants. Key innovations that occured during land plant terrestrialisation are indicated by coloured dots. Dates are indicated in million years ago (Mya).

1 Land plant evolution and key innovations: from the green algae to the angiosperms

1.1 Description of the different groups of plants

Colonization of the terrestrial environment by plants was one of the key transitions that made the Earth the unique planet that we inhabit today. Land plants emerged from the green algae, one of the oldest eukaryotic lineage. They are complex multicellular algae which exist as haploid individuals. Although, as in land plants, diploid cells (zygotes) are formed through the fusion of haploid cells (gametes) in charophyte algae, they generally undergo meiosis without prior cell division (Delwiche and Cooper, 2015). Land plants, otherwise known as embryophytes, emerged from aquatic environments around 470 million years ago (Mya) (Kenrick and Crane, 1997). As their name suggests, they undergo embryogenesis, which is the developmental process through which the zygote (the produce of gamete fusion) becomes a multicellular embryo (Rensing, 2016). The embryophyte life cycle thus alternates between multicellular haploid (gametophyte) and multicellular diploid (sporophyte) phases. Embryophytes are also characterised by the production of a hydrophobic, protective cuticle, that covers their surface, and is thought to have been a key innovation in conquering the terrestrial environment.

The group of living embryophytes that first evolved on land was the bryophytes (liverworts, mosses and hornworts), which have a haploid-dominant life cycle and are classified as “non-vascular” plants. Until recently, early land plant relationships were very uncertain, and because of their relative morphological complexity liverworts were assumed to be the “ancestral” group giving rise to all other embryophytes, probably because early fossilised spores are most similar to those of liverworts. However, the recent work of Puttick et al., 2018 strongly supports that the three groups forming the bryophytes (liverworts, mosses and hornworts) are monophyletic and thus all share the same common ancestor with the tracheophytes (vascular plants) (**Figure 1**). The simplicity of some liverworts is likely to reflect loss of structural diversity during the course of evolution.

The tracheophytes are thought to have arisen about 420 Mya, and are characterized by the presence of a lignified vasculature with identifiable xylem and phloem (Steemans et al., 2009). Approximately at the same time, plants developed a new body part: the root (**Figure 1**). In contrast to tracheophytes, bryophytes do not possess efficient sap-conducting vessels allowing them to transport solutes over long distances, nor specialized multicellular structures capable of extracting nutrients and water from the soil (**see Introduction, § 2.2**).

Tracheophytes are composed of three groups, the lycophytes which were the first extant tracheophyte group to emerge, the monilophytes which include ferns and horsetails and the Spermatophytes (seed plants) which is the most recent group to have emerged (**Figure 1**). A lack of vascular tissue in the bryophytes is thought to have limited plant size. However Lycophytes, equipped with a vascular system were the dominant group during the Carboniferous period (300 Mya-360 Mya) and could grew into massive 30 meters high trees, which dominated the landscape (Kenrick and Crane, 1997). Spermatophytes, which include gymnosperms and angiosperms appeared around 360 Mya (**Figure 1**). They are characterized by their ability to produce seeds and are the last group of plants which appeared on Earth (Kenrick and Crane, 1997). The first gymnosperms appeared at the end of the Carboniferous period 360 Mya and reached their peak in the Jurassic period, at the beginning of the Cretaceous period (200-150 Mya), before slowly declining during the angiosperm radiation. Angiosperms are thought to have first appeared about 125 Mya, and in addition to seeds, possess a further reproductive innovation: the flower (Friis et al., 2006) (**Figure 1**).

1.2 Plant Life cycles: the rise of the sporophyte

A characteristic shared by all land plants is the alternation between multicellular haploid and diploid phases. This contrasts with the situation in most charophyte algae where the zygote is formed of only one diploid cell (Bowman et al., 2016; Niklas et al., 2009), although a similar situation is observed in other lineages, such as brown algae.

Although the earliest land plants, like extant bryophytes, almost certainly had a haploid (gametophyte dominant) life cycle, the course of plant evolutionary history of plants, has been marked by a reduction in the dominance of the gametophytic phase (both in terms of size and life span) in favour of the sporophytic phase. Thus, in bryophytes, the gametophyte is dominant and autotrophic, whereas the existence of the sporophyte generation is reduced to a very short time window, and sporophytes are almost always nutritionally dependant on the gametophyte. The emergence of the tracheophytes marked the inversion of this dominance (**Figure 1**) (Friedman, 2013; Graham et al., 2000).

1.3 Two land plant models and their life cycles: *Marchantia polymorpha* and *Arabidopsis thaliana*

1.3.1 What is a model plant?

The term model plant was coined in the nineteen fifties, at the very beginning of the rise of *A. thaliana* as a key plant model. *A. thaliana* coexisted with other key models such as Antirrhinum (*Anthirrhinum majus*), Petunia (*Petunia x hybrida*) and Maize (*Zea mays*), which had been extensively studied over decades, and for which impressive banks of mutants (usually induced by the activity of endogenous transposons) and natural accessions were available (Meyerowitz, 2001; Somerville and Koornneef, 2002). *A. thaliana* rose to prominence however, due to its relatively short life cycle, small size, and ease of propagation. In addition, likely in part because it doesn't have a large endogenous transposon population, *A. thaliana* also has a small and quite simple genome (135 Mb). However, the point that underlay the truly meteoric rise of *A. thaliana* as a model plant, and which still makes it incredibly useful today, is its ease of Agrobacterium-mediated transformation and the associated capacity to generate both transgenic plants and stable mutants. *A. thaliana* as a model system for plant development was initiated in 1943 and became accepted by the scientific community in the eighties because of the different features which make an organism a convenient model to study (Meinke and Scholl, 2003). Numerous mutants are available, such as ethyl methane-sulfonate (EMS) mutants (Qu and Qin, 2014) and T-DNA insertion mutants (Qu and Qin, 2014b) in several stock centers such as the Arabidopsis Biological Resource Center (ABRC) or the Nottingham Arabidopsis Stock Center (NASC) and can also be very easily produced using CRISPR-Cas9 technology (Lee et al., 2018b). Chosen from an outset of plants with small genome size, *A. thaliana* is also the first plant organism with a fully sequenced genome published in 2000 (Meyerowitz, 2001; Somerville and Koornneef, 2002; The Arabidopsis Genome Initiative, 2000).

Since the *A. thaliana* whole-genome sequencing in 2000, many plant genomes have been sequenced. However during almost 10 years most plant genomes sequenced were angiosperm's and only in 2008 was the first bryophyte genome (*Physcomitrella patens)* sequenced, (Rensing et al., 2008). Perhaps because the *P. patens* genome was the first to be sequenced this raised *P. paten* to become the main bryophyte model plant. *M. polymorpha* was a very popular model plant in the early 1900s but fell into oblivion until the beginning of 21st century when genomic and genetic tools started to be available for plant to study evolution and development (Evo-Devo) (Ishizaki et al., 2008, 2013; Sugano et al., 2014). Although the complete chloroplast genome of *M. polymorpha* was one of the first sequenced (Ohyama et al., 1986), the whole genome took much longer to be sequenced. *M. polymorpha* was

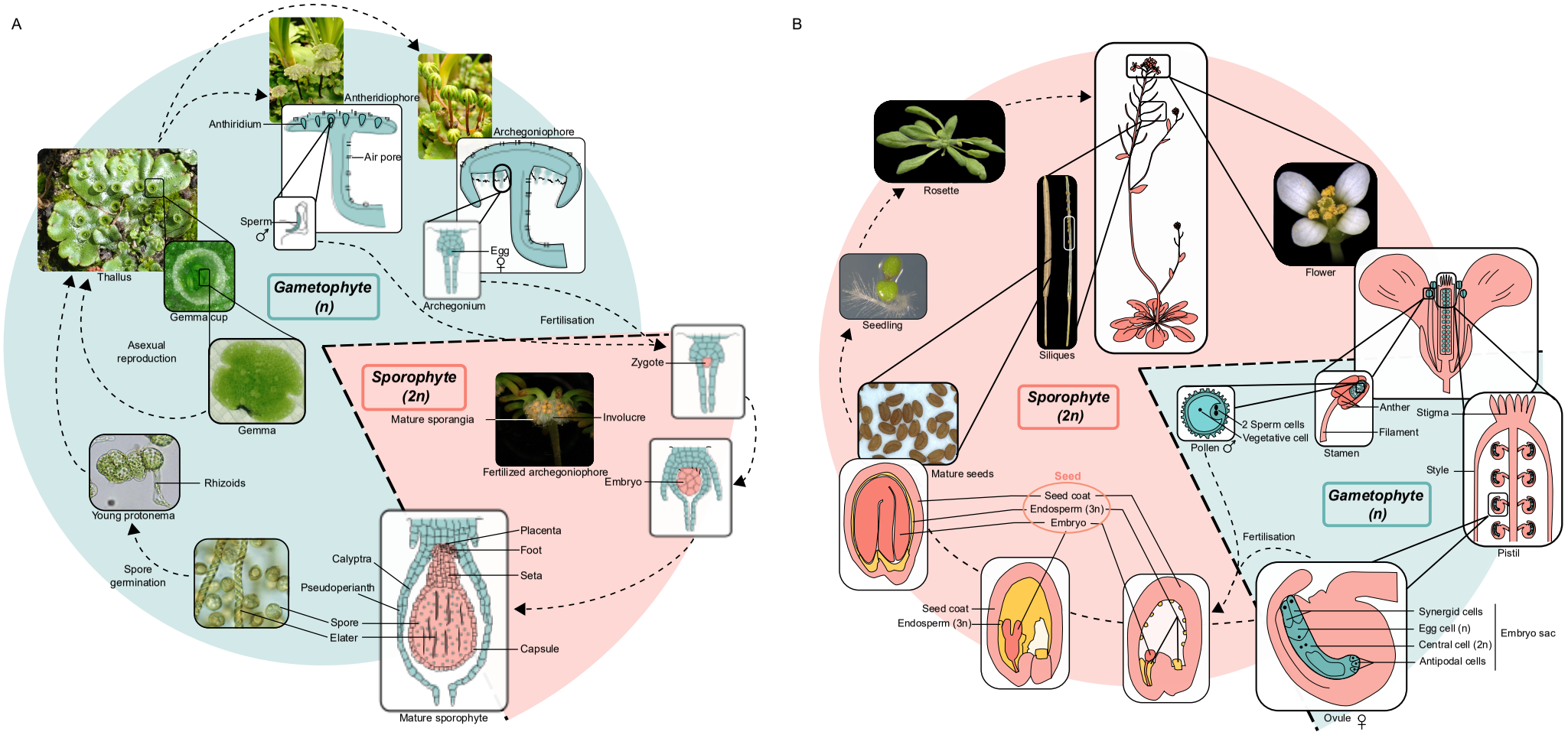

Figure 2 : Life cycles of *Marchantia polymorpha* and *Arabidopsis thaliana*.
M. polymorpha life cycle (A) is gametophytic dominant whereas *A. thaliana* life cycle (B) is sporophytic dominant. Alternation of the haploid gametophyte and the diploid sporophyte are represented in blue and pink respectively. *M. polymorpha* photos of germinated spores and spores and elaters are from Shimamura et al., 2016. *A. thaliana* photos of rosette, siliquees and flower are from Krämer et al., 2015.

eventually chosen for the community sequencing program at the Joint Genome Institute, Department of Energy, USA and the first version was published in 2017 (Bowman et al., 2017). Since then, newer versions have appeared (Montgomery et al., 2020) and gene annotations have been upgraded. CRISPR-Cas9 technology (Sugano et al., 2014) and homologous recombination (Ishizaki et al., 2013) has been developed, and sporeling and thallus can be transformed using *Agrobacterium* with very high efficiency (Ishizaki et al., 2008; Takenaka et al., 2000). The *M. polymorpha* genome is relatively small (approximately 280Mb), its life cycle is quite short and the plants are very easy to propagate (see below) and cross which are very good reason to use *M. polymorpha* as a model plant to study Evo-Devo (Bowman et al., 2016b, 2017; Shimamura, 2016). Compared to other transformable Bryophytes such as the moss *Physcomitrella patens* (Schaefer and Zrÿ d, 1997) or the hornwort *Anthoceros agrestis* (Frangedakis et al., 2021), *M. polymorpha* has fewer gene duplications facilitating genetic analysis. However, many biological processes in this species appear to have been "simplified" over the course of evolution (Bowman et al., 2016b).

Finally, it is important to bear in mind that whatever the model plant, neither *A. thaliana* or *M. polymorpha* are fully representative of their respective family or clade.

In the following paragraphs, I present the two plant models which have been used during my PhD: *Arabidopsis thaliana* and *Marchantia polymorpha*.

1.3.2 M. polymorpha.

M. polymorpha belongs to the liverwort order in the bryophyte clade and is thought to have emerged about 450Mya. As for other bryophytes, the autotrophic plant body of *M. polymorpha* is produced in the multicellular haploid gametophyte generation. The sporophyte is very highly reduced (more so than in many mosses for example), is only present for a very short window of time and is composed of a single sporangium. The gametophyte initiates development either from a unicellular haploid spore, the result of sexual reproduction followed by meiosis within the sporangium, or through vegetative propagation via the production of haploid multicellular propagules called gemmae (singular: gemma) which represent a form of asexual reproduction (Shimamura, 2016) (**Figure 2**).

Gemmae are produced in "gemma cups" which are bowl-shaped structures on the dorsal surface of the leaf-like structures formed by the adult gametophyte, the thalli (singular: thallus). They appear once in each bifurcation of the thallus. They are formed from single cells at the base of the cup which undergo repeated round of mitosis before detaching from the base

of the cup and being pushed upwards by the developing gemmae beneath. More than a hundred gemmae can be produced by a single gemma cup (Shimamura, 2016). Gemmae, which measure at maturity 1 to 2 mm, have a discoid shape and two apical notches (which have latent) meristematic activity are situated at opposite points on the extremity of the disk. Mature gemmae do not show dorso-ventral differentiation, and are dormant whilst in the cup. However once gemmae have been dispersed, a process that involves their propulsion from the thallus surface by rain splashes (Brodie, 1951), they will "germinate" upon contact with the ground. This process involves the rapid acquisition of dorso-ventral polarity, visible as the ventral development of smooth rhizoids from rhizoid precursor cells, which are initially present on both surfaces of the dormant gemma (Kato et al., 2020; Shimamura, 2016; Tarén, 1958). Rhizoids are unicellular filament cells which are found on the ventral surface of the thallus either growing perpendicular to the thallus, the smooth rhizoids, or growing parallel to the thallus, the pegged rhizoids (**see Introduction, §2-2**) (Jones and Dolan, 2012; Shimamura, 2016).

M. polymorpha is a dioecious plant producing male and female reproductive organs on different individuals. Sex is determined by the transmission of heteromorphic sex chromosomes, X in female individuals and Y in males (Ishizaki et al., 2002; Okada et al., 2000; Shimamura, 2016). Upon induction by environmental stimuli (long days and far red light), thalli develop umbrella-like structures: gametophores called respectively antheridiophores or archenoniophores in male and female individuals (**Figure 2**). The stalks of these reproductive structures are a prolongation of the thallus and form an inrolled structure. Archegoniophores are composed of a stalk topped by a receptacle that is divided into finger-like projections (**Figure 2**). A row of eggs, each surrounded by gametophytic tissues, forms between each finger (Shimamura, 2016). Antheridiophores have a similar morphology but with a flatter receptacle that is undivided and produces antheridia containing bi-flagellated mobile sperm (**Figure 2**). On contact with a drop of water, the antheridiophore receptacle releases the sperm which will find its way (by swimming and/or capillarity) to the eggs. Once a sperm has reached an egg, fertilization takes place, resulting in the development of a zygote that then divides mitotically to form a sporophyte embryo. The embryo develops surrounded by a maternal gametophytic tissue divided into three parts (**Figure 2**). The most inner is the calypthra, a protective structure covering the sporophyte, which is itself gathered by the pseudoperianth, which is itself gathered with the other developing embryos, surrounded by the involucre, a fluffy and transparent protective structure (**Figure 2**). At the junction between the sporophyte and the gametophyte, specialized transfer cells with wall ingrowth develop forming a nutrient transfer zone called the placenta (Ligrone et al., 1993). When the embryo becomes a mature sporophyte, it is retained under the receptacle of the archegoniophore, and is composed of

three diploid tissues. The foot, forms a proximal diploid interface between the maternal gametophore tissues and a second structure, the seta. The seta elongates as a stalk which suspends and then pushes the sporangium out of the involucre. The sporangium is the third and most distal tissue structure of the sporophyte. The sporangium produces two cell types: elaters (elongated sporophytic cells that die and become very hygroscopic, and which are responsible of the dispersal of the spores) and spores, the products of meiosis (**Figure 2**). Once dispersed, spores germinate by producing smooth rhizoids and form a new thallus, closing the loop/completing the life cycle (O'Hanlon, 2015; Shimamura, 2016).

It is thought that, although ancestral Bryophytes could probably produce stomata (air pores formed within the epidermis of most Embryophytes), this capacity was lost in liverworts (Harris et al., 2020; Puttick et al., 2018). Instead *M. polymorpha* produces stomata-like structures, called air pores, which play a similar role to that the stomata in permitting gas exchange but with no movement and less effective than stomata. They are composed of stack of four cells which form the "chimney" of the air pores. Beneath this chimney, an air chamber is present in which multiple photosynthetic filament cells are visible (Shimamura, 2016).

Finally, another feature of *M. polymorpha* (but also Bryophytes and Lycophytes) is the absence of true meristems (Jill Harrison, 2017). The meristem-like is composed of only one cell, the apical cell and thalli grow from a region of very small cells called the apical notch. Apical notches multiply as thalli expand and bifurcate (Shimamura, 2016).

1.3.3 A. thaliana.

A. thaliana belongs to the taxonomic family of the Brassicae in the eudicotyledonous group of angiosperm vascular plants. It is not a crop species, but belongs to the same family as rapeseed, cabbages, turnips, mustards etc… making it a very interesting model plant.

In contrast to *M. polymorpha*, but like most vascular plants, the dominant autotrophic part of the *A. thaliana* life cycle is produced in the multicellular diploid sporophyte generation, with the production of vegetative structures (in the case of *A. thaliana* a rosette of leaves), and reproductive structures (in the case of *A. thaliana* an erect inflorescence). As noted above, the *A. thaliana* life cycle is short, and plants can go from seed to seed in 3 months, or even less, under laboratory conditions. As in *M. polymorpha*, the *A. thaliana* reproductive phase is triggered by appropriate environmental conditions. The main plant body of *A. thaliana* is the rosette of leaves which at the appropriate time produce the inflorescence, a long stem where at the top of it, flowers are produced (**Figure 2**). The *A. thaliana* inflorescence bears flowers that are hermaphrodite and composed two external whorls of sterile organs (four sepals and 4

white petals), and two inner whorls of sexual organs comprising 6 stamens (male organs) and one pistil composed of two fused carpels (female organs) (**Figure 2**). The stamens and carpels produce very small multicellular gametophytes (Krämer, 2015).

The female gametophytes, also called embryo sacs (**Figure 2**), are produced in ovules that emerge from the internal carpel walls. Each carpel can produce 20 to 30 ovules (meaning that up to 60 ovules can be produced per flower). Within each ovule primordium, a specific cell called the megaspore mother cell undergo meiosis to give four megaspores, of which three degenerate and one undergoes limited mitosis to give the female gametophyte. Each female gametophyte is surrounded by maternal sporophytic tissues (the integuments and nucellus) and is composed of four specialized cell types: the egg cell (haploid) and the central cell (containing two haploid nuclei), two haploid synergids flanking the egg cell, and necessary for fertilization, and three haploid antipodal cells of unclear function (**Figure 2**). As in all angiosperms, both the egg cell and the central cell are fertilization competent and can thus be considered as female gametes (Krämer, 2015).

On the male side, the anther (at the tip of the stamen) produces male gametophytes in the form of pollens grain (**Figure 2**). Each pollen grain is derived from a microspore generated by meiotic divisions occurring within the developing anther. Post meiosis, each microspore develops a thick protective coat called the pollen wall. Each undergoes one round of mitosis to give a large vegetative and a smaller generative cell, that is engulfed by the vegetative cell. The generative cell then undergoes a further round of division to give two sperm cells (Krämer, 2015).

Angiosperms, and thus *A. thaliana,* are characterized by a unique double fertilization event, in which the two sperm cells, delivered to the ovules by the pollen tube after pollen grain arrival and germination on the receptive carpel surface, fuse with the egg cell and the central cell of the female gametophyte. This event triggers seed development, which will be described in detail in **section I-4 of the Introduction**.

2 The move to land: key innovations

2.1 Life on land

During their emergence onto land, the ancestors of land plants were confronted with a dramatically new environment that imposed severe constraints on their growth and development. In order to adapt, they innovated, both morphologically and physiologically

One of the most major challenges faced by land-colonizing plants was the low humidity of the Earth's atmosphere. This may have been an underlying factor in changes as profound as the transition from a gametophyte dominant to a sporophyte dominant life cycle, since unlike the dispersal of motile male gametes, the dissemination of spores and of seeds is not dependent on water (Delaux et al., 2012). The development of a waxy, hydrophobic cuticle on the plant surface also became very important to prevent desiccation, and may have gone hand in hand with the evolution of air pores and ultimately stomata, which became necessary for the controlled exchange of gases at the surface of photosynthetic organs. In addition to preventing desiccation, the cuticle probably also protected plants against UV radiation and pathogen attack (Yeats and Rose, 2013; Ziv et al., 2018). Cuticle structure, development and functions are explained further in **section 2.3 of the Introduction**. Another adaptation necessary for land life was the production of phenolic polymers (such as lignin and suberin) which, similarly to the cuticle (which contains the largely aliphatic polymer cutin), are used to form barriers against pathogen attack and spread, particularly upon wounding (Serrano et al., 2014; Ziv et al., 2018) but also contribute to the structural properties of many land plants through the formation of the vascular tissue.

Water is critical to all forms of life, but particularly so to plants, whose tissues grow though the generation of intracellular hydrostatic pressure, and whose energy production depends upon water-cleaving photosynthetic reactions. Water can move through plant tissues by diffusion and/or by capillarity, the later occurring mainly within the fibrous structures provided by plant cell walls, and both being constrained by physical parameters including gravity. Thus, in situations where water is obtained from the substrate (as on land), neither diffusion nor capillarity can provide sufficient water to support large plant body plans. Vascular tissues, facilitating the rapid long-distance movement of water through plant tissues, were therefore a critical innovation underlying the colonization of land by plants. Their formation depended upon hydrophobic polymers, particularly lignin, which reinforces the cell walls of specialized cell types called xylem vessels. Xylem vessels develop as continuous cell files, and ultimately die, forming "pipes". The reinforcement and "waterproofing" of the cell walls of these structures through the inclusion of lignin within their cell walls gives them unique properties, including the capacity to resist negative pressures within the water columns that they can maintain intact thanks to their water-resistant properties. The negative pressure in these columns is caused by their being dragged upwards by controlled evaporation from the mesophyll cells of aerial organs in a process called transpiration (Růžička et al., 2015).

The maintenance of efficient water movement is dependent upon two other factors, efficient water uptake from the soil, and a mechanism allowing the control of water evaporation from aerial surfaces. The former is provided, in vascular plants, by roots, and the later, by the

combination of the waterproof cuticle, and the acquisition of stomata which act as valves to control the transpiration stream. Stomatal opening thus promotes the transport of both water and nutrients from the root to the shoot in the transpiration stream. Roots also participate in the anchorage of the plants to the substrate and the uptake of nutrients and water (Raven, 2002).

As mentioned in the previous section, stomata are not restricted to tracheophytes. Some bryophytes (mosses and hornworts) also develop stomata but only on their sporophyte (which is not their dominant life-cycle phase) where they contribute to its dehiscence (Chater et al., 2017; Duckett et al., 2009; Pressel et al., 2018; Rich and Delaux, 2020). Many Bryophytes also develop air pores, which serve the same function as stomata, by permitting gas exchange between underlying mesophyll cells and the environment. However, in contrast to stomata, and despite some structural similarities the apertures of these structures do not open or close (Shimamura, 2016).

Bryophytes do not produce roots but developed functionally analogous structures called rhizoids which are uni (liverworts) or multi (mosses) cellular (Delaux et al., 2012; Jones and Dolan, 2012; Kenrick and Strullu-Derrien, 2014). Early during land plant evolution, the acquisition of mineral nutrients, and indeed water, by these root-like structures is thought to have been dramatically increased by the development of symbioses with microorganisms present in the soil. These interactions appear to have been critical for terrestrialization (Delaux et al., 2012, 2019; Humphreys et al., 2010).

2.2 Rhizoids: the 2 in 1 structure of liverworts, which combine the uptake of nutrients and water and their transport

Once they had arrived on the land, plants were not fully submerged by water and nutrients and thus developed novel adaptations to uptake water and nutrients and transport them to the whole plant body: rhizoids, roots and vasculature.

2.2.1 Rhizoids, roots and vasculature: three important innovations

Kenrick and Strullu-Derrien, 2014 define the root as “a multicellular organ characterized by special features including gravitropic response, endogenous branching, root hairs, and a protective root cap”. Roots are thought to have evolved independently in several clades between 416 to 360 million years ago, and in combination with efficient vascular systems, were clearly a major factor in allowing plant life to flourish (Hetherington et al., 2016; Kenrick and Strullu-Derrien, 2014; Strullu-Derrien et al., 2018).

Roots *"sensu stricto"* as seen, for example in the model plant *A. thaliana,* are therefore composed of three main structures : primary roots, lateral roots (the meristems of which are protected by the root cap evoked above) and root-hairs (Hopmans and Bristow, 2002). Root-hairs are tubular cell extensions which grow out from the epidermal cells of primary and lateral roots (Scheres et al., 2002). By increasing the effective root surface area, root hairs are critical factors in water and nutrient uptake.

Bryophytes did not evolve roots, but instead they developed rhizoids (Carol and Dolan, 2002; Pressel et al., 2008). Rhizoids are not restricted to land plants they also developed on the surface of the gametophyte of some aquatic streptophyte algae such as *Chara* (Lewis and McCourt, 2004) where they are either multicellular or unicellular. In the early land plants with a gametophyte dominant phase, rhizoids are unicellular in liverworts (except for *Haplomitrium* (Bartholomew-Began, 1991) and hornworts, but are multicellular and can be highly branched in mosses (Jones and Dolan, 2012; Motte et al., 2019; Tam et al., 2015).

In the liverwort *M. polymorpha*, two types of rhizoids can be distinguished: pegged rhizoids and smooth rhizoids (**Figure 3**). Smooth rhizoids are living cells with a diameter of 18 to 24 µm for maximum 30 mm length which grow perpendicular to the thallus (gametophytic photosynthetic tissue) and appear to function mainly to anchor plants to the substrate and it seems that they could also participate to water transport (Clee, 1943; Duckett et al., 2014; Kameriing, 1897; Shimamura, 2016). In contrast, pegged rhizoids are dead cells at maturity, and show extensive cell wall thickening, including the production of internal cell wall extensions called pegs which may prevent the cell body from collapsing (Kameriing, 1897). They generally grow parallel to the thallus all along the midrib and they tend to be narrower (6 to 24 µm of diameter) and shorter (8 to 20 mm) than smooth rhizoids (Duckett et al., 2014). In mature thallus, they form bundles enclosed by flaps of thallus tissue called ventral scales. Interestingly not all liverworts produce both types of rhizoids (Jones and Dolan, 2012; Shimamura, 2016), pegged rhizoids are restricted to complex thalloid liverwort suggesting they are an important evolutionary innovation (Villarreal A et al., 2016). Pegged rhizoids are almost undistinguishable from smooth rhizoids before peg development but after peg development and subsequent programmed cell death, they become very easily distinguishable from smooth rhizoids. During their differentiation the tips of nascent pegged rhizoids can still be peg-less, whereas the basal domain can be already completely full of pegs. Mainly thanks to their collection in bundles and dye uptake experiments, pegged rhizoids have been proposed to play a key role in water conduction (Duckett et al., 2014; Kameriing, 1897). Bundles of pegged rhizoids are also present in the stalk of the gametophores where they are thought to transport water by capillarity (Duckett et al., 2014; McConaha, 1941).

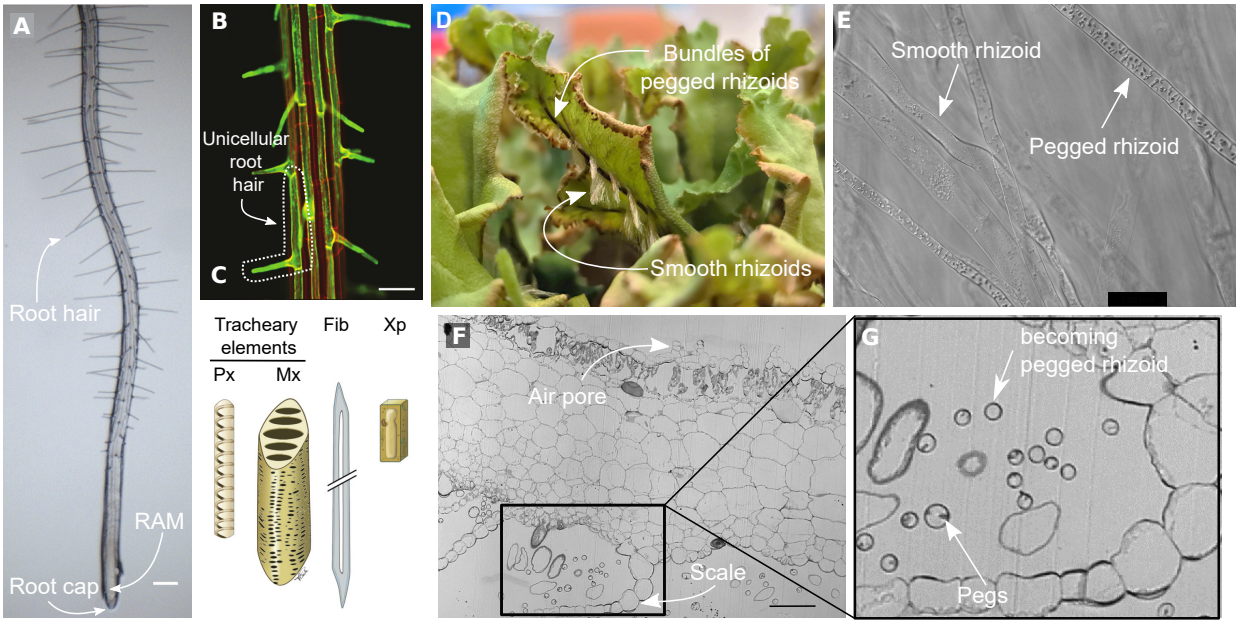

Figure 3: Description and structure of *M. polymorpha* rhizoids, root hairs and xylem in vascular plants.

(A-B) Root hairs are filament cells formed on the root of tracheophytes visible on a light microscopy photograph of *A. thalina* roots from Vissenberg et al., 2020. (A) The main zone of roots : at the tip the root cap which protects the root apical meristem (RAM) and further in the tissue, root hairs develop all around the root. Scale bar, 200µm. (B) Confocal microscopy photograph of a specific root-hair promoter (green) showing the unicellular root hair. Scale bar, 50µm. (C) Schematic reprensentation of the four differerent xylems found in Angiosperms: Tracheary elements (protoxylem (Px) and metaxylem (Mx)), fiber (Fib) and xylem parenchyma (Xp) from Schuetz et al., 2012. (D-G) The two types of rhizoids in *M. polymorpha* : pegged rhizoids and smooth rhizoids. (D) Underneath de thallus the bundles of pegged rhizoids and the beard of smooth rhizoids are growing respectively parallel and perpendicular to the thallus. Scale bar, 100µm. (E) DIC microscopy photograph of smooth rhizoid and pegged rhizoid. Scale bar, 50 µm. (F-G) Transverse section of thallus showing difference tissues. the air pores are on the dorsal surface whereas the bundle of pegged rhizoids with their pegs are growing inside the scales to form bundles. (G) is a higher magnification of the bundle of pegged rhizoids visible in the box in (F). Pegs are visible in the transverse section of pegged rhizoid. Scale bar, 100µm.

As discussed above, the evolution of true vascular tissues during land plant evolution contributed significantly to the emergence of higher plants by permitting the long distance transport of water and nutrients over long distances though stomatally controlled transpiration. (Bonfante and Genre, 2008; Delaux et al., 2012; Fukuda and Ohashi-Ito, 2019). The higher plant vasculature system is composed of xylem, phloem and cambium, all of which derive from the procambium. Xylem is composed of tracheary elements of which the most important are: the tracheids and vessel elements (**Figure 3**). They both have secondary cell wall thickenings, are dead at maturity and undergo programmed cell death as part of their differentiation programme (Ligrone et al., 2000; Růžička et al., 2015). These lignified thickenings provide the mechanical support for the entire plant. Despite their similarities, tracheid and vessel elements differ in their assembly and morphology. Tracheid elements are elongated overlap one another and are linked with each other by several pits (region without secondary cell wall) in their lateral wall. A pit is typically located at an opposing pit of a neighbouring tracheid forming pit pairs. In contrast, vessel elements arrange with each other by their end which are open wall forming a vertical file called vessel. Like tracheid elements, vessel elements also have pits on their lateral wall, allowing them to communicate with each other laterally (Růžička et al., 2015).

2.2.2 Similarities between rhizoids and root hairs

Filamentous cells develop at the plant surface interface in almost all land plants during their life cycle. Depending on the plants, two types of filamentous cells can be found: root hairs are found on the sporophyte of vascular plants whereas rhizoids develop on the rootless sporophyte or gametophyte of non-vascular and some vascular plants, the monilophytes and lycophytes (Banks, 1999, 2009). Both rhizoids and root hairs (Carol and Dolan, 2002; Pressel et al., 2008) elongate by tip growth but have slightly different diameter and length. Whereas the diameter of rhizoids varies from 6 to almost 30µm (depending of the type of rhizoids) in complex thalloid liverworts like *M. polymorpha*, root hairs in *A. thaliana* have approximately a dozen microns across and 1 mm length (De Baets et al., 2020; Duckett et al., 2014).

In contrast to root hairs which are thought to play role predominantly in nutrient uptake, rhizoid function was first shown to be involved in the anchorage of the plant to the substrate (Jones and Dolan, 2012). However, pegged rhizoids are also involved in the uptake of water and in nutrient transport. Moreover aqueous dyes are very quickly transported by capillarity between the pegged rhizoids of *M. polymorpha* supporting that in addition to classical transport of water within the pegged rhizoid, capillarity between the pegged rhizoids is also possible to transport water (Duckett et al., 2014). In addition, water can also be transported inside smooth rhizoids (even though these ones collapse easily) and pegged rhizoids (Clee, 1943; Jones

and Dolan, 2012). From an evolution point of view, since Mp*rsl1* mutant lack both type of rhizoids combined with the fact that smooth and pegged rhizoids are hard to distinguish early on suggested that pegged rhizoid evolved from smooth rhizoids (Honkanen et al., 2018; Villarreal A et al., 2016). In addition, the acquisition of pegged rhizoids has been proposed to be correlated with the ability of certain bryophytes to develop taller gametophores, as in the case in the complex thalloid liverwort, *M. polymorpha* (Duckett et al., 2014). Together these data support that pegged rhizoids are likely an important innovation for early land plants.

In addition to their functional similarities, the development of rhizoids and root-hairs which both developed from a single epidermal cell, has also been found to be regulated in a similar manner. Indeed, both are under the control of basic helix loop helix transcription factors (bHLH TF). The *Lotus japonicus* ROOTHAIRLESS LIKE (LRL) transcription factor, which is encoded by 5 homologous genes in *A. thaliana*, has been found to control the elongation of root hairs (Karas et al., 2005). Only one gene encoding this transcription factor is present in *M. polymorpha*, and has been shown to play a key role in rhizoid development (Breuninger et al., 2016). *ROOT HAIR DEFECTIVE6 (*At*RHD6)* and *RHD SIX-LIKE1 (*At*RSL1)* are required for root hair development in *A. thaliana* (Lin et al., 2015; Menand et al., 2007). Although, these genes are specific to land plants, members of the bHLH TF family to which the proteins that they encode can be found in green algae, suggesting the recruitment of these TF to rhizoid/root hair formation during terrestrialization (Jones and Dolan, 2012). In the moss *P. patens*, Pp*RSL1* and Pp*RSL2* are closely related to At*RHD6* and At*RSL1* respectively and are required for rhizoid growth and development. Indeed, the double mutant Pp*rsl1* Pp*rsl2* is defective in rhizoid development but not in the development of other tip growing cells (Jang and Dolan, 2011; Menand et al., 2007). Complementation of At*rh6* mutant with Pp*RSL1* rescues the root-hair phenotype supporting a conservation of protein function (Menand et al., 2007). Similarly, forward genetic screens in *M. polymorpha* supported the role of *RSL* genes in rhizoid development. Loss of function of Mp*RSL1*, the *M. polymorpha* orthologue of the *A. thaliana RSLs*, showed absence of rhizoids, but also, in this case, of other tip growing cells (such as papillae and gemmae) (Proust et al., 2016). In contrast, ectopic expression of Mp*RSL1* leads to only an excessive production of rhizoids including formation of rhizoids on both the ventral and the dorsal surface of the thallus. Together these data suggest that Mp*RSL1* controls rhizoid fate within epidermal cells. More recently, *FEW RHIZOIDS1* (Mp*FRH1*), which encoding a microRNA targetting the Mp*RSL1* transcript, was shown to act as a negative regulator of rhizoid development. Consequently, gain of function of Mp*FRH1* causes a severe reduction in rhizoid numbers (Honkanen et al., 2018; Thamm et al., 2020).

2.2.3 Pegged rhizoids also show similarity to xylem vessels

Although rhizoids can be easily compared to root hairs, rhizoids, and especially pegged rhizoids, also show many striking similarities with the internal water-conducting cells in mosses called hydroids and xylem vessels in vascular plants (Nakashima et al., 2012; Xu et al., 2014). All these structures are involved in water/nutrient transport and can be assimilated to vasculature-like and undergo programme cell death during their differentiation process.
Interestingly, the largest group of plant-specific TFs, the NAM, ATAF and CUC (NAC) domain proteins (or VASCULAR-RELATED NAC-DOMAIN (AtVND) in *A. thaliana*), control late development of moss and Angiosperm water conducting cells, including cell wall thickening but also associated traits such as salt and drought tolerance (Lv et al., 2016; Nakashima et al., 2012; Xu et al., 2014). In *A. thaliana* VND6 and VND7 activate genes involved in secondary cell wall biosynthesis of the xylem vessels and regulate xylem-specific programmed cell death (Fukuda and Ohashi-Ito, 2019; Kubo et al., 2005; Yamaguchi et al., 2010, 2011; Zhong et al., 2010). In the moss *P. patens*, three out of eight NAC TF also controls cell wall modification and programmed cell death of hydroids (filamentous cells with a similar functions to rhizoids) (Xu et al., 2014). The homology between moss and angiosperm gene regulatory network for xylem/hydroids is striking and could mean it was present in a common ancestor of land plants but lost in liverworts. This would depend whether NACs have a role in *M. polymorpha* pegged rhizoids which remains an opened question.

Until recently, the functional parallel between pegged rhizoids or hydroids and the xylem of vascular plants had not been demonstrated. However, recent work from (Brodribb et al., 2020) showed, for the first time, functional similarities between xylem in vascular plants and hydroids, in the moss *Polytrichum commune*. These parallels include vascular conducting tissue which are collapse-resistant while transporting water under tension and efficient regulation of leaves transpiration allowing photosynthetic gas exchange without cavitation inside the vascular tissue. Frustratingly few studies in *M. polymorpha* have been published to support this (Duckett et al., 2014). However, although the similar morphological structure of rhizoids strongly suggests that a parallel structure/function relationship between *M. polymorpha* pegged rhizoids and angiosperm xylem vessels is very likely since i) they both share a role in water transport ii) they both are collected together in bundles, iii) they both develop patterned secondary thickenings and developmental programed cell death, they are distinct and likely evolved independently. Indeed, pegged rhizoids arose late in liverwort evolution (they are found only complex thalloid liverworts) suggesting they are a derived and not an ancestral feature. They also showed a very different developmental origin since they are externalised and not internalised as the xylem or the hydroids and do not join end to end unlike xylem vessels.

2.3 Plant cuticle, the waterproofing layer of the plant surface, is one of the first innovations of land plants

Terrestrialization necessitates the need to control the movement of water within plant tissues. This need underlay the evolution of roots, rhizoids and vasculature as we discussed in the previous sections. However, these innovations do not limit the drying effect of the terrestrial environment. The colonization of land therefore necessitated adaptations allowing plants to prevent uncontrolled water loss. Plants addressed this problem by “waterproofing” their surfaces.

2.3.1 What is a plant cuticle?

2.3.1.1 The structure of the cuticle

The primary interface between land plants and their aerial environment is provided by the hydrophobic barrier, the cuticle. The cuticle, which is synthesized by epidermal cells (Kurdyukov et al., 2006; Samuels et al., 2008) and sometimes also covers the cell walls bordering substomatal chambers (Osborn and Taylor, 1990) is present in all land plants, from bryophytes (Buda et al., 2013; Budke et al., 2012; Lee et al., 2020; Renault et al., 2017) to angiosperms.

The concept of the cuticle was first proposed around two centuries ago (von Mohl, 1842, 1847). Since this time scientists have used diverse techniques to define and identify the cuticle structure, including Transmission Electron Microscopy (TEM), Scanning Electron Microscopy (SEM), confocal microscopy, and spectroscopic methods (Fernández et al., 2014; Heredia-Guerrero et al., 2014; Yeats and Rose, 2013). These studies have revealed a very heterogeneous structure. The structure and heterogeneity of the cuticle seems also to depend of the preparation of the samples (Guzmán et al., 2014) and the interpretation of the authors (Jeffree, 2007). The cuticle can differ dramatically in thickness from the nanometre to the micrometres scale (Jeffree, 2007). Cuticles are incredibly diverse in their structure, composition and properties, which themselves may vary between species, organs, genotypes, developmental stages, and environmental conditions etc (Fernández et al., 2016; Guzmán-Delgado et al., 2016; Knoche et al., 2004; Nawrath et al., 2013; Szakiel et al., 2012)… In an extreme case Guzmán et al., 2014 showed that structural differences may be observed even within the same cuticle section observed by TEM, confirming strong heterogeneity of the structure of the plant cuticle even at nanometric scale.

Despite this heterogeneity, most cuticles contain of a lipophilic matrix, called cutin which is a cross-linked matrix of insoluble monomers of long chain hydroxyl fatty acids, and

hydrophobic compounds, the waxes (Jeffree, 2007). Waxes can be intracuticular, within the cutin-matrix, or epicuticular wax crystals or wax films on the external surface of the cuticle. Structurally, the cuticle in seed plants can be divided into two parts: the cuticle proper forms the outer layer of the cuticle, is enriched in waxes and is sometimes is covered by additional wax structures such as epicuticular films and/or epicuticular wax crystals. The cuticle proper covers an inner zone, which is enriched in cutin with embedded polysaccharides and can be referred to as the cuticular layer (**Figure 4**) (Jeffree, 2007). However, this description probably oversimplifies a very complex picture since different plants, organs, and even fixation techniques can provide highly divergent images. In general, TEM observed cuticles are composed of two or more, more or less well defined layers with different electron-density distributions (after heavy metal staining) corresponding to the different parts of the cuticle. The intensity of these layers are very dependent on both the cuticle composition and sample preparation. Cuticles may also sometimes show lamella within their layers (Jeffree, 2007; Jeffree et al., 1975).

Another approach to studying cuticle structure which might, at first sight, seem less complex than studying the structure of intact cuticles *in planta*, has been to focus the analysis of the structure on some components or groups of components in a semi-purified form. For example, some studies focused their research on isolated waxes (Dragota and Riederer, 2007; Jeffree et al., 1975), cutin monomers (Graça and Lamosa, 2010; Ray and Stark, 1998), polysaccharides (Guzman-Puyol et al., 2015) or flavonoids (Domínguez et al., 2009). It has been suggested that different macromolecular arrangements of cutin components may be responsible for the variable ultrastructural cuticle patterns observed by TEM (Graça and Lamosa, 2010). However, separating out specific cuticle components is a complex undertaking and likely disrupts inter-molecular associations. In addition some components (such as "cutan" polymer found in the cuticles of some plant species, are highly resistant to extraction procedures (Mckinney et al., 1996).

In summary, due to the problems highlighted above, structure and chemical composition of cuticles are often difficult to link (Fernández et al., 2016).

2.3.1.2 The Composition of the cuticle

As previously mentioned, cuticles are incredibly diverse in their structure, composition and properties, in this section we will see that a lipophilic matrix and hydrophobic compounds, cutin and wax respectively are present in many cuticles. However, these polymers are themselves very diverse in chemical composition and present in highly variable proportions. Other components may include polysaccharides, phenolics and sometimes cutan (Fernández

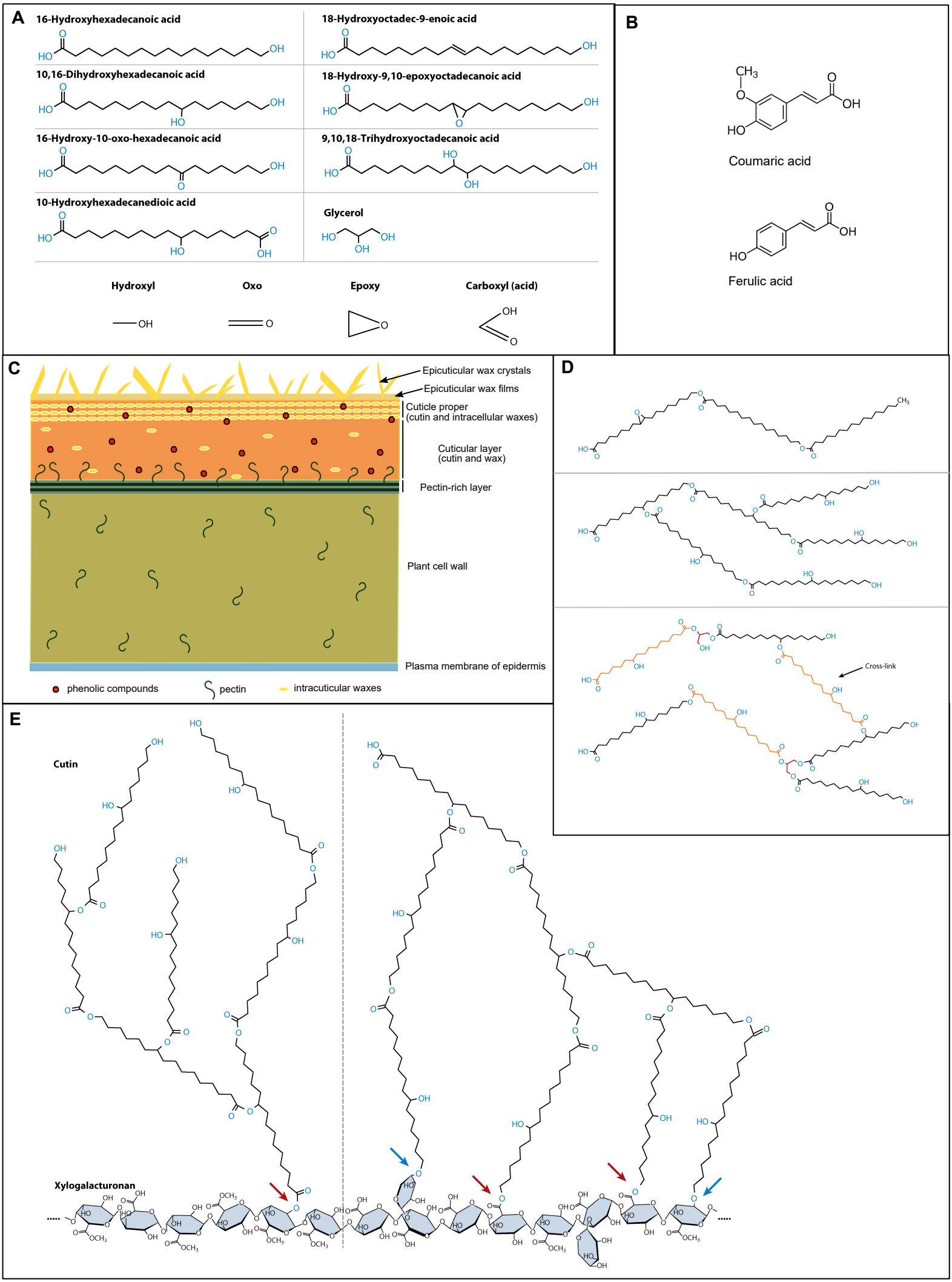
A
16-Hydroxyhexadecanoic acid
18-Hydroxyoctadec-9-enoic acid
10,16-Dihydroxyhexadecanoic acid
18-Hydroxy-9,10-epoxyoctadecanoic acid
16-Hydroxy-10-oxo-hexadecanoic acid
9,10,18-Trihydroxyoctadecanoic acid
10-Hydroxyhexadecanedioic acid
Glycerol
Hydroxyl
Oxo
Epoxy
Carboxyl (acid)
B
Coumaric acid
Ferulic acid
C
Epicuticular wax crystals
Epicuticular wax films
Cuticle proper
(cutin and intracellular waxes)
Cuticular layer
(cutin and wax)
Pectin-rich layer
Plant cell wall
Plasma membrane of epidermis
phenolic compounds
pectin
intracuticular waxes
D
Cross-link
E
Cutin
Xylogalacturonan

et al., 2016; Tegelaar et al., 1991). The complexity of the composition of each of them are overviewed below.

Waxes are a mixture of diverse very-long-chain aliphatic compounds containing between 22 and 48 carbon atoms that may carry an oxygen-containing functional group such as primary alcohols, esters, aldehydes, odd-chain numbered alkanes and ketones (**Figure 4**) (Jetter et al., 2006). The proportion between the different wax aliphatic compounds often varies within the different organs of the same plant and between species. In addition to these aliphatic chains, secondary metabolites as sterols, triterpenoids and phenylpropanoids may also be associated with cuticular waxes (Jetter et al., 2006; Li-Beisson et al., 2013). Waxes can be extracted from intact cuticles using solvents and its monomers analysed, for example by mass spectroscopy.

Although the fine structure of cutin polymers remains largely unknown, their composition has started to be elucidated. Cutin is a polyester composed mainly of C16-C18 hydroxy or hydroxyl epoxy fatty acid monomers (**Figure 4**) (Walton and Kolattukudy, 1972). These are esterified, mainly via their mid-chain hydroxyl groups into branched networks. Glycerol is also found as a monomer up to 14% of total monomer mass in cutin polymers (Pollard et al., 2008). Cutin cannot be extracted using solvents, but can be hydrolysed after solvent extraction, and analysed, by mass spectroscopy.

Others compounds can also be found in the cuticle such as polysaccharides, which are incorporated into the cutin matrix in which they may play a role in stiffness (Guzmán et al., 2014b). Phenolics can also be found in cuticle in the form of coumaric acid for example where they are often present in less than 1% in the cuticles (**Figure 4**) (Graça et al., 2002). They likely also contribute to cutin rigidity (López-Casado et al., 2007) but may also be important for UV protection. In addition to coumaric acid, in *A. thaliana* leaf tissue, ferulic acid has also been identified in the cutin polymer (Rautengarten et al., 2012). Phenolics can be released during cutin hydrolysis, but due to the potential presence of oxidative crosslinks between phenolic molecules, their abundance may be underestimated during such procedures.

The proportions of some compounds vary more than others in the different cuticle compartments, tissues and organs. For example, in waxes extracted from *A. thaliana* secondary alcohols and ketones which are almost absent from rosette leaves but respectively reach 23% in inflorescence stems and 14% in flowers (Bourdenx et al., 2011). As another example of variability, the cutin monomer α-ω-dicarboxylic acid which is usually found at less than 5% in most plant cutins, is much more abundant in *A. thaliana* where it represents more than 50% of total monomer mass (Pollard et al., 2008).

Figure 4: Schematic representation of the structure and composition of the cuticle of land plants. (A) Examples of cutin monomers and monomer functional groups, from Fich et al., 2016. (B) Examples of phenolic compounds found in cuticle. (C) The cuticle is composed of three zones. The zone closest to the cell wall is the cuticular layer. It is mainly composed of cutin and wax polymers, is closely linked to the cell wall and thus enriched in pectins. The middle zone is the cuticle proper, mainly composed of cutin polymers and intracellular waxes. Phenolics are also present in these two layers. Finally, the outer layer is the epicuticular waxes in which wax crystals cover wax films. (D) Example of cutin polymer. Diacids (orange) allow for cross-linking between cutin chains (arrow), as well as incorporation of glycerol (red) into the polymer, from Fich et al., 2016. (D) Examples of hypothetical cutin attachment to polysaccharides, using the pectin xylogalacturonan as an example. They may be joined through the single carboxyl end of the cutin dendrimer (left side of the dashed line) or its many hydroxyl ends (right of the dashed line). Arrows indicate possible covalent linkages between these two polymers: ester linkages (red) and ether linkages (blue), from Fich et al., 2016.

Finally, cutan may also be an important content of the cuticle, sometimes being present in similar quantities to cutin (Schmidt and Schönherr, 1982; Villena et al., 1999). It is a highly aliphatic matrix linked by ether bonds which is resistant to both solvent extraction and hydrolysis.

2.3.2 How to make a cuticle?

2.3.2.1 Cuticle biosynthesis within epidermal cells

Although they have different final chemical compositions, the biosynthesis of both cutin and wax starts with fatty acids. The main fatty acids used for cuticle biosynthesis have chain lengths of 16 or 18 carbons (C16/C18), although the actual ratio is unknown and is likely to vary between organs. They are synthesized in the plastids by the Fatty Acid Synthase complex and distributed to the endoplasmic reticulum (ER). The mechanism of intracellular trafficking of Fatty Acids from the plastids to the ER is still unknown. Once they have reached the ER membrane, acyl chains are activated to coenzyme–A (CoA) by long-chain acyl-CoA synthetases (LACS) (Haslam and Kunst, 2013; Jessen et al., 2011; Lü et al., 2009). The acyl-activation is common to both the wax and cutin biosynthesis pathways, and attributing LACS to specific pathways seems to be complicated. All nine LACS-encoding genes in the *A. thaliana* genome work redundantly or partially redundantly in lipid metabolism. In *in vitro* enzymatic assays most LACS proteins show higher enzymatic activity with saturated and monounsaturated 16 carbons fatty acids and mono and polyunsaturated 18-carbons fatty acids than with other fatty acids. (Lü et al., 2009; Pulsifer et al., 2012; Shockey et al., 2002). Three of the nine LACS are involved in cuticle biosynthesis, and are specifically localized in the endoplasmic reticulum (**Figure 5**). All three have been shown to activate fatty acids for production of cuticular lipids. *LACS1/ECERIFERUM8(CER8)* acts redundantly with *LACS2* to activate fatty acids for production of wax and for the incorporation of C16-C18 acyls groups into cutin (Lü et al., 2009; Weng et al., 2010). *LACS4* is also partially redundant with *LACS1* in providing substrates for cuticular wax biosynthesis (Jessen et al., 2011). More recently, Zhao et al., 2019 and colleagues showed that the cuticle of the triple mutant *lacs1lacs2lacs4* is permeable and has a severe decrease in wax and cutin loads confirming again the redundancy between these LACS-encoding genes, and the commonality between the substrates necessary for cutin and wax biosynthesis. Interestingly *LACS4* also functions partially redundantly with *LACS1* in pollen coat formation (Jessen et al., 2011). Although all LACS enzymes appear to function in lipid metabolism, they are not all ER localized or involved in the synthesis of extracellular lipids. For example, LACS9 is specifically associated with the outer envelope of plastids and is involved in the activation and export of plastid-derived fatty acids for triacylglycerol assembly. Moreover, seven of the nine *LACS* appear to be involved in seed

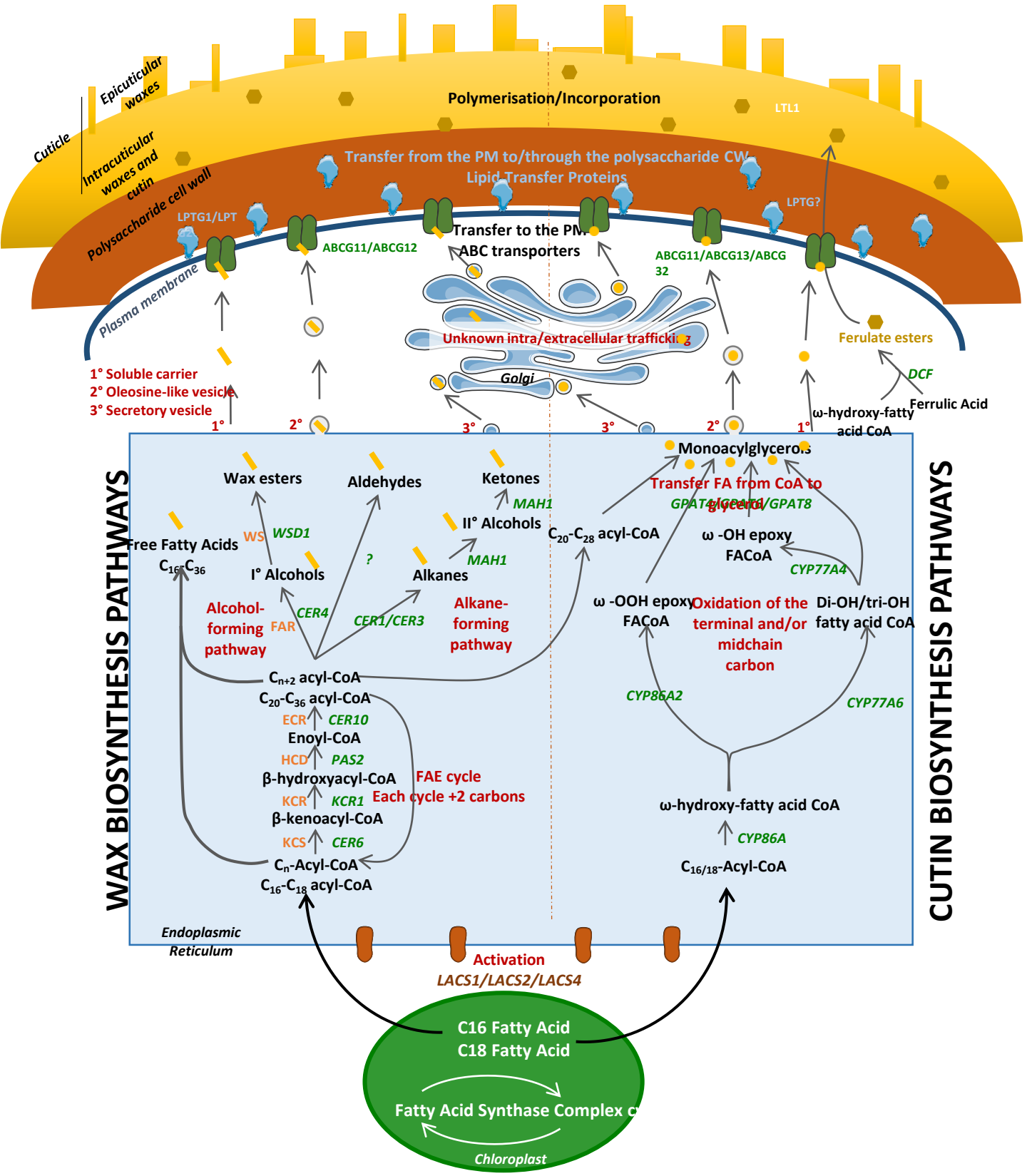

Figure 5: Cutin and wax biosynthesis pathways and cuticle formation on the surface of epidermal cells. The different steps of the two pathways are explained in the section INTRODUCTION I-3. Enzyme names are indicated in orange and their corresponding genes in green.

oil production: *LACS1*, *LACS2*, *LACS4*, *LACS6*, *LACS7*, *LACS8* and *LACS9* have overlapping roles in fatty acid beta-oxidation (Fulda et al., 2004; Jessen et al., 2015; Shockey et al., 2002; Zhao et al., 2010).

WAX.

Much of the wax biosynthetic process occurs within the endoplasmic reticulum and is composed of three majors steps. Once imported into the ER, C16-C18 acyl-CoA become substrates for the fatty acid elongase complex (FAE) (**Figure 5**). The activity of the FAE consists of four successive enzymatic reactions, catalysed by four distinct enzymes, that generate an acyl-CoA chain extended by two carbons. When carbon chains reach lengths of over 22 carbons, these acyl-CoA chains are classified as very long-chain fatty acyl CoA or VLCFA-CoAs. The first step of the fatty acid elongation cycle involves the condensation of two carbons from malonyl-CoA to the acyl-CoA chain and is catalysed by a β-ketoacyl-CoA synthase (KCS). The resulting β-ketoacyl-CoA is then reduced by a β-ketoacyl-CoA reductase (KCR) to β-hydroxyacyl-CoA which is dehydrated to enoyl-CoA by β-hydroxyacyl-CoA dehydratase (HCD). Finally, the FAE cycle is completed by another reduction reaction mediated by an enoylCoA reductase (ECR) to produce the +2 carbon elongated very-long-chain-acyl-CoA (**Figure 5**).

In *A. thaliana*, twenty-one KCS-encoding genes have been annotated (Joubès et al., 2008) including some with a wax synthesis activity. To date, CER6 is the only KCS which appears to have a strictly wax-specific function based on phenotypic and expression pattern analysis (Hooker et al., 2002; Millar et al., 1999). Likewise, several KCR-encoding genes have been annotated in the *A. thaliana* genome but only *KCR1* has been reported to reduce β-ketoacyl-CoA to β-hydroxyacyl-CoA (Beaudoin et al., 2009). The PASTICCINO2 (PAS2) protein, has been shown to dehydrate 3-hydroxyacyl-CoAs into enoyl-CoAs (Bach et al., 2008) but also (confusingly) contributes to cell division and cell differentiation, possibly through an antiphosphatase activity involved in the regulation of cyclin-dependant kinase A (Bellec et al., 2002; Da Costa et al., 2006; Harrar et al., 2003). Whether these two activities are linked remains a subject of debate. Some ER-localized enzymes involved in lipids synthesis are thought to form clusters on specific ER subdomains. The PAS1 protein has been proposed to act as a scaffold to recruit the FAE complex enzymes to such ER subdomains during wax biosynthesis (Roudier et al., 2010). Finally, Zheng et al., 2005 identified an enoyl reductase, CER10, responsible for the production of the elongated acyl-CoA (**Figure 5**).

Loss or partial loss of activity of the three last enzymes of the FAE complex (CER10, PAS2 or KCR1) results in a dramatic reduction in all major classes of very-long-chain-acyl lipids on the plant surface, and to severe developmental and cellular defects. These pleiotropic

phenotypes probably reflect that fact that these enzymes are involved in other metabolic pathways, including those involved in the production of sphingolipids which are necessary for basic cellular functions (Zheng et al., 2005).

Carbon chain elongation by the FAE cycle can end by the conversion of the VLCFA-CoA to free VLCFA by thioesterases. The resulting free VLCFA is then be incorporated directly into the cuticle by an unknown process. The FAE elongation products can also be used in the alcohol forming pathway to produce VLC-primary alcohols through the action of alcohol fatty acyl CoA reductases (FAR), such as ECERIFERUM4 (CER4*)* in *A. thaliana* (**Figure 5**)*.* CER4 only seems to be able to reduce C24 or C26 VLCFA-CoA into primary alcohols in the yeast heterologous system (Jenks et al., 1995; Rowland et al., 2006). Free primary alcohols can be incorporated into waxes or they can be esterified by a wax synthase to create wax esters. The only wax synthase (WS) functionally identified to date, and probably the main one in *A. thaliana,* is provided by the wax ester synthase/diacylglycerol acyltransferase 1 (WSD1) (Li et al., 2008). The *wsd1* mutant shows a severe reduction in alkyl esters and an absence of detectable wax esters in stems and leaves. More recently, *WSD1* has also been shown to contribute to drought tolerance (Patwari et al., 2019). WSD1 is part of a large protein family. The functions of many of the members of this family have not been fully characterised but the genes encoding these proteins show diverse expression patterns. Several other family members could also be implicated in wax biosynthesis including WSD11 which is thought to be involved in petal growth by providing waxes to the petal surface where they may act as a lubricant (Takeda et al., 2013). WDS6, WSD7 and WSD1 have also been shown to contribute to water, salt and abscisic acid (ABA) stress tolerance (Patwari et al., 2019).

Another possible destination for VLCFA-CoA produced by the FAE complex is the production of aldehydes, odd-chain numbered alkanes, secondary alcohols or ketones via the alkane-forming pathway. Alkanes can be produced from VLCFA-CoA via the formation of intermediate aldehydes. However, to date the enzyme responsible has not been identified. Nonetheless, Bernard et al., 2012 proposed a model in which CER3 (a VLCFA-CoA reductase) and CER1 (an alkane forming enzyme) form an enzymatic complex catalysing the formation of VLC-alkanes from VLC-acyl-CoA. Although they are, themselves, very abundant wax compounds, VLC-alkanes can also undergo further modifications to form secondary alcohols and ketones. In *A. thaliana*, MAH1, a mid-chain alkane hydroxylase from the cytochrome P450 family catalyses the production of VLC-secondary alcohols which can be further oxidized, by the same enzyme, into VLC-ketones (Greer et al., 2007).

CUTIN.

Similarly to wax biosynthesis, cutin biosynthesis occurs principally in the ER using C16-C18 fatty-acids as substrates. Once the C16-18 fatty-acids are activated by the transfer of a CoA group, the resulting product, C16/C18 acyl-CoA, undergoes oxidation of the terminal and/or mid-chain carbon followed by the transfer of the fatty acid from CoA to glycerol.

The oxidation step is catalysed by members of the CYP86 cytochrome P450 family such as ATT1/CYP86A2, CYP86A4, CYP86A8 and probably CYP86A7 (Li-Beisson et al., 2009; Molina et al., 2008; Voisin et al., 2009; Xiao et al., 2004). ω-hydroxy fatty acyl-CoA are hydroxyl fatty acyl-CoA with a carboxylic acid group and a primary hydroxyl group, and often carry one or two additional secondary hydroxyl groups. They are oxidised either on the terminal carbons, (mainly by members of the CYP86A family), or on a mid-chain carbon, (mainly by enzymes from the CYP77A family) (**Figure 5**) (Pollard et al., 2008).

Finally, the mature monoacylglycerol cutin monomers are generated by the enzymes of the Glycerol 3-Phosphate Acyltransferase or GPAT family (Fawke et al., 2019; Fich et al., 2016a; Li et al., 2007a). *A. thaliana* possesses ten genes annotated as GPATs but only eight of them have been shown to be potentially involved in the biosynthesis of apoplastic barriers. GPAT10 and GPAT9 appear to be required for membrane or storage lipid biosynthesis (Gidda et al., 2009; Nishida et al., 1993). The other GPATs cluster in a subfamily and have functions that affect the composition and/or quantity of cutin or suberin (Beisson et al., 2012). Suberin is another major polymer found in plants with similar functions and properties as cutin but is found in the roots, seed coats and abscission zones where it has a protective role (Franke and Schreiber, 2007; Philippe et al., 2020; Vishwanath et al., 2015). GPAT4, GPAT6 and GPAT8 are required for cutin biosynthesis where they have an sn-2 acyltransferase activity. In addition to acyltransferase activity, these three enzymes catalyse a dephosphorylation reaction during the condensation between glycerol and fatty-acyl CoA chains (Yang et al., 2010, 2012). The genes encoding these proteins are differentially expressed. *GPAT4* and *GPAT8* have been found to be expressed mainly in stems and leaves where they are required for the accumulation of C16 and C18 ω-hydroxy fatty acid and α,ω-dicarboxylic acid cutin monomers (Li et al., 2007). *GPAT6* is mainly expressed in flowers and catalyzes the production of three C16 monomers: 10,16-dihydroxypalmitate, hexadecane-1,16-dioic acid and 16-hydroxypalmitate (Li-Beisson et al., 2009). Interestingly, these three GPATs seem to preferentially catalyse the reaction of C16 and C18 fatty acids with hydroxyl or carboxyl groups suggesting there are probably undiscovered acyltransferases for the other cutin precursors such as the FA-CoA C20-C28 which are the main FA-CoA found in cutin polymers (Li-Beisson et al., 2013; Yeats and Rose, 2013). GPAT5 and GPAT7 are involved in suberin precursor synthesis and do not have phosphatase activity (Pollard et al., 2008; Yang et al., 2012). Finally,

GPAT1/2/3 are more divergent, in terms of protein sequence, compared to GPAT4/6/8 and GPAT5/7. Although GPAT1 seems to be required for tapetum and anther development (Zheng et al., 2003) no acyltransferase activity have been detected for this enzyme (Yang et al., 2012). GPAT2 and GPAT3 functions remain uncertain as mutants are not defective in lipid production and assays have revealed no acyltransferase activity with basic substrates for these enzymes. However, modelling and sequence similarities suggest that both proteins could possess a potential sn-2 acyltransferase activity (Zheng et al., 2003).

OTHER COMPONENTS.

In addition to aliphatic compounds, the cuticle also contains phenolic monomers synthesized via the phenylpropanoid pathway, such as coumaric acid or ferulic acid (Graça et al., 2002; Rautengarten et al., 2012). Incorporation of phenylpropanoid compounds into cutin requires BAHD acyltransferases such as DEFICIENT IN CUTIN FERULATE (DCF) which transfers ferulic acid from CoA to the terminal hydroxyl of omega-hydroxy-fatty acids (Rautengarten et al., 2012). Loss of DCF function does not cause any major alteration in cuticle permeability or cutin lipid monomer composition but a 90% decrease in ferulic acid content in *A. thaliana* non-suberized leaf tissue. This suggests that contrary to suberin, in which phenolic compounds play an important role in ensuring impermeability, this is not that case for the cuticle. (Gou et al., 2009; Rautengarten et al., 2012). In contrast with wax and cutin biosynthesis, the enzymatic reaction catalysed by DCF occurs in the cytosol (**Figure 5**) (Rautengarten et al., 2012).

How phenolic compounds are exported, how they are integrated into the cuticle and what roles they play during cuticle development are questions with very few concrete answers, although this is a fertile field of ongoing research (Biała and Jasiński, 2018).

2.3.2.2 Export of cuticle components from epidermal cells

After production of wax components and monoacylglycerols in the endoplasmic reticulum, cutin and wax precursors must be exported from the epidermal cell and transported to the cell surface. This transport involves two key steps: From the ER through the plasma membrane (PM) and from the PM through the polysaccharide cell wall (PCW) to the plant surface.

To reach the plasma membrane, cutin and wax precursors must cross the cytosol. To date very little is known about the intracellular trafficking of cuticular precursors. Several mechanisms have been hypothesised for the transport of wax and cutin monomers through

the hydrophobic cytosol. The first option is the role of the canonical secretory pathways. This last decade, McFarlane et al., 2014 and colleagues used mutants defective in vesicle trafficking to explore this option. *gnom-like1* and *echidna* mutants, respectively involved in Golgi-ER trafficking and vesicle trafficking from the trans Golgi network to the PM, have visibly fewer wax crystals (measured by scanning electron microscopy) on their stem surfaces and a reduction in wax load compared to wild-type. These results suggest that wax transport to the plasma membrane may depend partially on a Golgi-dependant mechanism that requires GNOM-LIKE1/ERMO1 (GNL1) and ECHIDNA (ECH). However, it is important to highlight that these mutants also have a defect in wax biosynthesis and a defective ER morphology (McFarlane et al., 2013; Nakano et al., 2009). Given the ER-localisation of wax biosynthetic enzymes, a disruption of the ER morphology in vesicle trafficking mutants may cause a disruption of the enzymes' organisation and a subsequent reduction of wax biosynthesis. The second option suggested by Samuels and McFarlane, 2012 is that lipids might be trafficking at sites of close contact between the ER and the PM through Lipid Transfer Proteins (LTP). Although no direct evidence for this trafficking mechanism of the cuticular precursors has been shown, such close contacts are known to exist in plants and animals and to be involved in the transport of other hydrophobic molecules (Larsson et al., 2007; Samuels and McFarlane, 2012).

Very few more recent papers have been published addressing the theory that vesicle trafficking could be involved in the export of cutin/wax monomers. It is likely that this is due to the fact that mutants in these processes are lethal or show severe developmental phenotypes. In the future the application of inducible knock-down approaches could be used to address this question.

Once at the plasma membrane, monoacylglycerols and wax precursors have been shown to exit the cell via polarly localized membrane transporters from the ATP-binding cassette subfamily G (ABCG). Full length transporters contain two nucleotide binding domains which hydrolyse ATP to provide energy for transport, and two multi-span transmembrane domains which allow substrate translocation across the membrane. However, some ABCG transporters exist as "half" transporters that must form homodimers or heterodimers to be functional. For example, the half transporter ABCG11 dimerizes with ABCG12/CER5 to mediate wax export. The need for both proteins in the functional complex is demonstrated by the fact that *abcg11* and *abcg11abcg12* mutants show the same decrease in extracellular wax quantity (Bird et al., 2007; Pighin et al., 2004). ABCG11 is also involved in cutin export since *abcg11* mutants also shows a reduced cutin load. Moreover, ABCG11 can homodimerize. This, together with the fact that *abcg12* mutants show no decrease in cutin load, suggesting that the homodimer ABCG11/ABCG11 may have specific functions in cutin export. Importantly

50% of total waxes are exported apparently normally in *abcg11abcg12* mutants, suggesting that other members of the ABCG family might be involved in wax transport (Bird et al., 2007). Consistent with this idea, a transporter closely related to ABCG11 and ABCG12, ABCG13, has been shown to contribute to cutin export in flowers (Panikashvili et al., 2011). Unlike the previously described ABC transporters, ABCG32 also called PERMEABLE CUTICLE 1(PEC1) is a full length transporter and is required for cutin precursors exportation since *abcg32* mutants display a reduction of 40% in some cutin precursors (**Figure 5**) (Bessire et al., 2011).

2.3.2.3 Cuticle assembly at the epidermal surface

How the compounds discussed in the previous sections assemble at the plant surface and form the cuticle is still little known. However, some studies suggested that cutin is likely to be the primary component deposited into the cuticle (during embryogenesis or organogenesis) whereas the wax deposition occurs later, and tends to be conditioned by environmental factors (Delude et al., 2016; Kannangara et al., 2007).

CUTIN POLYMERIZATION.

The identities and proportions of cutin monomers and their loads in diverse plants, organs, and tissues have been extensively studied. However, the information is almost always based on hydrolysed cuticles, making understanding how these different monomers are linked together in vivo difficult to ascertain. Several techniques based on spectrometry and Nuclear magnetic Resonance Spectroscopy (NMR) have been applied to try and decipher the structure and linkages within the cutin polymer. They revealed after partial depolymerisation primary and secondary ester linkages between the cutin monomers and covalent linkages between some cutin hydroxyl fatty acids and oligosaccharides (Graça et al., 2002; Tian et al., 2008). However, they might not be the only options for the assembly of the different monomers, these later can also be linked on the primary OH by a linear or on a secondary OH by a branched pattern as has been shown within tomato cutin but the relative proportion of the types of cross-links remain uncertain (Deas and Holloway, 1977; Deshmukh et al., 2003; Graça and Lamosa, 2010; Kolattukudy, 1977). To date, the ester links of glycerol OH groups remains unresolved. In vitro assays with the tomato *(Solanum lycopersicum)* cutin synthase SlCUS1 and a putative precursor of cutin polymer, 2-monoacylglycerol (2-MAG) in *A. thaliana* (Yang et al., 2010), showed a production of linear oligomers in aqueous solution by transesterification of the end-chain hydroxyls groups (Girard et al., 2012; Yeats et al., 2012, 2014). This CUS1 was the first enzyme identified in the polymerisation of the monomer (Girard et al., 2012; Yeats et al., 2012, 2014). The *CUS1* mutant exhibits a severe reduction of polymerised cutin in the tomato fruit cuticle (Girard et al., 2012; Yeats et al., 2012), in both the cuticular layer and cuticle proper.

More precisely, the esterification mediated by CUS1 involves mostly primary hydroxyl groups in vitro (Yeats et al., 2014) but probably also the secondary hydroxyl group of 9(10),16-dihydroxyhexadecanoic acid and both the primary and secondary hydroxyl groups of glycerol (Philippe et al., 2016). Girard et al., 2012 and Yeats et al., 2012 also showed that the polymerisation of the cutin monomers by CUS1 is extracellular and occurs where the cuticle is deposited.

Interestingly, although the *sicus1* mutant shows a polymerisation activity in vitro and in vivo the single mutant still has a very thin cuticle meaning that one or more additional enzymes are involved in the polymerisation of cutin.

It is possible that several other enzymes polymerise cutin monomers in various different ways, possibly via different groups, but CUS1 is a key component. These enzymes could belong to the same glycine–aspartic acid–serine-leucine (GDSL) motif lipase subfamily as CUS1.

Another possibility suggested in a few articles, is the auto-assembly of cutin monomers via a non-enzymatic mechanism involving cutinsomes; nanoparticles of partially polymerized cutin which are proposed to traverse the epidermal cell wall and self-assemble at its surface (Domínguez et al., 2010; Segado et al., 2020; Stępiński et al., 2017). It remains unclear if this process happened *in planta* or not. In addition, enzymes involved in polymerisation still need to be evoked for this mechanism to result in the production of a cuticle that cannot be extracted using solutes.

CUTIN LINKS TO CELL WALL POLYMERS.

Deposition of cutin and waxes occurs on the cell wall polysaccharide matrix. A gradient is formed in most plant surfaces where the most outer layer (the cuticle proper) is composed of waxes and cutin whereas the inner surface contains cutin and waxes but also polysaccharides (Jeffree, 2007). Treatments for cuticle isolation revealed the strong link between cuticle proper and cell wall, since pectinase treatment or pectinase and cellulose treatments have been found to be necessary to release the cuticle from the leaves of several plant species and from conifer needles respectively (Lendzian et al., 1986; Orgell, 1955).

In addition, several loss of function mutants affected in cuticle formation also show defect in cell wall organization, suggesting a coordination/cross-talk between the deposition of cell wall, including the cuticle layer, and the cuticle proper. An example of the cross talk between cell wall and cutin is the loss of function *gpat6* mutant in *A. thaliana* where not only a defect in cutin synthesis is detectable (Petit et al., 2016) but also significant changes in cell

walls (Philippe et al., 2020). Similar correlations have also been observed in the tomato fruit (Philippe et al., 2020). In *A. thaliana* another enzyme called DEFECTIVE IN CUTICULAR RIDGES (DCR), an acyltransferase from the BADH family, has been shown to have a key function in cuticle organization independently of cutin monomer composition and structure. Indeed, the corresponding mutant *dcr* showed a thinner cuticle proper as well as a thinner cell wall suggesting a feedback regulation between the formation of the cuticle and the cell wall, which could be necessary to equilibrate the cuticle-cell wall continuum (Mazurek et al., 2017).

More recently, the first details of the physical relationship between cutin deposition and associated polysaccharides has been published. They revealed that cellulose, pectin and hemicellulose are present in cutin embedded polysaccharides and strongly suggest that pectins play an important role in the cutin and polysaccharide continuum, at least in tomato fruit. Moreover, CUS1 function in the polymerisation of cutin monomers appears to be correlated with the deposition of methyl-esters within pectin (Philippe et al., 2020). This is coherent with other published data such as the observed role of the transcription factor SHINE (SHN) in the regulation of cutin synthesis but also in the regulation of cell wall polysaccharides through enzymes involved in pectin degradation and modifications (Shi et al., 2011).

From the point of view of plant growth, since both cutin and the underlying cell wall have to extend in a coordinated fashion, some level of cross talk between them seems indispensable.

WAX DEPOSITION.

Some studies suggested that cutin is likely to be the first component deposited into the cuticle whereas the wax deposition occurred later (Kannangara et al., 2007). However, to date the comprehension of wax deposition remains unclear.

In order to reach the cuticle, wax monomers have to cross the hydrophilic cell wall. Lipid Transfer Proteins were initially defined by their capacity to transfer phospholipids between membranes (Kader, 1996). They are extracellular proteins with a hydrophobic cavity, able to bind fatty acids and small enough to cross the cell wall pores (Beisson et al., 2003; DeBono et al., 2009; Kader, 1996; Kunst and Samuels, 2009; Zachowski et al., 1998). In *A. thaliana*, the glycosylphosphatidylinositol-anchored LTP (LTPG1) is involved in cuticular lipid composition. The loss-of-function mutant, *ltpg1*, showed defect in cuticular wax composition with a decrease of C29 alkanes but no changes on total wax and total cutin monomers. The authors suggested that the decrease in C29 alkanes is counterbalanced by an increase in other C29 waxes (secondary alcohols and ketones precisely) (Lee et al., 2009).

2.3.3 How is the cuticle production controlled post germination?

The cuticle is deposited and directly embedded in the cell wall of all aerial epidermis cells, suggesting that epidermal cell fate and cuticle deposition may share common regulatory pathways. The leaf surface is covered by different epidermal cell types. In many species, the pavement cells cover the majority of the leaf surface whereas some epidermal cells undergo specific differentiation processes which lead, for example, to the formation of stomata or trichomes. Interesting the distribution and development of these cells can also be influenced by cuticular properties. For example, *cer1*, *cer6* or even *wax2* which are all cuticle defective mutants involved in wax production, showed abnormal stomatal indices (Chen et al., 2003; Gray et al., 2000). However, it remains unclear how these factors are correlated. One possibility is that a defective cuticle could lead to changes in environmental perception by the epidermal cells and thus deregulate the stomatal density. Alternatively, the apoplastic signalling between cells involved in stomata patterning may be disturbed in cuticle-defective mutants, possibly due to changes in cell wall composition or structure as discussed above (Javelle et al., 2011).

Within the context of the regulation of cuticle formation, two major families of transcription factors need to be mentioned. The first one is the homeodomain-leucine zipper IV (HD-ZIP IV) transcription factor family comprising 16 members in *A. thaliana,* of which several have been shown to be involved in both differentiation and maintenance of epidermal cell fate and cuticle biogenesis (Abe et al., 2003; Ariel et al., 2007; Depège-Fargeix et al., 2011; Javelle et al., 2010; Peterson et al., 2013; San-Bento et al., 2014a; Takada et al., 2013; Vernoud et al., 2009). An overexpression of the HD-ZIP IV protein OUTER CELL LAYER11 in *Zea mays* (ZmOCL11*)* gave plants with quantitative and qualitative changes in cuticular wax compounds (Javelle et al., 2010) and showed that ZmOCL11 direct and indirect target genes are involved in cuticle formation including genes encoding ABCG transporters. The cognate binding site of HD-ZIP IV proteins is called the L1 box (Abe et al., 2001), and these sequences were found to be enriched in the promoters of ZmOCL11 targets. Similarly, the *BODYGUARD (BDG)* and *FIDDLEHEAD(FDH)* genes, both of which are required for normal cuticle formation in *A. thaliana*, contain L1 boxes upstream of their transcription start sites, which are bound by the HD-ZIP IV protein HDG1, suggesting a potential regulation by HD-ZIP IV proteins (Abe et al., 2001, 2003; Nakamura et al., 2006; Wu et al., 2011).

The second family of proteins is the SHINE transcription factor family in *A. thaliana*, which contains proteins from the APETALA2 (AP2/EREBP) clade, and includes SHINE1/WIN1, SHINE2 and SHINE3 (Aharoni et al., 2004; Broun et al., 2004). Silencing of the three SHN genes leads to organ fusions and defects in the expression of cuticle

biosynthesis genes but also of genes involved in pectin production and cell elongation, suggesting that these proteins, like some members of the HD-ZIP IV protein family, could have effects on epidermal cell differentiation (Shi et al., 2011). Alternatively, they could act as hubs mediating the crosstalk between cuticle deposition and cell wall composition evoked previously. In support of the first hypothesis, a positive regulator of genes encoding SHN1 transcription factors, the MIXTA-like MYB transcription factor MYB106, regulates the formation of trichomes (Oshima and Mitsuda, 2013). However, trichome formation also involves rapid cell expansion and cell wall modifications, meaning that the second hypothesis cannot be excluded.

In summary, the formation of a functional cuticle appears to be tightly linked to the acquisition and maintenance of epidermal identity and morphology (Delude et al., 2016; Javelle et al., 2011). This fact can render the targeted analysis of either process very complex.

Although cuticle production is almost always correlated with epidermal cell identity, a few exceptions exist. The first one is the cuticle covering the embryonic root cap and the emerging lateral root. The root cap is formed at the tip of the root in order among other things to protect the root apical meristem (Barlow, 2002). The embryonic root cap cuticle is composed of an TEM electron-opaque layer surrounded the root cap tip resembling the ultrastructure of aerial cuticle although its composition seems to slightly differ, possibly accounting for its relatively high permeability. Interestingly, this structure was not detected in the mutants of cutin biosynthesis genes such as *gpat4*, *lcr* or *bdg* (Berhin et al., 2019). Although the presence of a root cap cuticle was initially considered surprising, consistent with the expression of genes such as *BDG,* both lateral roots and the embryonic root pole appear to have epidermal identity similar to the aerial organs developing cuticle, at least based on the expression of HD-ZIP IV protein-encoding genes (Nakamura et al., 2006).

2.3.4 The functions of the cuticle post germination

The cuticle was a major innovation allowing the colonization of land by plants. It appears logical that, as hinted at above, the cuticle has a high diversity of functions within land plants.

2.3.4.1 Limiting water loss

One of the primary roles attributed to the cuticle is in limiting water loss. The chemical properties of the compounds of which cuticles are composed (notably hydrophobicity), are associated with the water barrier effect of the cuticle. The compounds that mediate this affect seems to be predominantly the cuticular waxes based on correlative studies (Bourgault et al., 2020). A positive correlation between an increase in wax amount and tolerance to drought stress has been reported in *A. thaliana* (Aharoni et al., 2004; Castorina et al., 2020; Cui et al., 2016; Kosma et al., 2009). In contrast, cutin seems to create a more selectively permeable barrier than wax. In general, permeability increased by two to four orders of magnitude when the waxes were removed by organic solvents (Schmidt and Schönherr, 1982). Alkanes are particularly non polar wax components and tend to be associated with decrease of water permeability of the cuticle. In contrast, triterpenoids which are nonaliphatic wax components are a less effective water permeability barrier (Leide et al., 2007; Buschhaus and Jetter, 2012). Thus the proportion of alkanes within the cuticle and not the total amount of waxes may have the most significant effect on the water permeability of the cuticle. This has been clearly illustrated with two pepper species with contrasting water loss rates (Parsons et al., 2012) and in *Prunus laurocerasus* leaves and *Pyrus communis* leaves in which cuticular waxes are responsible for respectively 96% and 99,5% of the total resistance of water diffusion (Burghardt and Riederer, 2006). A correlation is likely to exist between the chain length of cuticular waxes and the water permeability since the cuticle of plants in arid regions tend to have a longer chain length than the ones from plants in temperate regions (Bush and McInerney, 2015).

An interesting point linked to the cuticle permeability is the so called “lotus effect” which is the ability of some plants to form a water bead on the surface of the leaf. This water “repellent” effect has been clearly linked to the presence of epicuticular wax crystals which allow the formation of a pocket of air under the water droplets (Barthlott and Neinhuis, 1997). It seems that this mechanism allows the cleaning of the surface to prevent dust from filtering sunlight and thus preventing photosynthesis. It could also play an important role in washing away pathogen spores before they germinate.

Finally, triterpenoids found in waxes, particularly oleananes, lupines and ursanes are also thought to impact the permeability of cuticles to water vapour (Jetter et al., 2006; Schuster et al., 2017).

2.3.4.2 Protection against pathogens

Several studies have shown that the cuticle is an important element in providing protection against pathogen invasion. In contrast with the critical role of waxes in creating an efficient water barrier, it appears that the cutin polymer is likely more important in providing protection against pathogens. Highly counterintuitively, several mutants showed an increase in both leaf surface permeability and resistance to fungal pathogens, including mutants lacking the function of LCS2 (Bessire et al., 2007), BDG (Chassot et al., 2007) or DEWAX (Ju et al., 2017). Several potential mechanisms may explain why plant cuticle permeability is associated with increased resistance to fungal pathogens such as *Botrytis* (Ziv et al., 2018). Firstly, there is relatively little evidence that cutin acts as a physical barrier against pathogens. Instead it appears to be a source of signals that warn the plant of pathogen attack. Fungal pathogen ingress often involves cell wall digestion that can release cutin monomers and cell wall oligosaccharides (Aragón et al., 2017). These are perceived by the plants as Damage Associated Molecular Patterns (DAMPS) and trigger the plant to release antifungal diffusates and Reactive Oxygen Species (ROS) which inhibit the pathogen growth and infection (L'Haridon et al., 2011; Sela et al., 2013). These elicitors also trigger basic plant defence responses and cell wall repair responses (Aragón et al., 2017; Gilbert et al., 1996). It has been proposed that mutants in cuticle production could have increased basal levels of cutin monomers, and this show increased basal disease resistance (priming). Furthermore, increased cuticle permeability would facilitate the movement of anti-fungal components across the cell wall, enhancing their effects. Finally, pathogen-derived elicitors could also diffuse more rapidly into the epidermal cells and accelerate more classical pathogen activated responses. Interestingly however, not all cuticle mutants improve plant resistance to all pathogens. Indeed susceptibility to some bacterial pathogens may be enhanced in the same mutants that show reduced fungal pathogen susceptibility as demonstrated in the *A. thaliana shine* mutant (Sela et al., 2013).

In addition to protection against pathogens, the cuticle is also likely involved in protection against insects. This is again very dependent on the insect species. As an example, reproduction and feeding of aphids on *A. thaliana* leaves does not seem to be correlated with wax load and composition but are potentially affected by the defective cutin of cer1 mutants (Eigenbrode and Jetter, 2002; Negin et al., 2021). In general, glossy phenotypes with reduced epicuticular waxes have been shown to be correlated with greater resistance to insect attack (Shepherd et al., 1999) possibly because insects find it harder to "stick" to glossy leaves. Finally, a more recent paper in *Nicotiana glauca* showed that phloem feeding insects are only affected by cutin disruption, while oviposition was affected by wax crystal structure but not its chemical composition (Negin et al., 2021).

2.3.4.3 Protection against UV radiation

Cuticles can play an important role in UV light protection. Although the protein complexes involved in photosynthesis complex are designed to deal with moderate UV irradiation in many species, they can be damaged by excessive UV light. The cuticle can provide a protective layer with dense epicuticular wax crystals which will increase the reflection of UV irradiation and thus contribute to protecting the sensitive inner tissues preventing damage both to the chloroplasts and, indeed, to nuclear DNA (Krauss et al., 1997).

Specific compounds enhance UV protection, including hydroxycinnamic acid and related phenolics. Phenolics, covalently bound to the fatty acids of cutin, are thought to be responsible for the absorption of UV-B (Baur et al., 1998; Ju and Bramlage, 1999). Moreover, experiments on apple fruits confirm the protective role of phenolics as UV-A and UV-B filters, which can trap a massive proportion of these radiations before they reach the epidermal cells. (Solovchenko and Merzlyak, 2003).

Waxes are also important in protecting against UV radiation. The reflection of UV and visible light by waxes and epicuticular wax crystals has been quite extensively studied. In some species such as *Dudleya brittonnii*, a plant living in arid condition, up to 83% of UV-B radiation is reflected by epicuticular waxes (Mulroy, 1979). The epicuticular waxes of this plant but also of other species, contains high levels of triterpenoids and alkanes (Manheim et al., 1979). Consistent with the need to reconcile ongoing photosynthesis with UV protection, waxes have been shown to be better at reflecting UV light than visible lights in some cases (Holmes and Keiller, 2002).

Other, more esoteric roles for the cuticle include roles in insect attraction through the generation of petal iridescence. This phenomenon has been described in *Hibiscus trionum* and in *Eschscholzia californica* (California poppy) where the cuticle on iridescent petals forms regular folds which diffract sunlight. This pattern is recognized by bees much faster than non-iridescent flowers (Moyroud et al., 2017; Wilts et al., 2018).

2.3.4.4 Preventing adhesion and fusion of organs

Finally the cuticle plays key roles in plant development by preventing adhesion and fusion of developing organs (Ingram and Nawrath, 2017). Besides an increase of water loss, mutants with cuticle defect show morphological abnormalities. Numerous mutants have been reported during the development of vegetative and floral organs as well as during seed development, to combine cuticle defects and organ fusion. Interestingly, the adhesion and fusion of organs are mainly seen in cutin-defective mutants rather than wax-defective mutants. Good examples are loss of function alleles of *LCR* and *BDG* in leaves, and *ABCG11* and *FDH*

in vegetative organs and inflorescences (Bird et al., 2007; Jakobson et al., 2016; Kurdyukov et al., 2006; Panikashvili et al., 2010; Wellesen et al., 2001). Consistent with these results, expression and secretion of fungal and plant cutinases in *A. thaliana* leads to organ fusion (Sieber et al., 2000; Takahashi et al., 2010).

However, it is important to keep in mind that not all cutin-defective mutants show organ fusions as it is the case in *A. thaliana* with the *gpat4gpat8* mutant, which affects enzymes involved in cutin monomer biosynthesis. This mutant only shows a reduction in growth (Li et al., 2007). Such differences may reflect different degrees of defect severity since the triple mutants combination of *gpat4gpat8* with another cutin-defective mutant, lacking the ABCG32 transporter shows organ fusion as well as strong dwarfism (Fabre et al., 2016).

2.4 Key innovations in seed plants

The seed is a structure produced by all spermatophytes (gymnosperms and angiosperms). They are vital for plant survival since they ensure that the future plant, the embryo (usually the product of sexual reproduction), is nourished, protected and successfully dispersed by the mother plant.

Spermatophytes, which are inherently sessile have, over the course of evolution, innovated multiple means of seed dispersal. These include harnessing the movement of external agents such as air (for example in dandelion, with its flying akene (Seale and Nakayama, 2020), or pine trees with their winged seeds), water (the floating coconut seed), and animals (primates (Lambert and Garber, 1998) and birds which disperse the seeds within the fleshy angiosperm fruits or the “pseudo fruits” of gymnosperms such as yew, or insects such as hornets and ants which disperse *Stemona tuberosa* (Chen et al., 2017)). Some angiosperms have even developed elegant mechanical tricks to generate their own kinetic enery and “fling” their seeds away (for example *Cardamine hirsute* with the explosive dispersal strategy of the siliques (Hofhuis et al., 2016). This dissemination is critically important for the conquest of new environments by sessile plants. However, for this dispersal to be really successful seeds also require further qualities, such as the ability to survive in a quiescent state for long periods of time. Perhaps the most impressive example of this is a 30 000 year-old silene seed found in the Siberian permafrost that germinated and gave rise to a viable plant (Yashina et al., 2012). The ability of some seeds to remain viable, sometimes in extreme environments, over long time periods, is the culmination of multiple physiological and physical innovations that vary between species. They generally include the ability to delay germination until the environment is propitious (dormancy, which is conditioned by both physiological and physical factors), as well as the ability to maintain cell viability whilst in a highly dehydrated

and biochemically inactive state. However, these factors would count for nothing without the presence of significant amounts of nutrients within most seeds, which serve to support the embryo when it does eventually make the decision to germinate, and which allow it to grow until it reaches metabolic autonomy (through photosynthesis and efficient water and mineral uptake). These energy supplies, which can be impressive (there are about 1400 kcal in a medium sized coconut), make seeds the primary source of energy for most humans and agriculturally produced animals. How did these remarkable structures evolve?

2.4.1 The seed

2.4.1.1 The transition to seeds: from the early seed-like structures to the seed

The transition to seeds is likely to have appeared in the progymnosperms, the sister group of Streptophytes, in the late Devonian (370Mya). These progymnosperms had a vegetative structure typical of seed plants combined with a mode of reproduction via spores that is more typical of Ferns. Three major steps likely led to the transition from the progymnosperms to the Streptophytes (Doyle, 2006; Linkies et al., 2010; Taylor and Taylor, 2009). The first was the evolution of heterospory which is the production of morphologically distinct products of meiosis within separate organs considered as female (producing megaspores, and subsequently female gametophytes) and male (producing microspores, and subsequently male gametophytes (pollen). Heterospory is observed in some fern species. The evolution of the integuments, specialized organs that enclose the megaspore/megagametophyte-producing tissue (the nucellus) to give compound structures called ovules, is considered to be another key innovation. Finally the evolution of specialized structures associated with the ovule, that are capable of receiving pollen is considered to be a critical third innovation. Together these innovations underly the transition to water-independent plant reproduction. The discovery of several fossils from extinct progymnosperms has led to a better understanding of this transition to seed production. Some examples are explained below.

Archaeopteris, an extinct progymnosperm, may be a good example of the first step during the transition to seeds. This extinct progymnosperm was a tree that produced structurally distinct megaspores and microspores from separate sporangia. Over time, pre-ovules and ovules appeared, as seen in *Runcaria*, the oldest pre-ovule fossil. The female gametophyte is retained in the maternal sporophytic tissue of the ovule (Gerrienne and Meyer-Berthaud, 2007; Gerrienne et al., 2004). The oldest known fossil seed-bearing plant is *Elksinia polymorpha*, a so called “seed fern” belonging to the extinct Pteridospermatophyta, from the Late Devonian (DiMichele et al., 2006; Linkies et al., 2010; Niklas, 1997). In this species the

ovule (or pre-ovule) is partially enclosed in a cup-like structure called cupule. To date, the role of these cupules remain unknown although scientists hypothesized a role in seed protection and/or seed dispersal (Soltis, 2021). The cupule was then replaced in the later medulossan seed ferns by a true testa (also called a seed coat). The testa is derived from the integuments of the ovules), is composed of three layers, and encloses the female gametophyte and, after fertilization, the embryo (Doyle, 2006; Taylor and Taylor, 2009).

To summarize during the emergence of seed plants the sporophyte generation became dominant and in parallel the gametophyte became smaller but still nourished and protected the embryo. Ultimately the female gametophyte was fully retained within sporophytic tissues, and the seed was born. Seeds contributed to the evolutionary success of Streptophytes, as illustrated by the dominance of gymnosperms for around 300My (Willis and McElwain, 2014). Much more recently further reproductive innovations, including the development of the ovary, and importantly, double fertilization with the associated development of a gametophytic derived tissue, the endosperm (described below), are thought to have contributed to the explosive radiation of the angiosperms.

2.4.1.2 What is a seed?

To summarise; two of the three compartments of the seeds are the product of fertilisation in gymnosperms and angiosperms: the embryo and the endosperm. Seed are composed of three genetically distinct tissues: 1) the sporophytic embryo nourished by 2) the female gametophyte (or, in angiosperms the female gametophyte-derived endosperm), which is surrounded by 3) a coat derived from sporophytic tissues. Seeds develop from ovules which consist of one (gymnosperms) or two (most angiosperms) integuments surrounding the nucellus (the megasporangium). From a developmental point of view, the ovule can thus be considered as an unfertilized seed, the immature seed precursor (Gasser et al., 1998) and from an evolutionary point of view, as a megasporangium surrounded by integument(s) (Linkies et al., 2010). The integument(s) ultimately give rise to the testa or seed coat, usually after pollination.

GYMNOSPERM SEEDS.

The word gymnosperm comes from the Greek words: gymnos which means naked, and sperma, the seed. Gymnosperms form a monophyletic group within the spermaphyte, and, as their name suggests, produce naked seeds. Most gymnosperm seeds are produced on reproductive structures called cones, and can be found directly on the scales

(megasporophylls) of these cones. Gymnosperm ovules contain single multicellular female gametophytes that can produce several archegonia, each of which usually contains one egg cell (for example in pine, 2-3 archegonia are formed). Although some proliferation and nutrient storage can occur within the female gametophyte prior to pollination, the majority of seed development occurs after the fertilization of the ovule by sperm cells which can be motile or non motile, and are usually delivered by pollen grains. Pollination occurs when the male gametophyte i.e. the pollen grain, is deposited on the ovule. After pollination in most gymnosperms, one or more pollen tubes grow and transport the sperm cells to fertilize the egg cells which leads to development of embryos. In contrast, Ginkgo and Cycads release multiflagellated sperm from the pollen grains, which are captured in droplets of liquid extruded from the ovule, thus allowing the sperm to swim to the egg cell (Doyle, 2006). Several embryos may initiate development, but usually one "wins" and the others degenerate. A typical gymnosperm seed is thus composed of a single embryo covered of two other tissues (**Figure 6**). The first of these is the haploid maternal megagametophyte which absorbs nutrients from surrounding maternal tissues and nourishes the embryo, which in turn grows invasively into, and consumes, the megagametophyte tissues. The second is the diploid integument tissue which develops into the testa. Interestingly, most of the nucellus is replaced by the female gametophyte which is the main storage tissue in the Gymnosperm seed (Linkies et al., 2010).

Angiosperm seeds.

Angiosperms and gymnosperms show several morphological differences both in terms of the whole plant body and the seed. However, angiosperms arose from the gymnosperm lineage, and the seeds of gymnosperms therefore also likely share characteristics with those of the angiosperm ancestor. Nonetheless angiosperms, in terms of their reproductive development, developed three major innovations not found in gymnosperms: the flower, a complex of reproductive organs promoting pollination and fertilisation ii) the pollen-receptive ovary that encloses the ovules and develops into a fruit after fertilization and iii) double fertilization, which results in the production of the endosperm.

The angiosperm flower, is a complex of reproductive organs composed of a perianth surrounding and protecting the male reproductive organs (called stamens) and the female reproductive organs (called carpels) (Bateman et al., 2006). The female reproductive organs comprise one or more ovaries (thought to derive, like the organs of the perianth, from leaf-like structures). The ovules are attached by stalk-like structures to the inner surface of the ovary, which plays roles in pollen reception, selection and transmission, the transmission of nutrients from the maternal plant to the seed, and seed protection and dispersal (through fruit formation).

Fruits come in numerous shapes and forms and can sub-classed into multiple different

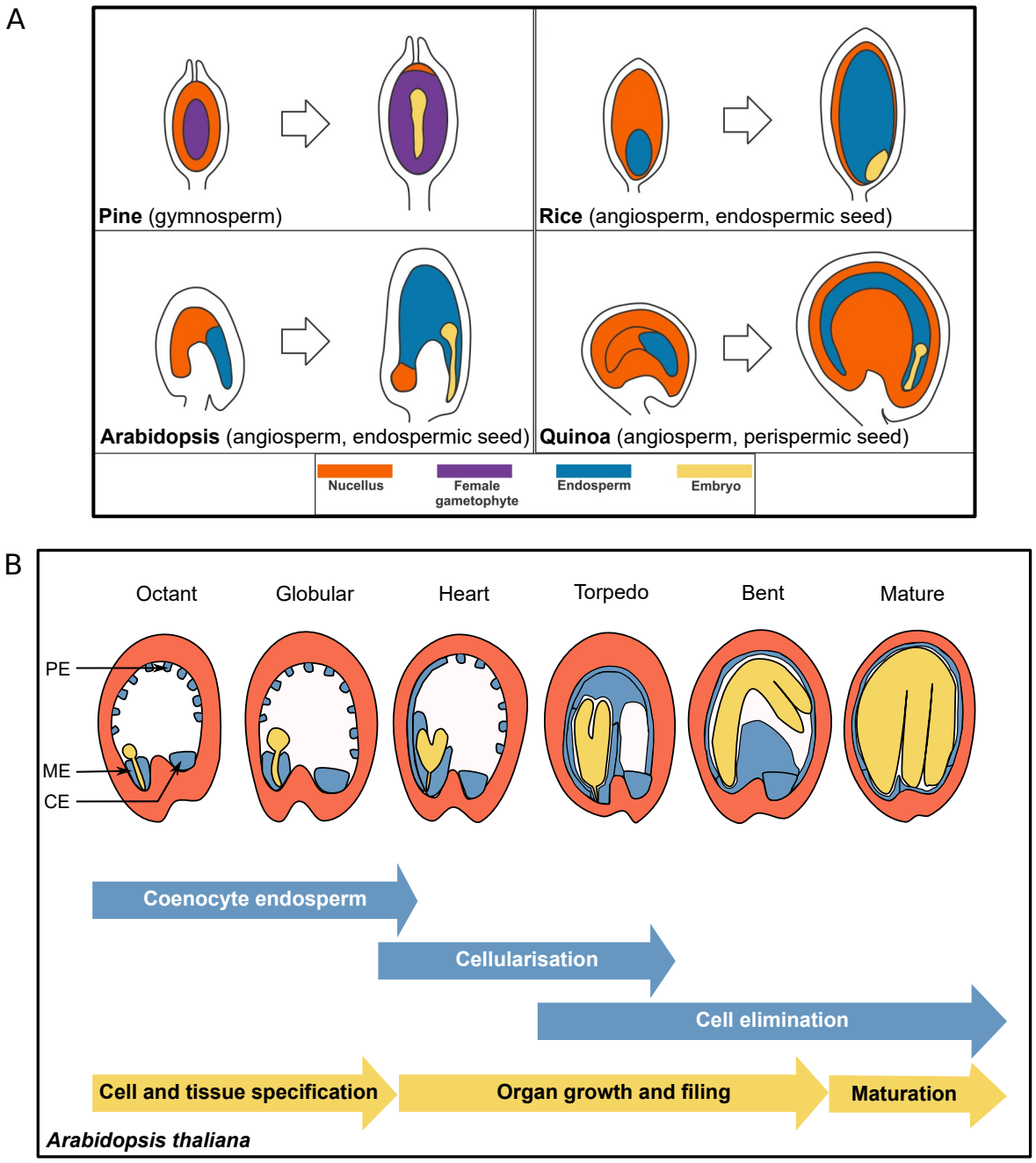

Figure 6: Seed development.
(A) Seed architecture of pine (gymnosperm, top left), rice (angiosperm endospermic seed, top right, Arabidopsis (angiosperm endospermic seed, bottom left) and quinoa (angiosperm, persipermic seed). Female gametophyte, nucellus, endosperm and embryo are represented in purple, orange, blue and yellow, respectively. Fertilization event is reprensented by the white arrow. From Lu and Magnani, 2018. (B) Schematic representation of the different stages of *A. thaliana* seed development. Maternal tissue are in red, endosperm in blue and embryo in yellow. The main phases of endosperm development (in blue) and embryo development (in yellow) are labelled. Different endosperms are represented : peripherical endosperm (PE), micropylar endosperm (ME) and the uncellularized chalazal endosperm (CE).

categories but these will not be described here (Łangowski et al., 2016). As described above, the angiosperm ovule is composed of diploid maternal tissue, in the form of the nucellus (megasporangium) surrounded by the integuments. Most angiosperms produce ovules with two integuments, the inner and the outer, which are morphologically and functionally distinct, and whose development is largely mutually independent (Endress, 2011; Gasser and Skinner, 2019).

Within the nucellus, during ovule development, a single maternal cell (MMC) is specified as the megaspore mother cell, and becomes morphologically distinct. This cell undergoes meiosis to give four daughter cells, of which one is selected to survive (and goes on to give the megaspore), whilst the other three usually degenerate. The megaspore then undergoes a series of mitotic divisions to give the female gametophyte. These steps are very similar to the situation in gymnosperm ovules. However, whilst in gymnosperms the female gametophyte can become quite large prior to fertilisation, and produce several archegonia, each containing an egg cell, in angiosperms the unfertilised female gametophyte is highly reduced. In most angiosperms only 3 rounds of mitosis occur, to give 8 nuclei, whilst in some more ancestral angiosperms, the mature female gametophyte contains only 4 nuclei (Friedman and Ryerson, 2009). The cells of the female gametophyte undergo cellularization and differentiate to give, at the distal pole (where the tips of the integuments meet to enclose the nucellus), an egg cell and 2 accessory cells called synergids, which are required for successful fertilization. More proximally a central cell is formed, which in 8 celled gametophytes is binucleate (double haploid), and in 4 celled gametophytes is mononucleate (haploid). 8 celled gametophytes also form “antipodal cells” (3) at the extreme proximal pole, adjacent to the “stalk” (funiculus) which attaches the ovule to the maternal tissues.

Understanding this organization is critical when describing the third particularity for angiosperm seeds, which is the development of the endosperm, the product of the unique, angiosperm-specific double fertilization event, which is described in more detail below, but which involves the fusion of the two genetically identical sperm cells carried to the ovule via the pollen tube with the egg cell (to give the embryo) and with the central cell, respectively (**Figure 6**). The endosperm is the result of central cell fertilization and, in 8 celled gametophyte-bearing species is triploid (the fusion of the two haploid central cell nuclei and one haploid sperm cell nucleus). In species with a 4 celled female gametophyte the resulting endosperm is thus diploid. Fertilization triggers the growth of the endosperm, and the embryo that it surrounds, a process that requires nutrients furnished by the mother plant through the nucellus and/or integuments. Endosperm characteristics and functions are described in the following section **§2.4.3.1, Introduction**. Angiosperm seeds are thus composed of three genetically distinct compartments organized like Russian dolls: i) the sporophytic embryo which gives the

new plant, surrounded by ii) the (usually triploid) endosperm, which is considered to be analogous to the nutrient storing female gametophyte tissues found in gymnosperms, and which nourishes the embryo and iii) the sporophytic maternal tissue, the seed coat which surrounds the endosperm (**Figure 6**).

Double fertilization in angiosperms has been proposed to be a major factor in their dramatic radiation. It provides a coordinated trigger for endosperm and embryo development, thus potentially minimising investment by the mother plant in unfertilized ovules. Furthermore, the role of the endosperm in absorbing maternal nutrients, combined with the genetic contribution of both parents to this tissue, also appears to have led to “parental conflicts” within the endosperm, similar to those described in the mammalian placenta. To anthropomorphise, in outcrossing species the male genome is geared to maximise maternal contributions to the development of each of his offspring, whilst the maternal genome(s) aims to minimise/equilibrate nutrient distribution to give the maximum number of viable seeds per plant. Since this conflict is played out at the developmental/physiological level within the endosperm, changes in genome dosage in the endosperm (for example if a tetraploid mother encounters pollen from a diploid father) can lead to severe defects in endosperm function and lethality, providing an instantaneous block to successful reproduction (reproductive isolation) between the two plants; the basis of speciation. Since plants can double their genomes rather easily, this mechanism has been evoked as a potential driver of the rapid angiosperm radiation (De Jong et al., 2005; Haig and Westoby, 1989; Lafon-Placette, 2019; Lafon-Placette and Köhler, 2016).

2.4.2 Seed development in Angiosperms requires double fertilization.

2.4.2.1 Generalities in seed development

As described above the development of the embryo and the endosperm is initiated by double fertilization which takes place in the ovule. The ovules develop within the ovaries which are located below pollen receiving and transmitting tissues called style and the stigma. The whole structure is called the carpel. As already mentioned, within each ovule the female gametophyte forms within the nucellus (which plays a role in nutrient provision) and the nucellus is enclose within the integuments. The female gametophyte is generally composed of 4 cell types derived from mitotic divisions: the egg cell, the synergids, the central cell and the antipodal cells (Dresselhaus et al., 2016).

The male gametophyte, in the form of the pollen grain, is produced within a separate floral organ, the stamen, which is composed of the anthers (where the pollen grains develop),

and the filament which raises the anther out of the flower. Pollen grains are again formed from the products of meiosis (microspores). Microspores undergo one round of mitosis to form a vegetative cell and a generative cell. The later then undergoes a second mitotic division to producing the two haploid sperm cells (gametes). The male gametophyte is thus even more highly reduced than the female gametophyte. Mature pollen is released from the anther and once it lands on a receptive stigma, it germinates to produce a pollen tube which grows towards the ovules guided by molecular and physical cues within in the tissues of the stigma, style and ovaries. Ultimately pollen attractants emitted by the ovules themselves guide the pollen tubes towards the distal opening (the micropyle) of the ovule (Mizuta and Higashiyama, 2018; Zhang et al., 2018).

Once within the ovule the pollen tube bursts within one of the two synergids cells flanking the egg cell, releasing the two sperm cells, one of which fuses with the egg cell, generating the zygote, while the other fuses with the central cell, generating the endosperm (Baroux et al., 2002; Berger, 2008). As noted above, since the sperm cells are generated by post meiotic mitoses, they are genetically identical as it is the case for the cells of the embryo sac. Thus the endosperm and the embryo usually carry the same genetic information, although they have a distinct fates (Dresselhaus et al., 2016).

Fertilization of the endosperm and embryo trigger their development, apparently largely independently. However endosperm fertilization has also been shown to be necessary to non cell-autonomously trigger the differentiation and expansion of the seed coat, probably via the production of auxin within the endosperm, and its transport to the seed coat tissues (Figueiredo and Köhler, 2018).

2.4.2.2 Seed Development in *Arabidopsis thaliana*

Much of the information provided above, although important for providing context, is rather general and can be applied to many species. However, to introduce the seed development work specifically carried out in my thesis, I will now concentrate on providing a more detailed overview of this process in the eudicotyledon angiosperm, *A. thaliana.*

THE EMBRYO.

The embryo develops through successive mitoses of the unicellular zygote during embryogenesis. This process can be divided into three parts : cell and tissue specification, organ growth and filling and dehydration (Dumas and Rogowsky, 2008). Embryogenesis starts directly after double fertilization. The zygote has an inherent basal (distal) apical (proximal)

polarity, that it inherits from the polarity of the egg cell, and elongates along the apical/basal axis in the first few hours after fertilization. The first cytokinesis is asymmetric and gives a large basal and a small apical cell (Bayer et al., 2017; ten Hove et al., 2015). The basal cell subsequently undergoes several divisions to become the suspensor. The suspensor is a largely transient structure which is involved in both taking up nutrients and hormones from the endosperm, and the integuments, during early embryo development and in anchoring the embryo within the seed (Kawashima and Goldberg, 2010). Although most of the suspensor undergoes programmed cell death relatively early during seed development, the upper cell of the suspensor contributes to the root apical meristem (RAM) of the embryo proper.

The apical cell of *A. thaliana* zygote divides with a rather stereotypical pattern to give the embryo proper. During this process, cells progressively acquire specific fates. One of the first to be acquired is protodermal fate, which is acquired by cells at the surface of the embryo, which will later give rise to the embryonic epidermis. Vasculature and ground tissue specificity is specified later as inner cells are produced through divisions. The upper tier of the ground tissue gives rise to the shoot apical meristem (SAM). During the early stages of embryogenesis, the embryo proper is more or less spherical (globular) (**Figure 6**). However, an important shape change transition occurs with the growth of the two nascent cotyledon primordia, which emerge on the flanks of the SAM to give a triangular and then a heart shaped embryo. (ten Hove et al., 2015). Subsequently the basal pole of the embryo differentiates into the root primordium. A massive amount is known about the early patterning of the embryo, which is regulated by cascades of transcription factors, signalling molecules, and, importantly, dynamic and complex auxin fluxes. This process has been very extensively reviewed (Bayer et al., 2017; Dumas and Rogowsky, 2008; ten Hove et al., 2015; Kawashima and Goldberg, 2010), and will not be discussed in detail here. The first stage of embryogenesis ends at around the heart stage, at which point all the main tissues and cell types that are found in the mature embryo have been specified and can be easily distinguished (ten Hove et al., 2015).

The second phase of embryogenesis involves embryo growth and the initiation of nutrient uptake and storage from the endosperm. The embryo grows through cell division and expansion, which force it to invade the endosperm tissues that surround it (see below). As the embryo grows its shape continues to change, and the progression through the torpedo, walking stick and bend cotyledon phases is used as a measure of the progression of seed development (**Figure 6**). The torpedo stage; occurs approximately 7-8 days after pollination (depending strongly on growth conditions). During this phase the embryo elongates from the base to the "tip" of the seed. However, once the cotyledons reach the tip of the seed, they are forced to bend over, effectively folding the embryo in two (walking stick and bent cotyledon stages). Ultimately, continued embryo expansion and elongation forces the tips of the cotyledons down

the proximal domain of the seed (next to the seed stalk/funiculus) (**Figure 6**). At this stage (mature green (approximately 13 days after pollination)) the embryo fills the entire seed, replacing most of the endosperm and is thus the biggest compartment within the seed. The mature embryo is composed of the two cotyledons (enclosing the SAM) and the hypocotyl (tipped by the nascent root meristem) (Le et al., 2010).

THE ENDOSPERM.

A. thaliana endosperm development can be divided into three temporally overlapping phases: coenocytic endosperm development (expansion), cellularization of the endosperm and elimination (**Figure 6**). Once the second sperm cell has fertilized the central cell, the endosperm rapidly develops into a multinucleate coenocyte through nuclear division in the absence of cytokinesis. This is accompanied by very rapid expansion of the endosperm and surrounding maternal tissues, which determines the final size of the seed. At the end of this phase, corresponding to the late globular-early heart stage of embryogenesis, a large vacuole occupies the centre of the endosperm cavity, with the endosperm cytoplasm and nuclei distributed over the endosperm periphery (Berger, 2003; Olsen, 2001).

Cellularization is initiated at the micropylar pole, around the embryo at the late globular stage-early heart stage and progresses until the late torpedo/walkingstick stage. The endosperm region near the chalazal (proximal) endosperm (CE) never cellularizes (Brown et al., 1999). The process of cellularization is rather mysterious and appears to be linked, to some extent, to ongoing nuclear proliferation (Sørensen et al., 2002). It presumably involves fragmentation of the central vacuole, although how this is achieved mechanistically remains unclear. After cellularisation three populations of endosperm cells exist 1) a peripheral cell layer, 2) internal cells (the central endosperm) and 3) the uncellularized chalazal endosperm (**Figure 6**).

The third stage of endosperm development initiates at around the heart stage around the embryo and progresses in a wave, closely following the wave of endosperm cellularization. During this phase, the central endosperm is rapidly eliminated make space for the growing embryo. This step involves the death of the endosperm, but also its physical separation from the embryo (see below). Unlike the central endosperm, the outer endosperm layer (the peripheral endosperm, PE) is persistent at maturity in *A. thaliana*. It develops as morphologically distinct cuboid cells. This layer plays roles in dormancy, germination and lipid storage (Bethke et al., 2007; Bryant et al., 2016; Penfield et al., 2004).

In summary, at maturity in *A. thaliana*, only one layer of endosperm remains surrounding the surface of the embryo. However endosperm development varies dramatically across the Angiosperms (Dumas and Rogowsky, 2008).

THE MATERNAL TISSUE.

The maternal tissues of the *A. thaliana* seed are composed of the integuments and the nucellus. The two integuments enclose the nucellus and the zygotic tissues. The nucellus is a largely transient structure. Initially, during megaspore selection and early embryo sac formation, it encloses the entire embryo sac, separating it from the integuments. However, the distal nucellus is eliminated well before ovule maturity, leaving only a small population of proximal nucellus cells that separates the embryo sac from the chalazal zone of the ovule into which nutrients are unloaded from the funiculus (Ingram, 2017). Consistent with this position, the function of the nucellus in *A. thaliana* appears to be the control of the nutrient transfer from maternal tissues to the embryo sac (prior to fertilization) and to the endosperm during early seed development (Lu and Magnani, 2018; Lu et al., 2021). After fertilization the unfertilized antipodal cells of the female gametophyte (which lie adjacent to the nucellus) degenerate, and this is followed by the degeneration of the distal part of the remaining nucellus (Ingram, 2017; Maruyama et al., 2015; Xu et al., 2016).

The different fates and morphologies of the seed tissues and compartments (such as the nucellus or the endosperm) appear to be determined by their role as a storage/transport compartment for nutrients. The timing and importance of these roles in different tissues is highly species specific, although three types of seeds have been classified based of their nutrient storage compartment. In perispermic seeds, such as *Amaranthus* and quinoa, the main nutrient storage compartment is, in fact the nucellus, which forms a persistent storage tissue called the perisperm, which is mobilized at germination. In these species the endosperm is very much reduced (Burrieza et al., 2014; Lu and Magnani, 2018; Magnani, 2018). The so called “endospermic seeds” such as those of maize or other cereals, contain a largely persistent endosperm, which stores large quantities of nutrients until germination, when they are remobilized to support the development of the germinating seedling (Sreenivasulu and Wobus, 2013). By contrast, in seeds with “transient” endosperm (such as *A. thaliana* or many legumes) the endosperm is completely or almost completely consumed during seed development by the embryo which thus become the main storage compartment (Weber et al., 2005). In reality these classifications are rather artificial. For example, in many cereals the nucellus forms a very transient “perisperm-like” storage tissue prior to fertilization that is rapidly eliminated and replaced by the endosperm after fertilization. In addition, some limited

elimination does occur around the embryo in cereals such as maize, whereas some endosperm does persist in *A. thaliana* at seed maturity (Doll et al., 2020; Grimault et al., 2015). The reality therefore appears to be a continuum in which nutrients pass through/are stored in the nucellus, and/or the endosperm prior to remobilization towards the embryo at different developmental time-points in different species. Since seed storage strategies also vary across basal Angiosperm, it is difficult to establish which strategy can be considered as "ancestral" (Friedman and Bachelier, 2013).

2.4.3 Coordination and regulation of the embryo/endosperm interface

During seed development the Russian doll organization of the three main seed compartments (maternal tissues, endosperm and embryo), and the controlled transfer of nutrients between them, necessitate very tight coordination and communication to ensure a successful developmental and metabolic outcome. How is this achieved?

2.4.3.1 The endosperm plays key roles in coordinating seed development

THE EVOLUTION AND FUNCTION OF THE ENDOSPERM.

Despite the importance of the endosperm during seed development but also in human and animal nutrition (80% of maize kernel is the endosperm), the evolutionary origins of the endosperm remain unclear. To date, two hypotheses as to the evolution of the endosperm persist but neither of them has tipped the balance in its favour. The first one has been suggested in 1900 by Sargant (SARGANT, 1900). It suggests that in seed-like structures the central cell was an additional egg cell. Thus, after fertilization two embryos would have developed simultaneously, with one adopting an "altruistic" function, and nourishing the second (Friedman, 1992; SARGANT, 1900). This hypothesis was supported by the observation that two embryos are sometime found in some basal gymnosperms (Gnetales, such as *Ephedra*), as a result from a double fertilization event (Carmichael and Friedman, 1996; Friedman, 1990). However, Gnetales are now considered not to be closely related to the direct ancestors of the Angiosperms, which has led to reduced support for this first hypothesis (Berger, 2003; Pires, 2014). The second hypothesis for the origin of the endosperm suggests that the endosperm derived from gametophytic structures which later acquired fertilization competence, tethering endosperm development to that of the embryo. The first factor that supports this hypothesis is the invasive growth of the embryo into the endosperm of angiosperms which is very similar to the observed interaction between the embryo and the nutritive female gametophytic tissues of gymnosperms. As evoked above, tethering endosperm development to fertilization, and thus

embryo development could save energy by preventing the investment of maternal resources on unfertilized gametophytes. The fertilization of the central cell, implying the input of a paternal genome, has also been proposed to provide a form of hybrid vigor to this tissue (Baroux et al., 2002; Linkies et al., 2010; Pires, 2014).

Although the evolutionary origin of endosperm may remain unclear, it has both a central position and a central role in seed biology, which is often underestimated or even completely ignored. First and foremost, it serves as a nutrient source for the embryo during seed development and at germination. In most monocotyledons species, the majority of the endosperm is persistent and will only be broken down during seed germination to release the nutrients it stored during seed filling (Ingram, 2017). Studies showed that during germination, hydrolytic enzymes are secreted from the outermost layer (aleurone layer) of the cereal endosperm during seed germination, and that these diffuse into the starchy central endosperm reserves, allowing them to be catabolised and thus provide energy that can be absorbed via a specialised embryonic structure called the scutellum, thought to be analogous to a single cotyledon, to allow the germination of the embryo and seedling establishment (Yan et al., 2014). Similarly, in *A. thaliana*, the single endosperm layer that remains at seed maturity accumulates lipids that are then catabolized into sucrose during germination (Penfield et al., 2004). However, in species such as *A. thaliana*, the main compartment used to store nutrients acquired from the mother plant during seed development is the embryo (Berger, 1999).

The role of the endosperm in supplying nutrients to the embryo is not restricted to germination but is also observed during seed development. Nutrients are absorbed from the maternal tissues of the plant by the endosperm at specialized interfaces such as the chalazal endosperm in *A. thaliana* which is characterized by the presence of many organelles, and is situated close to the residual nucellus and the zone into which phloem vessels are unloaded in the chalazal seed coat. Several studies suggest that this chalazal endosperm transfers minerals but also sugars which are themselves used as chalazal endosperm regulators (Lu et al., 2021; Otegui et al., 2002). Sugars have also been shown to enter endosperm at other sites than the chalazal endosperm in some Brassica species (Morley-Smith et al., 2008). It seems likely that some sugars diffuse symplastically through the integuments to the micropyle and are then actively transported into the micropylar endosperm (ME), and from there to the embryo. This process likely involves the transporter SUCROSE TRANSPORTER5 (SUC5), which is strongly expressed in the micropylar endosperm (Baroux and Grossniklaus, 2019; Baud et al., 2005), as well as a cascade of sugar transporters from the SWEET family (Chen et al., 2015). Similar pathways appear to be taken by amino acids, which are also unloaded into the chalazal seed coat (Karmann et al., 2018). In cereals, the transport of sugars, and other nutrients into the endosperm appears to be predominantly achieved within highly

specialized transport zones, showing specific cellular modifications such as the transfer cells observed within the Basal Endosperm Transfer Layer (BETL) of maize. Again molecular players such as sweet transporters are involved (Sosso et al., 2015). Once within the endosperm the path of sugars and other nutrients to the endosperm has not been extensively studied, but both sugars and amino acids appear to be exported out of the endosperm at the interface with the embryo, and are presumably absorbed into embryonic tissues (Doll et al., 2020). Intriguingly, although it is tempting to think that because of its very close location to the embryo, the Embryo Surrounding Region (ESR) of the maize endosperm, which envelopes the very early maize embryo, like the micropylar endosperm in *A. thaliana*, might provide nutrition to the embryo, some studies suggested otherwise (Olsen, 2004; Sabelli and Larkins, 2009).

The endosperm is also very important for allowing embryo growth. In many species it is the expansion of the endosperm which drives early seed growth and creates the space into which the embryo will subsequently expand. This is the case in *A. thaliana* (Berger et al., 2006; Li and Berger, 2012), where a balance between the growth-driving expansion of the endosperm and the growth restricting properties of the seed coat appear to condition the final size of the embryo (Garcia et al., 2005). Furthermore, a recent study in Brassica has elegantly shown that physical constriction of the seed during growth, not only limits seed size, but may also set the timing for the switch to seed maturation programmes (Rolletschek et al., 2021).

Finally, in addition to its roles in embryo nutrition during germination, the endosperm plays other key role in promoting seedling establishment post germination. In *A. thaliana*, a complex cross-talk between the embryo and endosperm is involved in ensuring that the decision to germinate is made at the correct time (Lee et al., 2010). Several studies showed that endosperm softening is required for the growth of the embryonic root during germination (Dutta et al., 1997; Lee et al., 2012b; Steinbrecher and Leubner-Metzger, 2017; Zhang et al., 2014). Moreover, mutants in specific cell wall modifying enzymes showed defects during the germination process (Iglesias-Fernández et al., 2011, 2013; Sechet et al., 2016; Shigeyama et al., 2016; Yan et al., 2014). Hormones directly affect the mechanical properties of the endosperm as revealed by analysis of the control of the expression of the wall softening *EXPANSIN2 (EXP2)* gene. Embryo expansion-induced mechanical cues in the endosperm have been proposed to play a key role in in triggering Gibberellin-dependent gene expression in the endosperm triggering changes in the physical properties of this later (Sánchez-Montesino et al., 2019).

Furthermore, during developmental endosperm elimination, the endosperm surrounding the embryo releases components rich in epitopes specifically detected by anti-extensin antibodies used in the production of the sheath, an extra-cuticular layer deposited on

the outer surface of the embryo as it develops (see **section 2.4.3.2**). Recently, the embryonic sheath was shown to act as a lubricant facilitating cotyledon emergence from the seed coat during germination (Doll et al., 2020). In addition, very recent work even suggests that endosperm-derived peptides may be involved in reinforcing the embryonic cuticle itself during germination, via a pathway similar to that used in integrity monitoring during casparian strip development (discussed in more detail below) (De Giorgi et al., 2021).

IMPORTANCE OF COORDINATING ENDOSPERM DEVELOPMENT WITH EMBRYO DEVELOPMENT.

The endosperm occupies a central position in the seed. It separates the embryo from the maternal nutrient source close to the chalazal pole and from the integuments. Thus, irrespective of its persistence in the mature seed, the endosperm is likely to assume a pivotal role during seed development. Consistent with this, analysis of rice mutants with altered embryo size has shown that a number of mutations specifically affect the endosperm, highlighting the role of the endosperm in embryo development (Hong et al., 1996). Some mutants present larger embryos than normal with reduced endosperm, whereas in others an enlarged endosperm occupies the space left by an embryo of reduced size. Thus, the endosperm likely exerts both positive and negative influences on embryo development.

The coordination between embryo and endosperm development necessitates a high level of communication between compartments. Symplastic connections (plasmodesmata) between the embryo proper and endosperm appear to be lost soon after fertilization (Ingram, 2010). As a result, communication must either involve the diffusion of signals across the apoplast between the two compartments, or mechanical cues. Mutants in genes expressed specifically in one compartment give information about compartment interdependence. In *A. thaliana* an outstanding example for this interdependence is shown in mutants that have lost the function of the endosperm-specific ZHOUPI (ZOU) protein. Loss of function *zou* mutants, instead of having a largely transient endosperm, have a completely persistent endosperm, apparently due to a defect in cell wall modifications that are usually required for endosperm cell wall softening and cell separation. The embryo cannot grow through the persistent endosperm and remains small, although it seems to mature normally since it undergoes desiccation and is capable of germinating to give morphologically normal plants (Fourquin et al., 2016; Kondou et al., 2008; Yang et al., 2008). The opposite is also true, embryo defects also affect endosperm development as can be in maize and *A. thaliana* with embryo-less mutants. In these mutants, the ESR, and later the EAS (Endosperm Adjacent to the Scutellum) does not develop properly in maize whereas in *A. thaliana* when the embryo dies at early stages, endosperm elimination does not occur normally, possibly due a lack of “crushing” by

the growing embryo, or potentially due to a lack of embryonic nutrient uptake (Doll et al., 2020; Fourquin et al., 2016; Ogawa et al., 2015a; Opsahl-Ferstad et al., 1997) . These examples illustrated the interdependence between embryo and endosperm development.

In addition, to nutritional transfer (discussed above) and peptide-mediated dialogues (of which an example is discussed in **§ 2.4.3.2**), mechanical interactions between the embryo and the endosperm have been proposed to regulate not only seed germination (discussed above), but also seed development.

CELL ELIMINATION DURING ENDOSPERM DEVELOPMENT.

We have previously seen that part of the endosperm is usually eliminated during seed development. This process may be dramatic, as in *A. thaliana* or in legumes, or very modest as in maize (Ingram, 2017). During this process, the endosperm cell walls are modified and progressively eliminated allowing embryo growth, which also appears to be required for the elimination process to proceed). The bHLH transcription factor ZHOUPI (ZOU) is required for *A. thaliana* endosperm elimination (**Figure 8**). A second bHLH transcription factor, INDUCER OF CBF EXPRESSION1 (ICE1), which has shown to act in a complex with ZHOUPI (ZOU) is also critical for endosperm breakdown (Denay et al., 2014; Fourquin et al., 2016; Xing et al., 2013). Because ZOU and ICE1 form an obligate heterodimer, endosperm cell elimination is absent in *zou* and *ice1* mutants.

Interestingly, transcriptome analysis has shown that, instead of cells generally accepted to be markers of developmental cell death in *A. thaliana* (Daneva et al., 2016), the primary, and early targets (based on the strength and timing of their expression in developing seeds, and their total lack of expression in *zou* mutants) are annotated as involved in cell wall modifications, and include genes encoding proteins such as Pectin Lyases and *REVERSIBLY GLYCOSYLATED POLYPEPTIDE 3* (*RGP3*), a direct target of the ZOU/ICE complex (Denay et al., 2014; Fourquin et al., 2016; Xing et al., 2013; Yang et al., 2008). Cell death marker genes, such as the early cell death marker *PUTATIVE ASPARTATIC PROTEINASE A3 (PASPA3)* which has no known function, and the nuclease encoding *BIFUNCTIONAL NUCLEASE1 (BFN1),* which plays a role in nuclear corpse clearance in roots (Fendrych et al., 2014) have only been found to be expressed later in endosperm development, although they are also downregulated in *zou* mutants. Furthermore, although *ZOU* and ZOU targets are expressed in seeds in which embryo growth arrests early, and endosperm cell walls undergo modification in these mutants, endosperm elimination and the expression of cell death marker genes is dramatically retarded (Fourquin et al., 2016). These data strongly support that ZOU/ICE complex does not act by directly triggering endosperm cell death, but rather that it

acts to mediate cell wall modification in the endosperm in order to prepare the endosperm to be eliminated in a process that involves mechanical crushing by the invasively growing embryo. (Fourquin et al., 2016).

2.4.3.2 Embryonic surface formation necessitates cross talk between endosperm and embryo

THE EMBRYONIC CUTICLE.

In comparison with the cuticle on the surface of the aerial organs, cuticles found in the seeds are poorly understood, largely because they are very thin, and also mainly situated internally, in complex tissues, making compositional analysis very complicated. In *A. thaliana* seeds, five cuticles are present. The first cuticle is external, and associated with the outer cell layer of the seed coat. It is likely that this cuticle both prevents the fusion between seeds as they develop, and has special properties allowing efficient mucilage release and seed hydration at germination (Panikashvili et al., 2009). The second cuticle found in seed is a discontinuous cuticle visible between the inner epidermis of the outer integument and the outer epidermis of the inner integuments, at their zone of fusion. Little is known about this cuticle, although some biosynthesis genes are expressed in the integuments and cutin-like material has been identified during early seed coat development (Creff et al., 2015; Molina et al., 2006, 2008). During seed development the cell wall housing this cuticle becomes progressively suberized to impermeabilize the mature seed, and traces of the original cuticle are lost (Fedi et al., 2017). There is also an additional cuticle layer made by the nucellus (O Cohen et al., 2019). The endosperm is also surrounded by a cuticle that is maternal in origin (produced by the inner cell layer of the inner integument). This endosperm-associated cuticle is considerably thicker than most of the other cuticles in the seed (approximately 10 times ticker) and appears to be involved in the barrier regulating water and oxygen entrance in order to avoid oxidation (Coen et al., 2019; Loubéry et al., 2018). The fourth, and innermost cuticle of the seed is the embryonic cuticle, and is found at the interface between the embryo and endosperm.

In *A. thaliana*, the embryonic cuticle is specific to the embryo proper and thus is absent from the suspensor. Moreover, in contrast to the cuticle of the aerial organs which is inherited during growth, the embryonic cuticle must form *de novo* (Creff et al., 2019; Delude et al., 2016). TEM analysis shows that the embryonic cuticle is deposited as patches during the globular stage of embryo development, and seems be continuous by the late-globular -early heart stage (Creff et al., 2019). As previously mentioned (**Introduction, §2.3**), cuticle formation and epidermal cell fate are difficult to separate, since cuticle formation appears to be an inherent property of the epidermis. Few, if any example of de novo epidermal specification and thus

cuticle formation occurs during post-embryonic development (with the possible example of (Lee et al., 2018)). Genes involved in epidermal specification such as *ARABIDOPSIS THALIANA MERISTEM LAYER1 (ATML1)* are expressed in the apical cell of the two celled embryo, suggesting that epidermal identity already exist at this stage, and may be a 'ground" state within the embryo proper (Lu et al., 1996). The timing of embryonic cuticle formation, suggests that, as expected, epidermal specification precedes embryonic cuticle formation. Consistent with this genes involved in the biosynthesis of the cuticle are expressed in embryo epidermal cells from around the 16 celled (dermatogen) stage in embryo development (Creff et al., 2019). De novo epidermal fate specification, and thus production of the embryonic cuticle occurs when the embryo is surrounded by the endosperm, and to date very little is known about how this proximity affects either event (Moussu et al., 2017). The extremely protected environment of the developing embryo also opens important questions regarding how the properties, and in particular the integrity, of the cuticle can be assured prior to embryo germination, when defects in the cuticle could lead to rapid water loss and death.

In *A. thaliana*, molecular and genetic analysis have revealed a central role for the two previously described basic helix-loop-helix transcription factor (bHLH TF), ZOU and ICE1 and their (indirect) targets in the establishment of embryonic cuticle integrity (**Figure 8**) (Denay et al., 2014; Yang et al., 2008). Interestingly, and consistent with the endosperm-specific expression pattern of *ZOU,* these genes are only required for embryonic cuticle integrity during seed development but not for cuticle formation in organs formed after germination. Recent work has started to elucidate the mechanisms via which the activity of the ZOU/ICE1 complex contribute to cuticle integrity. Cuticle integrity has also been found to depend on a (likely indirect) target of the ZOU/ICE complex, the subtilisin serine protease ABNORMAL LEAF SHAPE1 (ALE1) (Tanaka et al., 2001; Yang et al., 2008), but also the two GASSHO (GSO) - family leucine Rich Repeat receptor-like kinases (GSO1/SHENGEN3 and GSO2) (**Figure 7**). Consistent with its being a ZOU target, *ALE1* expression is restricted to the developing endosperm and strongly down-regulated in *zou* mutants. However *GSO1* and *GSO2* are expressed in the embryonic epidermis (Creff et al., 2019). Genetic analysis show that these factors act together in the same pathway to regulate cuticle integrity, but not cuticle biosynthesis (Creff et al., 2019; Xing et al., 2013; Yang et al., 2008). Interestingly, GSO1 is also known to be involved in ensuring the integrity of another apoplastic barrier, the Casparian strip (Pfister et al., 2014).

A recent study (Doll et al., 2020) has revealed that a two-way molecular dialogue between the embryo and the endosperm is necessary in order to ensure embryonic cuticle integrity. The missing factor in the pathway was a peptide related to the sulphated CASPARIAN STRIP INTEGRITY FACTORs (CIFs) that had previously been shown to bind to

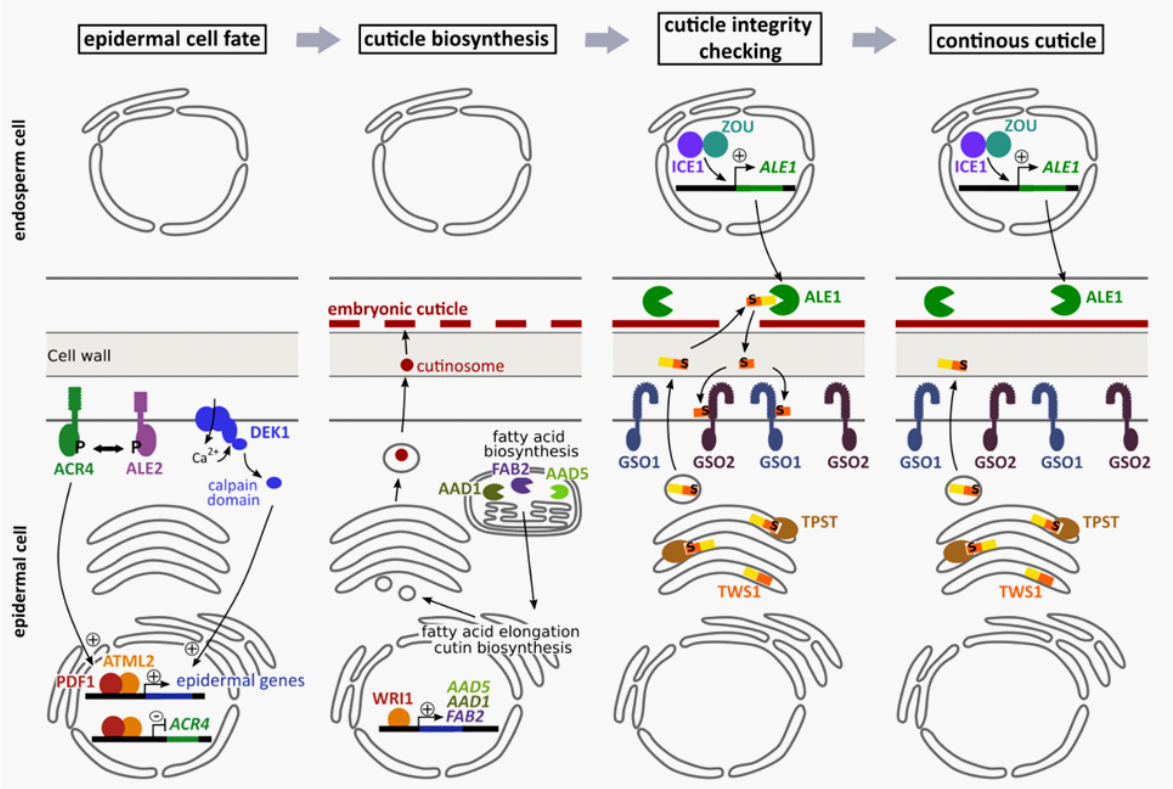

Figure 7: The different steps required for the embryonic cuticle formation in *A. thaliana*. For each step, the main molecular actors and their corresponding pathways are represented. As a first step, the most external cell layer of the embryo proper differentiates into an epidermis. Then, the epidermal cells start to produce cuticle components that are secreted into the apoplast to form a discontinuous “patchy” cuticle. A bidirectional exchange of signals between the embryo and the endosperm allows the detection of the gaps in this structure, mediates their closure, and thus ensures cuticle integrity. After the completion of cuticle gap closure, the pathway is shut down unless new gaps appear during embryo expansion. From Doll and Ingram., 2021, in press.

the GSO1 receptor during a unidirectional signalling process ensuring Casparian strip pathway integrity in the root (Doblas et al., 2017). In seeds, the CIF-related TWISTED SEED1 (TWS1) peptide is produced in an inactive form (with an inhibitory C-terminal extension that prevents receptor binding) in the embryo. To become active, the TWS1 peptide which is produced in the embryo, needs to be cleaved by ALE1, which removes the inhibitory C-terminal extension. This cleavage can only occur in the presence of gaps in the cuticle, that allow the TWS1 precursor to encounter its endosperm localized activator. Once activated, TWS1 can diffuse back across cuticular gaps and bind its receptors, GSO1 and GSO2. This triggers a poorly understood signalling event that ensures the closure of cuticle gaps. One this has been achieved, the intact cuticle separates the subtilase ALE1 from its substrate TWS1, turning off signalling (Doll et al., 2020). Interestingly, *ale1* shows a weaker cuticle phenotype than the *gso1 gso2* or *tws1* mutants, likely suggesting the presence of redundant subtilases in the endosperm (**Figure 7**).

How GSO-mediated signalling stimulated by TWS1 binding ensures cuticle gap closure remains unclear. However, in the root, CIF binding to GSO1 has been shown to generate apoplastic ROS, which are necessary for the oxidative crosslinking of Lignin monomers present around the nascent Casparian strip (Fujita et al., 2020) . It therefore seems likely that apoplastic ROS production may be a key factor acting downstream of GSO signalling in seeds. Although its composition remains unclear, staining of cotyledons with phenolic dyes (unpublished data) suggested an enrichment of the embryonic cuticle with phenolic compounds, which could be the targets of oxidative crosslinking. One potential hypothesis is that these phenolics could be crosslinked by apoplastic ROS and may act as a scaffold for the deposition of cutin and wax polymers to create an intact cuticle.

Interestingly, loss of GSO1 and GOS2 function also leads to a reduction in the phosphorylation of the MITOGEN ACTIVATED PROTEIN KINASE6 (MPK6) protein in seeds. MPK6 has also been shown to be required to be necessary for normal embryonic cuticle integrity. However how exactly MPK6 is involved in GSO signalling remains a mystery. The *mpk6* single mutants show several pleiotropic seed phenotypes which do not seem correlated. Indeed, in addition to a fragmented embryonic cuticle, *mpk6* mutants show bursting seed and abnormal seed size which are likely due to an independent role for MPK6 in the testa (Creff et al., 2019).

ROLES OF THE EMBRYONIC CUTICLE.

We have seen in the previous section that the embryo cuticle can restrict the apoplastic movement of peptides, a property that is important for ensuring its integrity. Other studies have

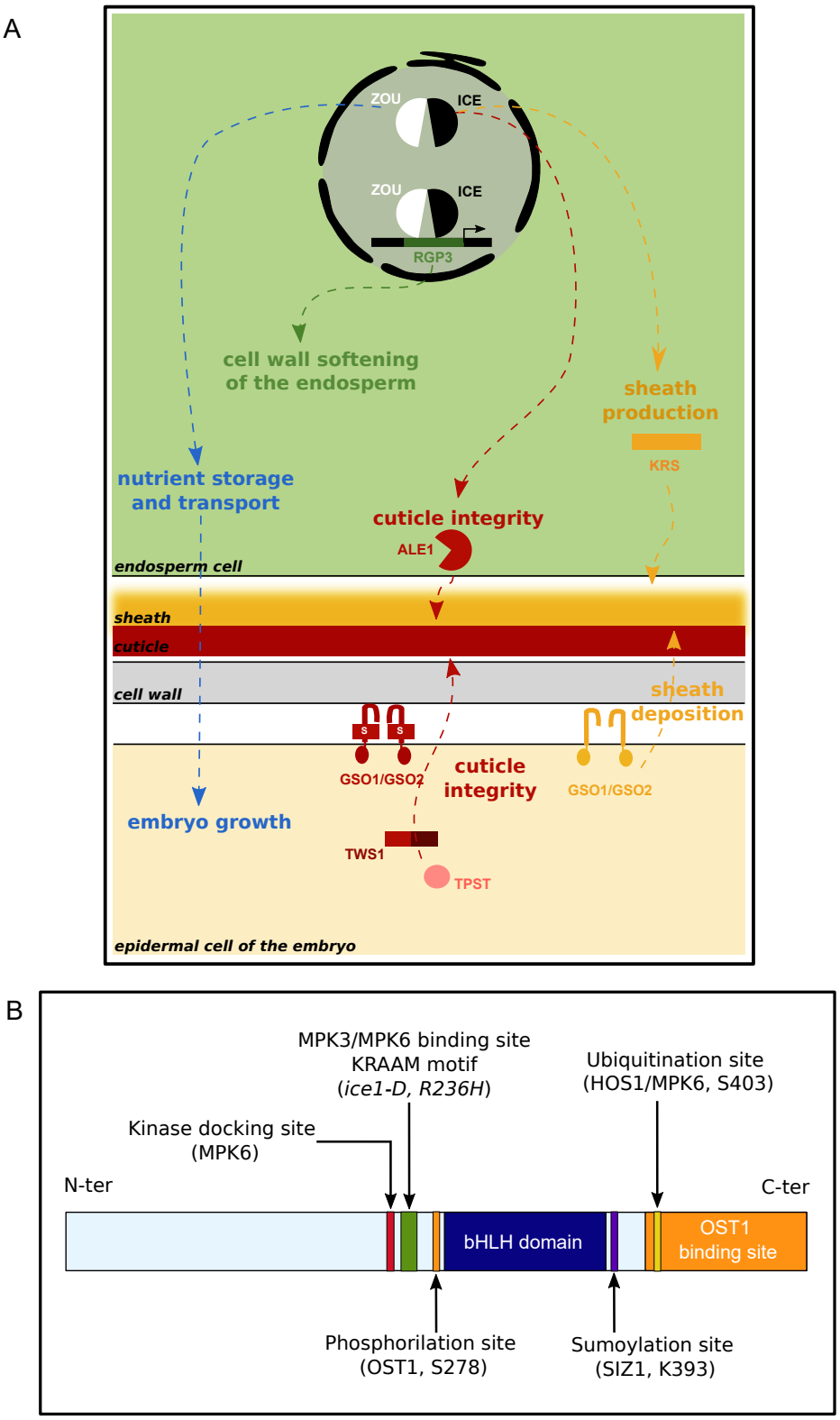

Figure 8 : ZOU/ICE-dependant signalling pathways and ICE1 post-translational regulators in other tissue.

(A) ZOU/ICE complex promote the nutrient storage and transport in the endosperm (in blue), the cell wall modifications of the endosperm (in green) whose the only direct target of ZOU/ICE complex is known, RGP3. ZOU/ICE complex also controls the formation of the embryo surface. The embryonic cuticle integrity (in red) which involves the GSO1/GSO2 receptors, the subtilisase ALE1, the peptide TWS1 and the TPST (for more informations see Figure 7 in the Introduction). The embryo sheath production and deposition (in yellow) involve the peptide KRS and GSO1/GSO2 receptors. (B) Post-translational regulators and their modification sites on ICE1. The modified amino-acid is indicated in the brakets with its corresponding regulator, except for the KRAAM motif, the binding site of MP3/MPK6, where the amino acid substitution and the name of the correpsonding gain of function mutant are mentioned in the brackets.

suggested the ability of the cuticle to prevent the leakage of developmentally important signals out of the developing embryo and into surrounding tissues could be an important factor in ensuring the stability of embryonic patterning and cell differentiation (Povilus et al., 2018; San-Bento et al., 2014). How early cuticle formation could affect other processes such as nutrient uptake from the surrounding endosperm remains unclear. However, the cuticle of the embryo remains rather permeable to small hydrophilic molecules throughout much of its development, particularly at the root pole (Berhin et al., 2019; Creff et al., 2019), presumably permitting nutrient uptake from the surrounding endosperm even after the death of the suspensor at the heart stage. Although it is tempting to suggest that nutrient uptake occurs predominantly at the embryo root pole it seems unlikely since expression of transporters in other species suggest that nutrients can transit over the entire embryo surface (Weber et al., 1997). The *A. thaliana* embryonic cuticle is thus likely to be more of a molecular filter than a hermetic barrier to nutrients (Doll and Ingram, 2021, in press).

THE SHEATH SURROUNDING THE EMBRYO.

The ZOU/ICE complex and the GSO-dependant signalling pathway are also involved in the formation of the embryo sheath. This structure is deposited on the cuticle surface, at the interface of the embryonic cuticle and the endosperm. It is thus the primary interface of the embryo with its environment. To date the exact composition of the embryo sheath remains unknown although it is enriched in components that are recognised by the anti-extensin antibody α-JIM12 (Moussu et al., 2017). Embryo sheath deposition is not affected in mutants involved in cuticle biosynthesis, and unlike the cuticle, its components are produced by the endosperm (Doll et al., 2020). During germination, Doll et al., 2020 showed that the sheath renders the embryo surface less adhesive, facilitating the escape of the cotyledons from the seed coat. This anti-adhesive property may also partially explain the role of the embryo sheath during seed development in permitting the embryo to separate from, and grow through the endosperm.

To date, little is known about the mechanisms underlying the production, deposition, and composition of the embryo sheath. ZOU activity is critical for sheath development, as is clearly visible from the complete absence of α-JIM12 immunolocalisation signal in *zou* mutant. The role of ZOU in sheath production appears to be mediated in part by a cysteine-rich peptide of STIGMA-SPECIFIC PROTEIN1 (STIG1) family, KERBEROS (KRS) (**Figure 8**). Although it belongs to the STIG1 family and thus show a cysteine-rich STIG1 domain and a signal peptide domain, the KRS peptide is distinguished from the other 5 members of this family in Arabidopsis by the presence of a non-conserved C-terminal region not found in other family members which is enriched in basic residues followed by a proline-enriched sequence (Moussu et al., 2017). Loss of KRS function also leads to a complete loss of α-JIM12

immunolocalisation signal in the developing endosperm. Like Loss of *ZOU* function, loss of KRS function also leads to a strong adhesion between the embryo and surrounding endosperm. However, unlike the situation in *zou* mutants, endosperm softening and elimination appear to occur normally in *krs* mutants. As a result, the embryos of *krs* usually expand normally, but occasionally "twist" due to adhesion between the embryo and residual endosperm (Moussu et al., 2017). Toluidine blue assay on *krs* mutant also showed a potential embryonic cuticle defect. However, how the process of cuticle deposition affects or is affected by sheath development remains unclear. Finally, timing of endosperm cell death does not seem to be affected in *krs* mutants (Moussu et al., 2017).

Interestingly, GSO1 and GSO2 -mediated signalling required for cuticle integrity, is also required for sheath formation. Unlike the situation in *zou* and *krs* mutants however, where α-JIM12 epitopes are never produced, defects in the GSO signalling pathway affect only the deposition of the sheath material on the cuticle surface, whilst the production of α-JIM12 epitopes occurs apparently normally. Like *zou* and *krs* mutants, mutants in the GSO signalling pathway show adhesion of the embryo to surrounding tissues, but this appears to be exacerbated by cuticle defects (Moussu et al., 2017). Extensins are known to be the targets of oxidative crosslinking via their tyrosine residues (Mishler-Elmore et al., 2021) and one hypothesis currently being investigated in the laboratory is that ROS produced at the embryo surface by GSO signalling could be involved in sheath deposition. It is also possible that sheath components could have a scaffolding function from the embryonic cuticle, however cuticle defects in sheath mutants (such as *krs)* are relatively weak (Moussu et al., 2017).

2.4.3.3 ZOU/ICE1 form a key hub coordinating embryo surface formation and endosperm development

WHAT DO WE KNOW ABOUT THE ZOU/ICE1 COMPLEX?

We have previously described the main functions of the ZOU/ICE complex in *A. thaliana* (**Figure 8**). However, studies suggested that ZOU is present in most other angiosperms (Catarino et al., 2016; Harris et al., 2020).

ZOU orthologues have been reported in both Monocotyledons *Zea mays* (maize) and *Orysa sativa* (rice) and in the leguminous *Glycine max* (soybean) (Dou et al., 2018; Feng et al., 2018; Grimault et al., 2015a; Zhang et al., 2017). In species with a more persistent endosperm such as *Z. mays*, the embryo invasion previously described is limited to a few cell layers surrounded the expanding embryo: the ESR and the endosperm associated with scutellum (EAS), (the endosperm surrounded the scutellum (part of the embryo)). Interestingly, the ZOU orthologue in maize, ZmZOU (also known as OPAQUE11), seems to only be involved

in ESR elimination (Feng and Song, 2018; Feng et al., 2018; Grimault et al., 2015), although detailed studies of the EAS in loss of function mutants for ZmZOU have not been carried out.

A.thaliana encodes two ICE proteins, ICE1 and ICE2. To date only loss of ICE1 function has been shown to affect seed development, although ICE2 acts redundantly with ICE1 in other tissues, an observation that I will investigate more fully in Chapter 1. Three ICE1 orthologues (a, b and c) exist in maize, two of which are expressed in seed and interact with ZmZOU in heterologous systems (unpublished data). A previous study in the laboratory showed no obvious macroscopic endosperm persistence in the Zm*icea* loss-of-function mutant. Analysis of the other Zm*ice* mutants has not been carried out so far but the absence of endosperm phenotype in Zm*icea* might be explained by redundancy between the ICE proteins (Feng et al., 2018; Grimault et al., 2015). To date no embryonic cuticle defect associated with loss of function of ZmZOU or ZmICE have been identified. In rice, where the endosperm is similar to that in maize, two ZOU orthologues have been found. However, only one shows some functional conservation regarding endosperm lysis and embryonic cuticle formation compared with *A. thaliana* ZOU (Dou et al., 2018). Interestingly, although developmentally soybean and *A. thaliana* endosperms are much more similar to each other than to Monocotyledon endosperms, only one of the *A. thaliana* ZOU orthologues in soybean partially rescues the A. thaliana zou seed phenotypes (embryonic cuticle and endosperm breakdown) (Zhang et al., 2017). To date, no studies have investigated the role of ICE orthologues during seed development in other species.

Based on the few functional studies that exist, it seems that the central role of ZOU in seed development is likely to be conserved through angiosperms. However, ZOU and ICE orthologues are also found in non-seed plants, from bryophytes to monilophytes. However, except one study which investigated the ZOU-independent role of ICE in stomatal development in *Physcomitrella patens* (Chater et al., 2016), no studies have looked at the functions of the ZOU/ICE complex in non-seed plants. Moreover, although seeds are fascinating, they can be challenging study systems and thus deciphering the role of ZOU/ICE complex in an early diverging plant might help to shed some light on basal function and regulation of the complex in plants. **This question will be addressed in Chapter 2 and Chapter 3 of this thesis using the early diverging plant model, *Marchantia polymorpha*.**

ICE1 IS POST-TRANSLATIONALLY REGULATED DURING STOMATA DEVELOPMENT AND COLD TOLERANCE.

In *A. thaliana* but also in other species, ICE1 also known as SCREAM1, has multiple functions in plants including regulation of cold tolerance and stomatal development (Chinnusamy et al., 2003; Kanaoka et al., 2008). ICE1 is involved in the production of stomatal air pores in the surfaces of aerial organs. In this pathway, it acts partially redundantly with its homologue ICE2 (SCREAM2), through interaction with the well-known class Ia bHLH transcription factors SPEECHLESS, MUTE and FAMA (Kanaoka et al., 2008; Putarjunan et al., 2019). In contrast to their strong seed phenotypes, *ice1-2* mutants show only very weak stomatal phenotypes due to redundancy with *ICE2*. The double mutant *ice1 ice2* does not produce any stomata, and is thus seedling lethal. Conversely, the dominant gain-of-function *ice1-D* mutant produces too many stomata on cotyledons and leaf surfaces, which seriously compromises plant viability (Kanaoka et al., 2008).

ICE1 was originally described for its role in cold responses, and loss of function of ICE1 leads to increased cold sensitivity and a failure to induce cold response genes. However, recently this role in cold tolerance has been questioned by Kidokoro and colleagues which showed that *CBF* genes are repressed by transgene-induced DNA methylation of ice1 (Kidokoro et al., 2020; Thomashow and Torii, 2020). Several proteins involved in post-translational regulation of ICE1 protein stability have been identified. In particular, ICE1 is post-translationally regulated during cold stress by HIGH EXPRESSION OF OSMOTICALLY RESPONSIVE GENES1 (HOS1), OPEN-STOMATA1 (OST1), SIZ1, and the MITOGEN ACTIVATED PROTEIN KINASEs, MPK3 and MPK6 (Ding et al., 2015; Dong et al., 2006; Li et al., 2017; Miura et al., 2011; Putarjunan et al., 2019; Zhao et al., 2017). HOS1 encodes a RING finger ubiquitin E3 ligase which directly interacts with AtICE1 and promotes its degradation via the 26S-proteasome. *hos1* loss-of-function mutants show increased ICE1 stability and a more sustained cold response whereas transgenic plants overexpressing *HOS1* show increased ICE1 degradation in cold and thus increased sensitivity to cold (Dong et al., 2006). In addition, a Ser-403 to alanine substitution (within the MPK6 phosphorylation site and HOS1 ubiquitination site) leads to increased ICE1 stability and improved freezing tolerance in *A. thaliana* (**Figure 8**) (Dong et al., 2006; Miura et al., 2011).

More recently, Li et al., 2017 and Zhao et al., 2017 have shown that the MKK5-MPK3/MPK6 cascade negatively regulates cold stress by leading to increased association with E3 ligases, promoting the ubiquitination of ICE1 and thus mediating its degradation via the 26S-proteasome (Li et al., 2017; Zhao et al., 2017). This MAP kinase cascade promotes the phosphorylation of ICE1 at Ser94, Thr366 and Ser403. In contrast, cold response is positively regulated by another MAP kinase cascade involving MEKK1-MKK2-MPK4, which also

suppresses the kinase activities of MPK3 and MPK6. Recently, Putarjunan et al., 2019 have deciphered the role of the KRAAM motif during stomatal development. Together with an upstream MPK docking motif, the KRAAM motif acts as a specific binding and phosphorylation site for MPK3 and MPK6. Thus, ICE1 ubiquitination via HOS1 and phosphorylation via the MKK5-MPK3/MPK6 cascade both act to decrease ICE1 protein stability post germination.

These studies of the post-translational regulation of ICE1 have been carried out on seedlings and vegetative leaves during cold stress and stomatal development. During seed development much less is known, although *ice1-D* mutants have been shown to cause precocious endosperm elimination, suggestion that KRAAM domain-mediated regulation occurs in the seed context (Denay et al., 2014), However, although public transcriptomes showed that known ICE1 regulators are expressed in seed, it remains unclear whether they play roles during endosperm development.

THE REGULATION OF THE ACTIVITY OF THE COMPLEX ZOU/ICE DURING SEED DEVELOPMENT : AN OPEN QUESTION!

The ZOU/ICE1 complex plays a central role during seed development as described above. Although our understanding of ZOU/ICE1 regulated processes is becoming clearer, the regulation of the activity of the ZOU/ICE1 complex itself remains a mystery. However, several lines of evidence converge to suggest that, although the tissue specificity of complex action is conferred by *ZOU* expression, it is the stability of the more broadly expressed ICE1 protein that acts to regulate ZOU/ICE1 complex activity in seeds. The observation that significantly altering levels of ZOU activity in seeds leads to little, if any phenotype (except when levels are very low), taken together with the observation that *ice1-D* mutants show early endosperm lysis (Denay et al., 2014; Feng et al., 2018; Grimault et al., 2015), support a hypothesis in which ICE1 levels, rather than ZOU levels are limiting for complex function in the endosperm. Unpublished confocal microscopy data on plant expressing an ICE1-D:GFP fusion under an endosperm promoter, suggest that, consistent with observations in other tissues, ICE1-D is stabilized in the developing endosperm compared to a simple ICE1:GFP fusion support this hypothesis.

Based on the results above, we hypothesize that the regulation of ICE1 stability is key in regulating ZOU/ICE1 complex activity in the endosperm. In addition, expression data and yeast two hybrid assay suggest that ZOU and ICE2 could form a heterodimer *in vivo* and that ICE2 might therefore also be involved in seed development. How ZOU/ICE1 activity is regulated in the endosperm, and the potential role of ICE2 in seeds, are **questions that will be addressed in Chapter 1 of this thesis.**

3 Aim of the thesis

The work carried out during my thesis aims to drive forward our knowledge about the functions of ZOU/ICE1 complex in seed development and more globally in land plants. To do this several subjects were addressed. In a first chapter, I will present a study aiming to elucidate the control of ZOU/ICE complex activity in *Arabidopsis thaliana* seeds. The second and a third chapters will focus on the potential ancestral functions of ZOU/ICE complex in the early emerging land plant, *Marchantia polymorpha*. In the second chapter, the characterization of *M. polymorpha* cuticle and an investigation the function of ZOU/ICE complex in cuticle development will be presented. In the third chapter I will describe the role of this complex in the formation of a novel water conducting tissue. In the third chapter, the characterization of *M. polymorpha* cuticle and an investigation the function of ZOU/ICE complex in cuticle development will be presented.

Bibliography

See general bibliography at the end of the thesis.

CHAPTER 1:

DOES DECIPHERING ZOU/ICE COMPLEX REGULATION SHED LIGHT ON ZOU/ICE FUNCTION DURING SEED DEVELOPMENT?

Preamble

As seen in the introduction, in *A. thaliana*, ICE proteins are strongly post-translationally regulated during cold tolerance and stomatal differentiation (Chinnusamy et al., 2003; Ding et al., 2015; Dong et al., 2006; Miura et al., 2007; Putarjunan et al., 2019). These regulations either stabilize or destabilize ICE proteins and are very diverse, from phosphorylation to ubiquitination or even sumoylation. However, although the function of ZOU/ICE1 complex in seeds has started to be elucidated, nothing is known about the regulation of ZOU/ICE1 complex activity in the endosperm (Creff et al., 2019a; Denay et al., 2014a; Doll et al., 2020c; Moussu et al., 2017a). Since ICE proteins are post-translationally regulated in other tissues and, in contrast to the situation for ZOU, for which changes in protein levels (with the exception of severe losses) appear not to affect function, ICE1 stabilization (gain of function) causes a precocious endosperm lysis (Denay et al., 2014a). This fact combined with the endosperm-specific expression of ZOU, has driven the hypothesis that ZOU and ICE1 affect complex activity differently. Whereas ZOU provides tissue specificity, ICE1 could be the main factor via which levels of complex activity are regulated. Based on information from other tissues, this regulation likely occurs through post-translational modifications. During my PhD I focused my attention on one of the known post-translational regulators of ICE1 the E3 ubiquitin ligase HOS1, already known to be involved in the destabilisation of the ICE proteins in other contexts (Dong et al., 2006a; Li et al., 2017). I also initiated experiments exploring the role of conserved KRAAM motif, recently discovered to be the binding site of two other negative regulators of ICE, the MAP kinases MPK3 and MPK6 (Putarjunan et al., 2019a). However, relatively few results have been obtained to date and this work will therefore not be presented in this thesis.

A second important point in this chapter was to understand why, contrary to the situation in stomatal development, *ICE1* does not appear to show significant functional redundancy with *ICE2* during seed development, despite the fact that *in silico* resources suggest that *ICE2* is co-expressed with *ICE1* in the endosperm.

Based on these questions, this chapter describes a study that uncovers the reason for the apparent lack of genetic redundancy between *ICE1* and *ICE2* during seed development.

This section is written as an article although some final validations are required before submission. We showed that, although at first sight ICE2 does not seem to play a role in seed development, ICE2 is not only co-expressed, but also interacts with ZOU. Functional redundancy has been revealed using a background lacking the E3 ubiquitin ligase HOS1, a known negative regulator of ICE activity in other tissues. Our data suggest that the E3 ubiquitin

ligase HOS1 is likely implicated in the post-translational regulation of the activity of both ZOU/ICE1 and ZOU/ICE2 complexes and that HOS1-mediated ubiquitination likely regulates the stability of both ICE proteins during seed development. Apparent lack of redundancy is caused by an apparently seed-specific phenomenon whereby ZOU/ICE1 heterodimers (and potentially ZOU/ICE2 heterodimers) are required to activate *ICE2* expression. This finding provides a cautionary example of how dangerous inferring genetic redundancy between different transcription factors based solely on genetic analysis of single and multiple mutants can be.

In a second section of this chapter, the genetic redundancy between ICE1 and ICE2 during seed development and in the other pathways is discussed in more detail as well as other putative regulators of the ZOU/ICE complex during seed development. This section describes the state of ongoing work and future directions for the project.

I) Negative regulation by HOS1 reveals cryptic genetic redundancy of ICE1 and ICE2 during seed development.

J. Loue-Manifel[1,2], A. Euzet-Rodriguez, A. Creff[1], S. Boeuf[1], E. Berenguer Peinado[1], Victor Girard, J. Goodrich[2], G. Ingram[1] and N. Dépège-Fargeix[1]

[1]Laboratoire Reproduction et Développement des Plantes, Université of Lyon, ENS de Lyon, UCB Lyon 1, CNRS, INRA, Lyon, France

[2]Institute of Molecular Plant Sciences, University of Edinburgh, Edinburgh, EH9 3BF Scotland UK

AUTHOR CONTRIBUTIONS

Jeanne Loue-Manifel carried out the genetic analysis presented in the paper and much of the phenotypic analysis. Some of the analyses of embryonic cuticle permeability and immunolocalizations were performed by Anais Euzet-Rodriguez, a master student that Jeanne Loue-Manifel supervised during the last year of her PhD. Yeast-two-hybrid experiments were carried out by Victor Girard, a master student supervised by Nathalie Dépège-Fargeix. Q-RT-PCR analysis to confirm the original observation made by Audrey Creff that *ICE2* expression is reduced in the *zou* mutant background were performed by Eduardo Berenguer Peinado. *In situ* hybridization was carried out by Sophy Boeuf. The article was written by Gwyneth Ingram with inputs from Jeanne Loue-Manifel, from Nathalie Dépège-Fargeix, and from Justin Goodrich. Jeanne Loue-Manifel prepared the figures.

ABSTRACT

The bHLH transcription factors INDUCER OF CBF EXPRESSION 1 and 2 (ICE1 and ICE2) act redundantly to regulate stomatal development and cold acclimation in *Arabidopsis thaliana*. In contrast, previous studies in seeds suggest that INDUCER OF CBF EXPRESSION 1, acting as a heterodimer with ZHOUPI (ZOU), plays an apparently non-redundant role in endosperm elimination and embryo surface formation. Here we have investigated this apparent lack of redundancy by studying the role of *ICE2* in seed development. We show that not only is this gene co-expressed with *ICE1* and *ZOU* in the endosperm, but that ICE2 can physically interact with ZOU. We demonstrate that ICE*2* expression is dependent upon ZOU activity, which masks functional redundancy between *ICE1* and *ICE2*. We show that this redundancy can nonetheless be revealed in a background lacking the ubiquitin E3 ligase HIGH EXPRESSION OF OSMOTICALLY RESPONSIVE GENES 1 (HOS1), a known negative regulator of the activity of ICE1 and ICE2 in other tissues. Our study thus demonstrates a previously undocumented role for *ICE2* in *A. thaliana* seed development and the dependency of the expression of this gene upon ZOU. In addition, we demonstrate that the E3 ubiquitin ligase HOS1 is likely implicated in the post-translational regulation of the activity of ICE1 and ICE2 in seeds.

INTRODUCTION

Genetic redundancy describes a situation where two or more genes perform the same biochemical function or can partially or fully substitute for the function of the other. In cases of full redundancy, loss-of-function of one redundant element has no apparent effect on the phenotype being monitored. An example of this phenomenon is provided by the HD-ZIP IV Transcription Factors (TFs) ARABIDOPSIS THALIANA MERISTEM LAYER 1 (ATML1) and PROTODERMAL FACTOR 2 (PDF2) which are necessary for epidermal specification during embryogenesis in *Arabidopsis thaliana*. Although loss of function of either protein does not significantly affect embryo development, loss of both proteins simultaneously leads to early embryo lethality due to severe epidermal defects (Ogawa et al., 2015b; San-Bento et al., 2014b). In backgrounds lacking ATML1, *PDF2* shows haploinsufficiency, revealing dosage dependency and highlighting the functional overlap between the two proteins (San-Bento et al., 2014b). Loss of function of ATML1 alone leads to an almost complete loss of giant cell formation in the sepal, illustrating a non-redundant role for this protein, likely linked to differences in gene expression/protein dosage between ATML1 and PDF2 in sepals (Meyer et al., 2017).

A second example of functional redundancy is provided by the GASSHO1 and 2 (GSO1 and GSO2) receptor kinases, which act fully redundantly to ensure cuticle integrity maintenance in the developing seed (Creff et al., 2019b; Doll et al., 2020d; Tsuwamoto et al., 2008). In contrast, GSO1 shows no genetic redundancy with GSO2 during integrity monitoring at a second apoplastic barrier, the Casparian strip (Pfister et al., 2014b). The lack of functional redundancy in Casparian strip integrity monitoring is due to the fact that unlike the situation in developing embryos, where GSO1 and GSO2 both bind the implicated ligand TWISTED SEED1 (TWS1) (Doll et al., 2020d), GSO2 is unable to bind the ligands implicated in Casparian strip monitoring (CIF1 and CIF2) (Okuda et al., 2020). Thus, tissue and/or process dependent changes in genetic redundancy between protein pairs can be caused by multiple factors including differences in relative gene expression between different tissues, or divergent interaction capacities with partner proteins.

Genetic redundancy is also observed between the basic helix-loop-helix (bHLH) transcription TFs SCREAM/ INDUCER OF CBF EXPRESSION 1 (ICE1) and ICE2, which act together during the development of the stomatal lineage through their hetero-dimerisation with the sequentially acting bHLH TFs SPEECHLESS (SPCH), MUTE and FAMA (Kanaoka et al., 2008b). Loss of ICE2 function does not affect stomatal development, and only very mild defects in stomatal differentiation are observed in backgrounds lacking ICE1. However, loss of function of both proteins leads to a complete lack of formation of stomata, leading to seedling lethality. In backgrounds lacking ICE1, *ICE2* shows haploinsufficiency (Kanaoka et al., 2008b). Similar redundancy has been demonstrated between ICE1 and ICE2 regarding their roles during the acquisition of freezing tolerance (Chinnusamy et al., 2003b; Kim et al., 2015b). ICE1 has more recently been shown to play a key role in regulating seed development via its interaction with the bHLH TF ZHOUPI (ZOU) (Denay et al., 2014b). This function was assumed to be non-redundant, due to the fact that loss of ICE1 function appear to phenocopy loss of ZOU function. However subtle modifications of the *zou* loss of function phenotype are difficult to quantify and, furthermore, *ice1 ice2* double mutants never produce seeds. As a result the role of ICE2, which is thought to have arisen from a duplication event within the Brassicaceae (Kurbidaeva et al., 2014), in seed development has not been studied.

The ZOU-ICE1 heterodimer plays two main roles in seeds development. The first is to regulate the elimination of the endosperm, the nutritive tissue surrounding the developing embryo in most angiosperm seeds. In *A. thaliana*, the endosperm is a transient tissue, that is progressively eliminated as the embryo grows, ultimately becoming restricted to a single and highly specialized peripheral cell layer that surrounds the embryo at seed maturity. The elimination of the so called “central” endosperm requires the activity of the ZOU-ICE1 complex, and seeds lacking either component contain a fully persistent endosperm and an embryo that

is viable, but much reduced in size (Denay et al., 2014b; Kondou et al., 2008b; Yang et al., 2008b). In parallel, the ZOU-ICE1 complex is necessary for the formation of the embryonic surface. Cuticle integrity is defective in both mutants, likely due to the fact that the expression of a key endosperm-specific component of a recently identified surface integrity-signalling pathway, ABBNORMAL LEAF-SHAPE1 (ALE1) (Creff et al., 2019b; Doll et al., 2020d; Tanaka et al., 2001b) is dependent upon the ZOU-ICE1 complex (Denay et al., 2014b; Grimault et al., 2015b; Yang et al., 2008b). Finally, ZOU function has been shown to be required for the formation of a glycoprotein-rich extra-cuticular structure, the sheath, which is necessary for embryo-endosperm separation during seed development and seedling germination (Doll et al., 2020e; Moussu et al., 2017b). The implication of ICE1 in sheath formation has not been studied to date.

Although ZOU is expressed exclusively in the endosperm, and thus likely gives spatial specificity to complex activity, previous studies in which levels of ZOU expression and/or ICE1 expression or activity have been manipulated, suggest that the level of complex activity may be regulated through modulation of ICE1 levels (Denay et al., 2014b; Grimault et al., 2015b). The activity and stability of the ICE1 protein is known to be regulated by both protein-protein interactions (Hu et al., 2013, 2019) and by a wide range of post-translational modifications such as sumoylation by the SUMO E3 Ligase SAP AND MIZ1 DOMAIN- CONTAINING LIGASE1 (SIZ1) (Miura et al., 2007b) ubiquitination by the ubiquitin E3 ligases HIGH EXPRESSION OF OSMOTICALLY RESPONSIVE GENES1 (HOS1) (Dong et al., 2006b), and CONSTITUTIVE PHOTOMORPHOGENIC 1 (COP1) (Lee et al., 2017a), phosphorylation by the SNF1-RELATED PROTEIN KINASE OPEN STOMATA 1 (OST1) and by the MITOGEN-ACTIVATED PROTEIN KINASES 3 and 6 (MPK6 and MPK3) (Ding et al., 2015b; Putarjunan et al., 2019b). Although less well studied, ICE2 is also known to be a target of HOS1 (Kim et al., 2015b), COP1 (Lee et al., 2017a) and likely of MPK3/6 (Putarjunan et al., 2019b). Ubiquitination by HOS1 destabilizes both ICE1 and ICE2 during the acquisition of cold tolerance (Dong et al., 2006b; Kim et al., 2015b).

Here we have used gene expression, protein interaction and genetic analysis of the regulation of endosperm elimination, cuticle formation and sheath formation to explore the apparent lack of functional redundancy between ICE1 and ICE2 in seed development. We reveal a cryptic genetic redundancy between ICE1 and ICE2 in the regulation of all three processes.

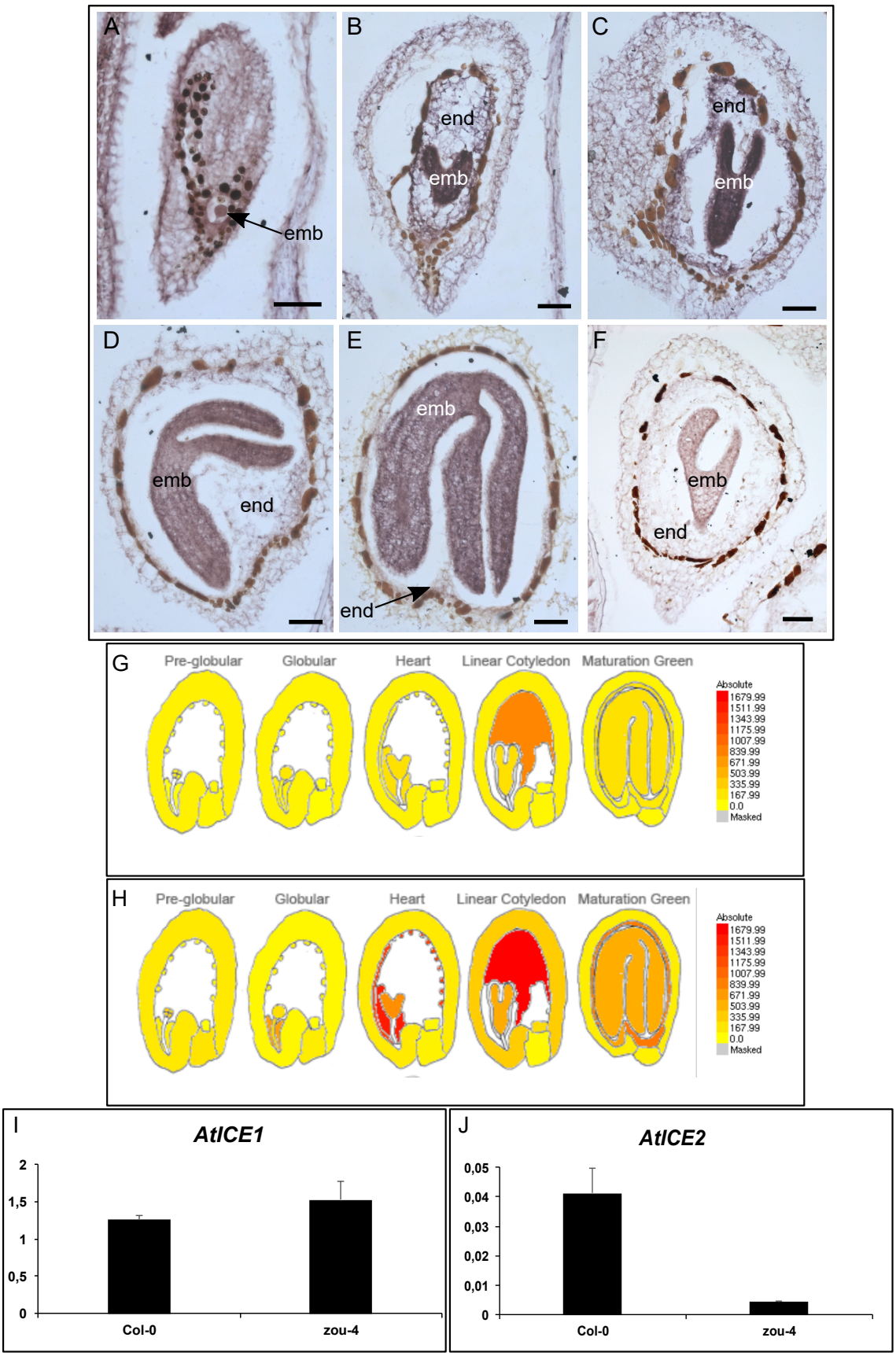

Figure 1 : Expression pattern of *ICE2* during seed development. (A-F) Images of in situ hybridizations of digoxigenin-labelled *ICE2* antisense (A-E) and sense probe (F), visualised by DIC microscopy. Four developmental stages are presented : globular stage embryo (A), old heart stage embryo (B), torpedo stage embryo (C), bent stage embryo (D) and mature stage embryo (E). Signal appears purple in the embryo, endosperm and seed coat. The endothelium stained in dark-brown is an artefact. emb is for embryo; end is for endosperm. Scale bar, 50µm. (F) *In silico* data from EFPbrowser showing the strong expression pattern of *ICE1* in the endosperm. (G) *In silico* data from EFPbrowser broadly confirms the expression pattern of *ICE2* in the endosperm. (H) Expression of *ICE1* relative to that of *EIF4* in the wild-type (Col-0) and *zou-4* siliques ; error bars reprensent standard errors. Five biological replicates were used. (I) Expression of *ICE2* relative to that of *EIF4* in the wild-type (Col-0) and *zou-4* siliques ; error bars reprensent standard errors. Five biological replicates were used.

RESULTS

APPARENT LACK OF REDUNDANCY IS NOT DUE TO A LACK OF EXPRESSION OF *ICE2* IN THE ENDOSPERM

In order to analyze potential roles played by ICE2 in the developing seed, we first asked whether ICE2 is expressed in seed tissues. Inspection of available *in silico* data revealed that like *ICE1, ICE2* is expressed in developing seed tissues, and particularly in the developing embryo and endosperm (Le et al., 2010b). Endosperm transcript levels of *ICE2* are considerably lower than those of *ICE1* at the linear cotyledon stage (244 vs 1679). *In situ* hybridization analysis was used to confirm the expression pattern of *ICE2* in developing seeds, and results broadly confirmed the pattern suggested by *in silico* data (**Figure 1**). Differences in the intensity of *in situ* hybridization signals in *A. thaliana* seed tissues compared with transcriptomic data have been previously highlighted (Francoz et al., 2016), and likely explain the apparently stronger expression in embryos in our experiments.

Mining of available transcriptomic data from whole silique samples (Xing et al., 2013b), revealed that at the linear cotyledon stage, *ICE2* expression showed a 6-fold reduction in gene expression levels in *zou* mutants compared to the situation in wild-type plants, suggesting that *ICE2* may be either a direct or indirect target of positive transcriptional regulation by the ZOU-containing TF complexes. This result was confirmed by multiple Q-PCR analyses (**Figure 1**).

APPARENT LACK OF REDUNDANCY IS NOT DUE TO AN INABILITY OF ICE2 TO INTERACT WITH ZOU

Apparent lack of functional redundancy between ICE1 and ICE2 in the endosperm could be explained by an inability of ICE2 to interact with the confirmed ICE1 binding partner ZOU. To exclude this possibility, yeast two hybrid analyses were carried out to assess the potential interaction of these two proteins "*in vitro"* (**Figure 2**). We conclude that not only are ICE2 and ZOU co-expressed in the endosperm, but that, in addition, they are capable of physically interacting.

LOSS OF *HOS1* FUNCTION LEADS TO A PARTIAL RESCUE OF THE *ICE1* LOSS OF FUNCTION PHENOTYPE

In order to assess the potential role of ICE2 in seed development the *ice2-1* loss of function mutant was obtained (Kanaoka et al., 2008b). This single mutant showed no quantifiable defects in seed development or seedling cuticle development (**Figure 3** and **Figure 4**). Analysis of the progeny of *ice1-2 ice2-1* +/- plants allowed us to confirm, as reported

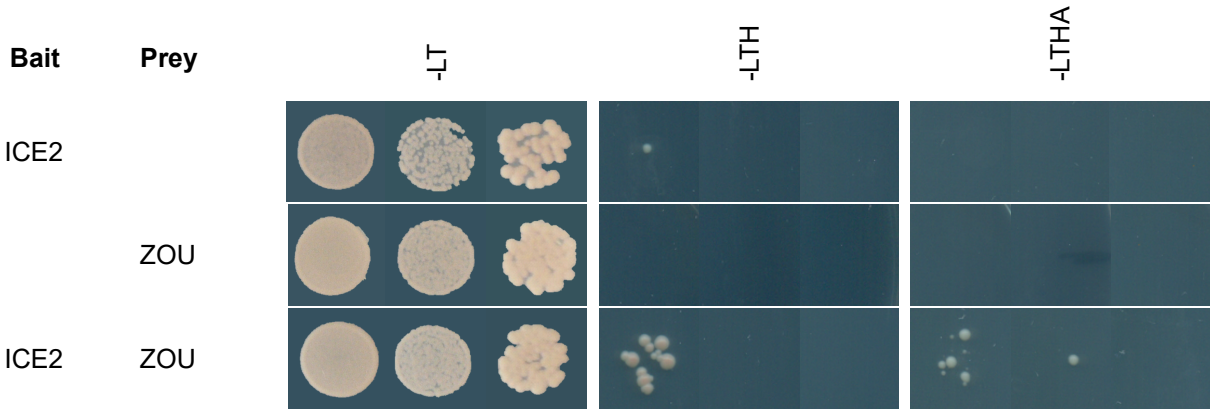

Figure 2 : ZOU and ICE2 interact in yeast.
Interactions tested in yeast. Empty boxes indicate empty vector controls. Growth on minimal non selective (-LT) and selective with low stringency (-LTH) and selective with high stringency (-LTHA) media is shown. the three dots are from the left to the right, no dilution, 1/10 dilution and 1/100 dilution.

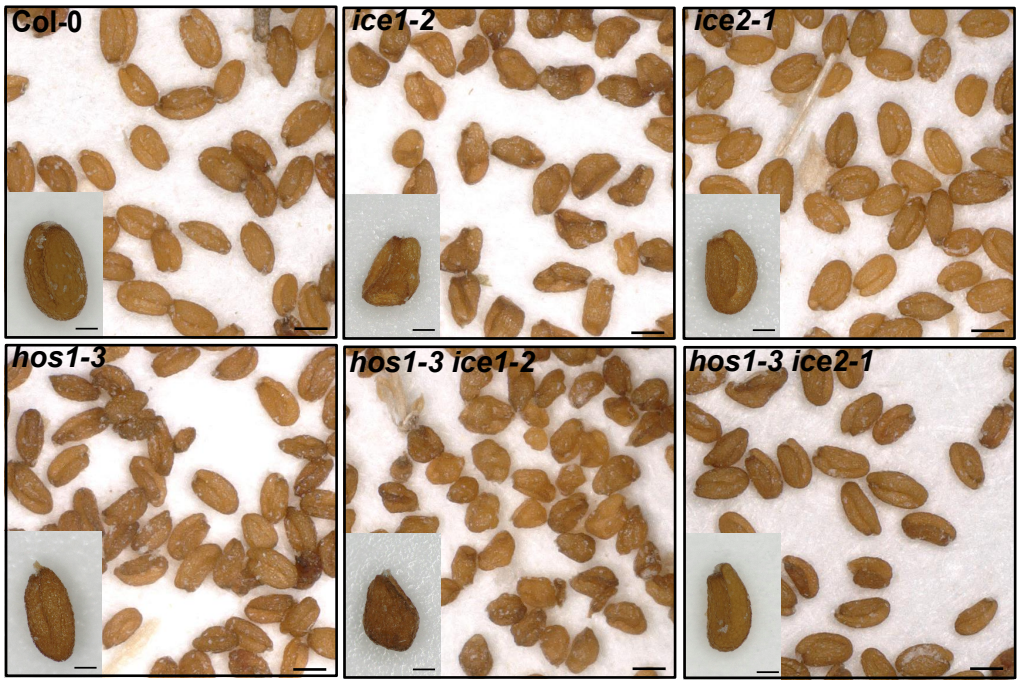

Figure 3 : Loss of function of *HOS1* and *ICE1* partially rescue the endosperm breakdown phenotype of *ice1-2* mutant. Pictures of individual and bulk of seeds showing the partial rescue by *hos1-3* of the *ice1-2* endosperm phenotype in *hos1-3 ice1-2* mutants. Scale bar, 250µm for the bulk of seeds and 100µm for individual seed.

previously (Kanaoka et al., 2008b), that *ice1-2 ice2-1* double mutants die as young seedlings due to a lack of stomatal development. However, in these segregating populations, it was not possible either to distinguish seeds containing double mutant endosperms through seed shape analysis, or double mutant seedlings, using qualitative toluidine blue staining (Creff et al., 2019b).

Our results support the idea that the apparent lack of functional redundancy between ICE1 and ICE2 as gauged by the phenotype of *ice1* mutants, is caused by the fact that that *ICE2* expression is partially ZOU, and thus ICE1 dependent. To test this hypothesis, we devised a strategy based on the idea that stabilizing the residual ICE2 protein present in an *ice1* mutant background could reveal a role for *ICE2* during seed development. Because loss of function of negative regulators such as COP1 and MPK6/MPK3 leads to strong pleiotropic defects in developing seeds and seedlings (Creff et al., 2019b; Deng et al., 1991), we focused our attention on the E3-ubiquitin ligase HOS1 which is known to destabilize both ICE1 and ICE2 in vegetative tissues. *In silico* data show that transcripts encoding HOS1 accumulate, albeit at relatively low levels, in the developing endosperm, as well as in other seed tissues. This ubiquitous expression in seeds was confirmed by *in situ* hybridization (**Figure S1**).

Single loss of function *hos1-3* mutants (MacGregor et al., 2013) and double *ice2-1 hos1-3* mutants produce seeds that are morphologically indistinguishable from those of wild-type plants, and, furthermore, show no defects in seedling cuticle permeability (**Figure 3** and **Figure 4**). Intriguingly however, double *ice1-2 hos1-3* mutants produced seeds that were visually “plumper” than those of *ice1-2* plants, and which contained larger embryos. Thus, loss of *HOS1* function appears to partially rescue the endosperm persistence phenotype of *ice1-2* single mutants. Furthermore, the seedlings of *ice1-2 hos1-3* mutants were both qualitatively, and quantifiably less permeable to toluidine blue than those of *ice1-2* single mutants (**Figure 3** and **Figure 4**).

RESCUE OF THE *ICE1* LOSS OF FUNCTION PHENOTYPE BY LOSS OF *HOS1* FUNCTION IS DEPENDENT UPON THE PRESENCE OF *ICE2*

In order to test the hypothesis that this partial rescue could be due to the stabilization of ICE2 due to loss of HOS1 activity, *ice1-2 hos1-3 ice2-1+/-* plants were generated and their progeny were analyzed. The seeds produced by these plants produced around 25% of seeds that had a very small embryo (similar to *ice1-2)* seeds, whilst the remaining seeds exhibited an *ice1-2 hos1-3* phenotype, or in some cases an intermediate phenotype. Our results support the hypothesis that the apparent rescue of the *ice1* mutant phenotype by loss of *HOS1* function

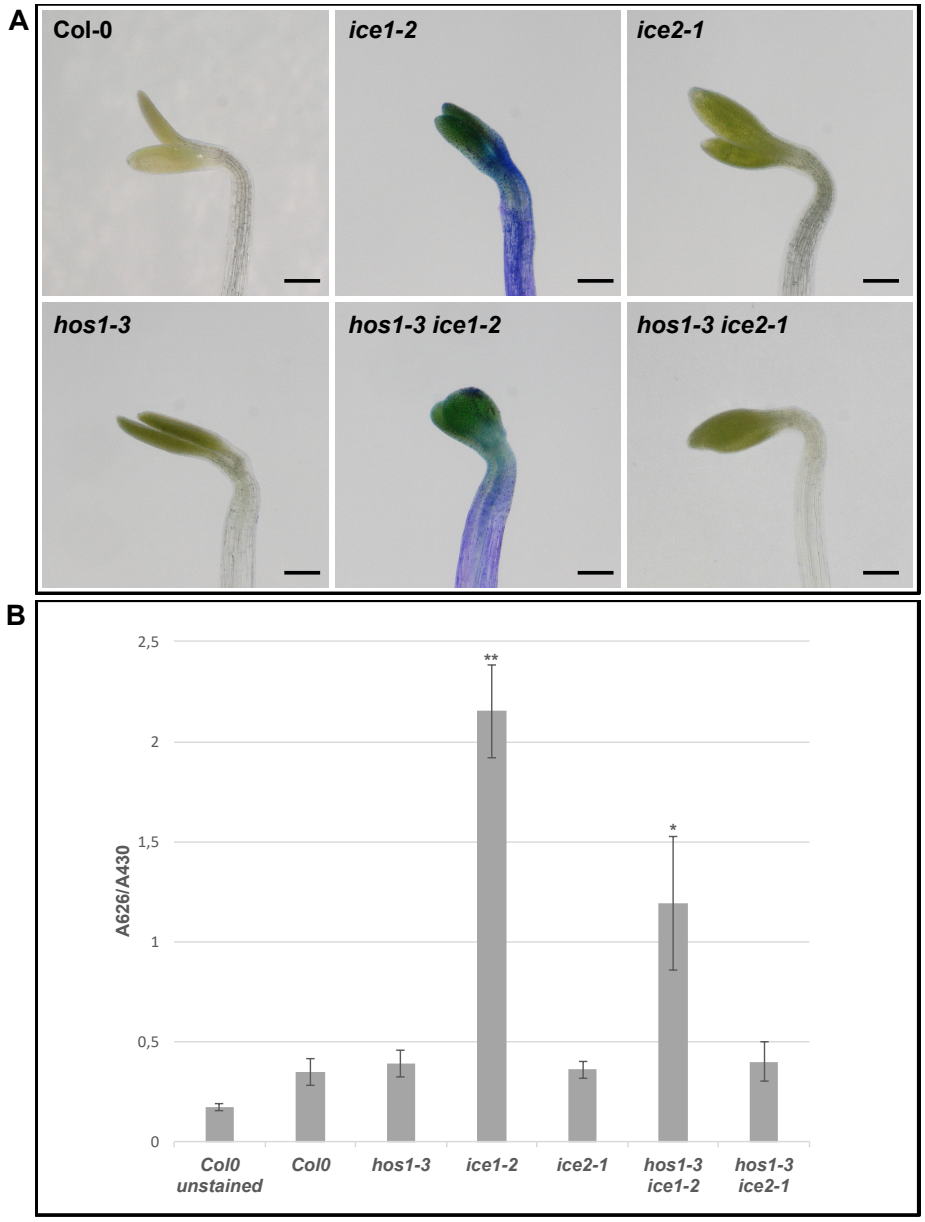

Figure 4 : Embryonic cuticle defect is partially rescued in *hos1-3 ice1-2* double mutants.
(A) Toluidine blue assays on etiolated cotyledons of wild-type (Col-0), *ice1-2* mutant, *ice2-1* mutant, *hos1-3* mutant, *hos1-3 ice1-2* mutant and *hos1-3 ice2-1* mutant. Scale bars 200µm. (B) Quantification of toluidine blue uptakes by the cotyledons of young seedlings, normalized to chlorophyll content. N= 18, 10 seedlings per repetition. * indicates statistical differences with ANOVA followed by Sheffe tests between *hos1-3 ice1-2* and the other genotypes. ** indicates statistical differences with ANOVA followed by Sheffe tests between *ice1-2* and the other genotypes. Error bars indicate standard deviations.

is due to the stabilization of ICE2 protein. When both ICE1 and ICE2 proteins are absent, phenotypes therefore revert to those of *ice1* single mutants.

ICE1 IS NECESSARY FOR SHEATH FORMATION

Our results support the fact that ZOU-ICE2 heterodimers may play a significant role in wild-type seed development, but that this role is masked by both genetic redundancies with, and transcriptional regulation by, ZOU-ICE1 heterodimers. In order to reveal the role of ICE2 in the presence of the ICE1 protein we sought to identify an ICE-dependent phenotype that might provide a more quantifiable readout than either endosperm persistence or cuticle permeability. Loss of ZOU function leads to a complete elimination of the embryo sheath, and extensive adhesion of the embryo and surrounding endosperm (Moussu et al., 2017b). We therefore investigated whether loss of ICE1 function also affects sheath formation, by carrying out immunolocalizations with the α-JIM12 antibody on imbibed seeds. As previously described (Doll et al., 2020; Lee et al., 2012), this antibody detects a continuous extra-cuticular structure on the surface of mature wild-type embryos. However, as has previously been shown for loss of ZOU function (Moussu et al., 2017), loss of ICE1 function leads to a complete elimination of JIM12 signal at the embryo surface, although signal in other tissues, such as the testa, is not affected (**Figure 5**). As for cuticle and endosperm phenotypes, a weak but distinct complementation of the sheath phenotype of the *ice1-2* mutant was observed in *ice1-2 hos1-3* mutant seeds in which patches of α-JIM12 labelling on the embryo surface, never observed in *ice1-2* single mutants, were detected.

LOSS OF *HOS1* FUNCTION LEADS TO AN APPARENT INCREASE IN SHEATH PRODUCTION WHICH IS ATTENUATED BY LOSS OF *ICE2*.

No visible difference in α-JIM12 signal intensity was observed between wild-type and *ice2-1* mutants. However, in contrast to the situation for endosperm elimination and cuticle integrity phenotypes, for which loss of HOS1 function does not generate an easily detectable "gain of ICE function" phenotype, loss of HOS1 leads to a significant increase in the intensity of sheath labelling with the α-JIM12 antibody compared to wild-type (**Figure 5**). This suggests that sheath biogenesis may provide a more quantifiable output for the ZOU/ICE1 pathway than either endosperm elimination or cuticle permeability. We therefore analyzed sheath production in *ice2-1 hos1-3* mutants, and found that loss of ICE2 function led to a reduction of the excess signal observed in *hos1-3* mutants to near wild-type levels, thus revealing the ICE2-dependency of embryo sheath formation during seed development.

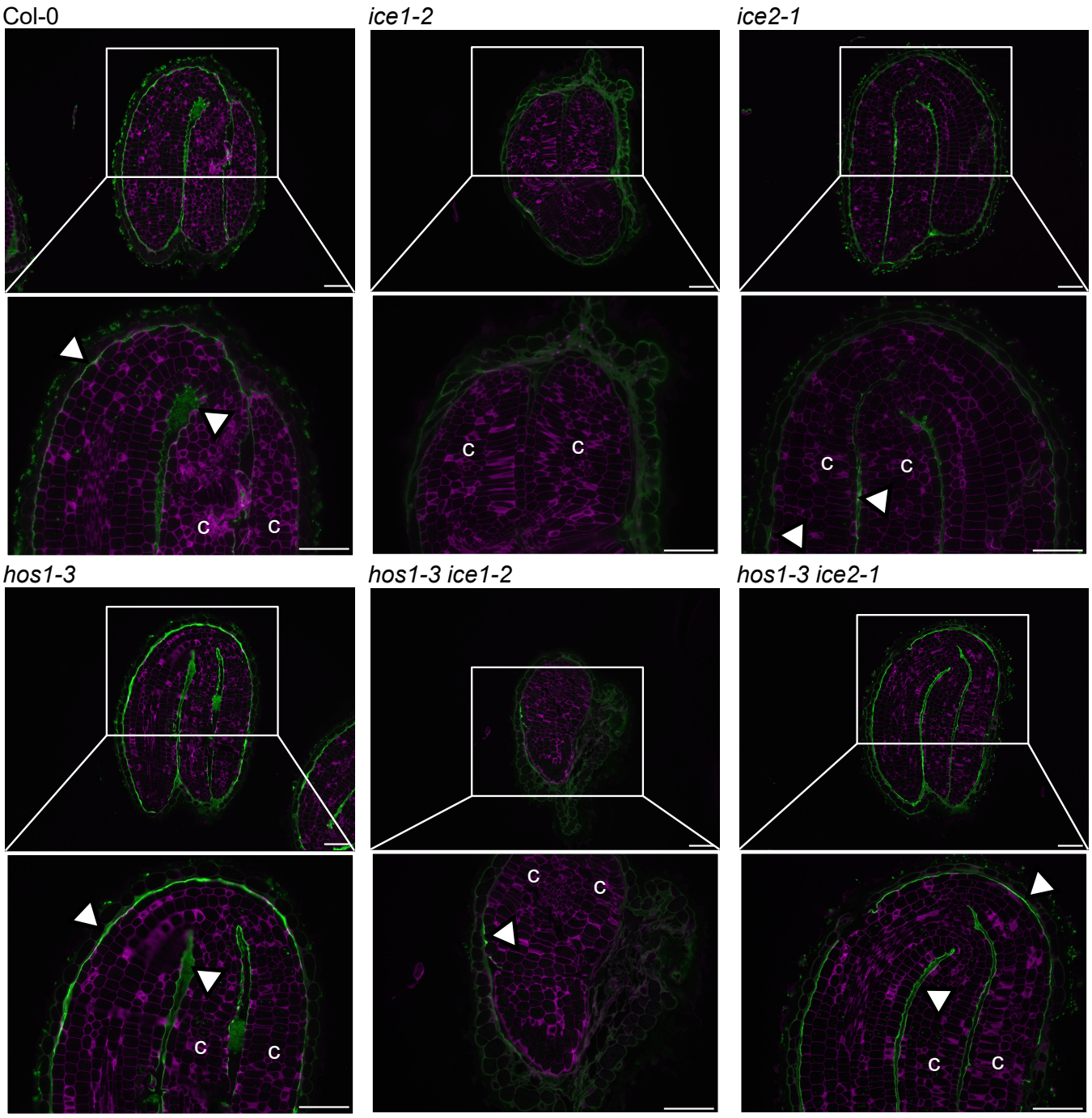

Figure 5 : Comparison of the immunohistochemical properties of the sheath in dessicated and imbibed seeds.
Seeds from Col-0, *ice1-2*, *ice2-1*, *hos1-3*, *hos1-3 ice1-2* and *hos1-3 ice2-1* subjected to immunolocalization with JIM12 rat monoclonat antibody (green) and post-stained with calcofluor white (magenta). Arrowheads indicate the sheath. c, cotyledon. Scale bars, 50µm.

MATERIALS AND METHODS

PLANT GROWTH.

Arabidopsis thaliana seeds were gas sterilized with chlorine (3mL HCl (33%) in 150mL bleach) for 2 hours and then sown on Murashige and Skoog (MS) medium with 0,5% sucrose in sterile condition, stratified for 2 days at 4°C and grown for 7 days in short-day conditions (8h light, 19°C). Seedlings were then transferred to compost (Argile 10 (favorit) and grown under short day conditions (8h light, 19°C) for two to three weeks before transferred to long day conditions (16h light, 21°C). All *A. thaliana* mutants used in this study were previously published: *zou-4* (Yang et al., 2008a), *ice1-2* (Denay et al., 2014a; Kanaoka et al., 2008a), *hos1-3* (Lazaro et al., 2012; Lee et al., 2012a), *ice2-1* (Kanaoka et al., 2008a). Both double mutants *hos1-3ice1-2* and *hos1-3ice2-1* were generated by crossing the respective single mutants. The ecotype Columbia-0 (Col-0) was used as a wild-type control. Sequence data from this article can be found in the GenBank/EMBL data libraries under the following accession numbers : *ZOU*, AT1G49770 ; *ICE1*, AT3G26744 ; *ICE2*, AT1G12860 ; *HOS1*, AT2G39810.1 .
Mutants are : *zou-4,* SALK_115353 ; *ice1-2*, SALK_003155 ; *ice2-1*, SAIL_808_Bio ; *hos1-3*, SALK_069312 .

YEAST TWO HYBRID ASSAY.

The Dual Hunter split ubiquitin-based system from Dualsystems Biotech was used to carry out yeast two-hybrid experiments (Möckli et al., 2007). Yeast protocols were performed as described by the manufacturer. Single bait and prey constructs were cloned by PCR-amplified cDNA fragments into pCR BluntII-TOPO vector (Invitrogen), and then transferred into the appropriate yeast vector.

QUALITATIVE AND QUANTITATIVE ANALYSIS OF TOLUIDINE BLUE PERMEABILITY.

To assess cuticle integrity, toluidine blue staining assays were performed (Tanaka et al., 2004). For qualitative toluidine blue staining tests, etiolated seedlings were used. Seedlings were stratified in the dark, exposed to a 6h light flash and then grown for 4 days in darkness. They were then stained for 2 min in 0.05% w/v Toluidine blue solution with 0.1% v/v Tween 20 and washed abundantly under tap water. Pictures were taken with a Keyence VHX900F digital microscope.

For quantitative toluidine blue staining test, 7-day old light-grown seedlings were stained in the same way. In order to extract toluidine blue and chlorophyll, the cotyledons of ten seedlings were collected and placed in 1mL of 80% ethanol for at least 3 hours in darkness. Toluidine blue content of the resulting solution was measured at 626nm with a spectrophotometer. This absorbance was then normalized using chlorophyll absorbance at 430nm, a wavelength not absorbed by toluidine blue. 6 repetitions were performed per condition (Xing et al., 2013a).

IN SITU HYBRIDIZATION ON SILIQUES.

In situ hybridization on siliques was performed as described in Yang et al 2008. Templates for antisense probe synthesis were PCR-amplified from pCRII vectors (ThermoFisher) containing full-length ORFs amplified from silique cDNA with primers containing 5'-extensions with T7 or SP6 RNA polymerase promoters (HOS1-HIS-F and HOS1-HIS-R for HOS1 and ICE2-geno-F and ICE2R for ICE2). Antisense RNA probes were then made using T7 or SP6 RNA polymerase as described in (Chanvivattana et al., 2004). Siliques were infiltrated with ice cold 4% paraformaldehyde (pH=7 adjusted with sulfuric acid) in PBS for three cycles of 20 minutes under vacuum. To increasing fixation efficiency, the two top corners of the siliques were cut. Siliques were dehydrated through an ethanol series, then into histoclear via an ethanol/histoclear series and finally embedded in Paraplast Plus (MC Cormick Scientific) Jackson, 1991. Sections of 6µm were cut with a HM355S microtome and stretched onto Superfrost Ultra plus™ (ThermoFisher Scientific) slides and then dewaxed and hydrated. Sections were then treated with 2x saline sodium citrate (20min) and digested with proteinase K in 50mM Tris-HCl, pH 7.5, 5mM EDTA for 15min at 37°C. Treatment for 2min with 0.2% glycine in PBS followed by a post-fixation with 4%% paraformaldehyde in PBS (10min, 4°C) were performed. Sections were then treated with 0.25% w/v acetic anhydride in 100mM triethanolamine (pH 8.0) for 10 min and finally rinsed and dehydrated through an ethanol series. An overnight hybridization was then carried out at 50°C with RNA probes (produced using DIG RNA labelling kit from Roche) diluted in DIG easy Hyb solution (Roche) following the manufacturer's instructions. Slides were washed in a solution containing 0.1% saline sodium citrate and 0.5% SDS, at 50°C, and then blocked for 1H in blocking solution (Roche) in TBS and for 30min in a BSA solution (1% BSA, 0.3% Triton-X-100, 100mM NaCl, 50mM MgCl2). Finally, 2h incubation at room temperature in a 1/3000 dilution of alkaline phosphatase-conjugated antidigoxigenin antibody (Roche) in BSA solution.

Alkaline phosphatase activity was detected in a reaction overnight in darkness in a revelation buffer (0.5 g/L of nitroblue tetrazolium (NBT) and O.2 g/L of 5-Bromo-4-chloro-3-

indolyl phosphate (BCIP). Slides were washed 4 times in water to stop the reaction and were mounted in Entellan (Sigma). Pictures were taken with Axio Imager 2 microscope (Zeiss).

IMMUNOLABELLING ON SECTIONS.

Mature and desiccated seeds were imbibed for 2-3 hours in water and punctured three times with a needle before being fixed as follow. Seeds were fixed in ice-cold PEM buffer (50mM PIPES, 5mM EGTA and 5mM MgSO4, pH6.9) containing 4% (w/v) paraformaldehyde under vacuum on ice (2 x 30 min) and overnight at 4°C. Samples were washed twice in PEM buffer and dehydrated by incubation in increasing concentrations of ethanol (50%, 70%, 80%, 90% and three times in 100%), for an hour each on ice under vacuum followed by an overnight incubation at 4°C in 100% Ethanol. Samples were then infiltrated with increasing concentrations of LR WHITE medium resin in absolute ethanol (30%, 50%, 70%, and three times in 100%), for an hour on ice under vacuum followed by an overnight incubation at 4°C for each bath. Seeds were then transferred into small Beam capsules (Electron Microscopy Sciences) and incubated overnight at 60°C for polymerisation. 1µm sections were cut on a Leica RM6626 microtome and floated onto adhesive slides (Superfrost Ultra plus™(ThermoFisher Scientific)). For immunolabelling, sections were first incubated for 45 minutes in PBS containing 2%(w/v) Bovine Serum Albumin (BSA). They were then incubated with a 10 fold dilution of primary antibody in PBS containing 0.1% BSA overnight at 4°C followed by one hour at room temperature. Sections were then washed three times in PBS for 5 minutes, then in PBS containing 0.1% Tween 20 (w/v) for 10 minutes and finally in PBS for 5 minutes. Incubation with a 100-fold dilution of an appropriate anti-rat secondary antibody (Alexa Fluor 488 conjugate, Invitrogen) in PBS with 0.1% BSA for one hour in the dark, in a wet chamber was then performed. The sections were washed three times in PBS for 5 minutes and counter-stained with a solution of 0.25ng/L of calcofluor (Fluorescent Brighter 28, Sigma Aldrich) in PBS for 5 minutes. Finally, sections were washed rapidly three times in PBS and mounted in Vectashield (Eurobio) (Moussu et al., 2017b). Observations were made using an Axio Imager 2 microscope (Zeiss).

RNA EXTRACTION AND QPCR ANALYSIS.

Replums were frozen in liquid nitrogen and total RNA was extracted using the Spectrum Plant Total RNA Kit (Sigma). Total RNAs were digested with Turbo DNA-free DNase I (Ambion) according to the manufacturer's instructions. RNA was reverse transcribed using the SuperScript VILO cDNA Synthesis Kit (Invitrogen) according to the manufacturer's protocol.

PCR reactions were performed in an optical 96-well plate using FastStart Universal SYBR Green Master Rox (Roche), in a final volume of 10 µl, according to the manufacturer's instructions. The following standard thermal profile was used for all PCR reactions: 95˚C for 10 min, 40 cycles of 95˚C for 10 s, and 60˚C for 30 s. As a reference, primers for the EIF4 and AP2M cDNA were used. PCR efficiency (E) was estimated from the data obtained from standard curve amplification using the equation $E = 10^{-1/slope}$. Expression levels are presented as $E^{-\Delta Ct}$, where $\Delta Ct = Ct^{GOI}-Ct^{HKG}$. GOI, Gene of Interest; HKG: Housekeeping genes.

TOLUIDINE BLUE PERMEABILITY.

To assess the cuticle integrity, toluidine blue staining assays were performed (Tanaka 2004). For qualitative toluidine blue staining test, etiolated seedlings were used (Creff et al 2019). Seedlings were stratified in the dark, exposed to 6h light flash and then grown for 4 days in darkness. They are then stained for 2min in 0.05% w/v Toluidine blue solution with 0.1% v/v Tween 20 and washed abundantly under tap water. Pictures were taken with a Keyence VHX900F digital microscope.

For quantitative assay of toluidine blue staining, 7-day old seedling were stained in the same way. In order to extract the toluidine blue stain and the chlorophyll, the cotyledons of ten seedlings were collected and placed in 1mL of 80% ethanol for at least 3hours in darkness. Toluidine blue staining of the resulting absorbance was measured at 626nm with a spectrophotometer. This resulting absorbance was then normalized with the chlorophyll absorbance at 430nm, a wavelength not absorbed by toluidine blue. 6 repetitions were performed per condition.

MICROSCOPY.

Mature and desiccated seeds were photographed with a Keyence VHX900F digital microscope. Light and fluorescent microscopy imaging was performed using a Zeiss AxioImager2.

DISCUSSION

Our work has revealed a previously undocumented role for ICE2 during *A. thaliana* seed development, where it acts redundantly, and likely as a complex with ZOU, to regulate endosperm elimination and embryo surface formation. This redundancy is in line with that observed between ICE1 and ICE2 function in other tissues. The fact that *ICE2* is expressed at lower levels than *ICE1* during wild-type seed development likely explains the fact that *ICE1* can completely compensate for loss of *ICE2* activity during normal seed development. *ICE2* expression levels during wild-type seed development would nonetheless, be expected to partially compensate for loss of *ICE1* function. However, we have shown that *ICE2* transcription appears to depend, either directly or indirectly, upon the activity of ZOU and thus, since ZOU acts as an obligate heterodimer, on ICE1 and potentially ICE2. The reduction of *ICE2* transcription engendered by a loss of ICE1-ZOU heterodimers may thus explain the very strong phenotype exhibited by *ice1* single mutants (**Figure 6**).

Despite the apparent dependence of *ICE2* upon ZOU complexes, we were able to show that loss of HOS1 function can lead to an *ICE2*-dependent partial rescue of the *ice1-2* mutant phenotype, suggesting that stabilization of residual ICE2 protein in the *hos1-3* mutant background is sufficient to partially compensate for loss of ICE1 function. This result highlights a previously undocumented role for HOS1 in seed development. However, how or even if the activity of HOS1 is regulated during seed development (for example at the level of expression or subcellular localization (MacGregor and Penfield, 2015) in seeds), remains to be elucidated. Furthermore, we show that loss of HOS1 function alone does not lead to observable changes in seed morphology or seedling cuticle permeability, suggesting that the proposed stabilization of ICE1 and ICE2 in this background does not cause a dramatic deregulation in seed development. The topology of the cuticle integrity monitoring pathway means that an increase in cuticle impermeability would not be a predicted result of excessive production of ZOU-dependent elements in the endosperm (Doll et al., 2020d). Nonetheless, previous work showed that plants expressing the gain of function ICE1 variant, ICE1-D show precocious endosperm elimination (Denay et al., 2014). One explanation for the discrepancy between this finding and the phenotype of *hos1-3* mutants could be the timing of *HOS1* expression. Based on *in silico* data and *in situ hybridization* (**Figure S1**) *HOS1* expression is strongest at early time points in endosperm development. In addition, it appears likely that other negative regulators of ICE activity, including the MPK6 and MPK3 proteins which are unable to bind the ICE1-D variant (Putarjunan et al., 2019b) act in parallel with HOS1 in the endosperm. Nonetheless, we have shown here that for one ICE-dependent process in the developing seed, namely embryo sheath deposition, the loss of HOS1 function generates a phenotype that is the inverse of that caused by loss of ICE function. Importantly the strong accumulation of

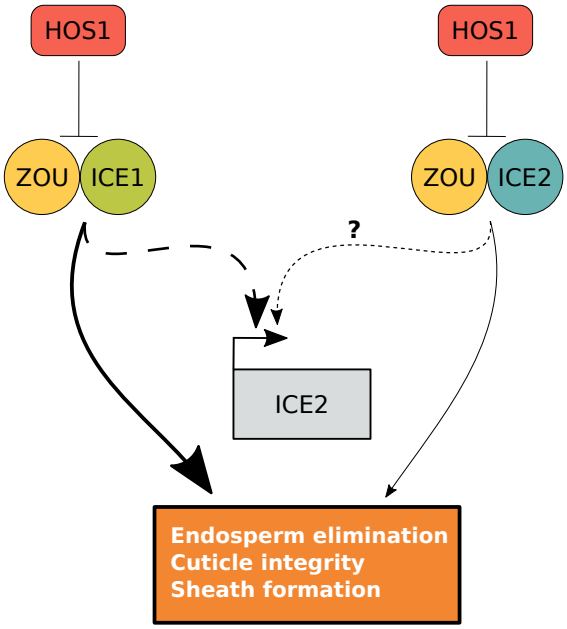

Figure 6: Schematic summary of the role and the HOS1-mediated regulation of ZOU/ICE1 and ZOU/ICE2 complexes in seed development highlighted in this study. HOS1 destabilizes the ZOU/ICE1 and ZOU/ICE2 complexes via its interaction and regulation of the ICE proteins. ZOU/ICE1 complex promotes seed development but also positively egulates ICE2 transcription. ZOU/ICE2 complex also promotes seed development in a more sublte way but whether this complex also influences ICE2 transcription remains to be confirmed.

sheath material observed in *hos1-3* mutants is attenuated in *hos1-3 ice2-1* mutants, again underlining the fact that ICE2 can make an important contribution to seed development, even in the presence of ICE1.

Taken together our results show that the *hos1-3* mutant background can this be used to reveal the functional relevance of ICE2 during seed development. Our work highlights the importance of understanding the molecular mechanisms underlying genetic redundancy (or apparent lack of genetic redundancy) before drawing mechanistic conclusions regarding gene/protein function.

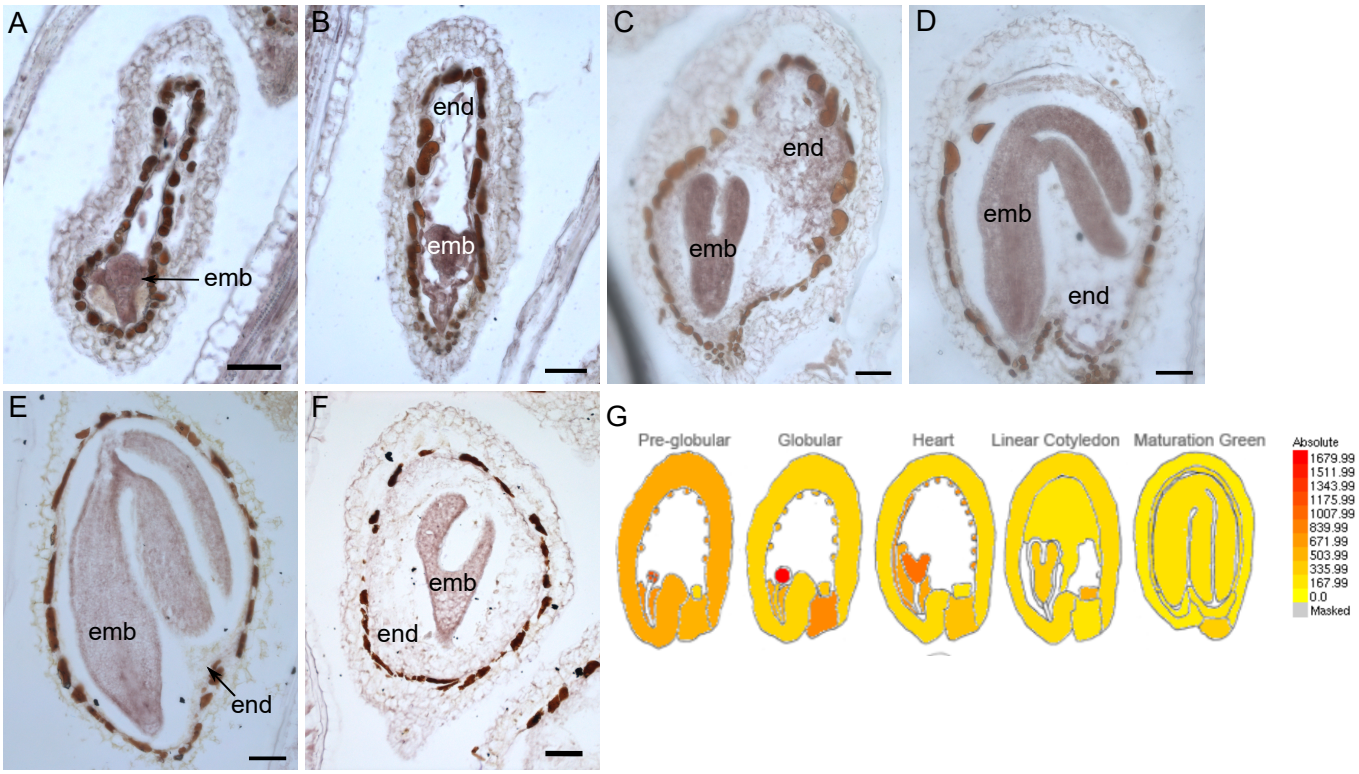

Figure S1 : Expression pattern of *HOS1* during seed development. (A-F) Images of in situ hybridizations of digoxigenin-labelled *HOS1* antisense (A-E) and sense probe (F), visualised by DIC microscopy. Four developmental stages are presented : globular stage embryo (A), heart stage embryo (B), torpedo stage embryo (C), bent stage embryo (D) and mature stage embryo (E). Signal appears purple in the embryo, endosperm and seed coat. The endothelium stained in dark-brown is an artefact. emb is for embryo; end is for endosperm. Scale bar, 50µm. (G) In silico data from EFPbrowser broadly confirms the expression pattern of *HOS1* in the endosperm.

Name	Sequence	project
ICE1-qPCR-F	GCTTTGATTTGATCAGGCAGT	qPCR ICE1
ICE1-qPCR-R	GTTTGCCTTGGATGTTTTCC	
ICE2-qPCR-F	CTCCTTGCCAAGTCCTAAAG	qPCR ICE2
ICE2-qPCR-R	CTAATCACCGCTTGTTGAAC	
EIF4-F	TTCGCTCTTCTCTTTGGCTCTC	qPCR EIF4
EIF4-R	GAACTCATCTTGTCCCTCAAGTA	
At5g46630-Fbis	TCAGGTGCCAATGTTCACAGC	qPCR AP2M
At5g46630-Rbis	ACCGCTCTTCTCCCAAACCTTG	
HOS1-HIS-F	TACGAGAGAAATCAACGGT	ISH HOS1
HOS1-HIS-R	CTGCGAATCTACGTCTCCT	
ICE2-geno-F	ATGAACAGCGACGGTGTTTGG	ISH ICE2
ICE2-R	CAAACCAGCGTAACCTGCTG	
ICE1 RP SALK	TTTGTAGGGCCTTTGTTGTTG	genotyping *ice1-2*
ICE1 LP salk	ATTCTTTGCTCTGCCTCTTCC	
LbB1-3 SALK	ATTTTGCCGATTTCGGAAC	
HOS1genoL	TGGACCGCATATTTCAGGTAG	genotyping *ice2-1*
HOS1genoR	AAGGCACGATAATGGTCTTCC	
LbB1-3 SALK	ATTTTGCCGATTTCGGAAC	
ICE2genoF	TGCATCCGACATCTTTTATCC	genotyping *hos1-3*
ICE2genoR	TAACTTCCGGAGATTCACCG	
Lb3	TAGCATCTGAATTTCATAACCAATCTCGATACAC	

Table1 : Primers used in this study.

II – Further considerations

We have shown that HOS1 likely regulates the stability of both ICE1 and ICE2 during seed development and that this regulation can be used to reveal the usually cryptic role of ICE2 during seed development. However very little is known about the post-translational regulation of *A. thaliana* ICE2 protein. Similarly to ICE1, ICE2 is thought to be phosphorylated by HOS1. Although the phosphorylation site has not been conclusively confirmed yet it seems to be conserved between ICE1 and ICE2 proteins (Kim et al., 2015c). Tools have been generated during this PhD to investigate the stability of the ICE1 and ICE2 proteins. Thus ICE1 and ICE2 variants mutated either in the KRAAM motif (R236H) or in the HOS1-ubiquitination site (S403A) to increased transactivation of ICE1 or ICE2, have been generated, introduced into wild-type plants and *ice1* mutants, and are currently being analysed. Phylogenetic analysis suggests that the *ICE2* gene in *A. thaliana* arose from a duplication of *ICE1*. However, whether this duplication has resulted in a neofunctionalization or subfunctionalization remains globally unclear. Several articles illustrated that ICE1 and ICE2 regulate the expression of *C-REPEAT BINDING FACTORS* (*CBF)* genes, involved in cold tolerance, and show unequal functional redundancy in inducing freezing tolerance (Fursova et al., 2009; Kim et al., 2015c). This unequal genetic redundancy of ICE1 and ICE2 is similar to that observed during seed development, where the, *ice2* seed phenotype resembles that of wild-type seeds, whereas the *ice1* seed phenotype is almost as severe as that of the *ice1ice2* double mutant. Unequal genetic redundancy is frequently observed in homologous gene pairs that have evolved through gene duplication in plants (Briggs et al., 2006).

Interestingly, in support of the idea that *ICE1* and *ICE2* may have functionally diverged since *ICE2* arose, it has been noted that a cathelicidin-like domain, a domain involved in antimicrobial resistance, is present only in the ICE2 protein (Kościuczuk et al., 2012; Kurbidaeva et al., 2014b; Tarasov et al., 2009). This domain may be responsible for the resistance to bacterial infection observed in plants overexpressing *ICE2* (Tarasov et al., 2009). However, although a gain of function mutant of ICE1 also exhibits enhanced disease resistance (Miura and Ohta, 2010; Zhu et al., 2011), it is unclear whether ICE1 has antimicrobial activity or not.

HOS1 is not the only known post translation regulator of ICE1. Li and colleagues and Zhao and colleagues have shown that the MKK5-MPK3/MPK6 cascade negatively regulates cold stress by leading to increased association with E3 ligases, promoting the ubiquitination of

AtICE1 and thus mediating its degradation via the 26S-proteasome (Li et al., 2017; Zhao et al., 2017). This MAP kinase cascade promotes the phosphorylation of ICE1 at Ser94, Thr366 and Ser403. In contrast, cold response is positively regulated by another MAP kinase cascade involving MEKK1-MKK2-MPK4, which also suppresses the kinase activities of MPK3 and MPK6. Recently, (Putarjunan et al., 2019a) deciphered the role of the KRAAM motif during stomatal development. Together with an upstream MPK docking motif, the KRAAM motif acts as a specific binding and phosphorylation site for MPK3 and MPK6. Under dark condition, the E3 ubiquitin ligase CONSTITUTIVE PHOTOMORPHOGENIC1 (COP1) also interacts with and degrades ICE1 proteins through ubiquitination pathways during stomatal development, leading also to its destabilization (Lee et al., 2017b). Whether this pathway also acts to regulate ICE stability, and thus ZOU/ICE activity in the endosperm remains unresolved. Although it is clear that mutants in *MPK6* affect embryonic cuticle development, this has been proposed to be due to their activity downstream of the ALE/GSO mediated embryonic cuticle integrity pathway (Creff et al., 2019a). Interestingly however, unpublished results from Audrey Creff, show that the expression of a constitutively active form of MPK6 specifically in the endosperm, causes the production of misshapen seeds. Whether this is a consequence of precocious endosperm breakdown remains to be resolved.

During cold tolerance acquisition, ICE1 can be phosphorylated by OPEN STOMATA1 (OST1) at Ser-278 increasing the activity of ICE1 in activating the transcription of *CBF3* (Ding et al., 2015a). (Ding et al., 2015a) have shown that when S278 is substituted with an aspartic acid this mimics a constitutive phosphorylation whereas S278 substituted with an alanine prevents phosphorylation. Similarly to OST1-mediated phosphorylation of ICE1, the sumoylation of ICE1 on Lys-393, mediated by the SUMO E3 ligase SAP AND MIZ1 DOMAIN-CONTAINING LIGASE1 (SIZ1), leads to its stabilization (Miura and Ohta, 2010; Miura et al., 2011). According to *in silico* data, all these genes are expressed during seed development and thus might also be involved in the stabilisation of the ZOU/ICE complex. In order to investigate the post-translational regulation of ICE1 during seed development, truncated and mutated versions of ICE1 targeting the different regulator modification sites will be introduced into different backgrounds and this, combined with genetic analysis should clarify potential roles for these regulators in the seed.

Finally, it is important to highlight the fact that identifying post-translational regulators of ZOU/ICE complexes in the endosperm, although providing valuable genetic tools, does not really answer the important question of why/how complex activity is regulated. Does post-

translational regulation by HOS1 or MPK6 for example occur downstream of specific developmental cues to coordinate seed development? Is complex activity altered by metabolic shifts and switches during seed development, for example reporting embryonic or maternal nutrient status? Although these possibilities are all plausible, their reality, and potential mechanistic basis remain totally unexplored.

Bibliography

See general bibliography at the end of the thesis.

CHAPTER 2

ARE THE ZOU/ICE FUNCTIONS IN EMBRYONIC SURFACE FORMATION IN *ARABIDOPSIS THALIANA* CONSERVED IN *MARCHANTIA POLYMORPHA*?

Preamble

As seen in the Introduction, in *A. thaliana*, the ZOU/ICE1 complex is involved in three genetically distinct pathways: ensuring embryonic cuticle integrity, orchestrating embryo sheath deposition and production and finally triggering endosperm lysis. The embryonic cuticle integrity pathway involves several proteins included the peptide TWS1, which after having been produced and sulfated in the embryo, can diffuse across gaps in the cuticle to be activated by cleavage at the embryo/endosperm interface by the subtilase ALE1. ALE1 production depends on the activity of the ZOU/ICE complex in the endosperm. Activated TWS1 can then diffuse back into the embryonic apoplast and bind GSO receptors at the surface of the embryo, ensuring embryonic cuticle integrity via a poorly understood mechanism that, by analogy with related pathways, likely involves the release of apoplstic ROS at the embryo surface (Doll et al., 2020; Fujita et al., 2020; Yang et al., 2008). The production of the embryo sheath involves another peptide, KRS, whose production also depends upon the activity of ZOU/ICE1 (Moussu et al., 2017) , and which belongs to a family of peptides previously proposed to be involved in ROS sensing (Wrzaczek et al., 2009). However, relatively little is known about sheath production and deposition. Anti-extensin antibodies such as α-JIM12 and α-LM1 label epitopes that are produced by the endosperm and accumulate in a continuous layer on the embryo surface where the sheath is formed. The production of these epitopes is eliminated in *zou, ice1* and *krs* mutants, whereas in mutants lacking components of the cuticle integrity signalling pathway it is only their deposition at the embryo surface that is defective (Moussu et al., 2017). Finally, endosperm lysis and elimination in the endosperm is also controlled by the ZOU/ICE1 complex. This process seems to involve cell wall softening and cell separation, followed by a physical crushing to the softened endosperm by the expanding embryo (Fourquin et al., 2016). This process appears to be largely independently of embryo cuticle development, and likely depends upon a distinct set of ZOU/ICE1 target genes (Xing et al., 2013). All these observations leave us with a complex picture of the function of the ZOU/ICE1 complex, in which it is difficult to ascertain what the overarching function of these proteins might be. This complexity is compounded by tha fact that, although seeds are fascinating, they can be challenging study systems due to their complex structural and genetic composition. Because the endosperm, where ZOU/ICE1 complexes act is derived from the female gametophyte, which in turn forms the majority of the plant body in early diverging land plants, we reasoned that deciphering the role of ZOU/ICE complex in these plants might help to shed some light on the ancestral function of this complex, and its regulation in plants. In this chapter a focus will therefore be placed on deciphering the ancestral role of ZOU/ICE complexes in *M. polymorpha.*

The first section of this chapter involves a study deciphering the existence and the role of ZOU/ICE complexes in *M. polymorpha*. We show the existence of two ICE proteins and two ZOU proteins in this species. We show that the interaction between ZOU and ICE proteins is conserved in *M. polymorpha* and that both MpZOU proteins and both MpICE proteins can complement the seed phenotypes of respectively *A. thaliana zou* and *ice1* mutants. We go on to demonstrate that two complexes, MpZOU2/MpICE2 and possibly MpZOU2/MpICE1 are involved the formation of the cuticle of gemmae, young dormant clones of the mother plant produced by asexual reproduction in *M. polymorpha*. Using dyes and microscopy techniques, as well as Mass Spectroscopy analysis, we confirmed that *M. polymorpha* cuticle contains both abundant phenolic compounds and some more classical aliphatic cuticle components and that MpZOU2 and both MpICE proteins are involved in the deposition of the cuticle but potentially also in determining its final composition. Finally, transcriptomic analysis revealed potential targets of ZOU/ICE complex function in *M. polymorpha*, supporting a hypothesis in which ZOU/ICE may be involved in ensuring the structural establishment of the cuticle rather than in regulating cuticle biosynthesis in *M. polymorpha* gemma.

The first section of this chapter is written as an article although some final validations are required before submission.

In a second section of this chapter, I focus on other potential roles of MpICE2 and MpICE1 during *M. polymorpha* development. Early expression of the genes encoding these proteins will be discussed. Parallels between the roles of ZOU/ICE in embryo sheath production and in ensuring embryonic cuticle integrity in *A. thaliana* and the role of ZOU/ICE in *M. polymorpha* will be addressed. The role of MpICE2 in the gamete-bearing tissue will be presented.

I - ZOU/ICE function in cuticle biogenesis is ancient

J. Loue-Manifel[1,2], YT. Lu[2], S. Knosp[3], J Just[1], S. Grey-Switzman, M. Erhardt[3], A. Hoguin, F. Simon, N. Dépège-Fargeix[1], G. Ingram[1], J. Goodrich[2]

[1]Laboratoire Reproduction et Développement des Plantes, Université of Lyon, ENS de Lyon, UCB Lyon 1, CNRS, INRA, Lyon, France

[2]Institut of Molecular Plant Sciences, University of Edinburgh, Edinburgh, Scotland

[3]Institut de Biologie Moléculaire des Plantes, Université de Strasbourg, Strasbourg, France

Author contributions

Studies of the permeability of the embryonic cuticle and seed shape quantifications have been performed by Jeanne Loue-Manifel. Yeast-two-hybrid experiments have been carried out by Yen-Ting Lu, Justin Goodrich and Antoine Hoguin, an L3 student supervised by Yen-Ting Lu. Expression analyses were performed by Jeanne Loue-Manifel and Yen-Ting Lu (for ZOU1 and ZOU2 Tdtomato reporter lines). Mass Spectrometry analysis has been carried out by Samuel Knosp on material produced by Jeanne Loue-Manifel. Material for RNA-seq analysis was produced by Jeanne Loue-Manifel. Jérémy Just carried out the bioinformatic analysis with input from Jeanne Loue-Manifel. TEM pictures of material prepared by Jeanne Loue-Manifel were taken by Mathieu Erhardt. Yen-Ting Lu and Shona Grey-Switzman cloned and transformed most of the CRISPR Cas9 constructs and constructs for GUS and TdTomato reporter lines, with input from Jeanne Loue-Manifel. The article was written by Jeanne Loue-Manifel and Gwyneth Ingram with inputs of Nathalie Dépège-Fargeix and Justin Goodrich.

Abstract

The evolution of land plants from aquatic ancestors involved several important innovations, including the production of a diffusion-limiting cuticle. Cuticles are found on the surfaces of all land plants, and are composed of complex polymers, of widely varying composition, but usually containing a significant proportion of aliphatic molecules. The formation of an intact cuticular membrane provide protection against multiple environmental stresses, but particularly against water loss to the dry terrestrial environment. In *A. thaliana*, two basic Helix-Loop Helix transcription factors, ZHOUPI (ZOU) and ICE1, have been shown to act non-cell autonomously in the endosperm of the seed to ensure the formation of an intact cuticle at the surface of the neighbouring embryo. ZOU and ICE1 act as a heterodimer, an association that we show is conserved in *Marchantia polymorpha*, an early land plant encoding two ZOU isoforms (MpZOU1 and MpZOU2) and two ICE1-like proteins (MpICE1 and MpICE2). Using genetic approaches, we show that, consistent with its expression in epidermal tissues, MpZOU2, in association with either MpICE1 or MpICE2, plays a role in the biogenesis of cuticle of young *M. polymorpha* propagules (gemmae). Transcriptomic analysis reveals that the loss of MpZOU2-containing complexes causes in a reduction principally in the expression of genes involved in cell wall modification and the homeostasis of apoplastic Reactive Oxygen Species. Biochemical analyses show that that the *M. polymorpha* gemma cuticle is composed of both aliphatic and phenolic compounds. Although loss of MpZOU function causes some changes in cuticle composition, these do not support a major defect in cuticle biosynthesis. Taken together our results point to a scenario in which, similar to their role at the embryonic surface in *A. thaliana,* ZOU/ICE complexes are required for the formation of a structurally intact cuticle in *M. polymorpha*, possibly though ensuring organised cuticle polymerisation, rather than directly in the regulation of the biosynthesis of cuticle monomers.

Introduction

Early land plants are thought to have evolved from charophyte freshwater green algae around 450 million years ago. This colonisation of land included the development of various key innovations necessary for survival in drier conditions (Puttick et al., 2018; Wickett et al., 2014). One of them was the development of components involved in water transport and permeability control. These include the biosynthesis and deposition of hydrophobic extracellular biopolymers like i) cutin, one of the main component of cuticle, ii) lignin, synthesized from phenolic precursors and deposited in secondary cell walls to provide structural support and facilitate long-distance water transport (the xylem in angiosperms) iii) and suberin, one of the main component of cork resulting from the polymerisation of lipids and

phenolics (Beisson et al., 2012; Fich et al., 2016; Weng and Chapple, 2010). In addition to cutin, which is a fatty acid derived polymer, the plant cuticle often also contains phenolic compounds such as ferulic and cinnamic acid derivatives, and cuticular waxes, a mixture of very-long-chain aliphatic compounds that render the cuticle highly impermeable to water (Yeats and Rose, 2013).

In contrast to angiosperms which synthesise both cutin and lignin, bryophytes synthesise only cutin. However, their genomes encode elements of the lignin-biosynthesis machinery. It was recently shown that these components play an essential role in both plant growth and cuticle deposition and function in mosses (Kriegshauser et al., 2021; Renault et al., 2017). Buda et al., 2013 also previously described the presence of phenolic residues in the cutin of moss cuticles. Recent phylogeny analysis strongly support that liverworts and mosses are sister groups (Puttick et al., 2018), and it therefore seems likely that the pre-lignin pathways highlighted in the moss *P. patens* could be also conserved in the liverwort *M. polymorpha,* as could be the distinctive phenolic-enriched cuticle.

In *A. thaliana*, during seed development the basic Helix-Loop-Helix transcription factor heterodimer ZHOUPI/INDUCER OF CBF EXPRESSION1 (ZOU/ICE1) has been shown to be involved in two genetically distinct processes: endosperm breakdown and embryo surface formation involving both the formation of the embryonic cuticle, and the production of the extra-cuticular embryo sheath (Denay et al., 2014; Moussu et al., 2017; Xing et al., 2013; Yang et al., 2008). Although both AtZOU and AtICE1 proteins can form homodimers in yeast, it has been shown that the heterodimerization of AtICE1 and AtZOU is required to activate target gene expression and is thus responsible for complex activity. Consistent with this, loss of *AtICE1* function, loss of *AtZOU* function and loss of function of both proteins simultaneously give very similar seed and embryo phenotypes (Denay et al., 2014). Although *AtICE1* has a broad expression pattern, and functions in multiple processes outside the seed including stomatal development and cold-tolerance (Chinnusamy et al., 2003; Kanaoka et al., 2008), *AtZOU* expression, and thus ZOU/ICE1 activity, is restricted to the developing endosperm.

The role of the ZOU/ICE1 complex in ensuring the formation of the embryo cuticle appears to be achieved at least partly through the transcriptional regulation (possibly indirect) of the subtilisin serine protease-encoding *ABNORMAL LEAF-SHAPE1 (AtALE1)* gene. AtALE1 acts in a complex dialogue between the embryo and the endosperm which ensures embryonic cuticle integrity and involves the two receptor-like kinases GASSHO1 and GASSHO2 (AtGSO1 and AtGSO2) and their ligand AtTWISTED SEED1 (AtTWS1) (Doll et al., 2020; Moussu et al., 2017). Like At*ale1* mutants, At*zou* and At*ice1* mutants show embryo

cuticle defects (Xing et al., 2013). In addition to regulating cuticle formation AtZOU, likely together with AtICE1, is also involved in the embryo sheath (Moussu et al., 2017). The embryo sheath is composed of a glycoprotein matrix that forms on the surface of the embryo outside the embryonic cuticle. Its deposition requires the coordinated production of material in the endosperm and signalling in the embryo. Molecular players involved in this process include the cysteine-rich peptide AtKERBEROS (KRS) whose expression is AtZOU dependent. Sheath deposition also requires the embryo expressed receptor like kinase AtGSO1 and AtGSO2, as well as AtALE1, suggesting functional links between the cuticle integrity pathway and sheath deposition (Moussu et al., 2017).

In *A. thaliana*, At*zou* and At*ice1* also show a persistency of the endosperm due to a lack of cell wall modifications and lysis of the endosperm. This problem in endosperm degradation prevents the embryo to grow through the endosperm leading to a collapse of the water filled endosperm cells during desiccation stage of seed development and thus shrivelling seed phenotype to At*zou* and At*ice1* mutants (Denay et al., 2014; Xing et al., 2013; Yang et al., 2008).

ZOU and ICE-encoding genes are conserved throughout land plants, in all of which at least one copy of each gene can be found. Given the extremely specific expression pattern of *AtZOU* in the endosperm, an Angiosperm-innovation, this observation raises the interesting question of whether the ZOU/ICE complex is conserved, and, if so the nature of its ancestral role (Catarino et al., 2016; Harris et al., 2020).

In contrast to seed plants, in bryophytes, autotrophic photosynthetic structures are predominantly formed by the haploid gametophytes, which release gametes that fuse to form reduced sporophytic structures that are often nutritionally dependent upon the parental gametophyte. In seed plants this situation is inverted, with the production of dramatically reduced gamotophytes, that develop within the sporophytic tissues. The endosperm, which together with the embryo is a product of the unique double fertilization process observed in angiosperms, appears to have arisen through the acquisition of fertilization competence within a non-egg cell of the much reduced female gametophyte (Buda et al., 2013). We propose that the functions of the ZOU/ICE1 complex in the endosperm, could be derived from ancestral gametophytic functions (for example in supporting the development of the sporophyte generation) in early land plants. Studying these functions may therefore provide valuable insights into the functions and regulation of ZOU/ICE1 in the endosperm, which are otherwise, very difficult to pinpoint precisely due to pleiotropic phenotypes of mutants, and the relative inaccessibility of this tissue.

To this end, we have carried out a study of the ZOU/ICE complex in the liverwort *Marchantia polymorpha*. We have used histology, genetics and biochemistry to show that *M. polymorpha* cuticle is composed of aliphatic and phenolic compounds. Moreover, we show that ZOU/ICE function in cuticle development is ancient since *MpZOU2* and both *MpICE* share functions in cuticle formation/polymerisation/composition of *M. polymorpha* gemmae.

RESULTS

THE *M. POLYMORPHA* GENOME CONTAINS TWO ZOU-ENCODING AND TWO ICE-ENCODING GENES.

Previous results in *A. thaliana* have shown that AtZOU and AtICE1, acting as heterodimers, are necessary to activate target promoter activity and mediate endosperm breakdown and embryo cuticle formation (Denay et al., 2014). Both proteins are ancient within land plant and at least one copy of each gene can be found in all land plants, raising the question of the ancestral role of ZOU and ICE (Catarino et al., 2016; Harris et al., 2020). BLAST searches and subsequent phylogenetic analysis revealed one *M. polymorpha* orthologue of AtZOU which was named *MpZOU1 (Mapoly0126s0029*) and a paralogue, which was named *MpZOU2 (Mapoly0012s0202*). Sequence comparisons showed that MpZOU1 was more similar to AtZOU in the bHLH domain (69,8%) and in the C-terminal region (28,4%) than MpZOU2 which shows 50,9% and 22,4% similarity respectively.

Whereas *P. patens* lack orthologues of AtZOU and gymnosperms such as *Pinus* has both orthologues of *MpZOU1* and *MpZOU2,* all Angiosperms (including *A. thaliana*) lack *MpZOU2*, and only those of *MpZOU1* are present. Interestingly, despite these losses, all land plant groups have at least one copy of ZOU suggesting that this protein retains functions that are indispensable for land plant biology (**Figure S1**).

AtICE1 and *AtICE2* are thought to have arisen from a duplication within the Brassica lineage (Kurbidaeva et al., 2014). We found two *M. polymorpha* co-orthologues of *AtICE1/AtICE2* which were named *MpICE1* (*Mapoly0150s0015*) and *MpICE2 (Mapoly0150s0016*). Sequence similarity in the bHLH domain and the C-terminal between MpICE2 and AtICE1 are respectively 85,9% and 60,4% whereas the similarity between MpICE1 and AtICE1 are 74,4% and 47,2% for the bHLH domain and the C-terminal region respectively. Phylogenetic analysis revealed that most land plants have several copies of the *ICE* gene, as is the case for *Zea mays,* where two co-orthologues and one potential paralogue of the *A. thaliana* genes have been described (**Figure S2**) (Grimault et al., 2015) .

THE ZOU/ICE COMPLEX IS CONSERVED IN *M. POLYMORPHA*

To test potential interactions between MpZOU and MpICE proteins, yeast-two-hybrid assays were carried out (**Figure S3**). Since the interaction between AtZOU and AtICE1 proteins has been shown to be mediated by their bHLH and C-terminal regions (Denay et al., 2014), constructs encoding both full length and N-terminally truncated (-T) versions were assembled and used to assess interactions. As indicated by growth on selective media, both MpZOU2 and MpZOU1 interact with both MpICE2-T and MpICE1-T. These results suggest that the ZOU/ICE interactions are likely conserved in all land plant and four potential heterodimers may form in planta: MpZOU1/MpICE1, MpZOU1/MpICE2, MpZOU2/MpICE1 and MpZOU2/MpICE2.

Furthermore, we found that both MpICE1-T proteins could interact with AtZOU and that AtICE1-T could interact with both MpZOU proteins.

MPZOU AND *MPICE* COMPLEMENT RESPECTIVELY *A. THALIANA ATZOU* AND *ATICE1* MUTANTS

Since the yeast-two-hybrid experiment suggested that cross-species interactions are possible between *A. thaliana* and *M. polymorpha* ZOU and ICE proteins, we tested whether MpZOU1 and MpZOU2, could complement loss of AtZOU function and whether MpICE1 and MpICE2 could complement loss of AtICE1 function. Homozygous *Atzou-4* mutants (Denay et al., 2014; Yang et al., 2008) were transformed with full length *MpZOU1* or *MpZOU2* cDNAs under the control of the *AtZOU* promoter and a *proAtZOU::AtZOU* construct was used as a positive control. In parallel, full-length *MpICE1* or *MpICE2* cDNAs under the control of the *AtICE1* promoter were introduced into homozygous *Atice1*-2 mutants (Denay et al., 2014). Mature dry seeds from multiple *Atzou*-4 lines transformed with either *proAtZOU::MpZOU1, proAtZOU::MpZOU2* or *proAtZOU::AtZOU* were compared to the seeds of *Atzou*-4 mutants, and wild-type plants. All three constructs were capable of fully rescuing the shrivelled seed phenotype of *Atzou-4* mutants. Similarly seeds from independent *Atice1*-2 lines transformed with *proAtICE1::MpICE1, proAtICE1::MpICE2* or *proAtICE1::AtICE1* were compared to wild-type and *Atice1-2* seeds. A full rescue of the *Atice1-2* shrivelled seed phenotype was observed for *proAtICE1::MpICE2* and *proAtICE1::AtICE1* in *Atice1-2*. However *proAtICE1::MpICE1* showed partial but not complete complementation of the *Atice1-2* phenotype.

Quantification of misshapen seeds of transgenic lines containing *pAtZOU::AtZOU*, *pAtZOU::MpZOU1* and *pAtZOU::MpZOU2* in the *Atzou-4* background and *pAtICE1::AtICE1* and *pAtICE1::MpICE2* in the *Atice1-2* background showed no significantly different from wild-type seeds. However, consistent with visual observations, 30% of transgenic seeds from lines

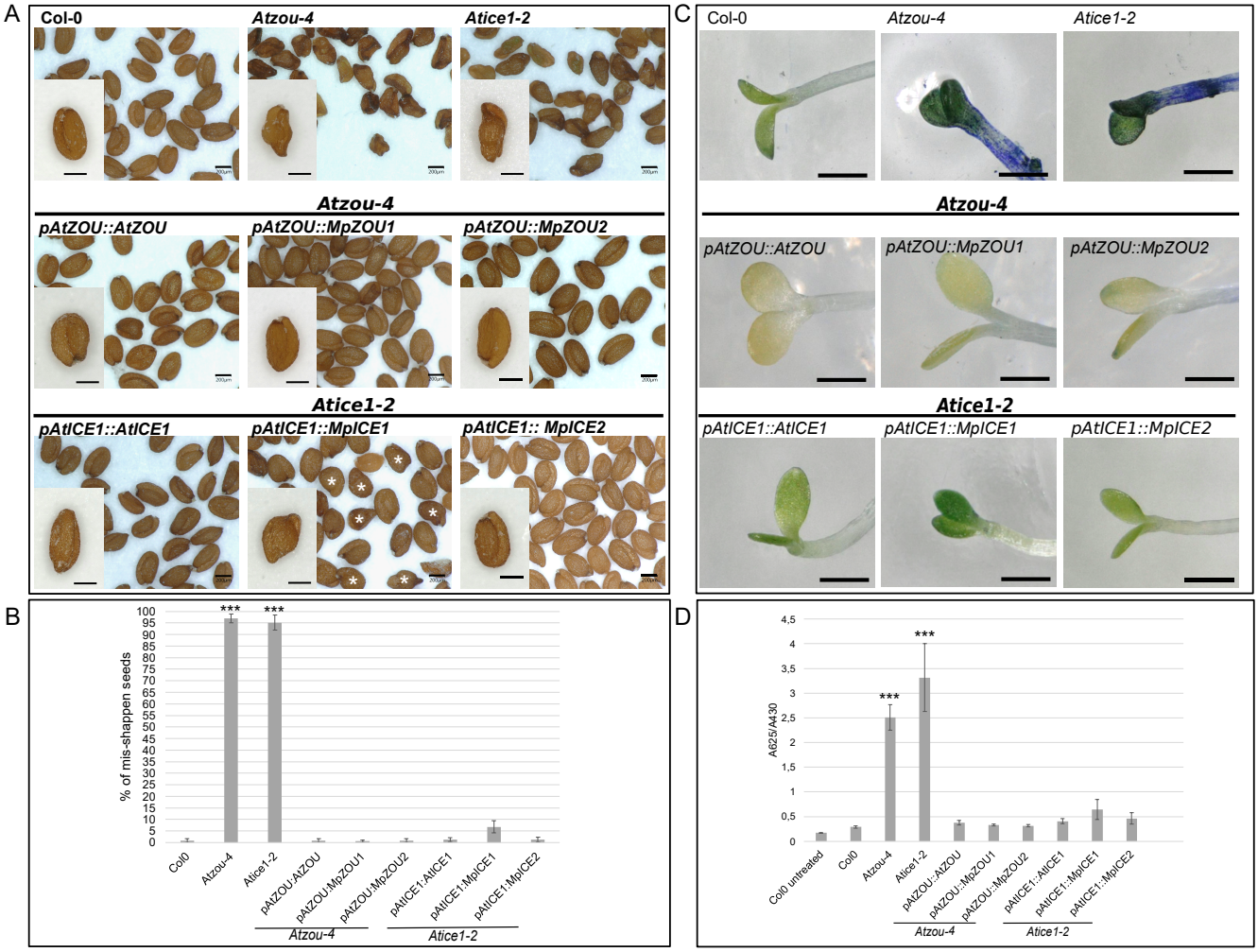

Figure 1 : MpZOU and MpICE complement seed and cuticle phenotypes of Arabidopsis At*zou-4* and At*ice1-2* mutants.

(A) Dry seeds of wild-type (Col-0), At*zou-4* mutant, At*ice1-2* mutant, pAtZOU::AtZOU, pAtZOU::MpZOU1 or pAtZOU::MpZOU2 in At*zou-4* mutant and pAtICE1::AtICE1, pAtICE1::MpICE1 or pAtICE1::MpICE2 in At*ice1-2* mutant. Partially complemented seeds are indicated by an asterisk. Scale bar, 200µm. (B) Quantification of misshappen dry seeds in different background. N=5, approximately 1000 seeds per repetition. *** indicates statistical differences with ANOVA. Error bars indicate standard deviation. (C) Toluidine blue assays on etiolated cotyledons of wild-type (Col-0), At*zou-4* mutant, At*ice1-2* mutant, pAtZOU::AtZOU, pAtZOU::MpZOU1 or pAtZOU::MpZOU2 in At*zou-4* mutant and pAtICE1::AtICE1, pAtICE1::MpICE1 or pAtICE1::MpICE2 in At*ice1-2* mutant. Scale bars 500µm. (D) Quantification of toluidine blue uptakes by the cotyledons of young seedlings, normalized to chlorophyll content. N= 6, 10 seedlings per repetition.. *** indicates statistical differences with ANOVA. Error bars indicate standard deviations.

expressing *pAtICE1::MpICE1* in *Atice1-2* are either misshaped or rounder than wild-type seeds (**Figure 1A and 1B**) but nonetheless plumper that *Atice1-2* mutant seed indicating partial complementation.

Finally, toluidine blue staining of etiolated young seedlings revealed a full rescue of the embryo cuticle defects of *Atzou-4* by *pAtZOU::MpZOU* , *pAtZOU::MpZOU1* and *pAtZOU::AtZOU2* in *Atzou-4,* and of *Atice1-2* by *pAtICE1::AtICE1*, *pAtICE1::MpICE1* and *pAtICE1::MpICE2*. Quantification and normalisation with chlorophyll absorbance confirmed the macroscopic cuticle rescue we observed (**Figure 1C and 1D**).

These results globally confirm the relevance of cross-species interactions demonstrated by yeast-2-hybrid experiments, and suggest that the properties of ZOU and ICE proteins have been conserved between bryophytes and angiosperms.

***MPZOU2* AND *MPICE2* ARE EXPRESSED IN THE DORSAL GAMETOPHYTE EPIDERMIS**

In order to analyse potential roles played by *MpZOU1, MpZOU2, MpICE1* and *MpICE2* in *M. polymorpha* development, we first asked where they are expressed in the gametophyte. Transcriptional reporter lines containing 5kb of regulatory sequences upstream of the start codon of the *MpZOU1* and the *MPZOU2* genes fused with either nuclear localised TdTomato fluorescent protein or to the *GUS* gene encoding β-glucoronidase were generated. Similarly, GUS and TdTomato transcriptional reporter lines were generated using 6.7kb and 5.3kb of regulatory sequences upstream of the start codon of *MpICE1* and *MpICE2* respectively.

The *pro*Mp*ZOU1:GUS* and *pro*Mp*ICE1:GUS* reporters showed a very similar expression pattern in 10-day-old thallus, predominantly on the ventral surface along the midrib, in the scales, the parenchyma and the rhizoids (**Figure 2**). Weaker expression of *pro*Mp*ZOU1:GUS* and *pro*Mp*ICE1:GUS* lines was also detectable in the dorsal epidermal cell layer, overlapping with the expression pattern of *pro*Mp*ZOU2:GUS* and *pro*Mp*ICE2:GUS* reporters (see below).

In contrast to the predominantly ventral expression of *MpZOU1* and *MpICE1*, the *pro*Mp*ZOU2:GUS* and *pro*Mp*ICE2:GUS* reporters were predominantly expressed in the dorsal epidermis of 10-day-old thallus(Fig GUS). However, weaker, but detectable expression was also detected in the ventral epidermis of *pro*Mp*ZOU2:GUS* thallus, overlapping with the expression pattern of *pro*Mp*ZOU1:GUS*. No detectable GUS staining was visible on the dorsal surface of the thallus of *pro*Mp*ICE1:GUS* reporter lines. Early expression of the genes of interest was also investigated. Interestingly, GUS staining was detected in the epidermis of developing gemmae of *pro*Mp*ZOU2:GUS* lines revealing an early expression of *MpZOU2*.

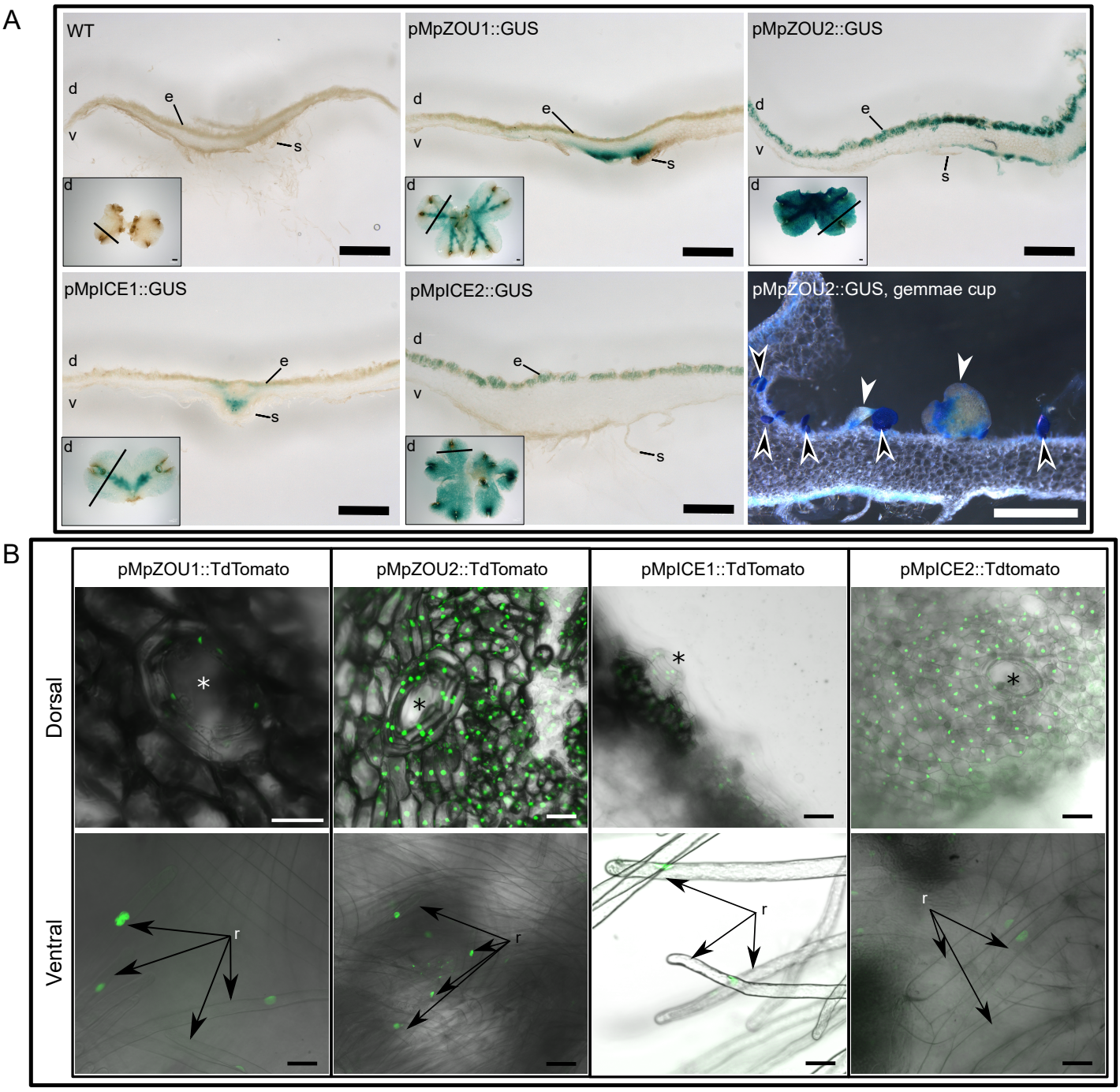

Figure 2 : Transcriptional reporter lines of Mp*ZOU1*, Mp*ZOU2*, Mp*ICE1* and Mp*ICE2* show an overlap of expression pattern. (A) Mp*ZOU2* and Mp*ICE2* promoter activity are restricted to the epidermis whereas the activity of Mp*ZOU1* and Mp*ICE1* promoters are limites to the ventral midrib. Transverse section of thallus of WT (Tak-1) and GUS reporter fusion of Mp*ZOU1*, Mp*ZOU2*, Mp*ICE1* and Mp*ICE2* promoters are the main photographes. Respective whole mount thallus are shown in the bottom left side of the transverse section picture. Black bar indicate the orientation of the section. Transverse section in the gemmae cup of pMpZOU2:GUS thallus show strong expression in developping gemmae (black and white arrowheads) and weaker expression in mature gemmae (white arrowheads). d, dorsale side of the thallus ; v, ventral side of the thallus ; e, epidermis ; s, scale where bundles of pegged rhizoids are found. Scale bar, 500µm. (B) Confocal microscopy images of Mp*ZOU1*, Mp*ZOU2*, Mp*ICE1* and Mp*ICE2* promoters fused to TdTomato fluorescent protein. Photographes of the dorsal surface of the thallus (first row) and ventral surface of the thallus with a focus on rhizoids (second row) show an overlap of expression pattern Mp*ZOU* and Mp*ICE*. Air pores are indicated with an asterisk. r, rhizoids. Scale bar, 50µm. Photographs of pMpZOU1::Tdtomato on the dorsal surface and pMpZOU2::TdTomato on the ventral surface are from Yen-Ting LU.

Early expression of *MpICE2* was not consistently detected in gemmae. Expression of *MpZOU1* and *MpICE1* was also detected in gemmae, predominantly in the rhizoid precursor cells (discussed in **Chapter 3, §II, Figure 1**).

15 day old thalli of nuclear TdTomato transcriptional reporter lines were also analysed and results were consistent with expression patterns observed in the GUS reporter lines. Expression of *pro*Mp*ZOU1:TdTomato-NLS* and *pro*Mp*ICE1:TdTomato-NLS* was easily detectable in rhizoids but could also be detected in air pore chamber cells and epidermal cells on the dorsal thallus surface (**Figure 2**). In contrast, *pro*Mp*ZOU2:TdTomato-NLS* and *pro*Mp*ICE2:TdTomato-NLS* lines confirmed a strong expression of *MpZOU2* and *MpICE2* in dorsal epidermal cells and air pore chambers. Despite the apparent absence of detectable signal in the ventral regions and rhizoids of *pro*Mp*ICE2:GUS* lines, expression in the rhizoids was detected for *pro*Mp*ICE2:TdTomato-NLS*. *MpZOU2* was again found to be expressed in rhizoids based on *pro*Mp*ZOU2:TdTomato-NLS* lines.

Expression data suggest, firstly, that both *MpZOU1, MpZOU2*, *MpICE1* and *MpICE2* are all expressed in both dorsal and ventral thallus tissues. However, the levels of expression of these genes differ, with *MpZOU1* and *MpICE1* expressed predominantly in the ventral surface and rhizoids and thus potentially involved in ventral parenchyma and rhizoid development, and *MpZOU2* and *MpICE2* predominantly expressed in the dorsal epidermis, and thus potentially sharing epidermal functions.

It should be borne in mind that the ICE proteins in *A. thaliana* are strongly regulated at the post-translational level (Ding et al., 2015; Dong et al., 2006; Miura et al., 2007, 2011; Putarjunan et al., 2019) and that gene transcription does not necessarily reflect protein levels. Translational reporters are under construction to address this issue.

M. POLYMORPHA **GEMMA CUTICLE IS COMPOSED OF BOTH ALIPHATIC AND PHENOLIC MOLECULES**

Plant cuticles contain a highly variable array of aliphatic molecules such as waxes and cutin (Yeats and Rose, 2013). To date very little is known about cuticle composition in *M. polymorpha*. Thus, we used the lipophilic dye Nile Red, originally used to stain the suberin-rich endodermis in *A. thaliana* roots (Greenspan et al., 1985; King, 1947), to see whether we could stain the cuticles of wild-type *M. polymorpha* gemmae. Subsequent analysis by confocal microscopy strongly suggests that the cuticle of *M. polymorpha* gemmae also contains aliphatic molecules (**Figure 3A**), as indicated by a very thin layer of Nile Red staining covering the surface of gemmae, which appears to be reinforced near the apical notch. Although bryophytes synthesize cutin, the main component of the cuticle, a recent study has shown that

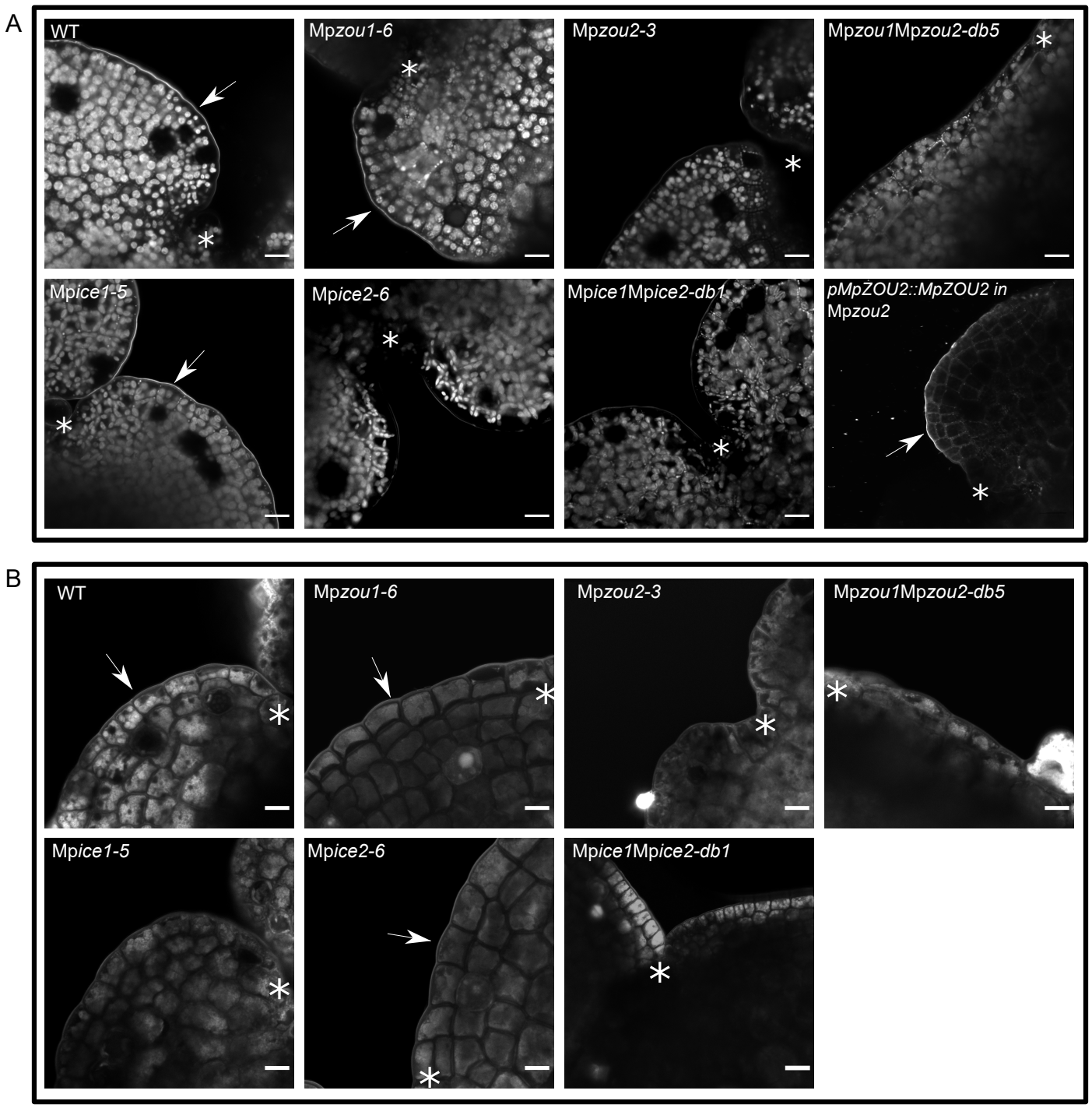

Figure 3 : Cuticle staining of *M. polymorpha* **gemmae with the lipophylic dye, Nile Red and the phenolic compounds dye, Diphenylborinic acid showed a critical role for Mp***ZOU2* **and both Mp***ICE* **in cuticle formation of gemmae.** (A) Nile Red staining of the gemmae cuticle indicates a cuticle defect in the Mp*zou2-3*, Mp*zou1zou2-db5*, Mp*ice2-6* and Mp*ice1ice2-db1* mutants. *, apical notch ; arrow indicates intact cuticle. Scale bar, 10µm. (B) Diphenylborinic acid stains the cuticle of wild-type (Tak-1) gemmae and indicates cuticle defect in Mp*zou2-3*, Mp*zou1zou2-db5*; Mp*ice1-5*, Mp*ice1ice2-db1* mutants. *, apical notch ; arrow indicates intact cuticle. Scale bar, 10µm.

proteins associated with the phenolic-based lignin-biosynthesis machinery of Angiosperms play an essential role in ensuring normal cuticle structure/deposition in mosses (Renault et al., 2017). Consistent with this finding (Buda et al., 2013) also described the presence of phenolic residues in the cutin of moss cuticles. Recent phylogenetic analysis strongly supports the idea that liverworts and mosses are sister groups (Puttick et al., 2018), and we therefore hypothesize that the pre-lignin pathways highlighted in *P. patens* could be also conserved in *M. polymorpha*, as could the distinctive dependence upon phenolic compounds for coordinated cuticle assembly. We therefore tested different staining techniques to assess the presence of phenolic compounds in the *M. polymorpha* cuticle. We concentrated on dyes previously reported to stain lignin, which is composed of phenolic compounds. We found that Diphenylborinic acid, which stains *A. thaliana* lignin (Corona-Carrillo et al., 2014; Reich et al., 2006) stains the cuticle of wild-type *M. polymorpha* gemmae (**Figure 3B**). Consistent with the staining results, mass spectrometry analysis of cuticles from wild-type *M. polymorpha* gemma demonstrated that several types of phenolics are present in relatively high quantity in the cuticle, in particular p-coumarate and ferulate (**Figure 4**).

BOTH *MPICE* AND *MPZOU2* GENES PROMOTE GEMMA CUTICLE FORMATION

To assess the potential role of the *M. polymorpha* ZOU and ICE proteins in cuticle development, CRISPR-Cas9 single loss of function mutants were generated for *MpZOU1, MpZOU2, MpICE1* and *MpICE2*. In addition, the double mutants, Mp*zou1* Mp*zou2* and Mp*ice1* Mp*ice2* were generated (**Figure S4 and S5**).

In *A. thaliana*, the cuticle is exclusively synthesized by epidermal cells (Ingram and Nawrath, 2017; Javelle et al., 2010) In *M. polymorpha,* nothing is as clear as it is in *A. thaliana* however some clues suggest that although epidermal cells are on both side of the thallus, the cuticle might be more pronounced on the dorsal surface. Indeed, the dorsal surface is the surface in direct contact with the air and environmental hazards while the ventral surface is in contact with the earth and therefore more protected than the dorsal surface from drying out. Moreover, cuticle has already been reported on the dorsal surface on the thallus, i.e. on air pore ledges (Schönherr and Ziegler, 1975; Xu et al., 2021). In addition to that, since Mp*ZOU2* and Mp*ICE2* show expression predominantly in the dorsal epidermis of the thallus, similarly to the expression of MpSBG9, a R2R3 MYB transcription factor involved in cuticle biosynthesis in *M. polymorpha* (Xu et al., 2021), we investigated whether *M. polymorpha* ZOU/ICE complex might be involved in cuticle development.

Confocal microscopy analysis after Nile Red staining of gemmae from the different backgrounds was carried out. Consistent with the results of expression analysis, Nile Red

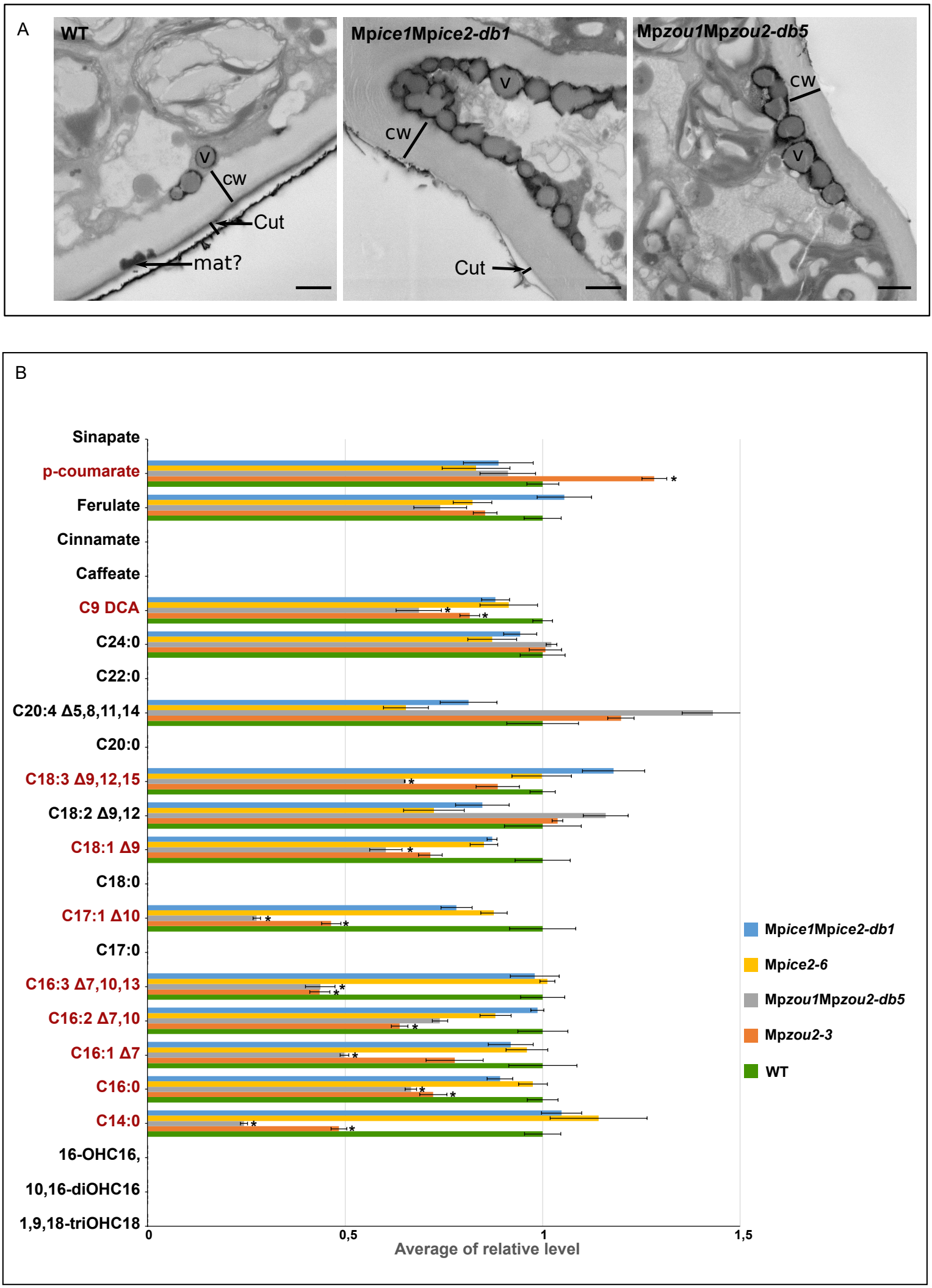
A
WT
V
CW
Cut
mat?
Mpice1Mpice2-db1
V
CW
Cut
Mpzou1Mpzou2-db5
CW
V
B
Sinapate
p-coumarate
Ferulate
Cinnamate
Caffeate
C9 DCA
C24:0
C22:0
C20:4 Δ5,8,11,14
C20:0
C18:3 Δ9,12,15
C18:2 Δ9,12
C18:1 Δ9
C18:0
C17:1 Δ10
C17:0
C16:3 Δ7,10,13
C16:2 Δ7,10
C16:1 Δ7
C16:0
C14:0
16-OHC16,
10,16-diOHC16
1,9,18-triOHC18
0
0,5
1
1,5
Average of relative level
Mpice1Mpice2-db1
Mpice2-6
Mpzou1Mpzou2-db5
Mpzou2-3
WT

Figure 4: MpZOU2 (and MpICE2 to a lesser extent) are critical for cuticle formation in *M. polymorpha* gemmae.

(A)Transmission electron micrographs of the gemmae cuticle showing alteration in Mp*zou1*Mp*zou2-db5* and Mp*ice1*Mp*ice2-db1* mutant cuticle layer compare to the WT (Tak-1). cw, cell wall; cut, cuticle; v, vesicles; mat?, putative material coming for deposition. Scale bar, 1µm. (B) Cutin compositional analysis of the gemma cuticle of Mp*ice2-6*, Mp*zou2-3*, Mp*ice1*Mp*ice2-db1* and Mp*zou1*Mp*zou2-db5* revealed gemma cuticle composition differences in Mp*zou2-6* and Mp*zou1*Mp*zou2-db5* compared to WT. DCA; dicarboxylic fatty acid. Compounds with statistical differences between the different backgrounds are highlighted in red. * indicates statistical differences with two-tailed t-test ($p<0.01$). Error bars indicate standard deviations, n=3.

stained gemmae fell into two categories. Whereas loss of function of *MpZOU1* and *MpICE1*, which are mainly expressed ventrally show WT-like cuticle staining, in Mp*zou2*, Mp*ice2*, Mp*zou1*Mp*zou2* and Mp*ice1*Mp*ice2* gemmae, the cuticle was much less strongly stained by Nile Red. Interestingly, the cuticle staining of Mp*ice2* mutants was stronger than that of Mp*ice1*Mp*ice2* double mutants suggesting either some functional redundancy (consistent with expression analysis), or reciprocal regulation between these genes. However, the potential redundancy observed for the MpICE proteins, does not seem to occur for the MpZOU proteins since staining of the Mp*zou2* mutant cuticle with Nile Red resembled that of the double mutant Mp*zou1* Mp*zou2*.

Based on our results it seems likely that MpZOU2 interacts *in planta* with MpICE2 and MpICE1 and the function of MpZOU2/MpICE heterodimers is to regulate cuticle biogenesis. The role of MpZOU2 in cuticle development was confirmed by the phenotypic rescue of *Mpzou2* with MpZOU2 cDNA driven by the endogenous MpZOU2 promoter, as shown by Nile red staining (**Figure 3A**). Similarly to our findings with Nile Red staining, the cuticle of Mp*zou1* gemmae was found to stain strongly with diphenylborinic acid whereas Mp*zou1*Mp*zou2*, Mp*ice1*Mp*ice2*, Mp*zou2* gemmae showed very weak cuticle staining (**Figure 3B**). Surprisingly, Mp*ice1* mutants stain less strongly than Mp*ice2* mutants. This observation again suggests a role for both MpICE proteins in the formation of the cuticle of *M. polymorpha* gemmae, but could indicate that these proteins act differently in the regulation of the deposition of phenolic and aliphatic components.

Transmission electron microscopy analysis of gemmae was applied to further explore the defects in gemma cuticle in Mp*zou2*, M*pice2,* Mp*zou1*Mp*zou2* and Mp*ice1*Mp*ice2*. Using this approach, the cuticle structure of *M. polymorpha* wild-type gemma was found to be very similar to *P.patens'* (Renault et al., 2017). It is composed of three visibly distinguishable layers: an inner grey layer, associated within the cell wall, a middle white layer probably corresponding to cutin and intracuticular waxes, and a dark outer-layer. These three layers were found to be fragmented in some cases and/or totally absent in the two double mutants Mp*zou1*Mp*zou2* and Mp*ice1*Mp*ice2* (**Figure 4**). Thus, it sometimes appears that the cell wall, (which does not seem to be defective in any of the mutants), is the most outer layer, directly in contact with the environment. Vesicles wrapped in electron-dense component and electron-dense components at the interface between the cell wall and the cuticle are also visible in the wild-type. This might be explained by there being materials coming via vesicles for deposition within the cuticle. In the two double mutants, Mp*zou1*Mp*zou2* and Mp*ice1*Mp*ice2* these electron-dense materials appear thicker and stuck around the vesicles suggesting a potential problem either in the transport (which is unlikely) or in the deposition of the materials within the cuticle.

In order to understand more about alterations in cuticle composition in mutants lacking MpZOU/MpICE complexes, Mass Spectrometry analysis of the cuticles of gemmae directly harvested from gemmae cups was carried out on wild type (Tak2xTak1), Mp*zou2*, Mp*ice2*, Mp*zou1*Mp*zou2* and Mp*ice1*Mp*ice2* plants. Several aliphatic molecules were found to be less abundant in some backgrounds. Statistically significant differences were only observed specificially in the Mp*zou1*Mp*zou2-db5* background for C18:3 Δ9,12,15, C18:1 Δ9 and C16:1 Δ7. By contrast, C14:0, C16:0, C17:1 Δ10, C16:2 Δ7,10, C16:3 Δ7,10,13 and C9 DCA (dichloroacetate) were statistically less abundant in both Mp*zou2-3* and Mp*zou1*Mp*zou2-db5* backgrounds compared to wild-type (**Figure 4**). Among the phenolics detected in WT gemma cuticle, only one, p-coumarate, showed a significant difference compared to wild-type. This compound was found to be more abundant specifically in Mp*zou2-3* gemma cuticle. None of the Mp*ice* mutants tested showed statistically significant differences in the amount of any of the molecules identified. However, when interpreting this data, it is important to bear in mind that some exotic/unexpected fatty acids or other molecules were not identified in the analysis and that important changes were therefore not detected. In addition, delipidation may have removed unpolymerized components, which would have masked potential defects in cuticle assembly.

WHAT ARE THE DIRECT/INDIRECT TARGETS OF MPZOU2?

To identify genes acting downstream of *MpZOU2* as effectors of cuticle biogenesis, we carried out transcriptional profiling (RNAseq) of gemmae of wild type (Tak2xTak1), Mp*zou2* and Mp*zou1*Mp*zou2* mutants.

Lists of genes differentially regulated in Mp*zou2* and Mp*zou1* Mp*zou2* double mutants were established. Because the Mp*zou2* single mutant used in our analysis was in the opposite gender type to our wild-type and Mp*zou1* Mp*zou2* double mutant alleles, and to increase rigour, the two lists were then combined and only genes misregulated in both mutant genotypes were retained. Since co-expression of ZOU and ICE1 genes activates transcription in several *in* planta assays in moss and tobacco (Denay et al., 2014; Feng et al., 2018) we concentrated on transcripts that were less abundant in mutants compared to wild type. Within this set of 565 differentially expressed genes (DEG), we identified numerous genes encoding proteins involved in cell wall modification and/or structure, including expansins, xyloglucan endotransglycosylases (XETs), and pectate lyases (**Figure 5**). At the level of cuticle biosynthesis, three genes identified by Bowman et al., 2017 as orthologues of key genes *in A. thaliana* cuticle biogenesis were present in our dataset, encoding orthologue of glycerol-3-

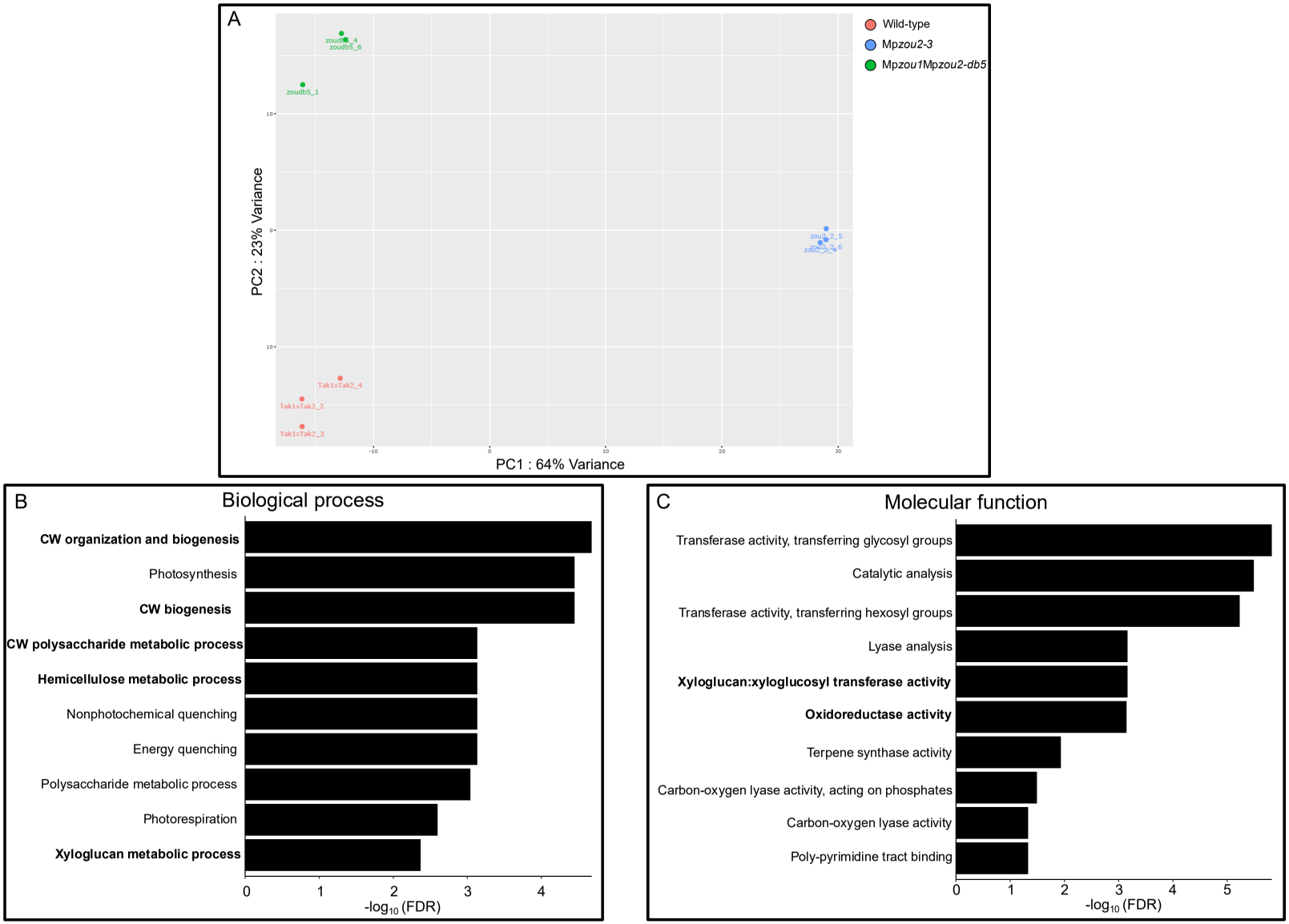

Figure 5 : RNA Sequencing analysis. (A) Principal Component Analysis (PCA) show distinct gene expression profiles across WT (Tak2 xTak1 progeny) in red, Mp*zou2-3* mutant in blue and Mp*zou1*Mp*zou2-db5* mutant in green. (B-C) Enriched Gene Ontology terms in Biological process (B) and Molecular Functions (C) for differential expresion genesdown regulated in Mp*zou2-3* single mutant and Mp*zou1*Mp*zou2-db5* double mutant. The top 10 significantly enriched GO categories ($p<0.01$)for each analysis. Significant enrichment is observed for cell wall (CW) structure and biogenesis (in bold) (B) and ROS production (in bold) (C). (http://plantregmap.gao-lab.org)

phosphate acyltransferase 6 (*GPAT6*) (*Mp7g03880*), a Cutin Synthase (*CUS*) (*Mp8g13940*), and an ABC transporter (*Mp8g12130*) (**Figure 5**) (Bowman et al., 2017).

Among the 565 DEGs, 339 DEGs have GO annotation and 81 GO terms were enriched. (http://plantregmap.gao-lab.org/) (**Figure 5**). Loss of function of Mp*zou2* and Mp*zou1*Mp*zou2* significantly affected cell wall biogenesis and structure.

The dataset was also strikingly enriched for gene encoding proteins encoding REDOX associated proteins. Of particular note were peroxidases, with 9 downregulated, of which 8 are predicted to encode class III peroxidases, Class III peroxidases have various roles, and are often associated with cell wall remodelling, including the polymerisation of phenolic units to form lignin, or the polymerisation of extensins (Mishler-Elmore et al., 2021; Rojas-Murcia et al., 2020) (**Table S1**). In addition, we found that a large number of genes encoding REDOX associated proteins were downregulated in our dataset, including genes encoding Aquaporins (associated with the transport of H2O2 (3), Tyrosinases (6), Polyphenol oxidases (4) and Dirigent proteins (2) (**Figure 5**). Despite the fact that analyses were carried out in different tissues, more than 50% of the genes belonging to this composite class have previously been identified as upregulated in plants lacking function of the MpTCP1 protein, which has been shown to be a key regulator of REDOX associated proteins (Busch et al., 2019). In addition a large number (7) of genes encoding Phytocyanin-domain proteins, also thought to be involved in ROS reactions (Nersissian et al., 1998; Reyt et al., 2020) were also downregulated in our dataset. Finally, we were interested to find that a gene encoding a STIG1-domain (cysteine-rich peptide) protein (*Mp3g18230*), as well as two EXTENSIN-encoding genes were downregulated in our dataset. Comparison with the *A. thaliana* showed that this protein was most closely related to KERBEROS, a key target of the ZOU complex in the *A. thaliana* endosperm, and necessary for the formation of the EXTENSIN-rich embryo sheath (Moussu et al., 2017). The STIG domain of the related protein GRIM REAPER (GRI) has been proposed to be involved in ROS sensing (**Figure S6**) (Wrzaczek et al., 2009).

Material and Methods

PLANT GROWTH

All wild-type plants used in the project were *Marchantia polymorpha* Takaragaike-1 (Tak-1) for the male or Takaragaike-2 (Tak-2) for the female (Ishizaki et al., 2008). Spores for transformation were the progeny of Tak2 x Tak1 (Ishizaki et al., 2008). Lines were asexually maintained and propagated through gemmae growth as described in Takenaka et al., 2000 and Okada et al., 2000 except that we used Johnson media (see details in Annexes)

complemented with 1.4% agar. Gemmae were transferred on plate to long-day conditions (16h, 21°C) for approximately 3 to 5 weeks, before harvesting the new generation of gemmae for further analysis.

Arabidopsis thaliana seeds were gas sterilized with chlorine (3mL HCl (33%) in 150mL bleach) for 2 hours and then sown on Murashige and Skoog (MS) medium with 0,5% sucrose in sterile condition, stratified for 2 days at 4°C and grown for 7 days in short-day conditions (8h light, 19°C). Seedlings were then transferred to compost (Argile 10 (favorit)) and grown under short day conditions (8h light, 19°C) for two to three weeks before transferred to long day conditions (16h light, 21°C). All *A. thaliana* mutants used in this study were previously published: the loss of function mutant At*zou-4* allele (Yang et al., 2008) was used for all complementation experiments as was the loss of function At*ice1-2* allele (Denay et al., 2014; Kanaoka et al., 2008). The ecotype Columbia-0 (Col-0) was used as a wild-type control.

GENERATION OF CRISPR-CAS9 KNOCK OUT MUTANTS

CRISPR-Cas9 mutants were generated as described in (Sugano et al., 2014). Two gRNAs for each gene were designed to generate single mutants (**Figure S3**). For ZOU constructs, the oligonucleotides encoding the sgRNA were first cloned into pGE_EN03 (**Table 1**). For both Mp*zou1* and Mp*zou2* single mutants, the sgRNA constructs were then introduced into pMpGE010 or pMpGWB401 destination vectors (containing the CAS9 protein). For double Mp*zou1* Mp*zou2* mutants, two separate constructs were introduced by co-cultivation with two *Agrobacterium GV3101* strains. For ICE constructs, the oligonucleotides encoding the sgRNA were also first cloned into pGE_EN03 and then introduced into pMpGE010 or pMpGWB401 destination vectors. For Mp*ice1* Mp*ice2* double mutants, the two sgRNAs were cloned into a single destination vector, pMpGE_EN04 and pBC-GE14 (**Table 1**) (Sugano et al., 2014, 2018).

YEAST-TWO HYBRID ASSAYS

The full length of *M. polymorpha* and *A. thaliana* ZOU and ICE1 proteins were expressed as fusions to the GAL4 DNA binding domain (bait constructs) or with the GAL4 transcriptional activation domain (prey constructs) and cloned into pGBKT7-GW or pGADT7-GW (Lu et al. 2010). The truncation of AtICE1, MpICE1 and MpICE2 was respectively residues 263-494, 443-710 and 389-692, based on Denay et al. 2014 for AtICE1 and on the alignment of AtICE1-T, MpICE1 and MpICE2. Matchmaker Y2HGold Yeast was co-transformed with bait and prey plasmids and transformants were selected on media lacking leucine and tryptophan

(-LW). Interaction of bait and prey constructs resulted in activation of reporter genes for histidine and adenine synthesis (-LWHA).

CLONING

Promoter regions of MpZOU1, MpZOU2, MpICE1 and MpICE2 were cloned using Gateway technology (Invitrogen). 5kb of regulatory sequences upstream of the start codon of the *MpZOU2* genes was PCR-amplified using MpZOU2_Prom_F and MpZOU2_Prom_3R primers for MpZOU2, cloned into pENTRDTOPO. From the resulting vector, *MpZOU2* promoter was introduced into pDONR221 using Topoisomerase I mediated ligation. 5kb of regulatory sequences upstream of the start codon of the *MpZOU1* genes was PCR-amplified using YT5F and YT5R primers with the Gateway extensions attB1-B2 and cloned by BP reaction into pDONR221 vector (**Table1**). 6.7kb and 5.3kb of regulatory sequences upstream of the start codon of *MpICE1* and *MpICE2* respectively genes were PCR-amplified using the pMpICE1b-F and pMpICE1b-R primers for *MpICE1* or the pMpICE1a-F and pMpICE1a-R primers for *MpICE2* with the Gateway extensions attB1-B2 and cloned by BP reaction into pDONR221 vector (**Table1**). Plasmids were purified and the expression vectors containing the transcriptional constructs were obtained by recombination with the destination vector pMpGWB104 or pMpGWB116 (Ishizaki et al., 2015) in LR clonase mediated reaction following the manufacturer's instructions.

For *Mpzou2* complementation, *MpZOU2* promoter and *MpZOU2* CDS PCR-amplified with and recombined in pMpGWB301 (Ishizaki et al., 2015) using Gibson Assembly mix (Biolab). Primers were designed with NEBuilder assembly tool: YT67F and YT67R for *MpZOU2* promoter and YT68F and YT68R for *MpZOU2* CDS (**Table 1**).

***M. POLYMORPHA* SPORELING TRANSFORMATION AND *A.THALIANA* FLORAL DIPPING TRANSFORMATION.**

M. polymorpha spores from Tak-2 x Tak-1 crosses, (approximatively 5 sporangia per transformation) were sterilised for 15minutes with 0.1% sodium hypochlorite (NaDCC) solution, spun for 1 minute at maximum speed in a microcentrifuge, resuspended in 500µL of water and grown 7 days into 50mL of OM51C (Takenaka 2000) liquid media under 130 rpm. agitation at 22°C, 16 hours light. *Agrobacterium*-mediated transformation of 7 day-old germinated spores was performed as previously described in Ishizaki 2008 unless otherwise described. Resulting cells were incubated under 16 hours light, 22°C. Gemmae from the second generation were subjected to further analysis. Sporeling transformation was performed for all constructs except for generating the Mp*zou2* complementation lines which required thallus transformation as described in (Kubota et al., 2013).

Constructs s of interest for the complementation of Mp*ICE* and Mp*ZOU* genes in *A. thaliana*, were electroporated into *Agrobacterium tumefaciens* strain GV3101 mp90. Bacteria were plated at high density onto Yeast Extract Broth (5g/L Beef extract, 1g/L Yeast extract, 5g/L Peptone, 5g/L Sucrose, 15g/L Bacto Agar) plates with the suitable antibiotics and incubated 2 days at 28°C. Bacteria were scraped off plates, suspended in 30mL of infiltration solution (MgCl2 10mM, sucrose 5% and Silwet-L-77 0.03%) and further diluted with 120mL of infiltration solution. At*ice1-2* or At*zou-4* flower buds were dipped in the bacterial solution for 10s, with gentle agitation, covered with plastic bags for 24h and allowed to set seeds. Primary transformants were selected on solid MS medium containing suitable antibiotics and then transferred to soil. T1 and T2 generation plants were selected on agar-solidified MS with antibiotics. T2 lines were genotyped and subjected to phenotypic and molecular analyses.

SEED-SHAPE ANALYSIS

Percentages of misshapen seeds were counted from images taken with the VHX900F digital microscope (Keyence), using the cell counter extension of the ImageJ software. For each genotype, seeds from 4 distinct mother plants were analysed with approximately 1000 seeds analysed per mother plant.

QUALITATIVE AND QUANTITATIVE ANALYSIS OF TOLUIDINE BLUE PERMEABILITY

To assess cuticle integrity, toluidine blue staining assays were performed (Tanaka et al., 2004). For qualitative toluidine blue staining tests, etiolated seedlings were used. Seedlings were stratified in the dark, exposed to a 6h light flash and then grown for 4 days in darkness. They were then stained for 2 min in 0.05% w/v Toluidine blue solution with 0.1% v/v Tween 20 and washed abundantly under tap water. Pictures were taken with a Keyence VHX900F digital microscope.

For quantitative toluidine blue staining test, 7-day old light-grown seedlings were stained in the same way. In order to extract toluidine blue and chlorophyll, the cotyledons of ten seedlings were collected and placed in 1mL of 80% ethanol for at least 3 hours in darkness. Toluidine blue content of the resulting solution was measured at 626nm with a spectrophotometer. This absorbance was then normalized using chlorophyll absorbance at 430nm, a wavelength not absorbed by toluidine blue. 6 repetitions were performed per condition (Xing et al., 2013).

HISTOCHEMICAL STAINING FOR GUS ACTIVITY OF WHOLE MOUNT THALLUS

Mp*ZOU1*, Mp*ZOU2*, Mp*ICE1* and Mp*ICE2* promoters were cloned into the pMpGWB104 vector and subsequently Tak2xTak2 spores were transformed (Ishizaki et al., 2015). Histochemical assays for GUS activity were performed according to Jefferson et al., 1987 with some minor modifications. Briefly, after three 20 minute vacuum infiltrations with the GUS staining solution (50mM sodium phosphate buffer, pH 7.2 ; 0.5mM potassium-ferrocyanide; 0.5mM potassium-ferricyanide; 10mM EDTA; 0.01% Triton ; 1mM 5-bromo-4-cloro-3-indolyl-Beta-glucuronic acid (Duchefa Biochemie, CAS number 114162-64-0), plants were incubated overnight at 37°C. They were then dehydrated by incubation in increasing concentrations of Ethanol (15%, 30%, 50%), for 20 minutes (per bath) at room temperature. Plants were then fixed in FAA fixative solution (10% formaldehyde, 5% acetic acid, 50% ethanol) for 45 minutes under vacuum followed by either 2 hours at room temperature or overnight at 4°C. Dehydration steps to remove the chlorophyll were then performed by incubation in further increasing concentrations in Ethanol (50%, 70%, 100%), for 20 minutes per bath at room temperature. Observations of GUS activity were made using a Keyence VHX900F digital microscope.

HISTOCHEMICAL STAINING FOR GUS ACTIVITY OF VIBRATOME-SECTIONED THALLUS

15 to 20 day-old transcriptional reporter lines (described in the previous section) were harvested and placed into a small plate. 5% Phytagel (Sigma CAS : 71010-52-1 ; P8169) at 50°-60°C was then poured onto the plants. The plate was then stored for 30 min to 1hour at 4°C to cool down before mounted onto the Leica VT1000 S Microtome. Approximately 10µm sections were performed and placed into 1%PBS solution before staining as described above. Observations of GUS activity were made using a Keyence VHX900F digital microscope.

CONFOCAL MICROSCOPY

Expression of proMpZOU1:TdTomato, proMpZOU2:TdTomato, proMpICE1:TdTomato and proMpICE2:TdTomato 10-day-old thallus were analysed by confocal microscopy using the SP8 Leica confocal microscope (Emission 581nm, Excitation 554nm).

HISTOCHEMICAL STAINING WITH NILE RED AND DIPHENYLBORINIC ACID

Mature gemmae were harvested directly from the gemmae cups and placed in filter baskets. Nile Red staining solution was prepared to contain 2µg/mL Nile Red (CAS number

7385-67-3) diluted in 50mM PIPES (SIGMA, CAS number 100037-69-2) at pH 7.0. Gemmae were incubated in this solution for 20 minutes at room temperature and then washed three times with water. Gemmae were mounted on slides and imaged with a LSM700 microscope (Leica) or SP8 confocal microscope (Leica) (553nm for excitation and 637nm for emission).

A similar staining procedure was used for Diphenylborinic acid as described in Corona-Carrillo et al., 2014. The staining solution was prepared to contain 0.5% of Diphenylborinic acid (CAS number 524-95-8) diluted in Ethyl acetate (CAS number 141-78-6). Gemmae were treated 10 minutes in ethyl acetate and the staining solution was then poured onto the gemmae for 10 minutes at room temperature and then washed three times successively with water. Gemmae were mounted on slides and imaged with a LSM700 microscope (Leica) or SP8 confocal microscope (Leica) (365nm for excitation and 418nm for emission)(Corona-Carrillo et al., 2014; Dimakos et al., 2016; Reich et al., 2006).

TRANSMISSION ELECTRON MICROSCOPY

Gemmae collected from 1month old mother plants of Mp*zou1* Mp*zou2-db5*, Mp*ice1* Mp*ice2-db1* and Tak2xTak1 progeny were directly immerged into the fixative solution composed of 3% glutaraldéhyde and 1% PFA. Gemmae was then fixed a second time following the OTO-fixation described in (Deerinck et al., 2010). EPON resin was used to embed the samples which were then sectioned by the serial-block-face module and imaged by scanning with the Zeiss Sigma VP300 (Gatan inc.) microscope at 4kV.

RNA EXTRACTION AND RNA-SEQUENCING

Gemmae from approximately 10 gemmae cups of Tak2xTak1 progeny, Mp*zou2-3*, Mp*zou1*Mp*zou2-5* thallus were harvested and frozen in liquid nitrogen before RNA extraction. In each case, three independent RNA samples were extracted for each genotype (1 RNA sample equals gemmae from approximately 10 gemmae cups). Gemmae were ground with two beads using the TissueLyser (1min, frequency 30/sec). Total RNAs were extracted in TRIzol. Briefly, 1mL of TRIzol were added in each tubes before the samples thawed and then were vortexed. After centrifugation (12,000 rpm, 10min, 4°C) ethanol was added to the supernatant to a final concentration of 35%. RNAs were purified using silica spin columns from Qiagen Plant RNA extraction kits. The rest of the RNA extraction was done according to the manufacturer's instructions. Genomic DNA contamination was removed from total RNA samples using the Turbo DNA-free DNase I (Ambion) according to the manufacturer's instructions. RNA integrity and quantity were checked using an Agilent Bioanalyzer 2100.

Sequencing of the 9 samples was carried out on an Illumina NextSeq 500 sequencer, using single end mode, leading to 50-54 million reads per sample, of length 75 bp.

Current reference genome sequence for *Marchantia polymorpha*, MpTak1v5.1 (Montgomery et al., 2020) has been built from a male individual. To allow a correct mapping of RNA-seq reads from both female and male individuals, we added to this genome sequence the scaffolds described to be specific to females from a previous version of the reference genome sequence (JGI v3.1, (Bowman et al., 2017), scaffolds 17, 18, 210, 227, 240, 250 and 497).

Reads were checked for quality and absence of adapters and contaminants with FastQC v0.11.9 (https://www.bioinformatics.babraham.ac.uk/projects/fastqc/). They were then mapped on the genome sequence using HISAT2 (Kim et al., 2015), in two-pass mode, using the reference genome annotation: a first mapping was performed with the complete dataset to discover putative new splice junction, before the per-sample mapping. Reads per gene were counted using FeatureCounts v1.5.1 (Liao et al., 2014). DESeq2 version 1.28.1 (Love et al., 2014) was used with R version 4.0.2 to perform the principal component analysis and the differential gene expression analysis. Genes having less than 6 reads in the sum of all samples were considered as non-expressed and discarded.

Mapping reads on a genome sequence containing both chromosomes U and V could theoretically lead to irrelevant results, for example in the presence of a pseudo-autosomal region or of scattered homologous genes (Bowman et al., 2017) having high sequence similarities between female and male genomes. To assess the specificity of reads matching on sex-determining chromosomes, we ran HISAT2 1000 times with a random seed and counted reads matching equally well U and V chromosomes. We observed an average of 45 of those reads in each sample, while at the same time an average of 125,000 reads was specific to chromosomes U or V, so we considered they would have a neglectable effect on the differential analysis.

CUTIN COMPOSITIONAL ANALYSIS

Protocol for cutin monomers analysis was adapted from Elejalde-Palmett et al., 2021; Li-Beisson et al., 2013 and Renault et al., 2017. Gemmae from Tak2xTak1 progeny, Mp*zou2-3*, Mp*zou1*Mp*zou2-db5*, Mp*ice2-6*, Mp*ice1*Mp*ice2-db1* mutants were harvested from the cups of 4-week-old thallus to have a minimum 10mg of lyophilised material per genotype. For each sample, about 10 mg of ground, lyophilized gemmae tissue was added to a pre-weighed 12 ml glass tube for processing. The tissue was delipidated by extensive washing with a series of

solvents, as follows. A total of 5 ml of isopropanol pre-heated to 85 °C was added to each sample and incubated at 85 °C for 10 min, then after cooling to room temperature, the samples were shaken at 1000 r.p.m. for 1h and centrifuged at 1,500g for 2 min to pellet most of the tissue. The supernatant was removed with a glass Pasteur pipette. The tissue was then washed with the following series of solvents: 2:1 chloroform: methanol, 1:1 chloroform: methanol, 1:2 chloroform: methanol, pure methanol. The samples were agitated with each of these solvents at 1000 r.p.m. for at least 1h and up to overnight, with centrifugation (as described above) after each wash. The tissue was then dried in SpeedVac at 40°C for 1h. The glass tube was weighed to determine the dry, delipidated tissue weight. A total of 1 ml of reaction medium (12:3:5 methanol: methyl acetate: 25% sodium methoxide) and 5 µg heptadecanoic acid and 10 µg pentadecalactone (internal standards) were added to each sample, and the mixture was then heated at 60 °C for 2h to depolymerize the cutin. The samples were then cooled to room temperature and 2 ml dichloromethane, 0.25 ml glacial acetic acid and 0.5 ml 0.9% NaCl in 100 mM Tris (pH 8.0) was added to each and vortexed to mix. Two phases were separated by centrifugation for 2 min at 1,500g. The lower, organic phase was transferred to a new vial and 1 ml of 0.9% NaCl in 100 mM Tris (pH 8.0) was added and mixed by vortexing. Two phases were again separated by centrifugation (2 min at 1,500g). Lower phase was recovered and dried on 0.5 g anhydrous sodium into a clean vial to remove any residual water. Each cutin sample was dried under a stream of nitrogen, then derivatized with 50 µl each of pyridine and N,O-bis(trimethylsilyl)trifluoroacetamide for 10 min at 90 °C. The samples were analysed by gas chromatography (GC) using an Agilent GC8890 coupled to a Leco Pegasus BT time-of-flight mass spectrometer. Data were analyzed with the ChromaTOF software, which was used to identify compounds in NIST chemical libray based on both retention index and fragmentation spectrum, and to calculate peak area from compound-specific extracted ion chromatogram. Peak areas were normalized to the internal standards and the dry, delipidated tissue weights.

Discussion

Our work has revealed a potentially very ancient and conserved role for ZOU/ICE complexes in cuticle development in land plants. Our results suggest that both the MpZOU2/MpICE1 and MpZOU2/MpICE2 complexes control the formation of the phenolic-enriched cuticle of gemmae in *M. polymorpha*.

REDUNDANCY OF ICE PROTEINS

Our results show that both MpICE proteins can interact with both MpZOU proteins in yeast. We show that the Mp*ICE1* and Mp*ICE2* expression patterns overlap in the dorsal epidermis of *M. polymorpha* thallus. Consistent with functional redundancy between the MpICE proteins, the Mp*ice1* Mp*ice2* double mutant shows a stronger cuticle phenotype in gemmae (as shown by staining) than either single mutant. A similar situation has been observed in *A. thaliana*, where AtICE1 and AtICE2 act redundantly during stomatal development (Kanaoka et al., 2008c). In this developmental pathway, both AtICE1 and AtICE2 form heterodimers sequentially with the key transcription factors SPEECHLESS, MUTE and FAMA. Similarly, to our observations in *M. polymorpha* for cuticle production in Mp*ice1* and Mp*ice2*, both At*ice1* and At*ice2* single mutants still produce functional stomata although At*ice1* has a stronger phenotype than At*ice2*. However, the double mutant At*ice1* At*ice2* does not produce any stomata. *Brachypodium,* another Brassicae*,* encodes two ICE proteins which, similar to *A. thaliana* also result from the Brassicae-specific duplication. However, unlike in *A. thaliana*, the loss of only *BdICE1* results in the total loss of stomata. *BdICE2* is nevertheless required for stomatal developmat but at a late stage of stomatal differentiation and function (Raissig et al., 2016).

The redundancy of ICE1 and ICE2 during seed development in *A. thaliana* has recently been studied (Loue-Manifel et al. in preparation, **Chapter 3**). The results of this work highlight the importance of understanding the tissue specific regulatory relationships between related transcription factors when drawing conclusions regarding the presence or absence of functional redundancy between family members. Finally, in a context of significant potential post-translational regulation (Ding et al., 2015; Dong et al., 2006; Li et al., 2017; Miura et al., 2007; Putarjunan et al., 2019) it is also important to bear in mind that the overlaps in gene expression highlighted in this article only reflect the RNAs levels due to the use of transcriptional reporter lines.

In *M. polymorpha*, the apparent redundancy observed for MpICE proteins does not appear to exist for MpZOU proteins. Despite the fact that the expression pattern of Mp*ZOU1* and Mp*ZOU2* overlap and that, furthermore, both genes could complement the At*zou* mutant, suggesting that their molecular mechanism of action could be similar, we found that the cuticle defects of Mp*zou1* Mp*zou2* double mutant appears very similar to those of Mp*zou2* single mutants. Our transcriptomics suggest that this apparent redundancy is not due to transcriptional regulation of Mp*ZOU1* by MpZOU2, since no reduction of expression of Mp*ZOU1* is observed in Mp*zou2* mutants. However, such a regulation cannot be completely

excluded since the strong ventral expression of Mp*ZOU1* might mask changes in gene expression in the dorsal epidermis.

As is the case in *M. polymorpha*, two At*ZOU* orthologues have been found both in rice and in soybean. However, in both cases, only one of the two genes (*OsZOU-1* in rice and *GmZOU-1* in soybean) is capable of (partial) complementation of the At*zou* mutants, suggesting that the molecular mechanisms underlying ZOU protein functions may diverge extensively in the Angiosperm lineage (Dou et al., 2018; Zhang et al., 2017). However, double mutants lacking these genes have not yet been characterized.

HOW DOES THE MPZOU2/ICE COMPLEX REGULATE CUTICLE DEVELOPMENT?

In *A. thaliana*, and in other species where ZOU and/or ICE function has been studied, little evidence exists to suggest that ZOU/ICE complexes directly regulate the biosynthesis of aliphatic cuticle components (Creff et al., 2019; Denay et al., 2014; Xing et al., 2013; Yang et al., 2008). Indeed, in *A. thaliana* it appears that one of the main functions of ZOU/ICE1 in regulating cuticle development is to ensure the correct production of the ALE1 protein, which is, in turn, necessary for cuticle integrity monitoring (Creff et al., 2019; Doll et al., 2020). Although three genes identified by Bowman and colleagues as orthologues of key genes in *A. thaliana* cuticle biogenesis were present in our transcriptomic dataset (Bowman et al., 2017), only one (an orthologue of *A. thaliana* glycerol-3-phosphate acyltransferase 6 (GPAT6)) can be truly considered to be potentially involved in cutin biosynthesis. The other two encode an ABC transporter and a Cutin Synthase (CUS), potentially involved in cutin monomer export and cuticle assembly respectively. Interestingly many more genes potentially involved in cell wall modification and/or the polymerization of phenolic monomers are downregulated in Mp*zou* mutants, than genes involved in aliphatic cuticle biosynthesis.

In terms of cell wall modification, a large number of genes encoding proteins with potential Xyloglucan Endo-transglycosylase activities, as well as pectin remodelling enzymes were identified as down regulated in mutants. Recent research has shown that pectins, xylans and xyloglucans may be intimately associated with the cutin of angiosperms, and that this association may be critical for the coordination of organ growth and cuticle deposition. ZOU/ICE1 could therefore play important regulatory roles in this process, potentially explaining the fragmented appearance of mutant cuticles (Hama et al., 2019; Philippe et al., 2020; Xin and Fry, 2021).

The second major group of genes down-regulated in plants lacking Mp*ZOU2* are genes encoding proteins that have been associated with defects in the deposition and/or oxidative

polymerization of the Lignin-rich Casparian strip in the *A. thaliana* root. These include several members of the UCLACYCLIN-like protein family (Plastocyanin domain-containing) , required in *A. thaliana* for the deposition of a specific lignified Casparian strip zone (Reyt et al., 2020), dirigent proteins (Hosmani et al., 2013) and secreted peroxidases similar to ones involved in the Reactive Oxygen Species (ROS)-mediated polymerization of lignin in the early Casparian strip (Fujita et al., 2020; Lee et al., 2013; Rojas-Murcia et al., 2020).

In addition to these peroxidases, which should, through their activity also act to detoxify apoplastic ROS, other proteins implicated in apoplastic ROS homeostasis including a catalase and several polyphenol-oxidases and tyrosinases and well as many other genes involved in the biosynthesis of secondary metabolites such as flavonoids, potentially implicated in ROS scavenging, particularly in Bryophytes, were downregulated (Chapman et al., 2019; Davies et al., 2020).

These findings could suggest that altering ZOU/ICE1 activity alters apoplastic REDOX homeostasis, and potentially the polymerization of aromatic components within the cell wall. This possibility is exciting since, in *A.thaliana*, the GASSHO1 receptor kinase implicated in embryo cuticle monitoring together with ALE1 is known, in the root endodermis, to act in lignin polymerization through the production of apoplastic ROS (Fujita et al., 2020).

The fact that our results suggest that the *M. polymorpha* cuticle, like that of *P. patens*, is enriched in phenolic components therefore opens the exciting possibility that ROS production could be a key function of MpZOU2/MpICE activity, and that ROS are subsequently implicated in the polymerization of phenolic cuticle components. The formation of a phenolic "scaffold" could, in turn, be necessary for directing the deposition of aliphatic components, similar to the situation in the root endodermis of *A. thaliana*, in which suberin deposition appears, to some extent, to depend upon lignin polymerization (Lee et al., 2013). It is important to note that the biochemical analysis carried out in the context of this work involves extensive delipidation and hydrolysis steps optimised to release monomers from polymerized plant cuticles. It is not clear to what extent a defect in polymerization might be revealed using this technique, since non-incorporated components are likely to be lost before analysis. In addition, some polymerization products involving phenolic components, or, potentially, cell wall proteins such as extensins, would not necessarily be detected in the analysis.

Finally, it is interesting to note that one of the genes down-regulated in the Mp*zou2* and Mp*zou1* Mp*zou2* double mutant encodes a protein closely related to AtKRS, a cysteine rich peptide implicated in embryo sheath formation in the seed (Moussu et al., 2017). At*KRS* expression is completely eliminated in At*zou* mutants. The STIG domain of the related protein AtGRIM REAPER has been proposed to be involved in ROS sensing (Wrzaczek et al., 2009),

further underlining links to ROS homeostasis. The embryo sheath is a structure enriched in epitopes specifically identified by anti-extensin antibodies, and two genes encoding EXTENSIN-like proteins also appear in our list of down regulated genes. Since extensins are known to undergo peroxidase-mediated oxidative polymerisation (Mishler-Elmore et al., 2021), it is therefore possible that these proteins are also targets of proposed ROS production downstream of ZOU/ICE activity. Further studies of extensin deposition in *M. polymorpha* gemmae and cuticles will be required to address this question such as immunolocalization with anti-extensins and ROS staining on the different mutants. CRISPR-Cas9 mutant of the closed homologue of AtKRS will also be generated as corresponding reporter lines.

Bibliography

See general bibliography at the end of the thesis.

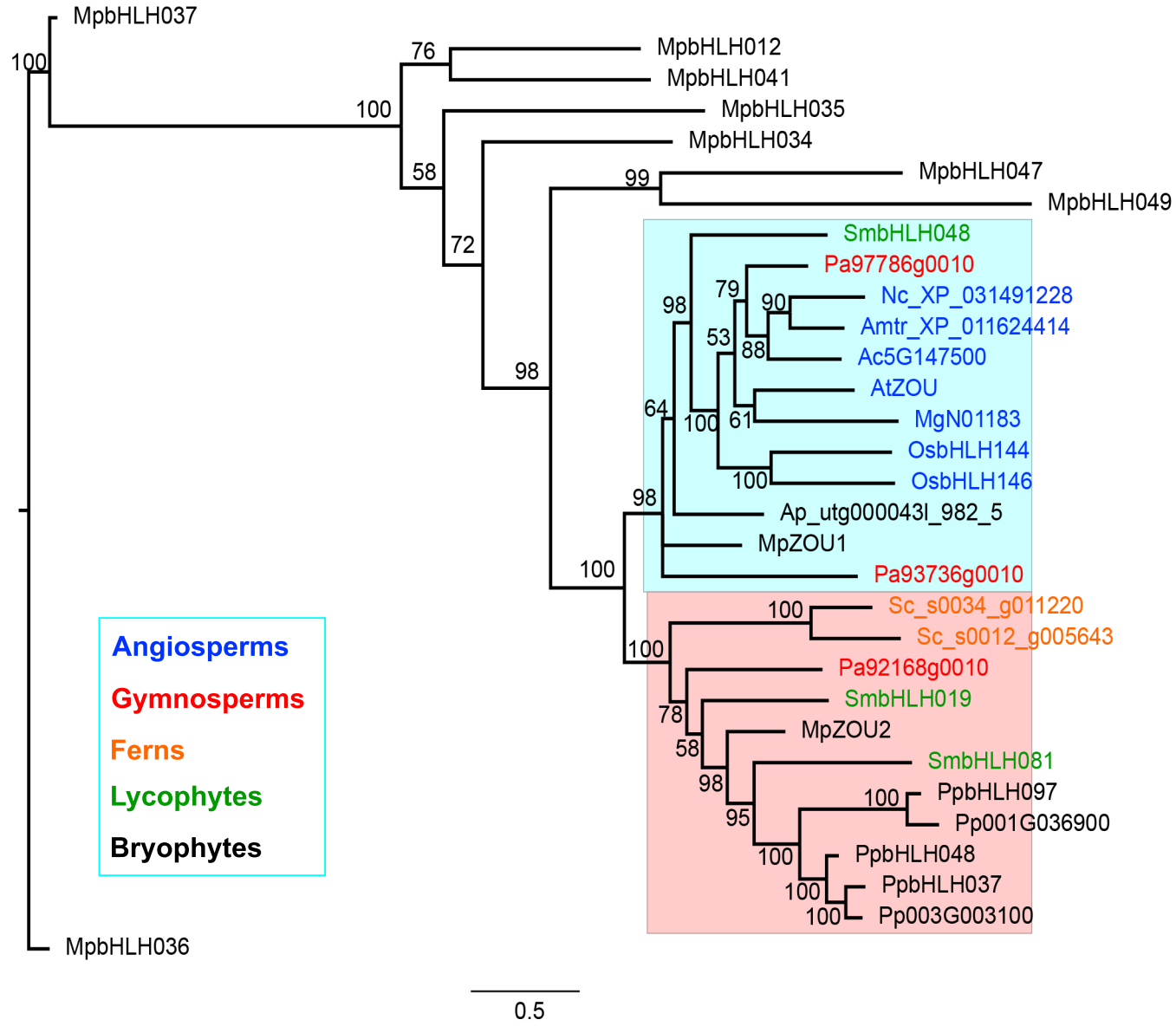

Figure S1 Phylogeny of land plant *ZOU* genes.
Bayesian phylogeny, rooted on MpbHLH36, with percent probabilities indicated on branches. The clade containing the *AtZOU* orthologues is highlighted in light blue, the ZOU2 clade containing an ancient paralogue in cerise. ZOU2 is not conserved in angiosperms, whereas mosses and ferns lack ZOU1. Where available the numbering of bHLHs follows that of Pires et al. Species abbreviations are At *Arabidopsis thaliana*, Mg *Mimulus guttifera*, Ac *Aquilegia coerula*, Nc *Nymphae colorata*, Amtr *Amborella trichopada*, Pa *Picea abies*, Sc *Salvinia cucullata*, Sm *Selaginella moellendorffii*, Aa *Anthoceros punctatus*, Pp *Physcomitrella patens*, Mp *Marchantia polymorpha*. Different taxonomic groupings coloured as shown in box on left.

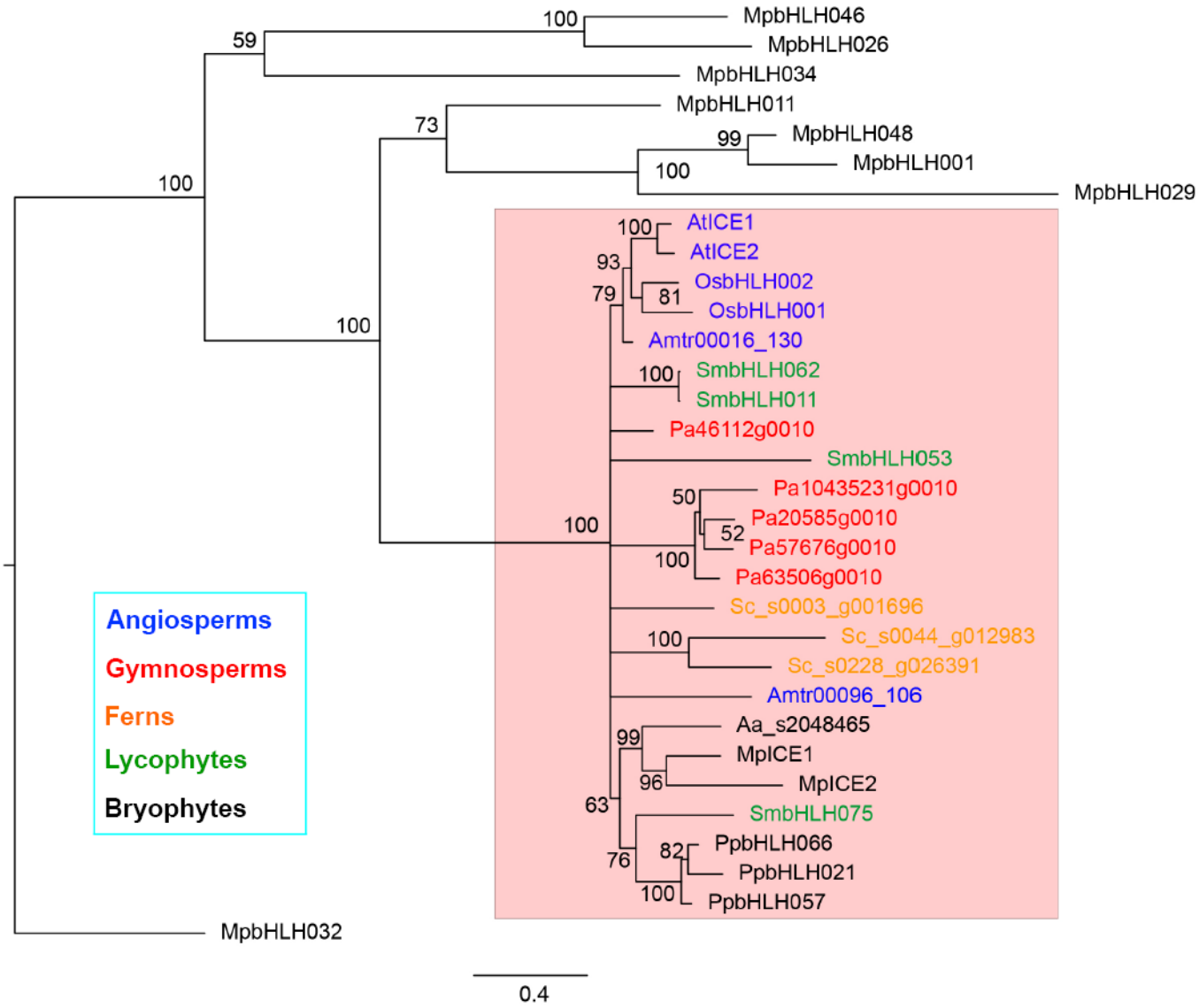

Figure S2 : Phylogeny of land plant ICE genes.
Bayesian phylogeny, rooted on MpbHLH032, with percent probabilities indicated on branches. The clade containing the *AtICE1* and *AtICE2* orthologues is highlighted in cerise. Species abbreviations are At *Arabidopsis thaliana*, Mg *Mimulus guttifera*, Ac *Aquilegia coerula*, Os, *Oryza sativa*, Nc *Nymphae colorata*, Amtr *Amborella trichopada*, Pa *Picea abies*, Sc *Salvinia cucullata*, Sm *Selaginella moellendorffii*, Aa *Anthoceros punctatus*, Pp *Physcomitrella patens*, Mp *Marchantia polymorpha*. Different taxonomic groupings coloured as shown in box on left.

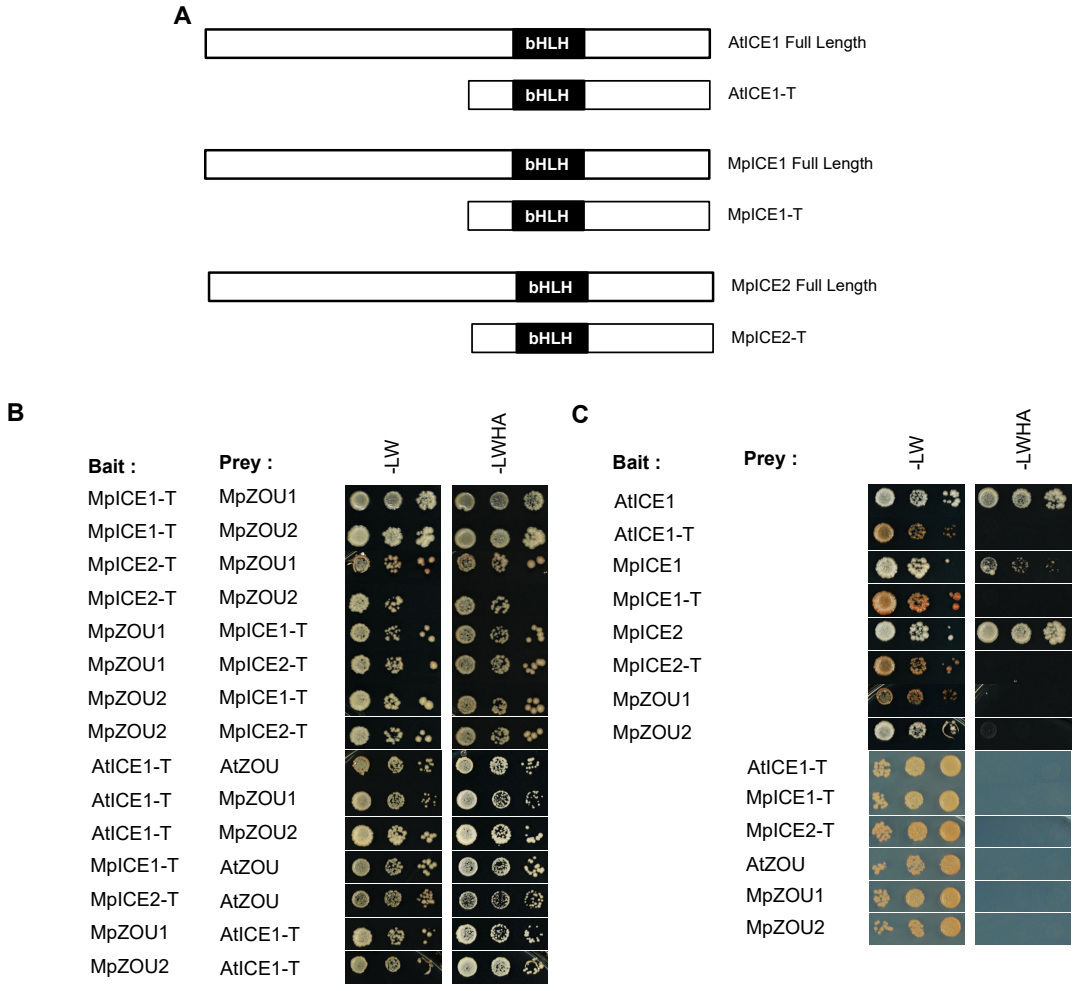

Figure S3 : Both MpZOU and both MpICE interact in yeast two hybrids.
(A) The MpICE proteins used in yeast two hybrids experiments : MpICE1-T and MpICE2-T are the truncated versions of MpICE1 and MpICE2 proteins respectively. (B-C) Interactions tested in yeast. Growth on minimal non selective (-LW) and selective (-LWHA) media is shown. (B) Yeast two hybrids show the interaction of both MpZOU with both MpICE. Both MpICE interact with AtZOU and both MpZOU interact with AtICE1. (C) Empty boxes indicate empty vector controls showing the autoactivation of the full length proteins of AtICE1, MpICE1 and MpICE2 but not of the respective truncated versions.The three dots of yeast are from the left to the right, no dilution, 1/10 dilution and 1/100 dilution.

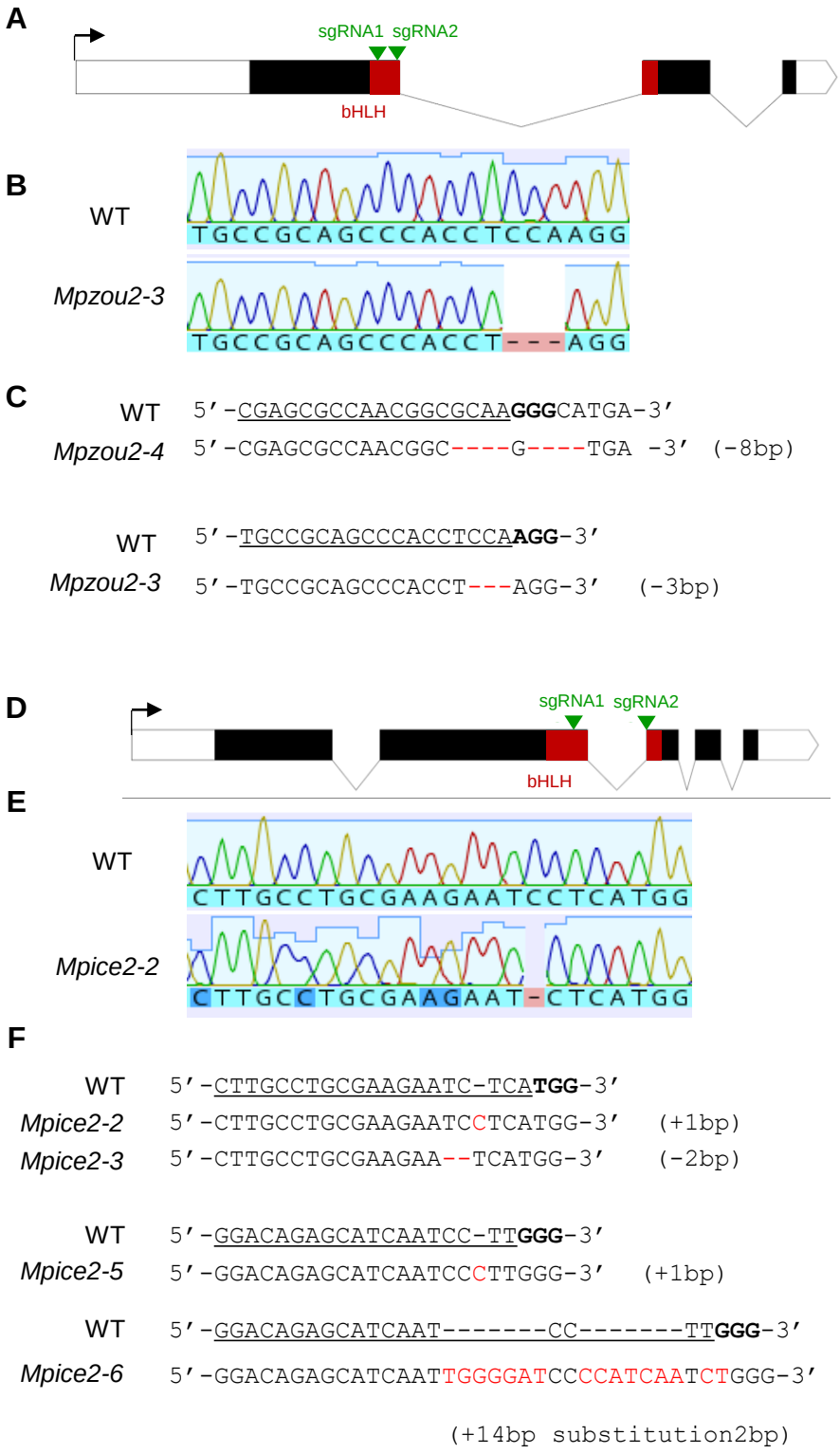

Figure S4: Mutant alleles produced by genome editing.
(A) Schematic of Mp*ZOU2* gene, filled rectangles indicate exons, untranslated regions are shown in blue and coding sequences in red. sgRNA1 and 2 target basic and loop regions of bHLH domain, respectively. (B) Chromatograms showing sequence alteration in Mp*zou2-1* allele. (C) Sequence of Mp*zou2* alleles. The sgRNA sequence is underlined in wild type (WT) and the PAM sequence shown in bold. The alleles were generated with sgRNA1 or sgRNA2. (D) Schematic of Mp*ICE2* gene, sgRNA targets basic region of bHLH domain. (E) Chromatograms showing sequence alteration in Mp*ice2-2* allele. (F) Sequence of Mp*ice2* alleles. The sgRNA sequence is underlined in wild type (WT) and the PAM sequence shown in bold. The alleles Mp*ice2-2* and Mp*ice2-3* were generated with sgRNA1 and Mp*ice2-5* and Mp*ice2-6* were generated with sgRNA2.

A

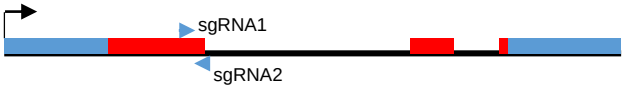

B

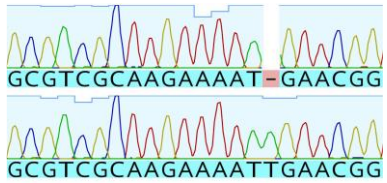

C

```
WT          5′-GCGTCGCAAGAAAA-TGAACGG-3′
Mpzou1-1    5′-GCGTCGCAAGAAAATTGAACGG-3′   (+1bp)
Mpzou1-5    5′-GCGTCGCAAGAAAATTGAACGG-3′   (+1bp)

WT          5′-GCGTCGCAAGAAAATG----------AACGG-3′
Mpzou1-6    5′-GCGTCGCAAGAAAATGTTCTCCACGTT-ACGG-3′   (+11bp -1bp = +10bp)

WT          5′-ATCACCTTGGAGTTGAGATGG-3′
Mpzou1-2    5′-ATCACCTTG-----GAGATGG-3′    (-5bp)
```

D



E

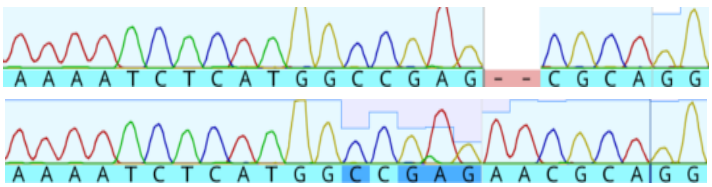

F

```
WT          5′-AAAATCTCATGGCCGA--------GCGCAGG-3′
Mpice1-2    5′-AAAATCTCATGGCCGAAAAATTCTGCGCAGG-3′  (+8bp)

WT          5′-AAAATCTCATGGCCGAG--CGCAGG-3′
Mpice1-4    5′-AAAATCTCATGGCCGAGT-CGCAGG-3′   (+1bp)
Mpice1-5    5′-AAAATCTCATGGCCGAGAACGCAGG-3′   (+2bp)

WT          5′-AAAATCTCA--------------------------------TGGCCGAGCGCAGG-3′
Mpice1-6    5′-AAAATCTCAGATTCATAAAATGAGATTCATAAAAATCTCAT--------CGCAGG-3′
            (+32bp -8bp = +24bp)
```

Figure S5: Mutant alleles produced by genome editing
(A) Schematic of Mp*ZOU1* gene, filled rectangles indicate exons, untranslated regions are shown in blue and coding sequences in red. sgRNA1 and 2 target basic and loop regions of bHLH domain, respectively. (B) Chromatograms showing sequence alteration in Mp*zou1-1* allele. (C) Sequence of Mp*zou1* alleles. The sgRNA sequence is underlined in wild type (WT) and the PAM sequence shown in bold. Mp*zou1-1* and Mp*zou1-5* have the same lesion but were independent isolates. The alleles were generated with sgRNA1 except Mp*zou1-2* which was from sgRNA2. (D) Schematic of Mp*ICE1* gene, sgRNA targets basic region of bHLH domain. (E) Chromatograms showing sequence alteration in Mp*ice1-5* allele. (F) Sequence of Mp*ice1* alleles. The sgRNA sequence is underlined in wild type (WT) and the PAM sequence shown in bold. The alleles were generated with sgRNA1.



Figure S6: Alignment of STIG1 domain of the 20 *M. polymorpha* STIG1-like proteins with the two *A. thaliana* STIG1 domains of KERBEROS and GRIM REAPER.

Alignment of the STIG1 sequence domains (highlighted in green) of the 20 MpSTIG1-like proteins with the two STIG1 domains of AtKERBEROS (AT1G50650-KRS) and AtGRIM REAPER (AT1G53130-GRI). The conserved cysteine residues in the STIG1 domains are highlighted in yellow. Red text is one of the genes down-regulated in the Mp*zou2* and Mp*zou1* Mp*zou2* double mutant encodes a protein closely related to AtKERBEROS. Blue text is one STIG1-like protein found down-regulated in the Mp*zou1* mutant.

Gene ID	*Annotations*	*L2FC Mpzou2/WT*	*L2FC Mpzou1Mpzou2/WT*
	Top HIT		
Mp3g18230	STIG1 domain	-1,679850021	-4,294301965
Mp2g10330	JA-Ile deactivating enzyme (CYP94B3)	-1,327924162	-0,940423885
Mp3g23170	MYB transcription factor	-2,707818682	-3,571246967
Mp3g07510	MYB transcription factor	-2,549523808	-3,185515099
Mp3g04970	Myb-like domain	-0,728540782	-0,879602916
	Cytochrome P450 related		
Mp6g19120		-3,657957976	-6,353718462
Mp6g11710	Germacradienol synthase / Germacradienol/germacrene-D synthase	-6,204110866	-6,053683434
Mp3g18510	(2Z,6Z)-farnesyl diphosphate synthase / ZFPS	-6,626048223	-5,281864582
Mp2g24750		-2,67491704	-4,685058499
Mp3g18500		-5,313832586	-4,634722289
Mp2g20490	5-epiaristolochene 1,3-dihydroxylase / EAH	-2,579323246	-4,269675605
Mp6g04630		-2,435226268	-3,75907174
Mp6g04600		-1,621785791	-3,460551583
Mp4g05010	Germacradienol synthase	-2,973629418	-3,198944876
Mp6g04320		-2,40527229	-3,085369455
Mp3g03420	AT2G26710.1 (BAS1,CYP72B1,CYP734A1)	-3,990297352	-2,693133848
Mp1g14660	Delta(24)-sterol reductase / Lanosterol Delta(24)-reductase	-1,255666607	-2,263541235
Mp8g14150		-2,914011212	-2,256330317
Mp7g00020		-1,682831136	-1,432359542
Mp1g04680		-0,771255534	-0,93503808
Mp1g25410	Potential ent-kaurenoic acid hydroxylase (KAO) - Gibberellin	-0,669700785	-0,660037592
Mp5g09870		-0,574703374	-0,497470976
	Peroxidases		
Mp5g17590	peroxidase 3 involved in casparian strip liginigcation RCI3	-4,144982045	-6,884261076
Mp5g13790	peroxidase 3 involved in casparian strip liginigcation RCI3	-2,284265005	-5,723168557
Mp7g19380	PRX53,(ascorbate peroxidase)	-3,097263959	-3,883401881
Mp5g04010		-3,604857165	-3,717339956
Mp4g14580	PER56, close to RCI3	-1,88302968	-3,362657017
Mp3g05740		-0,853313689	-3,004393956
Mp5g04000		-2,757875913	-2,881948515

Mp3g16820		-1,39306771	-2,597819369
Mp7g11550		-1,233857366	-1,724011788
	Cuticle related		
Mp8g13940	Cutin synthase	-1,555501731	-3,72514311
Mp8g12130	ABC transporter	-1,492170298	-1,268143618
Mp7g03880	GPAT6	-1,118071118	-2,064602519
	Cell wall modifications		
Mp3g09650	expansin	-5,534844879	-6,338062134
Mp2g18610	expansin	-3,822336091	-6,115673799
Mp3g09760	expansin	-3,429680852	-4,965898663
Mp5g20420	expansin	-2,084121598	-4,408311971
Mp8g18860	expansin	-2,404274208	-4,010961724
Mp4g06560	expansin	-1,56646211	-2,465096368
Mp1g26350	expansin	-1,071819623	-1,415005489
Mp4g01200	xyloglucan	-2,549715885	-4,556374471
Mp8g10190	pectate lyase	-2,080119452	-4,997598966
Mp8g00770	pectate lyase	-2,116247907	-1,343337421
Mp2g08500	EXT	-1,891224815	-3,912913768
	Flavonoids related		
Mp8g12170	Flavonoid 3',5'-hydroxylase	-2,441426329	-4,33476539
Mp8g09770		-3,730585551	-3,990691331
Mp8g10910	Anthocyanidin 3-O-glucosyltransferase	-1,086944081	-3,27859408
Mp5g06850	Flavone 3'-O-methyltransferase	-2,364954888	-2,774292226
Mp5g10800	Flavonoid 3'-monooxygenase	-1,682827538	-2,373857094
Mp5g06840	Flavone 3'-O-methyltransferase	-2,197659759	-2,33355098
Mp3g03440	UDP-GLYCOSYLTRANSFERASE 74C1-RELATED	-1,275111368	-2,294823317
Mp5g00520	Flavonol synthase	-2,979408361	-1,484288026
Mp4g14100	chalcone synthase (CHS)	-1,304809318	-0,753649336
Mp2g23890	Flavonol 3-O-glucosyltransferase	-1,311408514	-0,720219622
Mp5g20040		-2,9247462	-4,247452008
Mp6g17890		-1,810559503	-2,718923901
Mp5g21450		-2,832378901	-2,52059368
Mp6g17910		-2,054544579	-2,471884996

Mp5g14440		-2,410991923	-5,156006114
Mp5g14430		-2,674724977	-5,101156671
Mp5g19990		-2,804233277	-4,222960359
Mp5g20020		-2,733601262	-3,074832776
Mp5g15320		-2,018907212	-2,924461921
Mp8g06340		-1,478012301	-2,410671869
Mp5g21460		-2,244741873	-1,880548245
Mp6g17920		-0,814533533	-0,94227911
Mp6g10200		-1,18691394	-1,343674751
Mp7g01630		-1,226028973	-0,927557394
Mp2g18520		-0,760359516	-0,628892246
	UCLACYCLIN-like protein family		
Mp1g07620	UCC1	-3,356450435	-9,225060402
Mp3g20270	WAK type RLK	-2,479732009	-7,129624909
Mp3g17490	Another UCC	-1,583639863	-5,883546029
Mp2g14890	UCC1-like	-2,936340194	-4,724312999

Table S1 : List of gene dowregulated in Mp*zou2* and/or Mp*zou1*/Mp*zou2* double mutants.
L2FC means Log 2 FoldChange

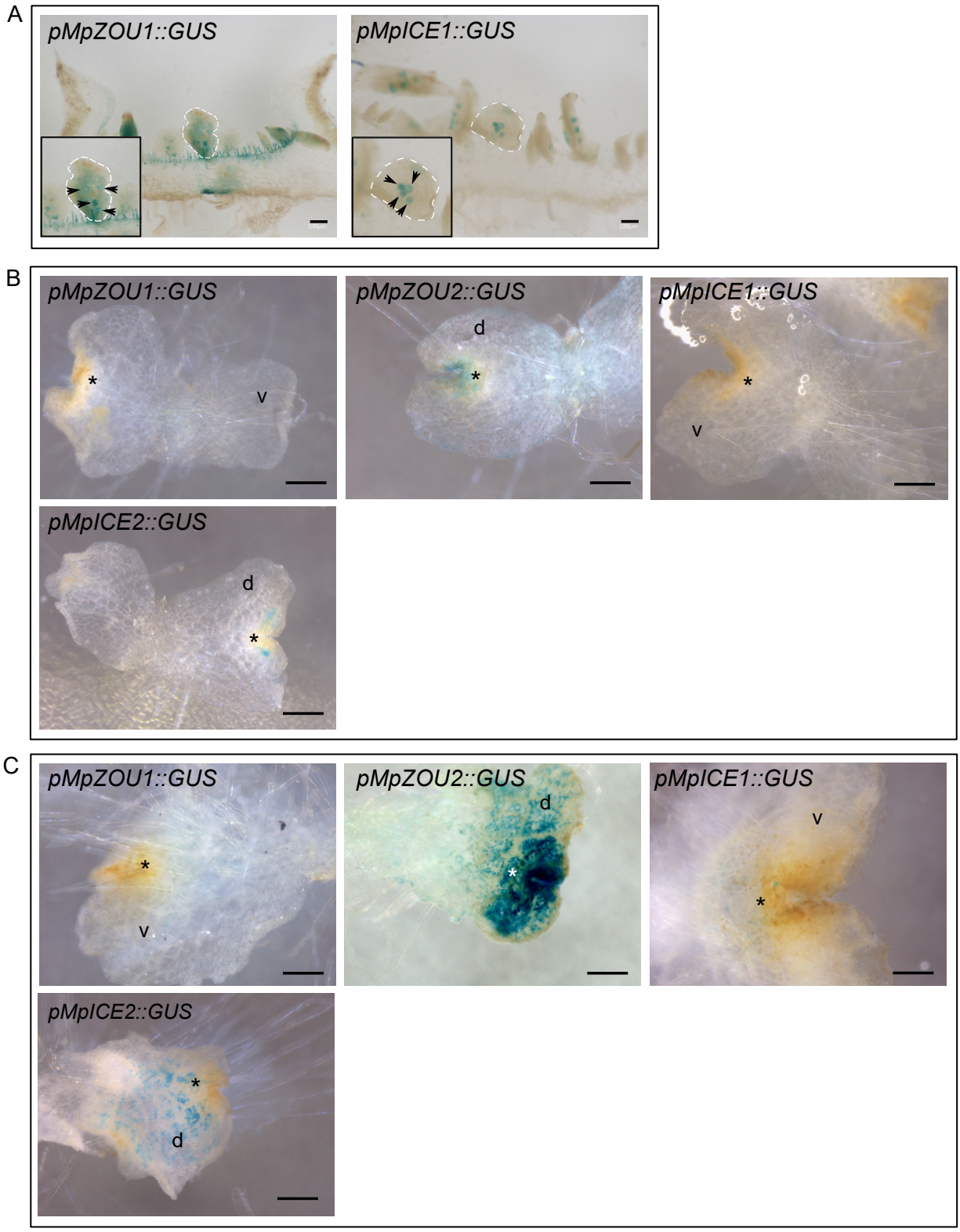

Figure 1: Transcriptional reporter lines of *pMpZOU1::GUS*, *pMpZOU2::GUS*, *pMpICE1::GUS* and *pMpICE2::GUS* show different expression pattern in gemma cup and gemma.
(A) Transverse section in a gemma cup of pMpZOU1:GUS and pMpICE1: GUS showed expression in primary rhizoid cells. Gemmae are surrounded by dashed white lines and the photograph in the left bottom corner is a higher magnification of a gemma; arrowhead indicates primary rhizoid cell. Scale bar, 100µm. (B-C) 3-day old (B) and 5-day old (C) young gemmae of GUS transcriptional reporter lines for *MpZOU1*, *MpZOU2* , *MpICE1* and *MpICE2* genes. In *MpZOU2* and *MpICE2* reporter lines, the GUS staining is limited to the apical notch region and detected in 3-day old gemmae. *MpICE1* promoter activity is also restricted to the region of the apical notch but starts at day 5. The low level of *MpZOU1* promoter activity does not allow to have a clear understanding and temporal expression pattern. v: ventral surface; d: dorsal surface; * apical notch. Scale bar 250µm

II – Do MpICE proteins have other ZOU-dependant roles and ZOU-independent roles?

II.1 Gene expression patterns.

In the work described above, we showed that the expression patterns of *MpZOU1* and *MpICE1* (mainly on the ventral surface of the thallus) differ from those of *MpZOU2* and *MpICE2* (seen mainly on the dorsal surface of the thallus). Nonetheless, these expression patterns seem to overlap slightly. The early post-gemma expression of *MpZOU1*, *MpZOU2, MpICE1* and *MpICE2* was also investigated using the transcriptional reporter lines described above during this thesis. This analysis showed that *MpZOU2* and *MpICE2* expression initiates around the apical notch about 3 days after germination and then spreads out across the dorsal surface of the thallus. *MpICE1* expression starts slightly later than that of *MpICE2* and *MpZOU2*, 5 days after germination around the apical notch and in the rhizoid primordia cells, shortly before pegged rhizoids start to be visible. Interestingly, although the early expression pattern of *MpZOU1* is very similar to that of *MpICE1*, the exact point at which *MpZOU1* expression initiates is less clear (**Figure 1**) (3 days after germination based on the data of Yen-Ting Lu, previous PhD student with J. Goodrich and 5 days after germination based on the data of Jeanne Loue-Manifel). These experiments were carried out under similar environmental conditions, but nonetheless, one possible explanation could be that *MpZOU1* expression is environmentally controlled. In order to confirm the exact expression of both *MpZOU* and *MpICE* genes, qRTPCR at different time points should be carried out.

II.2 Roles in surface formation.

In *A. thaliana*, the ZOU/ICE complex controls embryonic sheath production, likely via control of the production of the peptide KRS, and sheath deposition via control of the production of ALE1 (Moussu et al., 2017). The sheath is deposited outside the embryonic cuticle and incorporates endosperm-derived material rich in extensin-like molecules. Because of the conserved role of ZOU/ICE in suface development of *M. polymorpha* gemma, and that fact that a KRS-like peptide-encoding gene, as well as two extension-n-encoding genes are transcriptionally misregulated in mutants lacking *MpZOU* function, we tested whether immunolabelling of gemmae with anti-extensin antibodies might shed light on a putative KRS-related function in *M. polymorpha*. Immubolabelling with three anti-extensin antibodies, α-LM1, α-JIM12 and α-JIM19 (Lee et al., 2012; Paul Knox et al., 1995; Smallwood et al., 1994, 1994) was been carried out on the double mutants *Mpzou1Mpzou2* and *Mpice1Mpice2* and on wild-type. Although no obvious labelling was observed with α-JIM12 and α-JIM19, α-LM1 anti-

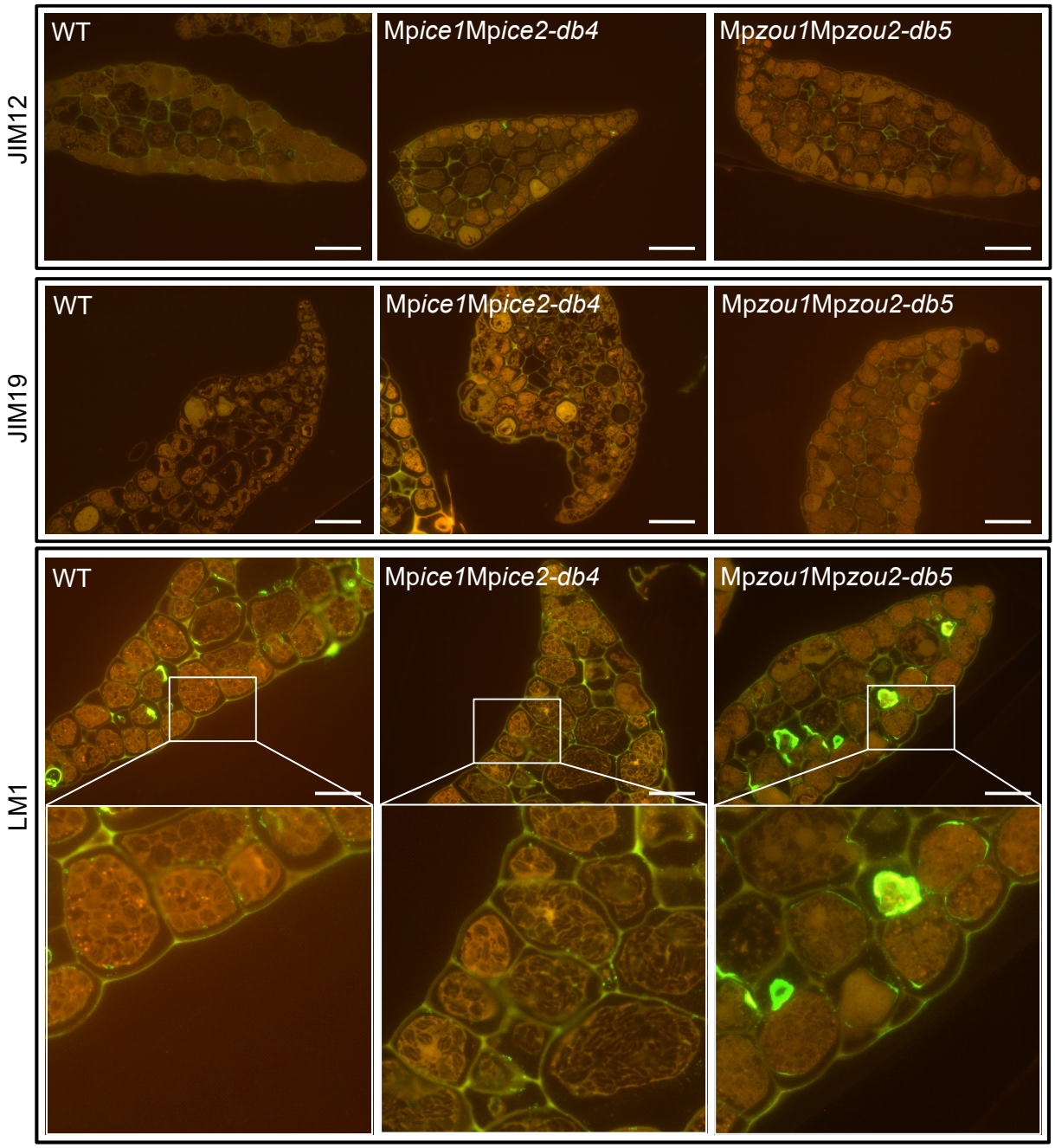

Figure 2: Analysis of mature gemma surface by immunolocalization with several different antibodies. Antibody signal is green and calcofluor signal is red. Immunolocalization with anti-extensin antibodies, JIM12 (first row), JIM19 (second row) and LM1 (third and fourth rows) are tested on wild-type (WT) gemmae, Mp*ice1*Mp*ice2-db4* and Mp*zou1*Mp*zou2-db5*, respectively 1st column, second column and thirsd column. Only LM1 antibody labeled gemma surface. Scale bar, 50µm.

extensin labelling was visible surrounding WT gemmae (**Figure 2**). A subtle difference between the mutants and the WT was visible with this antibody. α-LM1 labelling tends to be slightly fuzzier in the double Mp*zou1*Mp*zou2* mutant than in the wild-type and the double Mp*ice1*Mp*ice2* mutant. The fact that α-LM1, α-JIM12 and α-JIM19 can all detect the embryonic sheath in *A. thaliana*, but that only α-LM1 labelling was detectable in *M. polymorpha* gemmae, could suggest that carbohydrate decorations of extensins are different in the two species. Similar differences in sheath antigenicity were observed even between angiosperms, so this would not be suprising. However, it would be interesting to test more anti-extensin antibodies to see whether a more prominent structure is detectable and/or a more obvious phenotype is visible in *M. polymorpha* mutants laching ZOU and ICE proteins.

As with anti-extensin labelling, a stronger phenotype in Mp*zou1* Mp*zou2* mutants compared to the double Mp*ice1* Mp*ice2* mutant was also observed during with Nile red staining of the cuticle. However, no other ICE-encoding genes are present in the *M. polymorpha* genome. One possible explanation for this phenomenon, is that ZOU proteins from *M. polymorpha* can form functional, or partially functional homodimers in the absence of ICE. *A. thaliana* ZOU proteins have been shown to be capable of homodimerization (Denay et al., 2014), but functions for such homodimers have not been revealed. This possibility deserves further exploration in the future

Since the formation of the plant cuticle is thought to have been an innovation primarily to protect against uncontrolled water loss, we also decided to test whether desiccation tests could help us to shed light on the function of MpZOU2, MpICE1 and MpICE2. Gemmae from the different genotypes, together with wild-type gemmae, were directly put on soil in order to avoid stress-related phenotypes caused by the transfer from a humid environment (in vitro) to a much drier environment (soil). After 15 days, watering was stopped and plants were kept without watering for 18, 21 or 24 days, before being rewatered. The first obvious result of this study was the finding that wild-type *M. polymorpha* has a remarkable capacity to recover after a long period of desiccation (**Figure 3**). Mp*ice2* single mutants and Mp*ice1* Mp*ice2* double mutants were compared to wild-type plants and this revealed that plants lacking the function of both *MpICE* genes struggle to recover after 24 days without watering (**Figure 3**). This phenotype is also visible in the Mp*ice2* loss-of-function mutant but it tends to be less severe than in the double mutant. A parallel experiment comparing *Mpice1* with the double mutants Mp*ice1*Mp*ice2* and Mp*zou1*Mp*zou2* and the wild-type showed similar results. Double mutant plants were very small and brownish after treatment, whereas a less severe phenotype was observed in the single Mp*ice1* mutant. More data are required to draw conclusions from these observations. However, it is interesting to note that both Mp*ice1* and Mp*ice2* single mutants show similar recovery phenotypes, which are less severe than either double mutant. This

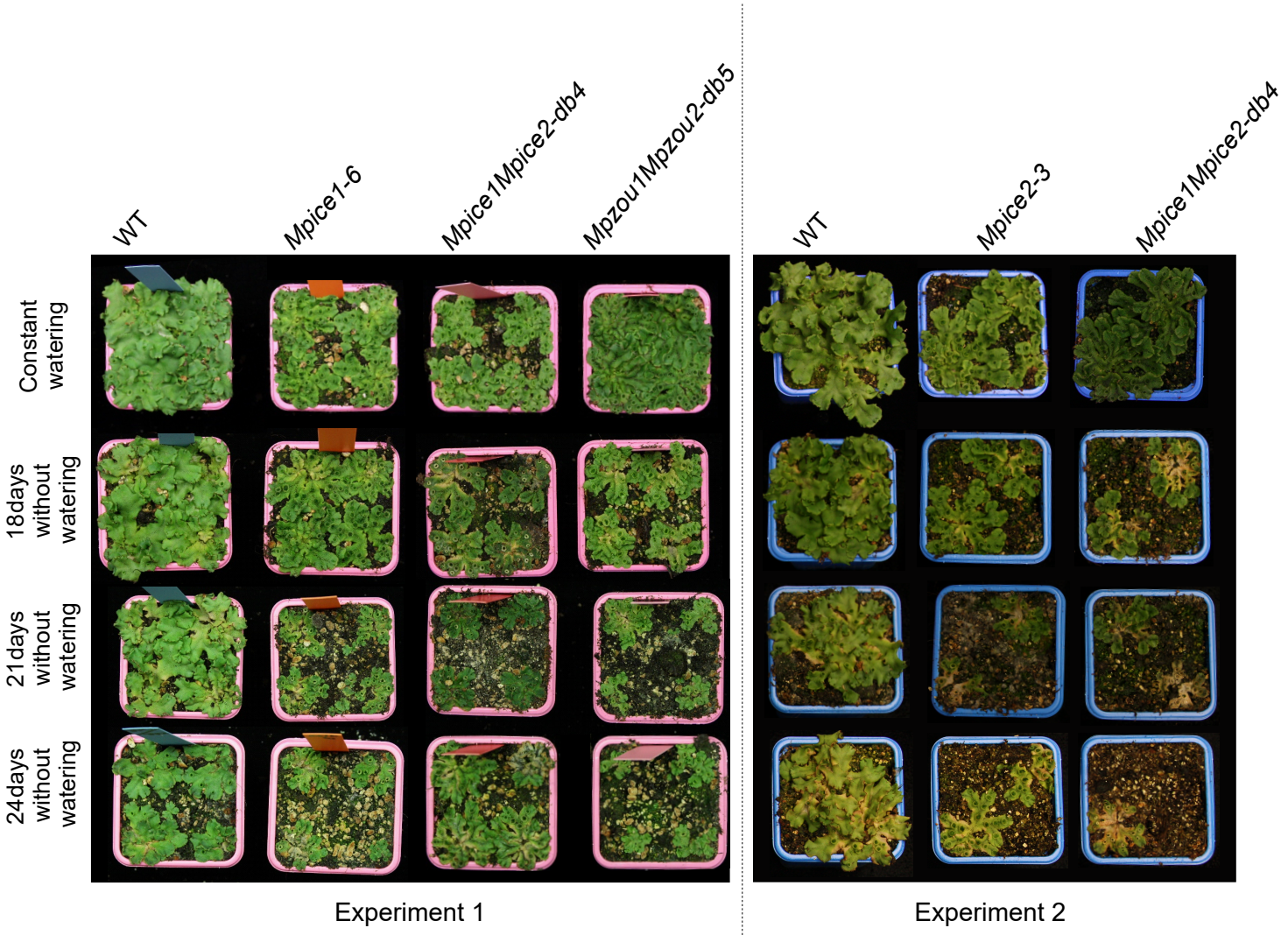

Figure 3: Mp*ice1*, Mp*ice2*, Mp*ice1*Mp*ice2* and Mp*zou1*Mp*zou2* mutants are more sensitive to water stress.

Constant watering is used as a control (first row) to compared with 18 days, 21 days and 24 days with water deficiency between WT (first two columns), Mp*ice1-6*, Mp*ice2-3*, Mp*ice1*Mp*ice2-db4* and Mp*zou1*Mp*zou2-db5*. These experiments show difficulties for both Mp*ice* single mutants and both double mutants Mp*ice1*Mp*ice2* and Mp*zou1*Mp*zou2* have difficulties of recovery from water stress. Plants were 15 days old when the dessication test starts. Experiment 1 and experiment 2 correspond to two independent experiments carried out under the same environnemental conditions.

indicates that phenotypes may not be uniquely attributable to cuticle defects and could be explained by the combination of both phenotypes observed in the double mutants: defective pegged rhizoid development (see **Chapter 3**) and defective cuticle development (assuming that the cuticle defect observed in gemmae of Mp*zou1* Mp*zou2*, Mp*ice1* Mp*ice2* and Mp*ice2* mutants is also visible in thallus, something which has been difficult to prove despite constant efforts).

II. 3 Other potential roles of MpZOU and MpICE proteins (excluding roles in pegged rhizoid formation)

MpZOU and MpICE proteins are involved in regulating the integrity and the composition of the gametophyte cuticle. Do MpICE and MpZOU mutants have other phenotypes which could be linked to a cuticle defect? What about the gamete-bearing gametophores?

As described in the next chapter, the gametophores of *Mpice1*, *Mpzou1*, *Mpzou1Mpzou2* and *Mpice1Mpice2* plants tend to try out before maturation. This appears to be due to the lack of pegged rhizoids, although cuticle defects may also compound this phenomenon. However, *Mpice2* and *Mpzou2* mutants produce viable gametophores, which allowed the potential role of MpICE2 and MpZOU2 in reproductive development to be investigated.

To address this question, crosses were carried out using *Mpice2* and *Mpzou2* mutants. Sporangia from both *Mpice2* x Tak1 (male wild-type) and *Mpice2* x *Mpice2* crosses show defects in spore dispersal (the sporangium does not burst and the spores are not released). Since this defect was only observed when Mp*ice2* was crossed as female suggests this might be due to a defect in maternal tissues surrounding the sporangia (i.e. calypthra or pseudoperianth, see **Figure 2**, Introduction) or it could be maternally inherited due to imprinting and differential expression of maternal. Similar crosses with Mp*zou2* were also carried out but unfortunately revealed female sterility for Mp*zou2* since no sporangia developed from this cross (**Figure 4**). The Tak2 (female wild-type) x Mp*zou2* cross was feasible but showed no obvious sporangium phenotype. Although further experiments need to be carried out to decipher the exact role of MpICE2 in sporangium development, we can suggest two possibilities to explain the phenotypes observed for *Mpice2* crosses. The first is that MpICE2 has a ZOU-independent role in sporangia. In *A. thaliana* and other Angiosperms, ICE proteins are involved in multiple pathways, involving interaction with different bHLH protein partners. It is therefore possible that other bHLH TFs might interact with MpICE2 to control sporangium development. Although, *M. polymorpha* does not have stomata, its genome

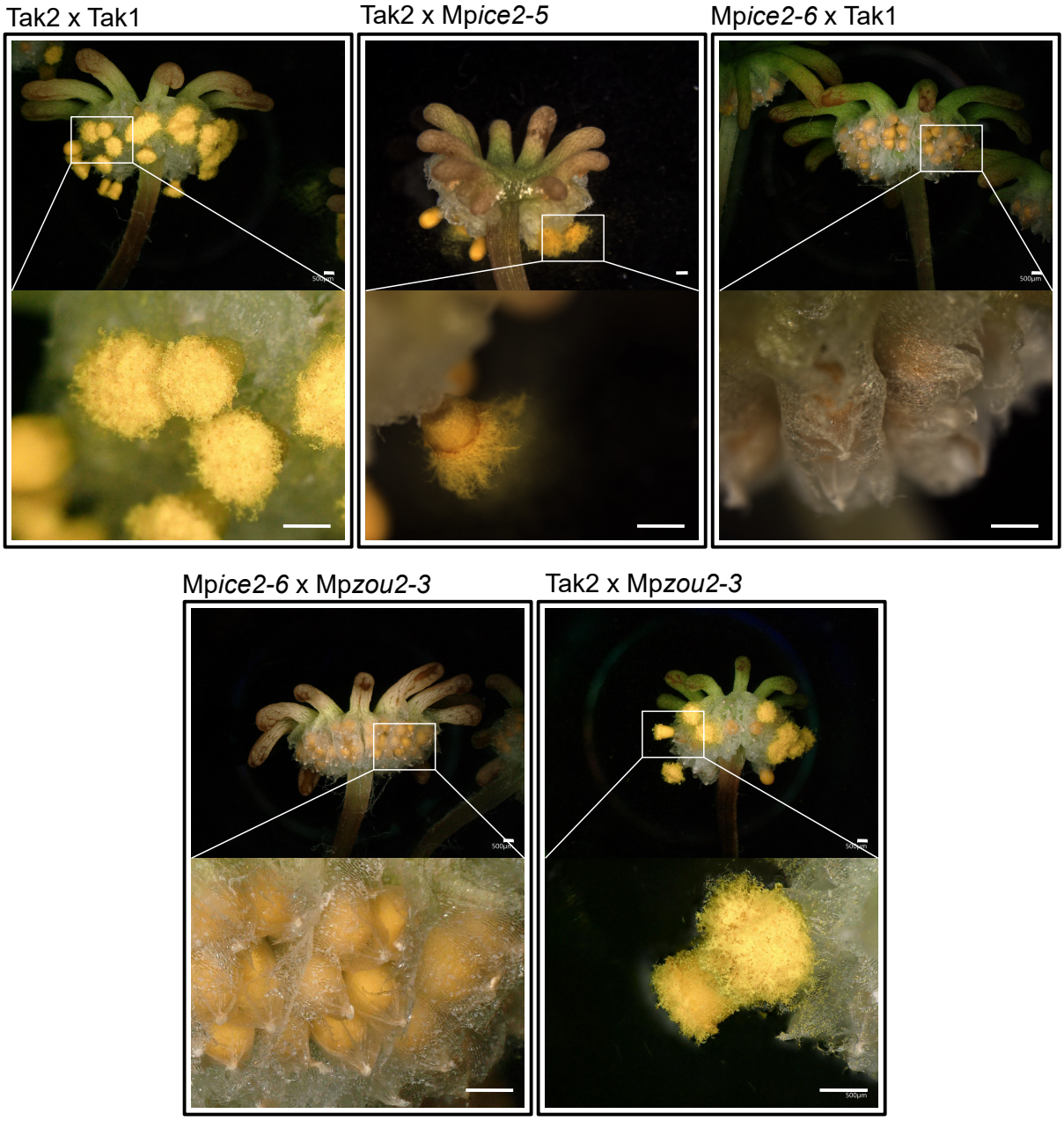

Figure 4: Defect in spore release occured only when Mp*ice2* is crossed as female.
Reciprocal crosses of Mp*ice2* (Mp*ice2-6* as female or Mp*ice2-5* as male) with either the wild-type (Tak1 or Tak2) or Mp*zou2* male (Mp*zou2-3*) revealed a maternally controlled defect of Mp*ice2*. The photographs of the second rows are higher magnification photographs of the white rectangle in the first row photographs. Scale bar, 500µm.

is therefore possible that other bHLH TFs might interact with MpICE2 to control sporangium development. Although, *M. polymorpha* does not have stomata, its genome contains a gene encoding a FAMA like protein (Harris et al., 2020). In *A. thaliana* FAMA is involved in the last differentiation step of stomata development, and it interacts with both AtICE1 and AtICE2 (Kanaoka et al., 2008). It is thus possible that MpFAMA interacts with MpICE proteins to control sporangium development. Another possibility, is that the phenotype observed when Mp*ice2* is used as a female is an attenuated version of the phenomenon that renders Mp*zou2* mutants sterile, and is thus ZOU dependent. To test these hypotheses, additional experiments are necessary, including further histological analysis of the abnormal sporangium development observed in Mp*ice2*xTak1 progeny. However, an ongoing collaboration between Jeanne Loue-Manifel, Justin Goodrich, Tomoo Shimada and Kenta Moriya suggests that the first explanation is correct.

Finally, although the regulation of cold tolerance acquisition by the ICE proteins has been proven many times in *A. thaliana*, cold tolerance experiments with double Mp*ice1* Mp*ice2* mutants compared to wild-type plants have not revealed any conclusive results (data not shown). Thus whether or not ICE-mediated cold tolerance is conserved through land plants is unclear. Similarly *A. thaliana* ICE proteins are involved in stomatal differentiation (Kanaoka et al., 2008). Since air pores in *M. polymorpha* have a similar function to stomata (Chater et al., 2017), and both MpICE and MpZOU2 showed strong expression pattern in air pores (data not shown), an analysis of air pores morphology in the different mutant lines produced in this thesis was carried out. Disappointingly, no drastic phenotype such as complete absence of air pores or a drastic diminution of air pore number were revealed either histologically or by SEM analysis in Mp*ice1*, Mp*ice2* or Mp*ice1*Mp*ice2* mutants, although Mp*ice1* Mp*ice2* mutants sometimes show a lighter green patchy thallus phenotype (**Figure 5**) suggesting a potential diminution of the number of air pores. However, although air pores in Mp*ice1* Mp*ice2* mutant tend to appear bigger, less neatly formed and have a “crushed” aspect compared to wild-type, no evidence proved conclusively that this phenotype is due to a specific function of MpICE in air pore development (**Figure 5**). Indeed it seems possible that this phenotype could be cuticle-related, since air-pores in *M. polymorpha* are surrounded by prominent cuticular extensions, or ledges, which are thought to be important for their function (Schönherr and Ziegler, 1975).

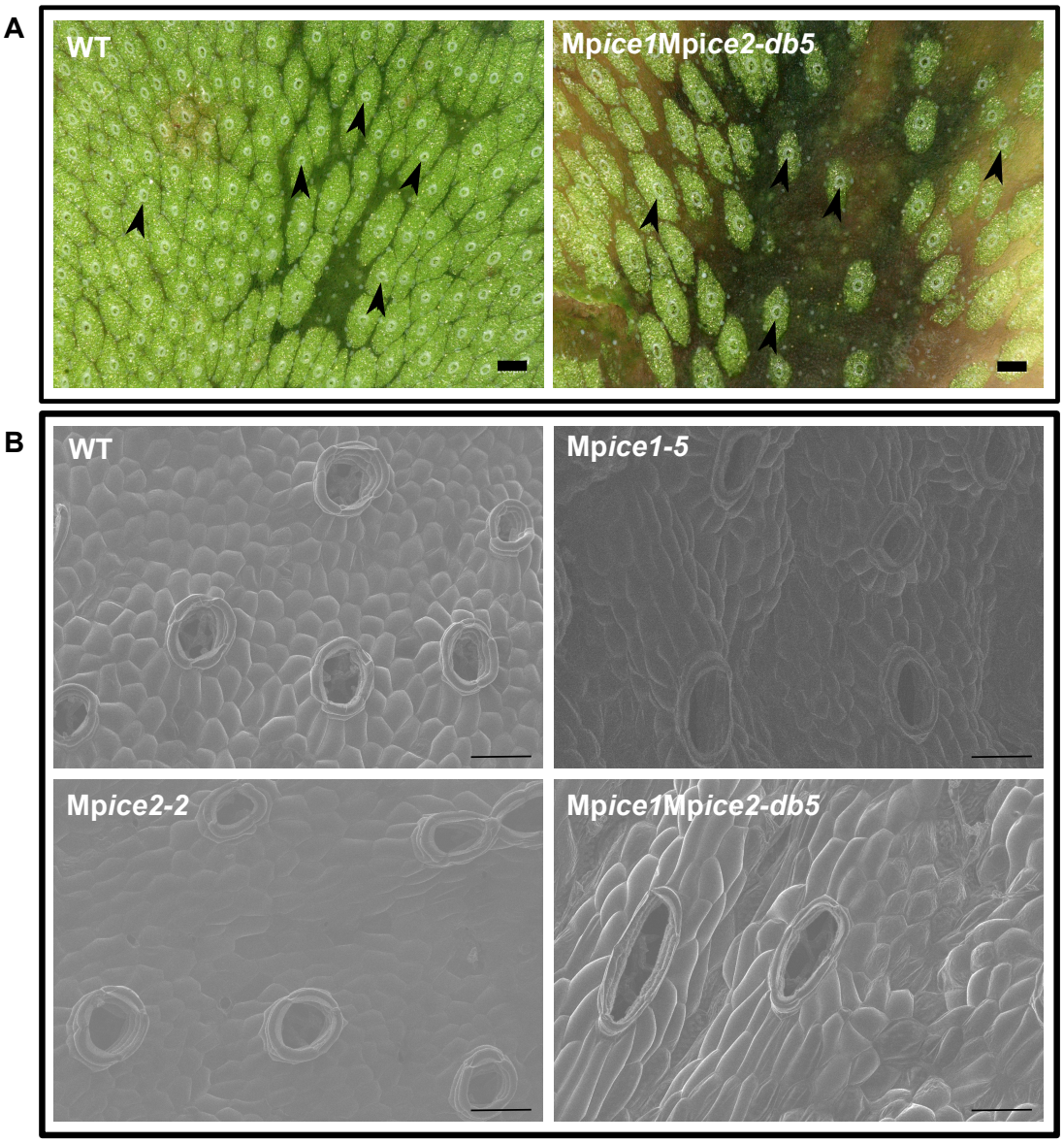

Figure 5 : Mp*ice1*Mp*ice2* double mutants have defective air pores.
(A) Photographs of 2-month old thallus of WT and Mp*ice1*Mp*ice2-db5* mutant showing a drastic decrease in the number of air pores around the midrib. Air pores are indicated by arrowheads. Scale bar, 200µm. (B) SEM micrographs of wild-type, Mp*ice1-5*, Mp*ice2-2* and Mp*ice1*Mp*ice2-db5* on the dorsal surface of 16-day old thallus. Mp*ice1*Mp*ice2-db5* show bigger and crushed air pores compared to WT and Mp*ice2-2* thallus surface. Mp*ice1-5* air pores seem to be slightly bigger and flatter than the WT. Scale bar, 50µm.

II.4 Material and Methods

Histochemical staining for GUS activity of vibratome-sectioned thallus.

15 to 20 day-old transcriptional reporter lines (described in **Chapter 2, § I**) were harvested and placed into a small plate. 5% Phytagel (Sigma CAS : 71010-52-1 ; P8169) at 50°-60°C was then poured onto the plants. The plate was then stored for 30 min to 1hour at 4°C to cool down before being mounted onto the Leica VT1000 S Microtome. Approximately 10µm sections were performed and placed into 1%PBS solution before staining as described above. Observations of GUS activity were made using a Keyence VHX900F digital microscope.

Histochemical staining for GUS activity in whole mount thallus.

Mp*ZOU1*, Mp*ZOU2*, Mp*ICE1* and Mp*ICE2* promoters were cloned as fusions to the GUS reporter via Gateway recombination using the pMpGWB104 destination vector and subsequently Tak2xTak2 sporelings were transformed (Ishizaki et al., 2015). Histochemical assays for GUS activity were performed according to Jefferson et al., 1987 with some minor modifications. Briefly, after three 20 minute vacuum infiltrations with the GUS staining solution (50mM sodium phosphate buffer, pH 7.2 ; 0.5mM potassium-ferrocyanide; 0.5mM potassium-ferricyanide; 10mM EDTA; 0.01% Triton ; 1mM 5-bromo-4-cloro-3-indolyl-Beta-glucuronic acid (Duchefa Biochemie, CAS number 114162-64-0), plants were incubated overnight at 37°C. They were then dehydrated by incubation in increasing concentrations of Ethanol (15%, 30%, 50%), for 20 minutes (per bath at each step) at room temperature. Plants were then fixed in FAA fixative solution (10% formaldehyde, 5% acetic acid, 50% ethanol) for 45 minutes under vacuum followed by either 2 hours at room temperature or overnight at 4°C. Dehydration steps to remove the chlorophyll were then performed by incubation in further increasing concentrations of ethanol (50%, 70%, 100%), for 20 minutes per bath at each step at room temperature. Observations of GUS activity were made using a Keyence VHX900F digital microscope.

Immunolabelling on sections.

Mature gemmae were directly harvested from the gemma cup and fixed in ice-cold PEM buffer (50mM PIPES, 5mM EGTA and 5mM MgSO4, pH6.9) containing 4% (w/v) paraformaldehyde and 1% (w/v) glutaraldehyde under vacuum on ice (2 x 30 min) and overnight at 4°C. Samples were washed twice in PEM buffer and dehydrated by incubation in increasing concentrations of ethanol (50%, 70%, 80%, 90% and three times in 100%), for an

hour each on ice under vacuum followed by an overnight incubation at 4°C in 100% Ethanol. Samples were then infiltrated with increasing concentrations of LR WHITE medium resin in absolute ethanol (30%, 50%, 70%, and three times in 100%), for an hour on ice under vacuum followed by an overnight incubation at 4°C for each bath. Seeds were then transferred into small Beam capsules (Electron Microscopy Sciences) and incubated overnight at 60°C for polymerisation. 1µm sections were cut on a Leica RM6626 microtome and floated onto adhesive slides (Superfrost Ultra plus^{TM}(ThermoFisher Scientific)). For immunolabelling, sections were first incubated for 45 minutes in PBS containing 2%(w/v) Bovine Serum Albumin (BSA). They were then incubated with a 10 fold dilution of primary antibody in PBS containing 0.1% BSA overnight at 4°C followed by one hour at room temperature. Sections were then washed three times in PBS for 5 minutes, then in PBS containing 0.1% Tween 20 (w/v) for 10 minutes and finally in PBS for 5 minutes. Incubation with a 100-fold dilution of an appropriate anti-rat secondary antibody (Alexa Fluor 488 conjugate, Invitrogen) in PBS with 0.1% BSA for one hour in the dark, in a wet chamber was then performed. The sections were washed three times in PBS for 5 minutes and counter-stained with a solution of 0.25ng/L of calcofluor (Fluorescent Brighter 28, Sigma Aldrich) in PBS for 5 minutes. Finally, sections were washed rapidly three times in PBS and mounted in Vectashield (Eurobio). Observations were made using an Axio Imager 2 microscope (Zeiss).

Desiccation test.

32 gemmae were sowed directly on soil (soil:perlite 1:1) under long-day conditions (16h, 21°C) (e.g. 4 gemmae per pot) to grow for 15 days under normal conditions. 8 plants e.g. 2 pots were then placed under one watering condition: continuous watering, 18 days without watering, 21 days without watering or 24 days without watering. Plants pictures after 24 days were obtained with a CANON EOS 450D camera equipped with objectives SIGMA 18-50mm.

Cold tolerance test.

8 gemmae per genotype were placed on a plate with Johnson media under short day conditions at 6°C. Plants grew 4 days or 17 days before being photographed with a CANON EOS 450D camera equipped with objectives SIGMA 18-50mm.

Production of Sporangia via genetic crosses in *M. polymorpha*.

1-month old thallus were transferred on soil (soil:perlite 1:1) and keep for adaptation for 2 weeks under 75% humidity, 21°C, long day conditions before induction of gametophore production with far red light (730 nm). Once gametophores were produced and were mature enough to be crossed, 20 archegoniophores were crossed in order to confirm the sterility and the observed phenotypes. Sperm was harvested from males by placing drops of water on the surface of the male receptacles, waiting until the water was cloudy with released sperm, then collecting and placing onto the female archegoniophores. After 4 weeks, sporangia were fully matured. To confirm the observed phenotype was not due to growth delay, extra sporangia were kept 4 extra weeks in observation. Pictures were taken with a Keyence VHX900F digital microscope.4 repetitions have been performed and 1 repetition is equivalent to 20 crossed-archegoniophores. This has been performed with the help of a L3 student, Louis Valay I supervised.

Air pores analysis.

A piece of sixteen-day old thallus grown in vitro was sectioned just after the apical notch, taped on and imaged at 5kV and -15°C using an Environmental scanning electron microscope (Hirox 3000). 2 month-old thallus grown in vitro on Johnsons media (see Annexe) was photographed near the midrib with a Keyence VHX900F digital microscope.

Bibliography

See general bibliography at the end of the thesis.

CHAPTER 3

Is the ZOU/ICE function in endosperm cell elimination in *Arabidopsis thaliana* conserved in *Marchantia polymorpha*?

Preamble

During angiosperm seed development, the endosperm is totally or partially degraded. This developmental process involves endosperm cell elimination followed by developmental cell death. In *A. thaliana*, ZOU/ICE complex activity in the endosperm promotes cell wall modifications that lead to thinning and cell separation. Previous transcriptomic studies showed that several genes involved in the modification of cell wall proteins and polysaccharides are downregulated in *zou* mutant, including *Reversibly Glycosylated Protein3* (Xing et al., 2013). *RGP3* is the only direct target of ZOU/ICE complex conclusively identified to date, and encodes a UDP-arabinose mutase participating in the plant cell wall biosynthesis/modification through arabinose metabolism (Denay et al., 2014; Rautengarten et al., 2012). ZOU-mediated cell wall modifications have been proposed to allow the deformation of endosperm cells under the pressure exerted by the expanding embryo, thereby priming them for pressure-induced cell death (bursting). This in turn facilitates the growth of the embryo (Fourquin et al., 2016). Another excellent example in which cell wall modification and cell death are tightly linked, is the differentiation of xylem vessels, discussed in **Introduction, § 2.2**.

Link between cell wall modifications and the conditioning of cells for developmental cell death is not an Angiosperm, or indeed a vascular-plant-specific phenomenon but is also seen in Bryophytes such as *M. polymorpha,* in which at least two tissue maturation programmes associate cell wall modifications and cell death. A good example is provided by *M. polymorpha* elaters which are dead, hygroscopic cells involved in spore release and found in sporangia. Another example is pegged rhizoids, which are dead cells with cell wall ingrowths involved in water transport. Again, pegged rhizoids are dead at maturity, and cell death is preceded by the development of complex cell wall modifications.

Finally, it is interesting to note that even in animal systems, extracellular matrix remodelling and cell death (in this case apoptosis) are often intricately linked (Shi et al., 1998).

In Chapter 2, I explored the putative parallels between the role of the ZOU/ICE complexes in *Marchantia polymorpha* surface formation (cuticle biogenesis) with their roles in embryo surface formation in *A. thaliana*. In this Chapter, I investigate another putative role for *M. polymorpha* ZOU/ICE complexes; the production of pegged rhizoids. This work was initiated by a previous PhD student in Goodrich group, Yen-Ting Lu, before I arrived in the group, but I carried out many of the experiments necessary to complete this study, and as I result I appear as co-first author on the resulting manuscript in preparation.

In a first section of this Chapter, presented as an article, we show that the MpZOU1/MpICE1 complex controls the development of a novel water conducting tissue, the pegged rhizoids. Data are presented showing that cell wall modifications and cell death are both key events occurring during this process, and parallels are discussed between the ZOU/ICE-mediated endosperm elimination process observed in *A. thaliana,* and the differentiation of pegged rhizoids.

The second section of this Chapter contains a more general discussion of open questions that our research has revealed, and describes potential future research perspectives.

I- The ZOU/ICE1 transcription factors control programmed cell death and formation of a novel water conducting tissue in the liverwort *Marchantia polymorpha*

YT Lu[1], J. Loue-Manifel[2,3]*, N. Bollier[4], E. De Leau[3], F. De Winter[4], P. Carella[5], S. Grey-Switzman, A. Hoguin, F. Simon, S. Schornack[5], N. Dépège-Fargeix[2],* R. Nishihama[6], *T. Kohchi[6], G. Ingram[2], M. Nowack[4], J. Goodrich[3]*

*co-authors

[1] Laboratory of Plant Developmental Signalling Nara Institute of Science and Technology, Nara, Japan

[2] Laboratoire Reproduction et Développement des Plantes, Université of Lyon, ENS de Lyon, UCB Lyon 1, CNRS, INRA, Lyon, France

[3]Institut of Molecular Plant Sciences, University of Edinburgh, Edinburgh, Scotland

[4] Department of Plant Biotechnology and Bioinformatics, University of Ghent, Ghent, Belgium

[5] Sainsbury laboratory, Cambridge, UK

[6] University of Kyoto, Japan

AUTHOR CONTRIBUTIONS

Yen-Ting Lu and Jeanne Loue-Manifel carried out the genetic analysis and the phenotypic analysis. Yen-Ting Lu carried out most of the cloning with the help of Erica De Leau, Freya de Winter and L3 students she supervised, Shona Grey-Swutzman, Antoine Hoguin and Francois Simon. Philip Carella did the thallus transformation of Mp*zou1.* Norbert Bollier carried out the microscopy analysis of the TdTomato reporter lines. GUS staining was performed by Jeanne Loue-Manifel. Yen-Ting Lu and Justin Goodrich performed the transcriptomic analysis. Phylogenetic analysis was performed by Justin Goodrich. Analysis of the complementation lines (toluidine blue permeability and seed shape quantification) was carried out by Jeanne Loue-Manifel. The article was written by Justin Goodrich with inputs from Jeanne Loue-Manifel, Moritz Nowack, Gwyneth Ingram, Norbert Bollier and Yen-Ting Lu. Jeanne Loue-Manifel prepared the main figures and Justin Goodrich the supplemental figures.

ABSTRACT

A key adaptation of plants to life on land is the possession of water conducting cells, which allow increase in size of aerial shoots and provide structural support. In vascular plants, water conducting cells in the xylem have two distinguishing features: they undergo programmed cell death at maturity, clearing cell contents to allow rapid water transport and in addition they have reinforced, patterned secondary cell walls which prevent cell collapse under negative pressure. Complex thalloid liverworts have independently evolved a novel externalised water conducting tissue, composed of bundles of pegged rhizoids. Pegged rhizoids are distinct from normal (smooth) rhizoids as they have secondary cell wall thickenings (pegs) and they are dead at maturity. We identify orthologues of the *A. thaliana ZHOUPI* and *INDUCER OF CBF EXPRESSION1* genes, required for endosperm cell death and elimination in seeds, as key regulators of pegged rhizoid differentiation in *Marchantia polymorpha* and show that they promote expression of cell wall and cell death genes. Our results suggest that the genetic control of developmental cell death is conserved in land plants and it has been independently recruited in liverworts to facilitate pegged rhizoid differentiation.

In *A. thaliana*, the basic helix loop helix transcription factors ZHOUPI (ZOU) and INDUCER OF CBF EXPRESSION1 (ICE1) act as a heterodimer with various key roles during seed development, including promoting the cell death and elimination of endosperm and the formation of an intact embryonic cuticle (Denay et al., 2014; Fourquin et al., 2016; Yang et al., 2008). Both proteins are conserved throughout land plants (Catarino et al., 2016; Harris et al., 2020), raising the question of their role in plants lacking seed or endosperm. To address this, we characterised their orthologues in the model liverwort *M. polymorpha*. Phylogenetic analysis indicates that *M. polymorpha* has a single orthologue of *A. thaliana ZOU*, *Mp4g19650* here designated Mp*ZOU1* and a second paralogous gene Mp*ZOU2* (*Mp8g04130*) that derives from an ancient duplication likely present in the common ancestor of land plants (**Figure S1**). The position of the two introns in the *M. polymorpha* and *A. thaliana* genes is conserved, also consistent with a common evolutionary origin. There are also two *M. polymorpha* co-orthologues of the *A. thaliana ICE* genes, Mp*ICE1* (*Mp4g04920*) and Mp*ICE2* (*Mp4g04910*) which derive from a more recent duplication, after the divergence of liverworts and mosses (**Figure S2**). We did not find *ICE* or *ZOU* genes in any green algae genomes, suggesting that they arose early in evolution of land plants. Here we characterize Mp*ZOU1* and Mp*ICE1* which we found to share discrete functions in rhizoid development.

We first tested whether the *M. polymorpha* proteins could interact with one another using a yeast two hybrid assay. Indeed, MpZOU1 and MpICE1 interact both with each other,

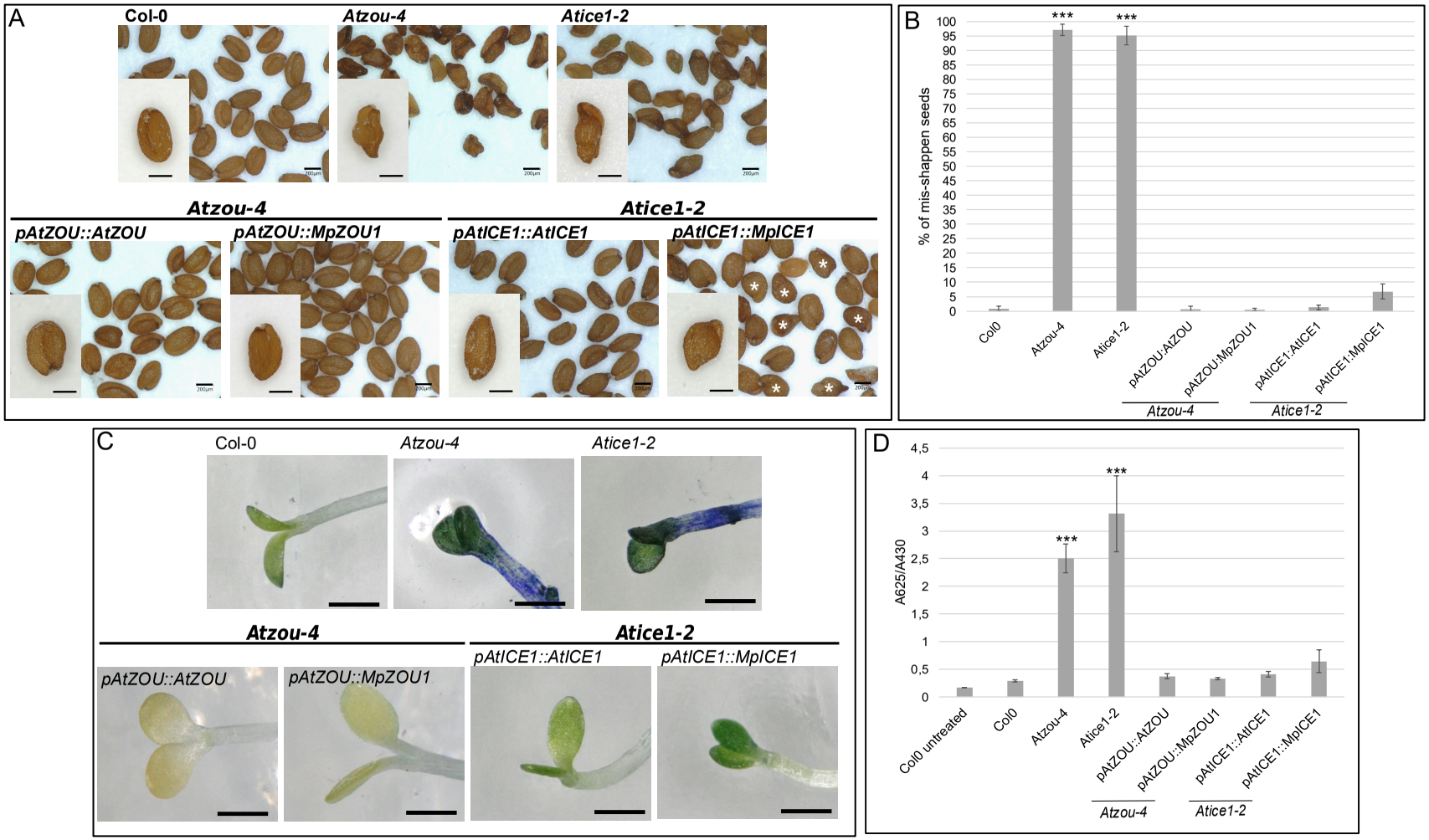

Figure 1 : MpZOU and MpICE complement seed and cuticle phenotypes of Arabidopsis At*zou-4* and At*ice1-2* mutants. (A) Dry seeds of wild-type (Col-0), At*zou-4* mutant, At*ice1-2* mutant, pAtZOU::AtZOU, pAtZOU::MpZOU1 or pAtZOU::MpZOU2 in At*zou-4* mutant and pAtICE1::AtICE1, pAtICE1::MpICE1 or pAtICE1::MpICE2 in At*ice1-2* mutant. Partially complemented seeds are indicated by an asterisk. Scale bar, 200µm. (B) Quantification of misshappen dry seeds in different background. N=5, approximately 1000 seeds per repetition. *** indicates statistical differences with ANOVA and Sheffe tests (p-value 0.01). Error bars indicate standard deviation. (C) Toluidine blue assays on etiolated cotyledons of wild-type (Col-0), At*zou-4* mutant, At*ice1-2* mutant, pAtZOU::AtZOU, pAtZOU::MpZOU1 or pAtZOU::MpZOU2 in At*zou-4* mutant and pAtICE1::AtICE1, pAtICE1::MpICE1 or pAtICE1::MpICE2 in At*ice1-2* mutant. Scale bars 500µm. (D) Quantification of toluidine blue uptakes by the cotyledons of young seedlings, normalized to chlorophyll content. N= 6, 10 seedlings per repetition.. *** indicates statistical differences with ANOVA. Error bars indicate standard deviations.

and also with *A. thaliana* AtICE1 and AtZOU, respectively (**Figure S3**). Further, the full-length ICE proteins had transcriptional activation activity in yeast and a C-terminal portion that included the bHLH domain was sufficient for interaction with ZOU proteins. We next tested whether the *M. polymorpha* genes could rescue the seed phenotypes of their corresponding *A. thaliana* mutants when expressed in transgenic seed from the *A. thaliana* ZOU or ICE promoters. Both Mp*ZOU1* and Mp*ICE1* rescued the cuticle defects of At*zou-4* and At*ice1-2* mutants as measured by toluidine blue staining of etiolated seedlings (**Figure 1A and 1B**). The seed of At*zou* and At*ice* mutants contains a small embryo which does not fill the seed, due to the presence of a persistent endosperm which impedes embryo growth. In addition, the seed is shrivelled, due to the collapse of the watery endosperm cells during seed maturation and desiccation. In At*zou-4* mutants, expression of either the At*ZOU* or Mp*ZOU1* coding sequences from the At*ZOU* promoter gave a full rescue, with a large embryo filling the oval shaped seed and no shrivelling (**Figure 1C and 1D**). In At*ice1-2* mutants, expression of At*ICE1* gave a full rescue, whereas Mp*ICE1* gave a partial rescue such that many seed had larger embryos than in At*ice1-2* and less shrivelling but were misshapen relative to wild type (**Figure 1C and 1D**). Collectively these data support that the ZOU ICE partnership arose early in land plant evolution and the properties of the proteins have been broadly conserved in bryophyte and angiosperm lineages thought to have diverged about 430 million years ago.

To determine the developmental function of *MpZOU1* and *MpICE1* in *M. polymorpha*, we first examined their expression using transcriptional reporters comprising 5 and 6.6kb of regulatory sequences upstream of the start codons, respectively, fused either to the *GUS* gene encoding ß-glucoronidase or nuclear localised TdTomato fluorescent protein. The $_{pro}$*MpZOU1:GUS* and $_{pro}$*MpICE1:GUS* reporters were expressed strongly in 20 day old thallus tissue and with similar patterns, in ventral tissues around the midrib that included the parenchyma, scales and rhizoids (**Figure 2A**). We also examined $_{pro}$*MpZOU1:TdTomato-NLS* and $_{pro}$*MpICE1:TdTomato-NLS* reporters in two week old thallus and observed strong signals in the thallus, emerging rhizoids and developing pegged rhizoids where pegs were present at the base of the rhizoid but not yet at the tips (**Figure 2**). Overall these results indicated that Mp*ZOU1* and Mp*ICE1* might share common functions, including roles in ventral parenchyma and or rhizoid development

We next created multiple independent loss of function alleles of Mp*ZOU1* using genome editing to create frameshift mutations in the region encoding the bHLH domains (**Figure S4**). The alleles are likely to be null as they are predicted to cause premature termination of translation, truncating the proteins and removing the highly conserved bHLH domain. We first examined whole mount, cleared thallus tissue of 12 day old plants using differential interference contrast microscopy, as this allowed us to check large number of

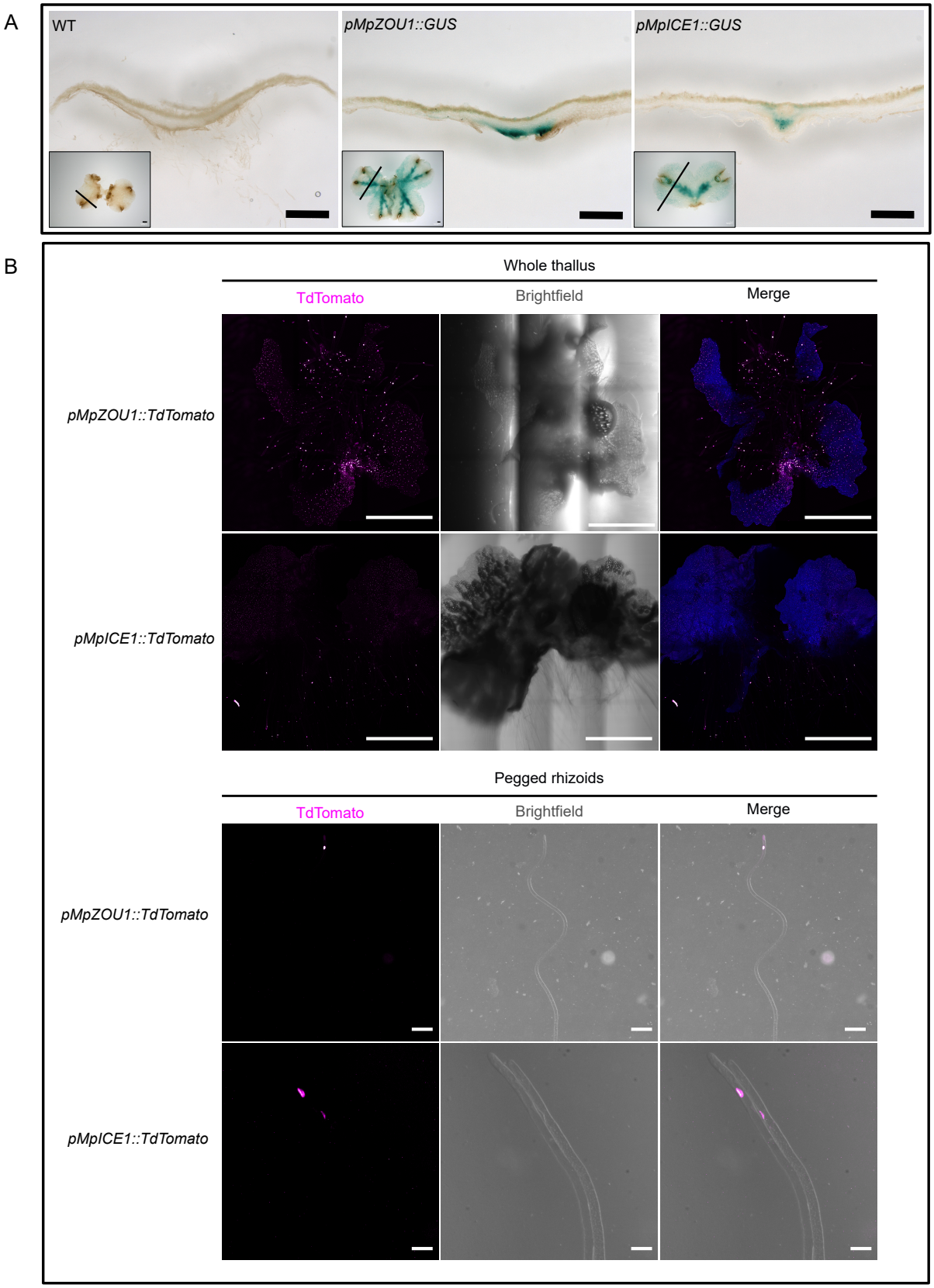

Figure 2 : Transcriptional reporter lines of Mp*ZOU1* and Mp*ICE1* show expression in rhizoids. (A) Mp*ZOU1* and Mp*ICE1* promoter activity are restricted to the ventral surface of the thallus where the pegged rhizoids are formed. Transverse section of thallus of WT (Tak1) and GUS reporters fusion of Mp*ZOU1* and Mp*ICE1* promoters are the main photographs. Respective whole mount thallus are shown in the bottom left side of the transverse section photographs. Scale bar, 500µm (whole mount) and 100µm (vibratome secions). (B) Confocal microscopye images of Mp*ZOU1* and Mp*ICE1* promoters fused to TdTomato-NLS fluorescent protein. Photographs of the whole mount thallus and of the ongoing pegged rhizoids are shown in the first and second panel. Scale bar, 1mm (whole mount) and 200µm (rhizoids).

rhizoids. Wild type plants had a mixture of smooth and pegged rhizoids, whereas the mutants had smooth rhizoids but lacked any pegged rhizoids (**Figure 3**). To confirm that this phenotype was due to disruption of Mp*ZOU1,* we complemented the mutant phenotype by introducing a transgene expressing the Mp*ZOU1* coding sequence (*$_{pro}$MpZOU1::MpZOU1 CDS*) into the Mp*zou1-1* mutant background and observed that pegged rhizoids were present (**Figure 3**). We next performed genome editing of Mp*ICE1* and identified independent mutant alleles (**Figure S4**). The Mp*ice1* mutants had a very similar phenotype to Mp*zou1* (**Figure 3**), consistent with Mp*ZOU1* and Mp*ICE1* acting together and being required to promote pegged rhizoid differentiation in thallus tissue. To test the effects of over-expression, we made transgenic plants that expressed Mp*ZOU1* or Mp*ICE1* coding sequences under the control of the constitutive Mp*EF1* promoter (Althoff et al., 2014). In plants that expressed *$_{pro}$MpEF1:MpZOU1 CDS*, all rhizoids differentiated as pegged rhizoids and no smooth rhizoids were present (**Figure 3**). In addition, the development of pegged rhizoids was accelerated. In wild type, no pegged rhizoids were visible on 3-day old gemmae and they did not become morphologically discernible, via presence of pegs until day 5-6. By contrast, in three day old transgenic plants most rhizoids were already pegged rhizoids. However, unlike plants that mis-express Mp*RSL1*, in which rhizoids are produced from the dorsal epidermis as well as ventrally (Proust et al., 2016), rhizoids were only produced ventrally (**Figure 3**) suggesting that Mp*ZOU1* expression was not sufficient to cause epidermal cells to develop as rhizoids but rather to promote differentiation in existing rhizoids. We also generated *$_{pro}$MpEF1::MpICE1* transgenic plants, however rhizoid development appeared normal in these lines (**Figure 3**), suggesting that *MpZOU1* is the factor giving spatial specificity or limiting the activity of the MpZOU1/MpICE1 heterodimer. Since ICE is known to be strongly post-translationally regulated in *A. thaliana* during stomata development and cold tolerance (Chinnusamy et al., 2003; Ding et al., 2015; Dong et al., 2006; Lang and Zhu, 2015; Putarjunan et al., 2019), the absence of phenotype in *$_{pro}$MpEF1::MpICE1* might also suggest that the post-translational regulation of MpICE1 is conserved limiting the activity of MpZOU1//MpICE1 complex.

To identify genes acting downstream of MpZOU1/MpICE1 as effectors of pegged rhizoid differentiation, we carried out transcriptional profiling (RNAseq) of 12-day old gemmae of wild type, Mp*zou1* and Mp*ice1* mutants. Since MpICE1 activated transcription in yeast assays (**Figure S3**), and co-expression of ZOU and ICE1 genes activates transcription in several *in planta* assays in moss and tobacco (Denay et al., 2014; Feng et al., 2018), we looked for transcripts that were less abundant in mutants compared to wild type. Consistent with their shared phenotype, a large and statistically significant fraction of the down regulated genes were common to the two mutants (**Figure S5**). Within this set of 119 genes, we identified numerous genes involved in cell wall modification and potentially linked to peg production

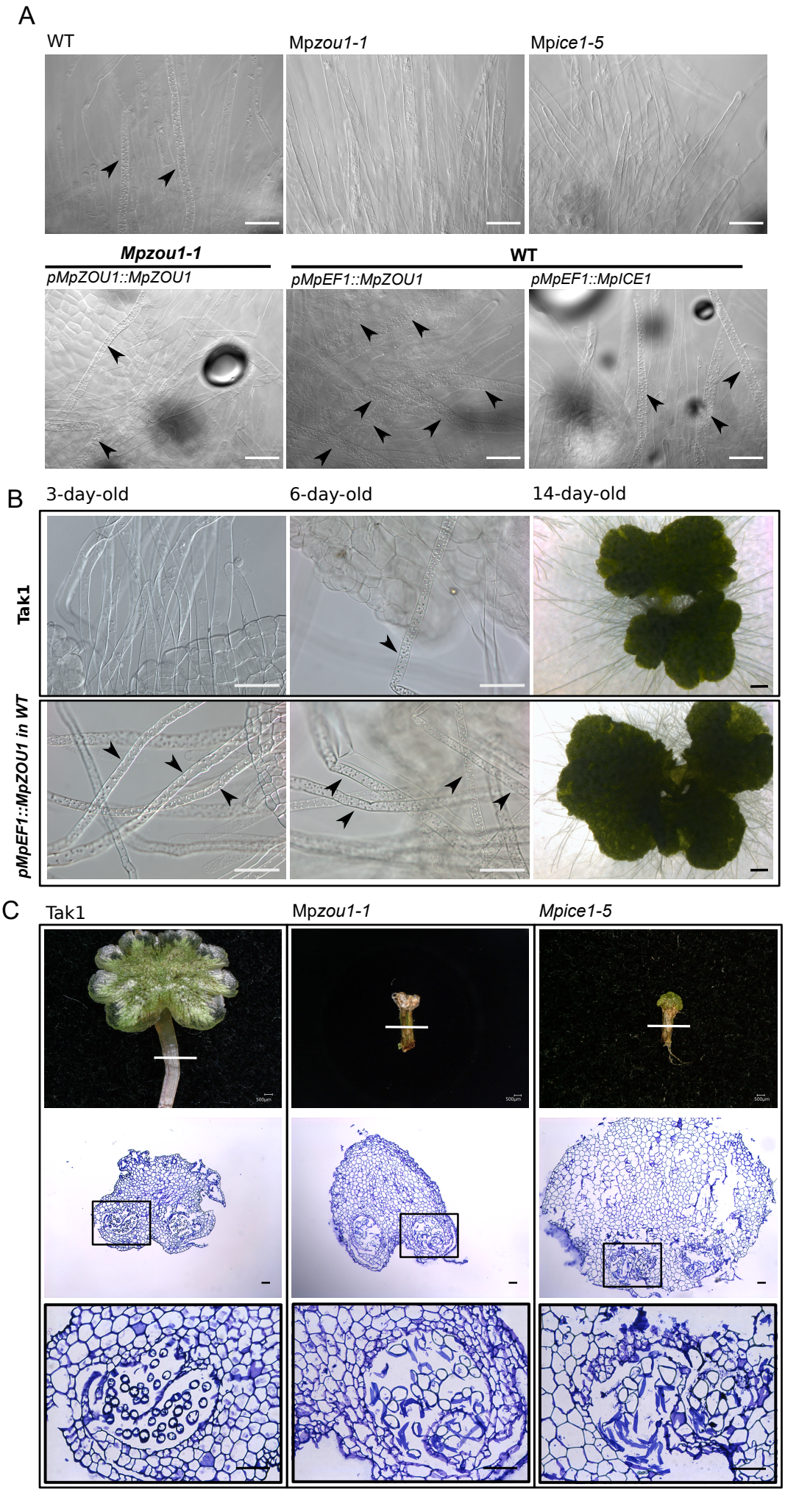
A
WT
Mpzou1-1
Mpice1-5
Mpzou1-1
pMpZOU1::MpZOU1
WT
pMpEF1::MpZOU1
pMpEF1::MpICE1
B
3-day-old
6-day-old
14-day-old
Tak1
pMpEF1::MpZOU1 in WT
C
Tak1
Mpzou1-1
Mpice1-5

Figure 3: *MpZOU1* and *MpICE1* promote pegged rhizoids differentiation and *MpZOU1* over expression causes excess pegged rhizoid formation.
(A) Clearing of 10-day old thallus. Mp*zou1-1* and Mp*ice1-5* are missing pegged rhizoids compared to the WT (wild-type), the complementation *pMpZOU1::MpZOU1* in Mp*zou1-1* and *pMpEF1::MpICE1*. In contrast the ectopically expressed *MpZOU1*, *pMpEF1::MpZOU1* shows an overproduction of pegged rhizoids. Arrowheads indicate pegged rhizoids. Scale bar, 100µm. (B) The two first columns show clearing of 3-day-old and 6-day-old young plants. Arrowheads indicate pegged rhizoids. Scale bar, 50µm. The third column show absence of rhizoids on the dorsal surface of *pMpEF1::MpZOU1* in WT. Scale bar, 1mm. Pictures from Yen-Ting LU. (C) Gametophores of *Mpzou1-1* and Mp*ice1-5* are defective in pegged rhizoids and very short and dry. First row are photographs of Tak1 (wild-type male), Mp*zou1-1* and Mp*ice1-5*. Scale bar, 500µm. White line indicates transverse section realised in the embedded stalk showed in the second and third rows. Black square in the second row indicate the zoom in visualised in the third row. Scale bar for the second and third rows are 50µm.

including several predicted rhamnogalacturonan endolyases and xyloglucan endotransglycosylases (**Table S1**). In addition, there were also several genes linked to developmental programmed cell death (dPCD). Notably, *Mp8g07700* encoding a type II metacaspase was strongly downregulated. In *A. thaliana* there are six type II metacaspases (MC4-9), cysteine proteases with various roles in cell death and immunity (Bollhöner et al., 2013, 2018), with Metacaspase9 (MC9) associated with cell death during xylem differentiation (Olvera-Carrillo et al., 2015). Phylogenetic analysis indicates that there are four type II metacaspases in *M. polymorpha*, and that the duplications occurred since the divergence of Bryophyte lineages so they are equally related to AtMC4-9. In addition, five genes encoding DUF679 Domain Membrane proteins (DMP) were down regulated. *A. thaliana* encodes ten DMP proteins of which DMP4 expression is tightly associated with various developmental programmed cell death (dPCD) processes including xylem differentiation and endosperm breakdown. Phylogenetic analysis indicates 11 DMP genes in *M. polymorpha*, again equally related to AtDMP1-10. Lastly, the aspartyl protease PASPA3 is another marker and likely effector for dPCD in *A. thaliana*. We did not detect misexpression of the two *M. polymorpha* PASPA3 homologues, but six aspartyl proteases with weak similarity to *A. thaliana* PASPA3 that were downregulated and may play a similar role in dPCD. The dataset was also strikingly enriched for peroxidases, with 17 downregulated, of which 16 are predicted to be class III, i.e. secreted and apoplastic. Class III peroxidases have various roles, and are often associated with cell wall remodelling, including the polymerisation of phenolic units to form lignin (Rojas-Murcia et al., 2020). We also compared the 119 genes with a single cell RNA seq dataset from 4 day old thallus tissue and found that a statistically significant fraction (35 genes, $p= 8.8 \times 10^{-13}$, hypergeometric test) were expressed in 2 cells that were likely pegged rhizoids and notably included the metacaspase and 7 DMP4 like genes.

Pegged rhizoids are an innovation found in complex thalloid liverworts and their presence is correlated with species in which the gametangiophores are elevated above the thallus on stalks, facilitating spore dispersal via wind (Duckett et al., 2014; Villarreal A et al., 2016). In *M. polymorpha*, two grooves run up the stalk and are densely packed with pegged rhizoids, implicated in water transport to the receptacles (Duckett et al., 2014; Shimamura, 2016). In the stalks of Mp*zou1* and Mp*ice1* mutants, transverse sections showed that normal pegged rhizoids were absent from the grooves and instead smooth rhizoids lacking pegs and larger in diameter were present. Occasionally rhizoids developed pegs, but these were smaller and extended less far into the lumen of the rhizoid, suggesting that they were not fully differentiated (**Figure 3**). Strikingly, the gametangiophores of mutants were typically shorter than wild type and did not survive for long, shrivelling and drying out even when grown in humid conditions. Most likely as a result the mutants were not fertile either as males or females.

These results are consistent with the presence of pegged rhizoids in stalks being important for hydration and viability of the aerial gametangiophores.

The pegged rhizoids of *M. polymorpha*, unlike xylem, are external to the thallus and have become internalised in the stalk due to inrolling of thallus tissues to form the stalk (Duckett et al., 2014; Shimamura, 2016). They are believed to have evolved a role in water transport independently of xylem via convergent evolution (Duckett and Pressel, 2020). Notably they have acquired structural reinforcement, via pegs, which help to prevent collapse during desiccation, and dPCD to clear cellular contents. Consistent with this evolutionary convergence, we find that the ZOU/ICE partnership has been recruited as a master transcriptional regulator in *M. polymorpha* and promotes expression of cell wall modifying genes and dPCD genes. In *A. thaliana* the ZOU/ICE heterodimer is required for the breakdown of endosperm that permits growth of the embryo during seed development. This involves programmed cell death of endosperm cells and is marked by expression of dPCD genes such as *PASPA3* and *DMP4* (Olvera-Carrillo et al., 2015), but differs in that cell walls and debris are eliminated post mortem and expansion of the embryo is required to trigger cell death (Fourquin et al., 2016). Nonetheless, it raises the possibility that ZOU/ICE genes played a role in dPCD in early land plants and that this has been recruited to different roles in the *M. polymorpha* gametophyte and the angiosperm endosperm. Given that the pegged rhizoids are a derived feature of complex thalloid liverworts it will be interesting to know whether ZOU/ICE have a more general role in dPCD processes. For example, the elaters in the sporophyte are involved in spore dispersal and are also dead at maturity, with distinctive secondary thickenings.

Materials and Methods

YEAST-TWO HYBRID ASSAYS.

The full length of *M. polymorpha* and *A. thaliana* ZOU and ICE1 proteins were expressed as fusions to the GAL4 DNA binding domain (bait constructs) or with the GAL4 transcriptional activation domain (prey constructs) and cloned into pGBKT7-GW or pGADT7-GW (Lu et al. 2010). The truncation of AtICE1, MpICE1 was respectively residues 263-494 and 443-710 based on Denay et al. 2014 for AtICE1 and on the alignment of AtICE1-T and MpICE1. Matchmaker Y2HGold Yeast was co-transformed with bait and prey plasmids and transformants were selected on media lacking leucine and tryptophan (-LW). Interaction of bait and prey constructs resulted in activation of reporter genes for histidine and adenine synthesis (-LWHA).

M. POLYMORPHA SPORELING TRANSFORMATION AND *A. THALIANA* FLORAL DIPPING TRANSFORMATION.

M. polymorpha spores from Tak-2 x Tak-1 crosses, (approximatively 5 sporangia per transformation) were sterilised for 15minutes with 0.1% sodium hypochlorite solution, spun for 1 minute at maximum speed in a microcentrifuge, resuspended in 500µL of water and grown 7 days into 50mL of OM51C (Takenaka 2000) liquid media under 130 rpm. agitation at 22°C, 16 hours light. *Agrobacterium*-mediated transformation of 7 day-old germinated spores were performed as previously described in Ishizaki 2008 unless otherwise described. Resulting cells were incubated under 16 hours light, 22°C. Gemmae from the second generation were subjected to further analysis.

Constructs of interest for the complementation of Mp*ICE* and Mp*ZOU* genes in *A. thaliana*, were electroporated into *Agrobacterium tumefaciens* strain GV3101 mp90. Bacteria were plated at high density onto Yeast Extract Broth (5g/L Beef extract, 1g/L Yeast extract, 5g/L Peptone, 5g/L Sucrose, 15g/L Bacto Agar) plates with the suitable antibiotics and incubated 2 days at 28°C. Bacteria were scraped off plates, suspended in 30mL of infiltration solution (MgCl2 10mM, sucrose 5% and Silwet-L-77 0.03%) and further diluted with 120mL of infiltration solution. At*ice1-2* or At*zou-4* flower buds were dipped in the bacterial solution for 10s, with gentle agitation, covered with plastic bags for 24h and allowed to set seeds. Primary transformants were selected on solid MS medium containing suitable antibiotics and then transferred to soil. T1 and T2 generation plants were selected on agar-solidified MS with antibiotics. T2 lines were genotyped and subjected to phenotypic and molecular analyses.

QUALITATIVE AND QUANTITATIVE ANALYSIS OF TOLUIDINE BLUE PERMEABILITY.

To assess cuticle integrity, toluidine blue staining assays were performed (Tanaka et al., 2004). For qualitative toluidine blue staining tests, etiolated seedlings were used. Seedlings were stratified in the dark, exposed to a 6h light flash and then grown for 4 days in darkness. They were then stained for 2 min in 0.05% w/v Toluidine blue solution with 0.1% v/v Tween 20 and washed abundantly under tap water. Pictures were taken with a Keyence VHX900F digital microscope.

For quantitative toluidine blue staining test, 7-day old light-grown seedlings were stained in the same way. In order to extract toluidine blue and chlorophyll, the cotyledons of ten seedlings were collected and placed in 1mL of 80% ethanol for at least 3 hours in darkness. Toluidine blue content of the resulting solution was measured at 626nm with a spectrophotometer. This absorbance was then normalized using chlorophyll absorbance at

430nm, a wavelength not absorbed by toluidine blue. 6 repetitions were performed per condition (Xing et al., 2013). Data were subjected to an ANOVA test, and where differences were detected, a Scheffe test was used to whether significant differences existed between specific genotypes.

SEED-SHAPE ANALYSIS.

Percentages of misshapen seeds were counted from images taken with the VHX900F digital microscope (Keyence), using the cell counter extension of the ImageJ software. For each genotype, seeds from 4 distinct mother plants were analysed with approximately 1000 seeds analysed per mother plant. Data were subjected to an ANOVA test, and where differences were detected, a Scheffe test was used to whether significant differences existed between specific genotypes.

HISTOCHEMICAL STAINING FOR GUS ACTIVITY OF WHOLE MOUNT THALLUS.

Mp*ZOU1* and Mp*ICE1* promoters were cloned into the pMpGWB104 vector and subsequently Tak2xTak2 spores were transformed (Ishizaki et al., 2015). Histochemical assays for GUS activity were performed according to Jefferson et al., 1987 with some minor modifications. Briefly, after three 20 minute vacuum infiltrations with the GUS staining solution (50mM sodium phosphate buffer, pH 7.2 ; 0.5mM potassium-ferrocyanide; 0.5mM potassium-ferricyanide; 10mM EDTA; 0.01% Triton ; 1mM 5-bromo-4-cloro-3-indolyl-Beta-glucuronic acid (DuchefaBiochemie, CAS number 114162-64-0), plants were incubated overnight at 37°C. They were then dehydrated by incubation in increasing concentrations of Ethanol (15%, 30%, 50%), for 20 minutes (per bath) at room temperature. Plants were then fixed in FAA fixative solution (10% formaldehyde, 5% acetic acid, 50% ethanol) for 45 minutes under vacuum followed by either 2 hours at room temperature or overnight at 4°C. Dehydration steps to remove the chlorophyll were then performed by incubation in further increasing concentrations in Ethanol (50%, 70%, 100%), for 20 minutes per bath at room temperature. Observations of GUS activity were made using a Keyence VHX900F digital microscope.

HISTOCHEMICAL STAINING FOR GUS ACTIVITY OF VIBRATOME-SECTIONED THALLUS.

15 to 20 day-old transcriptional reporter lines (described in the previous section) were harvested and placed into a small plate. 5% Phytagel (Sigma CAS : 71010-52-1 ; P8169) at 50°-60°C was then poured onto the plants. The plate was then stored for 30 min to 1hour at

4°C to cool down before mounted onto the Leica VT1000 S Microtome. Approximately 10µm sections were performed and placed into 1%PBS solution before staining as described above. Observations of GUS activity were made using a Keyence VHX900F digital microscope.

CRISPR-CAS9 GENE EDITING.

CRISPR-Cas9 mutants were generated as described in (Sugano et al., 2014). Two gRNAs for each gene were designed to generate single mutants. The oligonucleotides encoding the sgRNA were first cloned into pGE_EN03. For Mp*zou1* and Mp*ice1* single mutant, the sgRNA constructs were then introduced into pMpGE010 destination vectors (containing the CAS9 protein) and sporelings were transformed using *Agrobacterium* GV3101 strain. (Sugano et al., 2014, 2018).

MICROSCOPY.

12-day old thallus were placed between the slide and slip cover with a drop of chloral hydrate: glycerol (7:1) solution overnight and analysed using a Zeiss axioimager 2 with Differential Interference contrast (DIC).

To image pMpZOU1::TdTomato and pMpICE1b::Tdtomato lines, gemmae were directly grown in chamber slides Nunc™Lab-Tek™II filled with 5mL of B5 Gamborg medium. Chamber slides were placed in a 21°C growth chambers under continuous light from SpectraluxPlus NL36W/840 Plus (Radium Lampenwerk) fluorescent bulbs during 7 days. Images were acquired on a Leica SP8X spectral confocal microscope inverted system equipped with a 460–670 nm super continuum white light laser. Imaging was conducted using either a 10× air objective (HC PL APO 10×/0.40 CS2), a 20× air objective (HC PL APO 20×/0.75 CS2) or a 40× water immersion objective (HC PL APO 40×/1.10 W CORR CS2).

Excitation laser wavelength and captured emitted fluorescence wavelength window were 561 nm, 570–625nm for TdTomato and 488nm, 650-700nm for Chlorophyll autofluorescence. To limit chlorophyll signal in the tdTomato channel time-gating was used.

RNA EXTRACTION AND RNASEQ.

12-day old thallus were harvested, frozen in liquid nitrogen and grounded with a pestle and a mortar to have minimum 100mg of ground powder. In each case, three independent RNA samples were extracted for each genotype. Total RNAs were extracted in TRIzol. Briefly,

1mL of TRIzol were added in each tubes before the samples thawed and then were vortexed. After centrifugation (12,000 rpm, 10min, 4°C) ethanol was added to the supernatant to a final concentration of 35%. RNAs using silica spin columns from NEB biologicals (catalogue NES-5-008). After centrifugation (11,000 g, 30sec, RT) the flowtrough was discarded and 700µL of RW1 buffer (Qiagen) was added before centrifugation (11 000 g, 30sec, RT). The flow through was discarded and 500µL of RPE buffer (Qiagen) was added before centrifugation (11 000 g, 2min, RT). The column was finally dried out with another 2 minutes centrifugation at RT before elution of the RNAs with 40µL RNAse-free water. RNA quality was checked by running the samples on agarose gel and directly used for either RNASeq analysis (see section RNASeq) or reverse transcripted for qPCR expression analysis as follow.

Total RNAs were extracted as described in RNA extraction section and sent to Edinburgh Genomics for quality control, cDNA preparation, library preparation and sequencing with Illumina HiSeq. Sequencing data were analysed using Salmon and then DESeq2 system.

PLANT GROWTH

All wild-type plants used in the project were *Marchantia polymorpha* Takaragaike-1 (Tak-1) for the male or Takaragaike-2 (Tak-2) for the female (Ishizaki et al., 2008). Spores for transformation were the progeny of Tak2 x Tak1 (Ishizaki et al., 2008). Lines were asexually maintained and propagated through gemmae growth as described in Takenaka et al., 2000 and Okada et al., 2000 except that we used Johnson media (see Annexe) complemented with 1.4% agar. Gemmae were transferred on plate to long-day conditions (16h, 21°C) for approximately 3 to 5 weeks, before harvesting the new generation of gemmae for further analysis.

Arabidopsis thaliana seeds were gas sterilized with chlorine (3mL HCl (33%) in 150mL bleach) for 2 hours and then sown on Murashige and Skoog (MS) medium with 0,5% sucrose in sterile condition, stratified for 2 days at 4°C and grown for 7 days in short-day conditions (8h light, 19°C). Seedlings were then transferred to compost (Argile 10 (favorit)) and grown under short day conditions (8h light, 19°C) for two to three weeks before transferred to long day conditions (16h light, 21°C). All *A. thaliana* mutants used in this study were previously published: the loss of function mutant At*zou-4* allele (Yang et al., 2008a) was used for all complementation experiments as was the loss of function At*ice1-2* allele (Denay et al., 2014a; Kanaoka et al., 2008a). The ecotype Columbia-0 (Col-0) was used as a wild-type control.

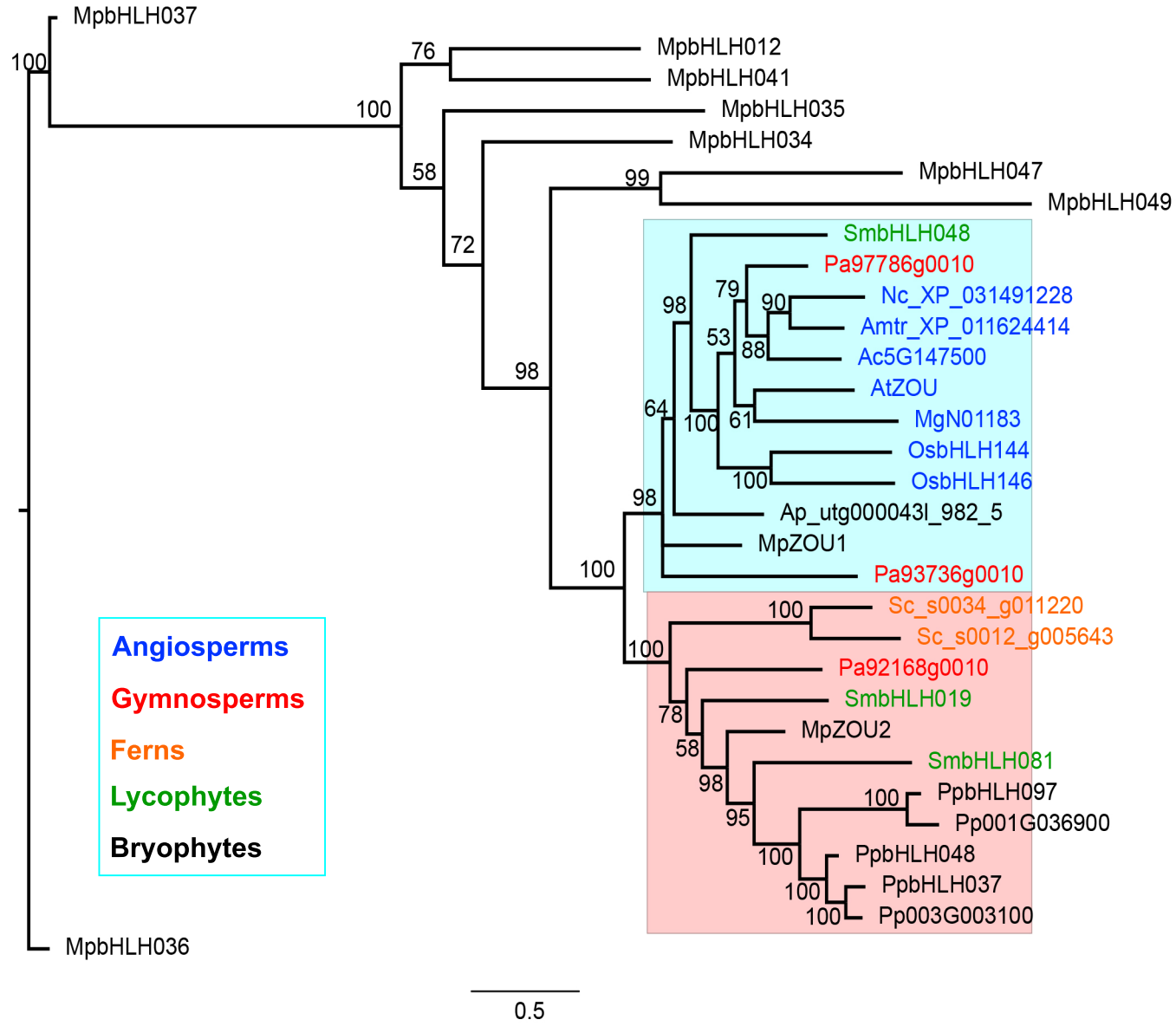

Figure S1 Phylogeny of land plant *ZOU* genes.
Bayesian phylogeny, rooted on MpbHLH36, with percent probabilities indicated on branches. The clade containing the *AtZOU* orthologues is highlighted in light blue, the ZOU2 clade containing an ancient paralogue in cerise. ZOU2 is not conserved in angiosperms, whereas mosses and ferns lack ZOU1. Where available the numbering of bHLHs follows that of Pires et al. Species abbreviations are At *Arabidopsis thaliana*, Mg *Mimulus guttifera*, Ac *Aquilegia coerula*, Nc *Nymphae colorata*, Amtr *Amborella trichopada*, Pa *Picea abies*, Sc *Salvinia cucullata*, Sm *Selaginella moellendorffii*, Aa *Anthoceros punctatus*, Pp *Physcomitrella patens*, Mp *Marchantia polymorpha*. Different taxonomic groupings coloured as shown in box on left.

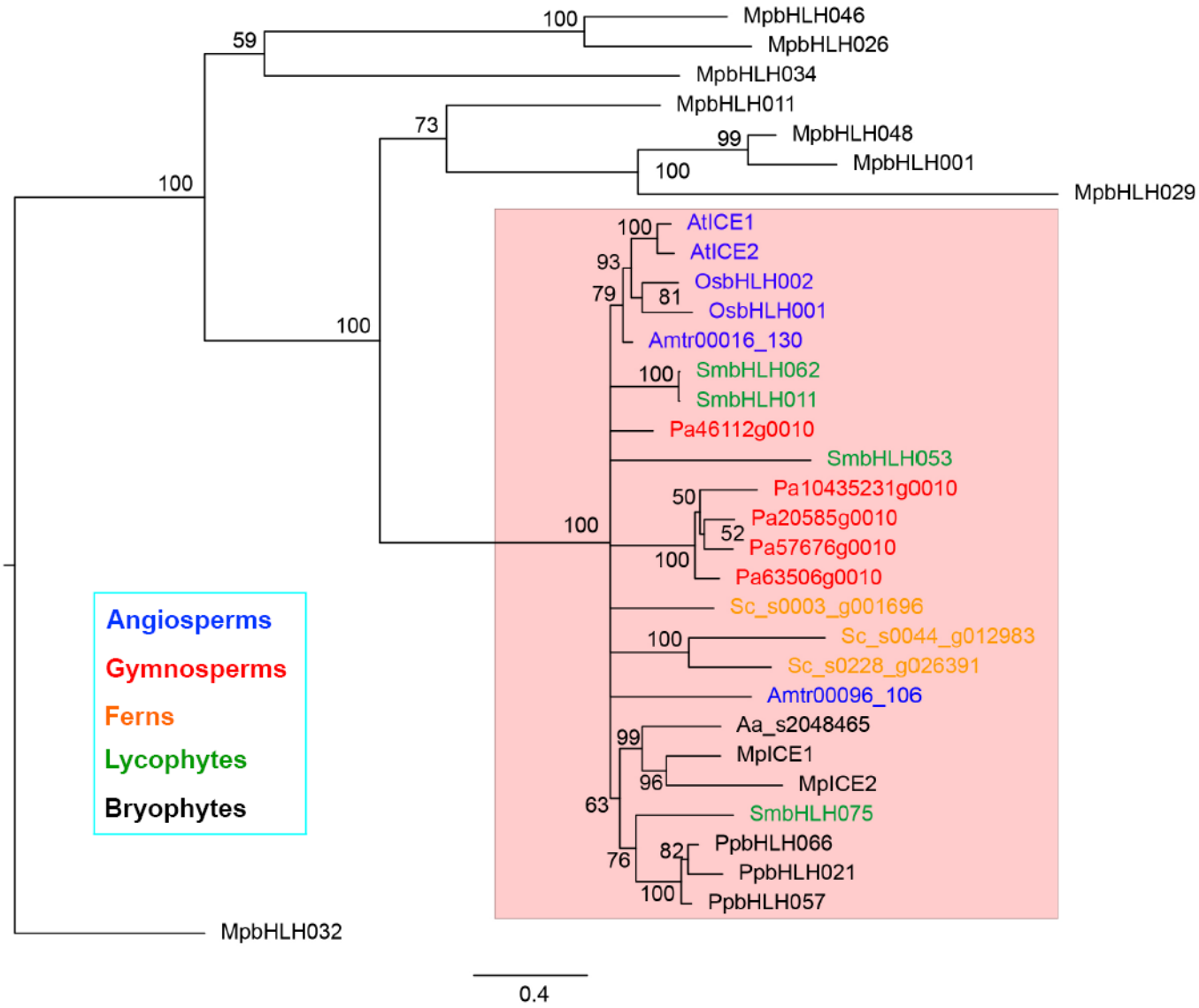

Figure S2 : Phylogeny of land plant ICE genes.
Bayesian phylogeny, rooted on MpbHLH032, with percent probabilities indicated on branches. The clade containing the *AtICE1* and *AtICE2* orthologues is highlighted in cerise. Species abbreviations are At *Arabidopsis thaliana*, Mg *Mimulus guttifera*, Ac *Aquilegia coerula*, Os, *Oryza sativa*, Nc *Nymphae colorata*, Amtr *Amborella trichopada*, Pa *Picea abies*, Sc *Salvinia cucullata*, Sm *Selaginella moellendorffii*, Aa *Anthoceros punctatus*, Pp *Physcomitrella patens*, Mp *Marchantia polymorpha*. Different taxonomic groupings coloured as shown in box on left.

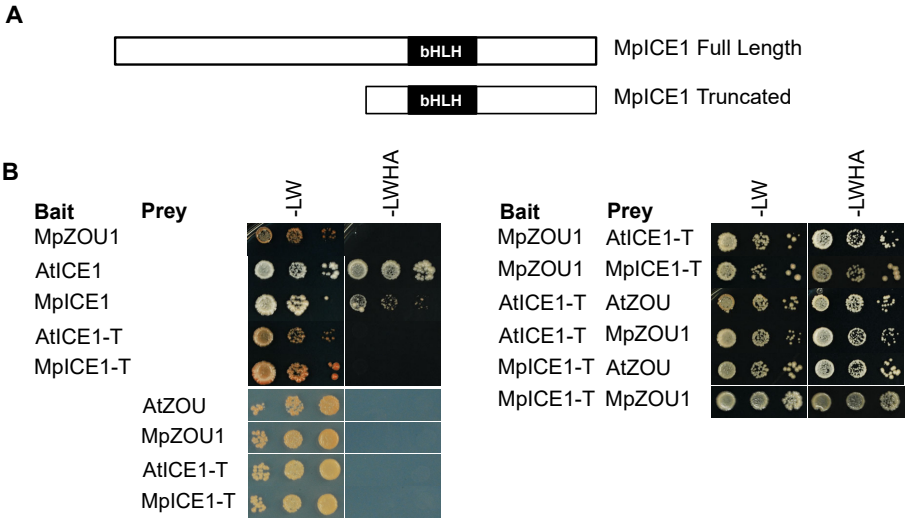

Fig S3 : MpZOU1 and MpICE1 interact in yeast two hybrids and with AtICE1 and AtZOU respectively. (A) The proteins used in yeast two hybrids experiments. (B) Interactions tested in yeast. Empty boxes indicate empty vector controls. AtICE1-T and MpICE1-T indicate respectively AtICE1 truncated and MpICE1 truncated as shown in (A). Growth on minimal non selective (-LW) and selective (-LWHA) media is shown.

A

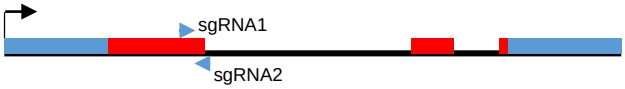

B

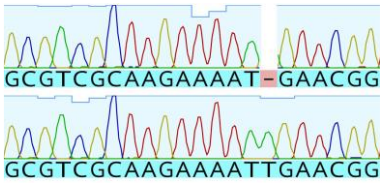

C

WT 5′-GCGTCGCAAGAAAA-TGAA**CGG**-3′

Mpzou1-1 5′-GCGTCGCAAGAAAATTGAACGG-3′ (+1bp)

Mpzou1-5 5′-GCGTCGCAAGAAAATTGAACGG-3′ (+1bp)

WT 5′-GCGTCGCAAGAAAATG----------AA**CGG**-3′

Mpzou1-6 5′-GCGTCGCAAGAAAATGTTCTCCACGTT-ACGG-3′ (+11bp -1bp = +10bp)

WT 5′-ATCACCTTGGAGTTGAGA**TGG**-3′

Mpzou1-2 5′-ATCACCTTG-----GAGATGG-3′ (-5bp)

D



E

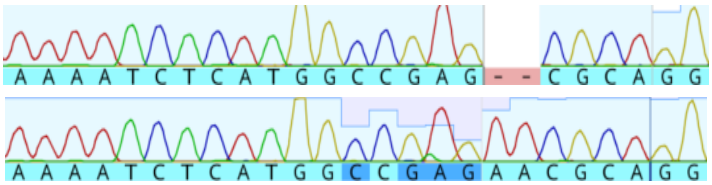

F

WT 5′-AAAATCTCATGGCCGA--------GCGC**AGG**-3′

Mpice1-2 5′-AAAATCTCATGGCCGAAAAATTCTGCGCAGG-3′ (+8bp)

WT 5′-AAAATCTCATGGCCGAG--CGC**AGG**-3′

Mpice1-4 5′-AAAATCTCATGGCCGAGT-CGCAGG-3′ (+1bp)

Mpice1-5 5′-AAAATCTCATGGCCGAGAACGCAGG-3′ (+2bp)

WT 5′-AAAATCTCA----------TGGCCGAGCGC**AGG**-3′

Mpice1-6 5′-AAAATCTCAGATTCATAAAATGAGATTCATAAAAATCTCAT--------CGC**AGG**-3′

(+32bp -8bp = +24bp)

Figure S4: Mutant alleles produced by genome editing

(A) Schematic of Mp*ZOU1* gene, filled rectangles indicate exons, untranslated regions are shown in blue and coding sequences in red. sgRNA1 and 2 target basic and loop regions of bHLH domain, respectively. (B) Chromatograms showing sequence alteration in Mp*zou1-1* allele. (C) Sequence of Mp*zou1* alleles. The sgRNA sequence is underlined in wild type (WT) and the PAM sequence shown in bold. Mp*zou1-1* and Mp*zou1-5* have the same lesion but were independent isolates. The alleles were generated with sgRNA1 except Mp*zou1-2* which was from sgRNA2. (D) Schematic of Mp*ICE1* gene, sgRNA targets basic region of bHLH domain. (E) Chromatograms showing sequence alteration in Mp*ice1-5* allele. (F) Sequence of Mp*ice1* alleles. The sgRNA sequence is underlined in wild type (WT) and the PAM sequence shown in bold. The alleles were generated with sgRNA1.

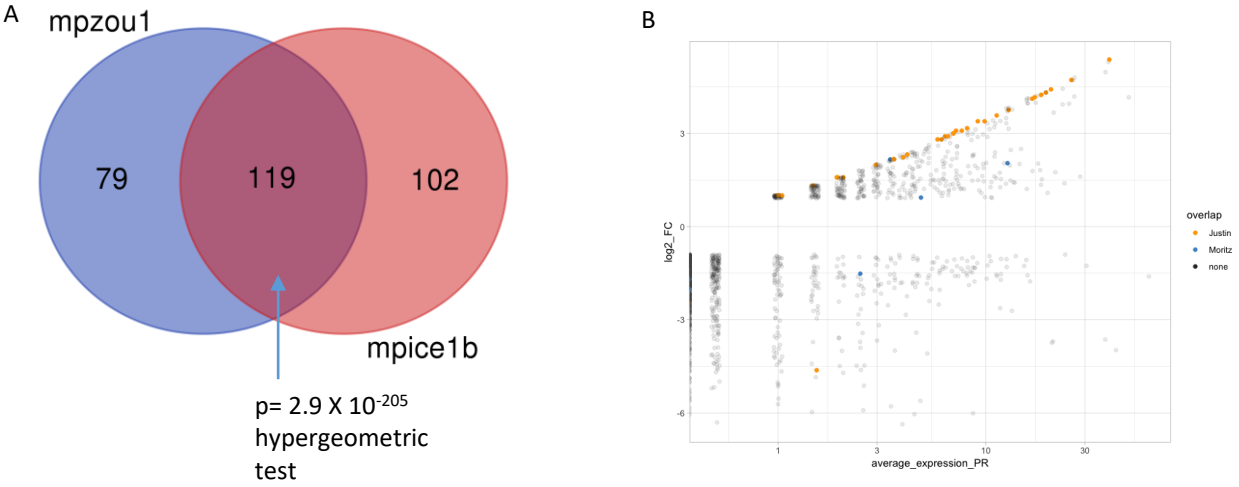

Figure S5: Transcriptional profiling of 12 day old thallus tissue and overlap with scRNAseq data. (A) Number of transcripts with reduced abundance (log2 fold change <-2, FDR < 0.05) relative to wild type in 12 day old thallus. (B) Overlap of scRNAseq data from presumed pegged rhizoid cells with RNAseq dataset (orange) with average expression level in pegged rhizoid (x axis) and expression relative to average expression in other cell types. The 35 genes downregulated in zou and ice mutants are also highly expressed in pegged rhizoids relative to other cell types.

Gene ID	*Annotation*	*L2FC Mpzou1/WT*	*L2FC Mpice1/WT*
	Cell Wall Modification		
Mp4g03640	D-mannose binding lectin protein	-7,308547264	-8,689340194
Mp3g06900	Expansin	-3,334748823	-6,165767015
Mp5g22020	FASCICLIN-like arabinogalactan 2	-5,381568334	-2,686180513
Mp8g02360	Proline rich extensin signature	-3,190385544	-5,652239957
Mp3g03160	Rhamnogalacturonan endolyase	-8,8	-8,1
Mp2g13580	Rhamnogalacturonan endolyase	-8,6	-8,7
Mp2g13570	Rhamnogalacturonan endolyase	-8,2	-7,8
Mp5g20220	Rhamnogalacturonan endolyase	-5,885335982	-7,252274609
Mp7g11130	Rhamnogalacturonan endolyase	-3,84641169	-2,264821661
Mp5g20220	Rhamnogalacturonan endolyase	-5,885335982	-7,252274609
Mp4g00700	Xyloglucan endotransglycosylase	-9,8	-10,6
Mp4g00680	Xyloglucan endotransglycosylase	-7,839091308	-7,907304139
Mp4g00670	Xyloglucan endotransglycosylase	-6,051564703	-5,409005562
Mp4g00690	Xyloglucan endotransglycosylase	-5,685791453	-5,754003905
Mp2g02380	Xyloglucan endotransglycosylase	-5,328890025	-5,397103167
	Cell Death		
Mp8g07700	Metacaspase	-5,98687609	-4,337532352
Mp6g12240	DUF679 containing DMP-like	-8,53321704	-9,328491709
Mp5g12180	DUF679 containing DMP-like	-6,547208129	-7,533705979
Mp5g12170	DUF679 containing DMP-like	-4,56976316	-5,50409815
Mp4g17600	DUF679 containing DMP-like	-3,708551749	-5,019035685
Mp4g17620	DUF679 containing DMP-like	-2,173907669	-2,324182094
	Protease		
Mp5g16420	Aspartyl protease	-10,79466634	-9,565979272
Mp5g16430	Aspartyl protease	-9,366918598	-8,215863957
Mp5g16410	Aspartyl protease	-6,990028668	-7,058242037
Mp5g12100	Aspartyl protease	-5,922008559	-7,22629013
Mp5g16350	Aspartyl protease	-4,965458929	-5,22836089
Mp5g12090	Aspartyl protease	-4,263418673	-2,942451302
Mpzg01030	ATP-dependent Clp protease	-3,088101055	-3,143609532
Mp8g14580	Metalloprotease	-2,48692834	-2,498577119

Gene ID	*Annotation*	*L2FC Mpzou1/WT*	*L2FC Mpice1/WT*
	Redox		
Mp5g06310	Peroxidase	-9,881484643	-6,51345322
Mp5g17080	Peroxidase	-9,128887961	-9,197099693
Mp5g17030	Peroxidase	-8,904455447	-3,423555011
Mp5g02520	Peroxidase	-8,185049792	-3,406338144
Mp5g17120	Peroxidase	-8,164674098	-8,23288664
Mp5g17130	Peroxidase	-8,105389317	-8,891553292
Mp5g17110	Peroxidase	-7,062941802	-7,062087351
Mp2g24530	Peroxidase	-6,58548836	-6,24048508
Mp6g21140	Peroxidase	-5,785625602	-5,853838371
Mp5g19410	Peroxidase	-5,585295307	-8,852405877
Mpzg01380	Peroxidase	-5,236155709	-6,026463768
Mp4g14270	Peroxidase	-5,033286376	-5,105498111
Mp5g09230	Peroxidase	-4,505291281	-4,338896425
Mp5g02600	Peroxidase	-3,203014465	-2,607079395
Mp1g22970	Peroxidase	-3,021317617	-4,255561426
Mp5g10750	Peroxidase	-2,99377374	-6,845421615
Mp5g06280	Peroxidase	-2,474439263	-3,115963437
	Other		
Mp4g03020	Aquaporin	-7,214844725	-5,358732309
Mp1g29040	Aquaporin	-4,750690852	-3,029208179

Table 1: List of genes downregulated in Mp*zou1* and/or Mp*ice1* compared to WT.
L2FC corresponds to Log2 Fold Change

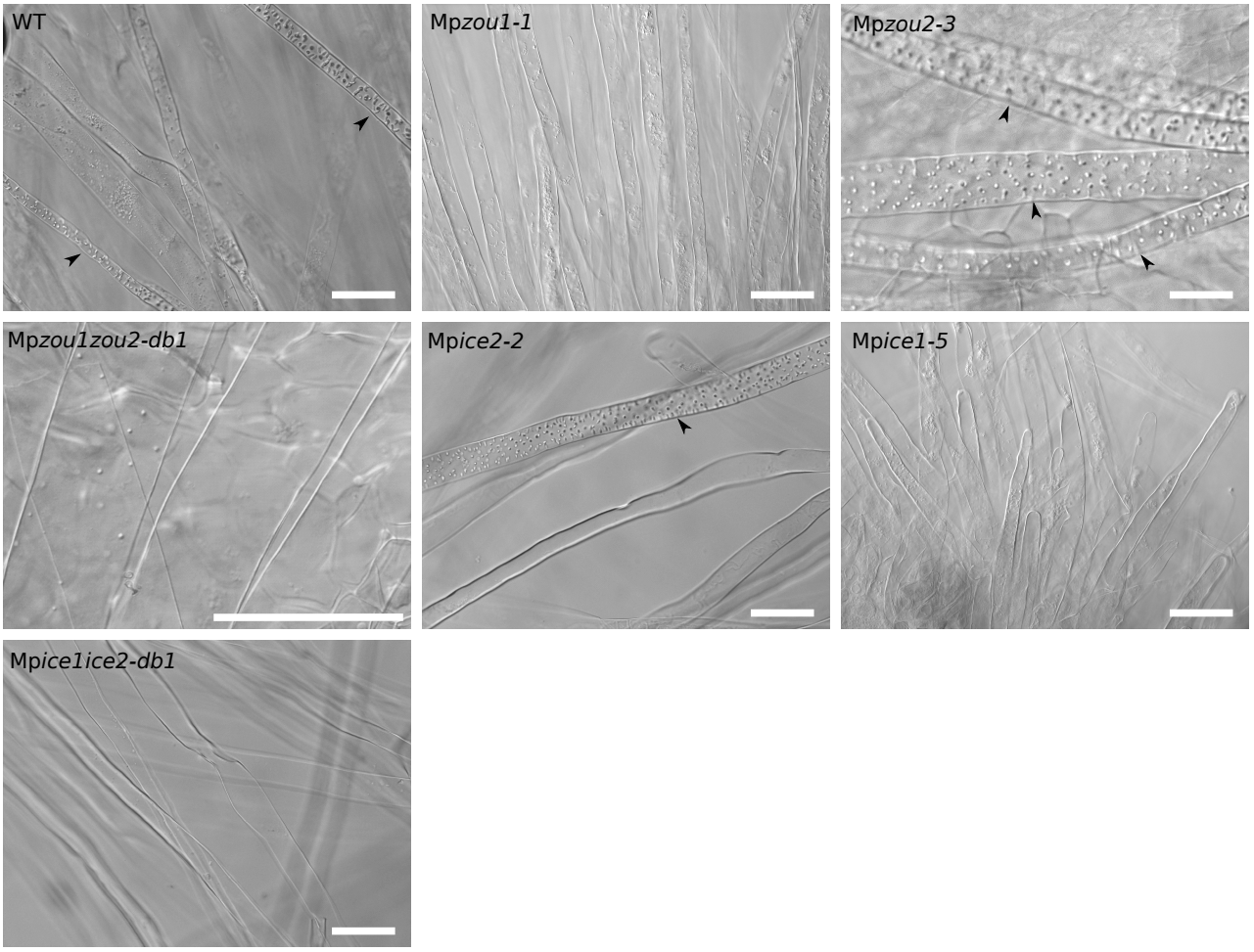

Figure 1 : MpZOU1 and MpICE1 promote pegged rhizoids differentiation in the gametophyte.
Mp*zou1zou2-db1* and Mp*ice1ice2-db1* are also defective in pegged rhizoids in the stalk but not Mp*zou2-3* and Mp*ice2-2* single mutants. Arrowheads indicate pegged rhizoids. Scale bar, 100µm.

II- Further considerations

As seen in the introduction and discussed in this previous section, *M. polymorpha* contains two types of rhizoids: living rhizoids called smooth rhizoids and pegged rhizoids which are dead at maturity. MpZOU1 and MpICE1 appear to control the development of the pegged rhizoids in both the gametophyte but also in the “stalks” of the gametophores. In the single mutants, Mp*zou1* and Mp*ice1*, the lack of pegged rhizoids (and possibly other factors) causes early drying of the gametophores and a drastic reduction in their size. As described above, *M. polymorpha* encodes two ICE proteins, MpICE1 and MpICE2, and two ZOU proteins, MpZOU1 and MpZOU2. My work has shown that MpZOU2 and both MpICE proteins are involved in cuticle development in gemmae. Thus two protein complexes, MpZOU2 MpICE1 and MpZOU2 MpICE2 apopear to be involved in cuticle formation. The slightly overlapping expression patterns of the two ZOU-protein encoding genes, and the two ICE encoding genes in the ventral epidermis of *M. polymorpha* raised the question of whether functional redundancy also exists between the different complex components with respect to pegged rhizoid development. To answer this question, pegged rhizoid development was investigated in the gametophytes and gametophores of the following CRISPR-Cas9 mutants: Mp*zou2*, Mp*ice2*, Mp*zou1* Mp*zou2* and Mp*ice1* Mp*ice2* (**Figure 1 and 2**). Mp*zou2* and Mp*ice2* showed no defect in pegged rhizoid development either in their gametophyte or in the stalk of their gametophores, suggesting that *MpZOU2* and *MpICE2* play either minimal or highly redundant roles in the control of pegged rhizoid formation. This observation was confirmed by the phenotypes of both double mutants Mp*zou1*Mp*zou2* and Mp*ice1*Mp*ice2* which resembled the single mutants, Mp*zou1* and Mp*ice1* in terms of pegged rhizoid formation. This is contrary to the augmentation of cuticle phenotypes observed in double mutants compared to Mp*zou2* and Mp*ice2*.

This discrepancy regarding the functional redundancy of the MpZOU/MpICE complexes deserves to be investigated in more detail. One possibility is that our assays for pegged rhizoid formation are not accurate enough to detect subtle differences in the timing of rhizoid differentiation of, indeed the number of pegged rhizoids formed. It would also be interesting to investigate whether $_{pro}$*MpZOU2::MpZOU1-CDS* or $_{pro}$*MpZOU1::MpZOU2-CDS* can complement the cuticle phenotype of Mp*zou2* or the pegged rhizoid phenotype of Mp*zou1* mutants, in order to test whether complexes show functional specificity that is independent of their expression patterns. Similar experiments could also be carried out using the *MpICE* genes.

Finally MpZOU1/MpICE1 complex activity involves extensive cell wall remodelling to thicken the rhizoid walls and to generate pegs, which are outgrowths composed of cell wall

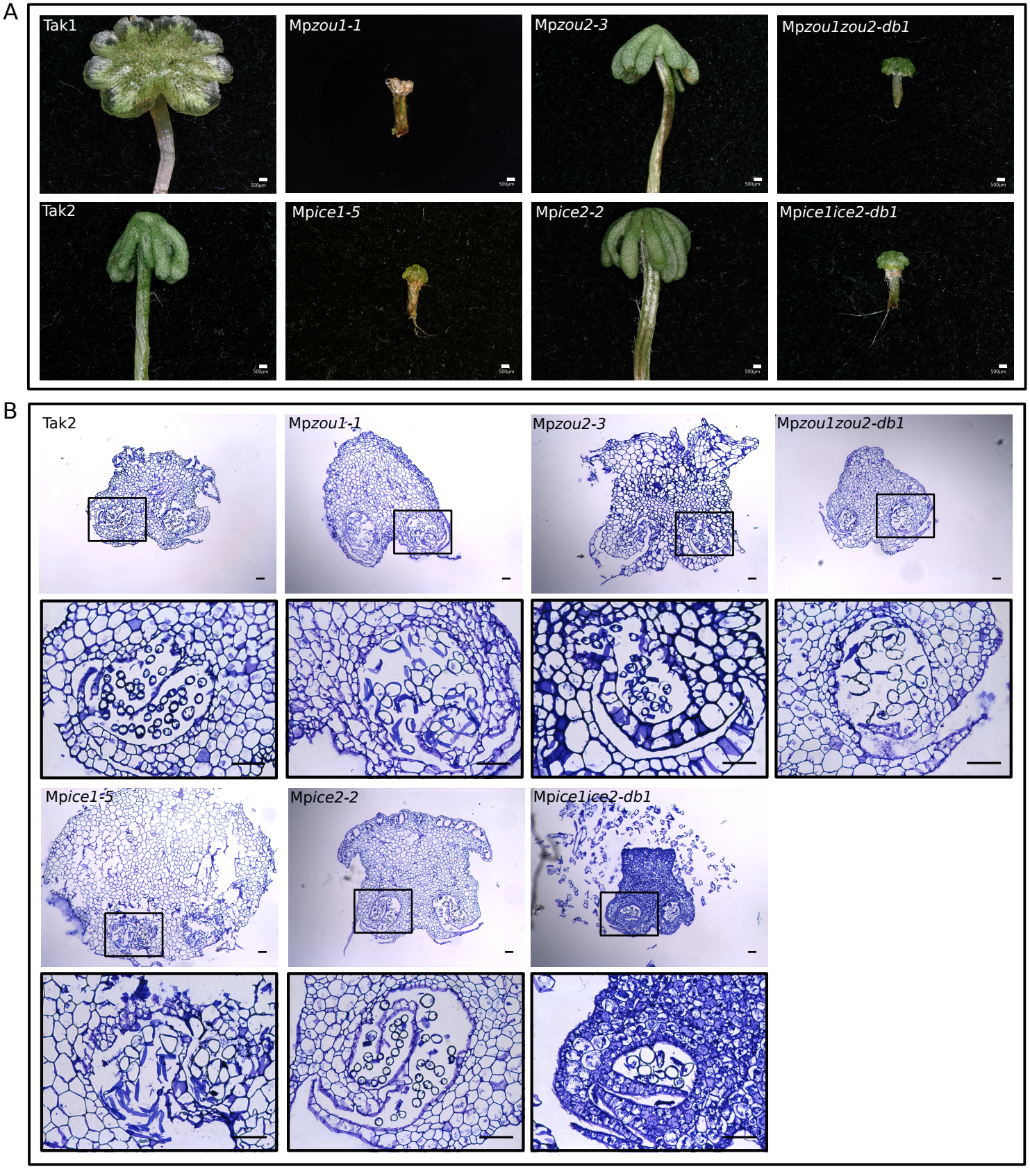

Figure 2 : MpZOU1 and MpICE1 promote pegged rhizoids differentiation in the gametophore stalks. Mp*zou1zou2-db1* and Mp*ice1ice2-db1* are also defective in pegged rhizoids in the stalk but not Mp*zou2-3* and Mp*ice2-2* single mutants. (A) Gametophores of Mp*zou1-1* and Mp*ice1-5* are similar to Mp*zou1zou2-db1* and Mp*ice1ice2-db1* gametophores, they are very short and dry. In contrast with Mp*zou2-3* and Mp*ice2-2* gametophores which are WT-like (Tak1 or Tak2). Scale bar, 500µm. (B) Mp*zou1zou2-db1* and Mp*ice1ice2-db1* are also defective in pegged rhizoids in the stalk but not Mp*zou2-3* and Mp*ice2-2* single mutants. Row 1 and 3 are transverse sections of embedded stalks. Black squares in row 1 and 3 are higher magnification showed in row 2 and 4. Scale bars, 50µm.

material. These modifications are followed by cell death, although the functional link between the two processes remains unclear. Does cell wall remodelling lead to cell death, or is cell death triggered independently of cell wall remodelling by the MpZOU1/MpICE1 complex. This question is relevent given the superficial similarity between the functions of MpZOU1/MpICE1 in rhizoids and AtZOU/AtICE1 in the breakdown *of the A. thaliana* endosperm. In the endosperm it has been shown that cell wall modification (in this case thinning and softening) precedes and is a prerequisite for endosperm cell death, which is also promoted by the physical crushing of the softened endosperm by the growing embryo (Fourquin et al., 2016). Whether cell death in the pegged rhizoids of *M. polymorpha* can truly be functionally equated to the cell elimination process observed in the developing endosperm remains an open question.

GENERAL DISCUSSION AND PERSPECTIVES

I The regulation of the activity of the ZOU/ICE complex: Conservation and divergence.

The work presented in this thesis has confirmed that not only are ZOU and ICE proteins conserved in *M. polymorpha*, but that the ZOU/ICE complex is also conserved and is thus likely to have been an early and important factor for gene regulation in land plants. My work has also underlined intriguing parallels between the function of the ZOU/ICE complexes in *M. polymorpha* and those in seed plants, relating to the regulation of cell elimination/death, and the formation of the cuticle. However, despite this apparent molecular and functional conservation, my work has also pinpointed interesting points of divergence.

One of the main questions that I hoped to address during my PhD was how the activity of the ZOU/ICE complex in seeds is regulated, and whether regulatory mechanisms might have already been recruited in early land plants, and could potentially help in the eludidation of complex function. Previous work in *A. thaliana* had suggested that ZOU/ICE complex in the endosperm activity is likely controlled at the level of ICE1 stability. My work has confirmed that this is the case, by revealing the role of HOS1 in the endosperm. I have also revealed an additional role for ZOU/ICE1 in regulating the transcription of *ICE2,* highlighting the likely complex nature of regulatory interactions in this tissue.

Complementation experiments using MpICE1 and MpICE2 suggests that MpICE1 post-translational regulation could be divergent from that of AtICE1 and AtICE2. This difference might be explained in terms of the conservation of the important KRAAM motif in MpICE1. In *A. thaliana*, both ICE1 and ICE2 proteins interact with other bHLH class Ia transcription factors SPEECHLESS MUTE AND FAMA to specify three cell-state transitional steps leading to stomata differentiation. During this developmental process, ICE1 serves as a scaffold to recruit SPCH and MPK3/6. The association of MPK3/6 and ICE1 leads to phosphorylation and degradation of ICE1 protein by an unknown proteosomal pathway. In addition to the phosphorylation of ICE1 and through its interaction with SPCH, ICE1 brings SPCH into proximity with MPK6 which thus phosphorylates SPCH leading to its dowregulation. Together, this inhibits stomatal cell fate (Putarjanan 2019). To date, we do not know if this mechanism is conserved in seed development through the ZOU/ICE complex However, similarly to the overproduction of stomata when ICE1 is stabilized in ICE1-D (mutated in the KRAAM domain), endosperm lysis is precocious suggesting again a stabilisation and gain of activity of ICE1 (Denay et al., 2014a). My preliminary results on the embryo sheath also support this. Published data also confirm a role of MPK6 in embryonic cuticle formation through the ALE1/GSO

signalling pathway. However the MPK6 loss-of-function mutant is also affected in seed size and seed bursting, phenotypes that are unlikely related to the ALE1/GSO pathway.

In *M. polymorpha* ICE proteins the KRAAM motif is only partially conserved in MpICE1 (KRGGT motif and not KRAAM). MpICE1 only partially rescues the A. thaliana *ice1-2* seed phenotype potentially due to altered interactions with putative regulators, such as AtMPK6 in the complemented line. Interestingly, during an unpublished study carried out during my Master degree, I showed that ZmICEa, a very divergent ICE variant from maize that lacks a KRAAM domain, fully complements the *ice1-2* seed phenotype and, moreover gives stomatal phenotypes similar to those of ICE1-D when expressed in Arabidopsis. It is therefore possible that the KRGGT motif in MpICE1 leads to excessive destabilization of the MpICE1 protein, at least in *A. thaliana*. However, partial complementation could also be due to other factors, and merits further exploration. MpICE2 which gives a full rescue of the seed phenotype in *A. thaliana* has a more conserved KRAAM motif since only one amino acid changed from a methionine to a leucine (KRAAL motif). This raises the question of a possible difference in the regulation of MpZOU1/MpICE1 and MpZOU2/MpICE2 complexes in *M. polymorpha*.

Interestingly, no interaction in yeast between PpICE1 and AtMPK3/6 has been highlighted although MPKs are present in Physcomitrella genome. This absence of interaction might suggest that the MPK3/6-mediated post-translational regulation of ICE is not an ancient mechanism, and may have appeared later during land plant evolution. This is supported by the fact that *A. thaliana* MPK3 and MPK6 orthologues are not found in either *Physcomitrella patens* or *M. polymorpha* (González-Coronel et al., 2021). However, other MPKs could functionally replace MPK3 or MPK6 in the regulation of ICE in Bryophytes. HOS1 is also known to negatively regulate ICE1 and ICE2 in *A. thaliana* during stomatal development, cold tolerance and more recently seed development. Interestingly, *M. polymorpha* also seems to have one HOS1 protein (Mapoly0088s0017). However, to date more tools need to be generated to address divergence in the ZOU/ICE complex at the level of its regulation. In addition to post-translational regulation, it would be particularly interesting to assess whether transcriptional regulation, such as that that I have revealed for *ICE2* in seeds, is a feature in lower land plants. My results in *M. polymorpha* suggest that this may not be the case, however this possibility, and the molecular basis for my observations in *A. thaliana* seeds, again require further study.

bHLH transcription factors are the second largest transcription factors family in Angiosperms. They are involved in many developmental processes and cellular differentiation events. Twenty subfamilies of bHLH transcription factors found in Angiosperms (out of a total of 26) are also present in early land plants suggesting that bHLH transcription factors appeared before.(Catarino et al., 2016; Pires and Dolan, 2010). Most characterised plant bHLH

transcription factors bind to the conserved G-box (5'-CACGTG-3') and G-box related DNA sequences (Giuliano et al., 1988; Hao et al., 2021). Since ZOU and ICE are bHLH transcription factors they likely bind to G-box sequences. Detailed comparative analysis of genes acting downstream of ZOU/ICE complexes (which could be identified by combining omics approaches such as by ChIP seq and RNASeq) would help to identify whether the direct targets of ZOU/ICE complexes are conserved in *A. thaliana* and *M. polymorpha*. Transactivation in the heterologous system *Physcomittrella patens* already confirmed genetic data showing the necessity for the *A. thaliana* ZOU and ICE proteins to form heterodimers in order to activate *RGP3* gene promoter via its G-box sequence (Denay et al., 2014a). It would be interesting to carry out parallel omics experiments, combined with similar transactivation approaches using the *M. polymorpha* ZOU and ICE proteins to determine how target specificity of the M. polymorpha ZOU/ICE complex is defined.

II The ZOU/ICE complex in the control of *M. polymorpha* gemma cuticle and *A. thaliana* embryonic cuticle formation

In *A. thaliana*, ZOU/ICE1 heterodimers are required for the formation of a functional embryonic cuticle. Interestingly this function appears not to involve the regulation of the biosynthesis of cognate cuticle components such as cutin monomers, but rather an implication in pathways involved in a pathway involved in cuticle integrity monitoring. Although the main molecular actors of this pathway have been elucidated, how pathway activation leads to the production of an itact embryonic cuticle remains a mystery, potentially because the composition of the embryonic cuticle is also enigmatic. Published and unpublished data from the group have suggested the potential importance of phenolic components in the *A. thaliana* embryonic cuticle. Several dyes generally used to stain phenolic-enriched polymers (such as lignin and suberin) have been tested and can stain the embryonic cuticle, including Fluorol Yellow dye which is mostly used to stain cutin and suberin, but also Auramine O which is specifically used for suberin and lignin staining (unpublished data from N. Doll and AC Marsollier and (Creff et al., 2019a)). Interestingly, comparative analysis of embryonic cuticle staining of *zou* mutant and wild-type revealed a decrease of cuticle staining in *zou* suggesting that phenolic compounds are reduced in the *zou* embryonic cuticle or at least that phenolic compounds within the embryonic cuticle are less easily detectable by dyes in this mutant. The presence of phenolic compounds (particularly Sinapic acid) in the embryonic root cuticle was confirmed by Berhin and colleagues (Berhin et al., 2019). The origin of these phenolic componds in unclear, although the expression of genes encoding several enzymes involved in the biosynthesis of specialized phenolics, including SPERMIDINE HYDROXYCINNAMOYL

TRANSFERASE (SHT) (Grienenberger et al., 2009) is strong in the developing endosperm of Arabidopsis, and almost completely lost in *zou* mutants (unpublished results). Thus some components of the embryo cuticle, as well as the extensin enriched extracuticular sheath could be derived from the endosperm and produced under the control of ZOU/ICE.

Interestingly, the cuticles found at the surface of Bryophyte gametophytes also appear to be enriched in phenolic compounds (Kong et al., 2020; Renault et al., 2017; Loue-Manifel et al., in preparation). In this context it is important to remember that the endosperm is derived from the female gametophyte in Angiosperms, albeit as a fertilized derivative. Taken together these results could support a tentative but tantalising hypothesis in which the control of embryonic cuticle formation in angiosperms by ZOU/ICE complexes may have evolved from an ancestral role in the formation of the cuticle of the gametophyte of the ancestor of early diverging land plants such as *M. polymorpha*. One possibility is that phenolics and/or crosslinkable cell wall proteins such as extensins could serve as a scaffold to allow the correct deposition and polymerisation of cutin and waxes in both contexts. The common denominator might be a dependence upon ROS-mediated cross-linking, mediated, in the case of the embryo at least, by the activity of the cuticle integrity signalling pathway. However ROS staining of the embryos of *zou* mutants has not revealed conclusive defects in ROS production (Nicolas Doll, unpublished data), probably due to the technical constraints of such experiments. Likewise, preliminary results in *M. polymorpha* did not show any conclusive differences between *Mpzou1Mpzou2* and *Mpice1Mpice2* double mutants, *Mpzou2, Mpice2* and the WT. However, only one type of ROS (H202) has so far been assayed, and differences in cuticle permeability likely make results very difficult to interpret due to differential access to reagents. Other dyes exist and would need to be tested in *M. polymorpha*.

Specific p-coumarate antibodies have been developed to label cell walls in grasses (Tranquet et al., 2009). INRA-COU1 antibody can recognize free p-coumaric acid and p-coumarate esters whereas esterified p-coumarates are recognized by INRA-COU2 (Tranquet et al., 2009). Since we hypothesized that cuticles of *A. thaliana* embryo and *M. polymorpha* gemma might have a similar phenolic enriched composition and p-coumarate is one of the most abundant phenolic compounds in *A. thaliana* aerial organ cuticles, these two antibodies have also been tested on both species. Unfortunately, neither INRA-COU1 nor INRA-COU2 labelled cuticles in *M. polymorpha* gemma (unpublished data from J. Loue-Manifel and AC. Marsollier)) Gemma cuticle composition also confirms an enrichement in phenolics compounds. However, among the phenolics detected in WT gemma cuticle, only one, p-coumarate, showed a significant difference compared to wild-type. This compound was found to be more abundant specifically in Mp*zou2-3* gemma cuticle. None of the Mp*ice* mutants tested showed statistically significant differences in the amount of any of the molecules identified. However, when interpreting this

data, it is important to bear in mind that some exotic/unexpected fatty acids or other molecules were not identified in the analysis and that important changes were therefore not detected. In addition, delipidation may have removed unpolymerized components, which would have masked potential defects in cuticle assembly. However, when interpreting this data, it is important to bear in mind that some exotic/unexpected fatty acids or other molecules were not identified in the analysis and that important changes were therefore not detected. In addition, delipidation may have removed unpolymerized components, which would have masked potential defects in cuticle assembly.

III What is the link between pegged rhizoid formation, cuticle biogenesis and endosperm cell death?

My work has elucidated two functions of *M. polymorpha* ZOU/ICE complexes. Whereas MpZOU1/MpICE1 predominantly controls pegged rhizoid fate, MpZOU2/MpICE2 and potentially MpZOU2/MpICE1 also control cuticle formation in gemmae. Complex specific function appears likely to be determined by expression patterns. Extensive RNASeq analysis from different mutant backgrounds in two different tissues revealed that ZOU/ICE complexes in *M. polymorpha* appear to activate the expression of a large number of peroxidase-encoding genes, as well as numerous genes involved in cell wall modification and genes linked to apoplastic ROS responses and metabolism. The similarities between these datasets suggest potential mechanistic connections between the role of ZOU/ICE1 complexes in cuticle formation, discussed above, and in pegged rhizoid development. Indeed, like cuticle development, pegged rhizoid development involves remodelling of the cell wall to create the pegs which seem to have a specific signature under UV lights for example (Duckett et al., 2014). This might indicate the presence of large quantities of ROS-crosslinked phenolics. A lack of ROS production in mutants lacking ZOU/ICE complexes could, via an unknown mechanism, be behind the observed regulation of peroxidases in our datasets. Bryophyte cuticles are also enriched in phenolic compounds which might also be crosslinked by ROS-dependent peroxidases. In the future it would be fascinating to assess whether growing *M. polymorpha* in the presence of ROS scavengers can lead to similar transcriptomic changes to those seen in mutants lacking ZOU/ICE complexes, or, indeed, to phenotypes reminiscent of those observed in such mutants.

One particularly interesting discovery from my transcriptomic analysis was the finding that the expression of the closest *M. polymorpha* homologue of the ZOU-regulated *AtKRS* gene, which is required for the production of the extensin-rich embryo sheath in *A. thaliana,* is

also significantly reduced in Mp*zou2* and Mp*zou1*Mp*zou2* mutants. The fact that AtKRS belongs to the family of potential ROS sensing/regulated STIG peptides could prime a hypothesis whereby ROS-dependent extensin production, modification and/or polymeration could be a common factor involved in scaffolding cell wall modifications involved in both cuticle deposition and pegged rhizoid formation. Interestingly in the Mp*zou1*, Mp*ice1* transcriptomic analysis, another predicted STIG-encoding genes is downregulated, strengthening this possibility (Figure S6, Chapter 2). It is interesting, in this context, to note that elicitor induced stress-lignin in Spruce appears to contain large quantities of an extensin-like protein that has been proposed to play a scaffolding function (Lange et al., 1995).

How cuticle formation, pegged rhizoid formation and endosperm elimination are linked mechanistically is less clear. There are obvious superficial parallels between pegged rhizoid formation and endosperm elimination since both processes ultimately involve cell death. However it is interesting to note that while, at least in dicotyledonous plants, endosperm elimination, even if only partial, usually involves, or even depends upon the almost complete dismantling of cell wall, and presumably their recycling, the opposite is true in pegged rhizoids, where death is associated with extreme cell wall thickening. From this point of view pegged rhizoid formation superficially resembles xylem vessel formation much more strongly than it resembles endosperm elimination. Consistent with this view, transcriptomic analysis of *zou* mutants (Xing et al., 2013a) showed that genes whose expression was reduced or lost in *zou* mutants could globally be divided into two classes. The first contained genes whose expression was also reduced in *ale1* mutants, and included genes implicated in stress response, including oxidative stress and ROS responses (Creff et al., 2019a). The second contained genes whose expression was completely unaffected in *ale1* mutants, and whose function was associated either with sheath formation (KRS, being a rare example of a gene in this later class with a link to ROS) or, predominantly, with cell wall degradation (for example pectin lyases). Several genes involved in simple sugar metabolism also fell into this second category. Based on this is seems plausible that the role of ZOU/ICE complexes in endosperm elimination is relatively “new” (or at least highly derived), and associated with nutrient recycling, and the switch of the endosperm from a sink to a source tissue during seed development. Linking this function to the reinforcement of the embryo cuticle may have been an innovation in seed plants aimed at coordinating nutrient fluxes in the seed. This intriguing hypothesis is currently being tested in the Ingram group.

Finally, I would like to point out that although during my PhD I managed to show tantalising similarities between two evolutionary very distant plant models, *A. thaliana* and *M. polymorpha,*

these two models remain distinct points on a very wide and diverse evolutionary tree. They do not necessarily reflect “the norm” in plants belonging to the same clade, group or even family. *A. thaliana* and *M. polymorpha* therefore cannot be considered to be representative of the angiosperms or the bryophytes respectively. As a result, comparing gene functions and/or regulatory machanisms between these two species, although it may provide glimpses of potential commonalities and divergence, cannot be considered to provide conclusive proof of functional conservation at any level.

REFERENCES

Abe, M., Takahashi, T., and Komeda, Y. (2001). Identification of a cis-regulatory element for L1 layer-specific gene expression, which is targeted by an L1-specific homeodomain protein. Plant J. Cell Mol. Biol. *26*, 487–494.

Abe, M., Katsumata, H., Komeda, Y., and Takahashi, T. (2003). Regulation of shoot epidermal cell differentiation by a pair of homeodomain proteins in Arabidopsis. Dev. Camb. Engl. *130*, 635–643.

Aharoni, A., Dixit, S., Jetter, R., Thoenes, E., van Arkel, G., and Pereira, A. (2004). The SHINE clade of AP2 domain transcription factors activates wax biosynthesis, alters cuticle properties, and confers drought tolerance when overexpressed in Arabidopsis. Plant Cell *16*, 2463–2480.

Althoff, F., Kopischke, S., Zobell, O., Ide, K., Ishizaki, K., Kohchi, T., and Zachgo, S. (2014). Comparison of the MpEF1α and CaMV35 promoters for application in Marchantia polymorpha overexpression studies. Transgenic Res. *23*, 235–244.

Aragón, W., Reina-Pinto, J.J., and Serrano, M. (2017). The intimate talk between plants and microorganisms at the leaf surface. J. Exp. Bot. *68*, 5339–5350.

Ariel, F.D., Manavella, P.A., Dezar, C.A., and Chan, R.L. (2007). The true story of the HD-Zip family. Trends Plant Sci. *12*, 419–426.

Bach, L., Michaelson, L.V., Haslam, R., Bellec, Y., Gissot, L., Marion, J., Costa, M.D., Boutin, J.-P., Miquel, M., Tellier, F., et al. (2008). The very-long-chain hydroxy fatty acyl-CoA dehydratase PASTICCINO2 is essential and limiting for plant development. Proc. Natl. Acad. Sci. *105*, 14727–14731.

Banks, J.A. (1999). GAMETOPHYTE DEVELOPMENT IN FERNS. Annu. Rev. Plant Physiol. Plant Mol. Biol. *50*, 163–186.

Banks, J.A. (2009). Selaginella and 400 Million Years of Separation. Annu. Rev. Plant Biol. *60*, 223–238.

Barlow, P.W. (2002). The root cap: Cell dynamics, cell differentiation and cap function. J. Plant Growth Regul. *21*, 261–286.

Baroux, C., and Grossniklaus, U. (2019). Chapter Twenty-One - Seeds—An evolutionary innovation underlying reproductive success in flowering plants. In Current Topics in Developmental Biology, U. Grossniklaus, ed. (Academic Press), pp. 605–642.

Baroux, C., Spillane, C., and Grossniklaus, U. (2002). Evolutionary origins of the endosperm in flowering plants. Genome Biol. *3*, reviews1026.

Bartholomew-Began, S.E. (1991). A morphogenetic re-evaluation of Haplomitrium Nees - (Hepatophyta) (Schweizerbart'sche Verlagsbuchhandlung).

Bateman, R.M., Hilton, J., and Rudall, P.J. (2006). Morphological and molecular phylogenetic context of the angiosperms: contrasting the 'top-down' and 'bottom-up' approaches used to infer the likely characteristics of the first flowers. J. Exp. Bot. *57*, 3471–3503.

Baud, S., Wuillème, S., Lemoine, R., Kronenberger, J., Caboche, M., Lepiniec, L., and Rochat, C. (2005). The AtSUC5 sucrose transporter specifically expressed in the endosperm is involved in early seed development in Arabidopsis. Plant J. *43*, 824–836.

Baur, P., Stulle, K., Schönherr, J., and Uhlig, B. (1998). Absorption of UV-B to blue light radiation by leaf cuticles of selected crop plants. Gartenbauwissenschaft *63*, 145–152.

Bayer, M., Slane, D., and Jürgens, G. (2017). Early plant embryogenesis—dark ages or dark matter? Curr. Opin. Plant Biol. *35*, 30–36.

Beaudoin, F., Wu, X., Li, F., Haslam, R.P., Markham, J.E., Zheng, H., Napier, J.A., and Kunst, L. (2009). Functional characterization of the Arabidopsis beta-ketoacyl-coenzyme A reductase candidates of the fatty acid elongase. Plant Physiol. *150*, 1174–1191.

Beisson, F., Koo, A.J.K., Ruuska, S., Schwender, J., Pollard, M., Thelen, J.J., Paddock, T., Salas, J.J., Savage, L., Milcamps, A., et al. (2003). Arabidopsis genes involved in acyl lipid metabolism. A 2003 census of the candidates, a study of the distribution of expressed sequence tags in organs, and a web-based database. Plant Physiol. *132*, 681–697.

Beisson, F., Li-Beisson, Y., and Pollard, M. (2012). Solving the puzzles of cutin and suberin polymer biosynthesis. Curr. Opin. Plant Biol. *15*, 329–337.

Bellec, Y., Harrar, Y., Butaeye, C., Darnet, S., Bellini, C., and Faure, J.-D. (2002). Pasticcino2 is a protein tyrosine phosphatase-like involved in cell proliferation and differentiation in Arabidopsis. Plant J. Cell Mol. Biol. *32*, 713–722.

Berger, F. (2003). Endosperm: the crossroad of seed development. Curr. Opin. Plant Biol. *6*, 42–50.

Berger, F. (2008). Double-fertilization, from myths to reality. Sex. Plant Reprod. *21*, 3–5.

Berger, F., Grini, P.E., and Schnittger, A. (2006). Endosperm: an integrator of seed growth and development. Curr. Opin. Plant Biol. *9*, 664–670.

Berhin, A., de Bellis, D., Franke, R.B., Buono, R.A., Nowack, M.K., and Nawrath, C. (2019). The Root Cap Cuticle: A Cell Wall Structure for Seedling Establishment and Lateral Root Formation. Cell *176*, 1367-1378.e8.

Bernard, A., Domergue, F., Pascal, S., Jetter, R., Renne, C., Faure, J.-D., Haslam, R.P., Napier, J.A., Lessire, R., and Joubès, J. (2012). Reconstitution of plant alkane biosynthesis in yeast demonstrates that Arabidopsis ECERIFERUM1 and ECERIFERUM3 are core components of a very-long-chain alkane synthesis complex. Plant Cell *24*, 3106–3118.

Bessire, M., Chassot, C., Jacquat, A.-C., Humphry, M., Borel, S., Petétot, J.M.-C., Métraux, J.-P., and Nawrath, C. (2007). A permeable cuticle in Arabidopsis leads to a strong resistance to Botrytis cinerea. EMBO J. *26*, 2158–2168.

Bessire, M., Borel, S., Fabre, G., Carraça, L., Efremova, N., Yephremov, A., Cao, Y., Jetter, R., Jacquat, A.-C., Métraux, J.-P., et al. (2011). A member of the PLEIOTROPIC DRUG RESISTANCE family of ATP binding cassette transporters is required for the formation of a functional cuticle in Arabidopsis. Plant Cell *23*, 1958–1970.

Bethke, P., Libourel, I., and Jones, R. (2007). Rebirth and death: Nitric oxide and reactive oxygen species in seeds. Comp. Biochem. Physiol. A. Mol. Integr. Physiol. *146*, S56.

Biała, W., and Jasiński, M. (2018). The Phenylpropanoid Case – It Is Transport That Matters. Front. Plant Sci. *9*, 1610.

Bird, D., Beisson, F., Brigham, A., Shin, J., Greer, S., Jetter, R., Kunst, L., Wu, X., Yephremov, A., and Samuels, L. (2007). Characterization of Arabidopsis ABCG11/WBC11, an ATP binding

cassette (ABC) transporter that is required for cuticular lipid secretion. Plant J. Cell Mol. Biol. *52*, 485–498.

Bollhöner, B., Zhang, B., Stael, S., Denancé, N., Overmyer, K., Goffner, D., Van Breusegem, F., and Tuominen, H. (2013). Post mortem function of AtMC9 in xylem vessel elements. New Phytol. *200*, 498–510.

Bollhöner, B., Jokipii-Lukkari, S., Bygdell, J., Stael, S., Adriasola, M., Muñiz, L., Van Breusegem, F., Ezcurra, I., Wingsle, G., and Tuominen, H. (2018). The function of two type II metacaspases in woody tissues of Populus trees. New Phytol. *217*, 1551–1565.

Bonfante, P., and Genre, A. (2008). Plants and arbuscular mycorrhizal fungi: an evolutionary-developmental perspective. Trends Plant Sci. *13*, 492–498.

Bourdenx, B., Bernard, A., Domergue, F., Pascal, S., Léger, A., Roby, D., Pervent, M., Vile, D., Haslam, R.P., Napier, J.A., et al. (2011). Overexpression of Arabidopsis ECERIFERUM1 Promotes Wax Very-Long-Chain Alkane Biosynthesis and Influences Plant Response to Biotic and Abiotic Stresses. Plant Physiol. *156*, 29–45.

Bourgault, R., Matschi, S., Vasquez, M., Qiao, P., Sonntag, A., Charlebois, C., Mohammadi, M., Scanlon, M.J., Smith, L.G., and Molina, I. (2020). Constructing functional cuticles: analysis of relationships between cuticle lipid composition, ultrastructure and water barrier function in developing adult maize leaves. Ann. Bot. *125*, 79–91.

Bowman, J.L., Sakakibara, K., Furumizu, C., and Dierschke, T. (2016). Evolution in the Cycles of Life. Annu. Rev. Genet. *50*, 133–154.

Bowman, J.L., Kohchi, T., Yamato, K.T., Jenkins, J., Shu, S., Ishizaki, K., Yamaoka, S., Nishihama, R., Nakamura, Y., Berger, F., et al. (2017). Insights into Land Plant Evolution Garnered from the Marchantia polymorpha Genome. Cell *171*, 287-304.e15.

Breuninger, H., Thamm, A., Streubel, S., Sakayama, H., Nishiyama, T., and Dolan, L. (2016). Diversification of a Transcription Factor Family Led to the Evolution of Antagonistically Acting Genetic Regulators of Root Hair Growth. Curr. Biol. *26*, 1622–1628.

Briggs, G.C., Osmont, K.S., Shindo, C., Sibout, R., and Hardtke, C.S. (2006). Unequal genetic redundancies in Arabidopsis – a neglected phenomenon? Trends Plant Sci. *11*, 492–498.

Brodie, H.J. (1951). The splash-cup dispersal mechanism in plants. Can. J. Bot. *29*, 224–234.

Brodribb, T.J., Carriquí, M., Delzon, S., McAdam, S. a. M., and Holbrook, N.M. (2020). Advanced vascular function discovered in a widespread moss. Nat. Plants *6*, 273–279.

Broun, P., Poindexter, P., Osborne, E., Jiang, C.-Z., and Riechmann, J.L. (2004). WIN1, a transcriptional activator of epidermal wax accumulation in Arabidopsis. Proc. Natl. Acad. Sci. U. S. A. *101*, 4706–4711.

Brown, R.C., Lemmon, B.E., Nguyen, H., and Olsen, O.-A. (1999). Development of endosperm in Arabidopsis thaliana. Sex. Plant Reprod. *12*, 32–42.

Bryant, F.M., Munoz-Azcarate, O., Kelly, A.A., Beaudoin, F., Kurup, S., and Eastmond, P.J. (2016). ACYL-ACYL CARRIER PROTEIN DESATURASE2 and 3 Are Responsible for Making Omega-7 Fatty Acids in the Arabidopsis Aleurone. Plant Physiol. *172*, 154–162.

Buda, G.J., Barnes, W.J., Fich, E.A., Park, S., Yeats, T.H., Zhao, L., Domozych, D.S., and Rose, J.K.C. (2013). An ATP Binding Cassette Transporter Is Required for Cuticular Wax

Deposition and Desiccation Tolerance in the Moss Physcomitrella patens[W]. Plant Cell *25*, 4000–4013.

Budke, J.M., Goffinet, B., and Jones, C.S. (2012). The cuticle on the gametophyte calyptra matures before the sporophyte cuticle in the moss Funaria hygrometrica (Funariaceae). Am. J. Bot. *99*, 14–22.

Burrieza, H.P., López-Fernández, M.P., and Maldonado, S. (2014). Analogous reserve distribution and tissue characteristics in quinoa and grass seeds suggest convergent evolution. Front. Plant Sci. *5*.

Busch, A., Deckena, M., Almeida-Trapp, M., Kopischke, S., Kock, C., Schüssler, E., Tsiantis, M., Mithöfer, A., and Zachgo, S. (2019). MpTCP1 controls cell proliferation and redox processes in Marchantia polymorpha. New Phytol. *224*, 1627–1641.

Carmichael, J.S., and Friedman, W.E. (1996). Double fertilization in Gnetum gnemon (Gnetaceae): its bearing on the evolution of sexual reproduction within the Gnetales and the anthophyte clade. Am. J. Bot. *83*, 767–780.

Carol, R.J., and Dolan, L. (2002). Building a hair: tip growth in Arabidopsis thaliana root hairs. Philos. Trans. R. Soc. B Biol. Sci. *357*, 815–821.

Castorina, G., Domergue, F., Chiara, M., Zilio, M., Persico, M., Ricciardi, V., Horner, D.S., and Consonni, G. (2020). Drought-Responsive ZmFDL1/MYB94 Regulates Cuticle Biosynthesis and Cuticle-Dependent Leaf Permeability. Plant Physiol. *184*, 266–282.

Catarino, B., Hetherington, A.J., Emms, D.M., Kelly, S., and Dolan, L. (2016). The Stepwise Increase in the Number of Transcription Factor Families in the Precambrian Predated the Diversification of Plants On Land. Mol. Biol. Evol. *33*, 2815–2819.

Chanvivattana, Y., Bishopp, A., Schubert, D., Stock, C., Moon, Y.-H., Sung, Z.R., and Goodrich, J. (2004). Interaction of Polycomb-group proteins controlling flowering in Arabidopsis. Development *131*, 5263–5276.

Chapman, J.M., Muhlemann, J.K., Gayomba, S.R., and Muday, G.K. (2019). RBOH-Dependent ROS Synthesis and ROS Scavenging by Plant Specialized Metabolites To Modulate Plant Development and Stress Responses. Chem. Res. Toxicol. *32*, 370–396.

Chassot, C., Nawrath, C., and Métraux, J.-P. (2007). Cuticular defects lead to full immunity to a major plant pathogen. Plant J. Cell Mol. Biol. *49*, 972–980.

Chater, C.C., Caine, R.S., Tomek, M., Wallace, S., Kamisugi, Y., Cuming, A.C., Lang, D., MacAlister, C.A., Casson, S., Bergmann, D.C., et al. (2016). Origin and function of stomata in the moss Physcomitrella patens. Nat. Plants *2*, 16179.

Chater, C.C.C., Caine, R.S., Fleming, A.J., and Gray, J.E. (2017). Origins and Evolution of Stomatal Development1[OPEN]. Plant Physiol. *174*, 624–638.

Chen, G., Wang, Z.-W., Qin, Y., and Sun, W.-B. (2017). Seed dispersal by hornets: An unusual insect-plant mutualism. J. Integr. Plant Biol. *59*, 792–796.

Chen, L.-Q., Lin, I.W., Qu, X.-Q., Sosso, D., McFarlane, H.E., Londoño, A., Samuels, A.L., and Frommer, W.B. (2015). A Cascade of Sequentially Expressed Sucrose Transporters in the Seed Coat and Endosperm Provides Nutrition for the Arabidopsis Embryo[OPEN]. Plant Cell *27*, 607–619.

Chen, X., Goodwin, S.M., Boroff, V.L., Liu, X., and Jenks, M.A. (2003). Cloning and characterization of the WAX2 gene of Arabidopsis involved in cuticle membrane and wax production. Plant Cell *15*, 1170–1185.

Chinnusamy, V., Ohta, M., Kanrar, S., Lee, B.-H., Hong, X., Agarwal, M., and Zhu, J.-K. (2003). ICE1: a regulator of cold-induced transcriptome and freezing tolerance in Arabidopsis. Genes Dev. *17*, 1043–1054.

Chinnusamy, V., Ohta, M., Kanrar, S., Lee, B., Hong, X., Agarwal, M., and Zhu, J.-K. (2003c). ICE1: a regulator of cold-induced transcriptome and freezing tolerance in Arabidopsis. Genes Dev. *17*, 1043–1054.

Clee, D.A. (1943). The Morphology and Anatomy of Fegatella conica in relation to the Mechanism of Absorption and Conduction of Water. Ann. Bot. *7*, 185–193.

Coen, O., Lu, J., Xu, W., De Vos, D., Péchoux, C., Domergue, F., Grain, D., Lepiniec, L., and Magnani, E. (2019). Deposition of a cutin apoplastic barrier separating seed maternal and zygotic tissues. BMC Plant Biol. *19*, 304.

Corona-Carrillo, J.I., Flores-Ponce, M., Chávez-Nájera, G., and Díaz-Pontones, D.M. (2014). Peroxidase activity in scutella of maize in association with anatomical changes during germination and grain storage. SpringerPlus *3*, 399.

Creff, A., Brocard, L., and Ingram, G. (2015). A mechanically sensitive cell layer regulates the physical properties of the Arabidopsis seed coat. Nat. Commun. *6*, 6382.

Creff, A., Brocard, L., Joubès, J., Taconnat, L., Doll, N.M., Marsollier, A.-C., Pascal, S., Galletti, R., Boeuf, S., Moussu, S., et al. (2019). A stress-response-related inter-compartmental signalling pathway regulates embryonic cuticle integrity in Arabidopsis. PLOS Genet. *15*, e1007847.

Cui, F., Brosché, M., Lehtonen, M.T., Amiryousefi, A., Xu, E., Punkkinen, M., Valkonen, J.P.T., Fujii, H., and Overmyer, K. (2016). Dissecting Abscisic Acid Signaling Pathways Involved in Cuticle Formation. Mol. Plant *9*, 926–938.

Da Costa, M., Bach, L., Landrieu, I., Bellec, Y., Catrice, O., Brown, S., De Veylder, L., Lippens, G., Inzé, D., and Faure, J.-D. (2006). Arabidopsis PASTICCINO2 is an antiphosphatase involved in regulation of cyclin-dependent kinase A. Plant Cell *18*, 1426–1437.

Daneva, A., Gao, Z., Van Durme, M., and Nowack, M.K. (2016). Functions and Regulation of Programmed Cell Death in Plant Development. Annu. Rev. Cell Dev. Biol. *32*, 441–468.

Davies, K.M., Jibran, R., Zhou, Y., Albert, N.W., Brummell, D.A., Jordan, B.R., Bowman, J.L., and Schwinn, K.E. (2020). The Evolution of Flavonoid Biosynthesis: A Bryophyte Perspective. Front. Plant Sci. *11*, 7.

De Baets, S., Denbigh, T.D.G., Smyth, K.M., Eldridge, B.M., Weldon, L., Higgins, B., Matyjaszkiewicz, A., Meersmans, J., Larson, E.R., Chenchiah, I.V., et al. (2020). Micro-scale interactions between Arabidopsis root hairs and soil particles influence soil erosion. Commun. Biol. *3*, 1–11.

De Giorgi, J., Fuchs, C., Iwasaki, M., Kim, W., Piskurewicz, U., Gully, K., Utz-Pugin, A., Mene-Saffrane, L., Waridel, P., Nawrath, C., et al. (2021). The Mature Endosperm Governs Early Seedling Development: A Focus on Cuticle Formation (Rochester, NY: Social Science Research Network).

De Jong, T.J., Van Dijk, H., and Klinkhamer, P.G.L. (2005). Hamilton's rule, imprinting and parent-offspring conflict over seed mass in partially selfing plants. J. Evol. Biol. *18*, 676–682.

Deas, A.H.B., and Holloway, P.J. (1977). The Intermolecular Structure of Some Plant Cutins. In Lipids and Lipid Polymers in Higher Plants, M. Tevini, and H.K. Lichtenthaler, eds. (Berlin, Heidelberg: Springer), pp. 293–299.

DeBono, A., Yeats, T.H., Rose, J.K.C., Bird, D., Jetter, R., Kunst, L., and Samuels, L. (2009). Arabidopsis LTPG Is a Glycosylphosphatidylinositol-Anchored Lipid Transfer Protein Required for Export of Lipids to the Plant Surface. Plant Cell *21*, 1230–1238.

Deerinck, T.J., Bushong, E., Thor, A., and Ellisman, M. (2010). NCMIR methods for 3D EM: A new protocol for preparation of biological specimens for serial block face scanning electron microscopy. Nat Cent. Microsc Imag Res 6–8.

Delaux, P.-M., Nanda, A.K., Mathé, C., Sejalon-Delmas, N., and Dunand, C. (2012). Molecular and biochemical aspects of plant terrestrialization. Perspect. Plant Ecol. Evol. Syst. *14*, 49–59.

Delaux, P.-M., Hetherington, A.J., Coudert, Y., Delwiche, C., Dunand, C., Gould, S., Kenrick, P., Li, F.-W., Philippe, H., Rensing, S.A., et al. (2019). Reconstructing trait evolution in plant evo-devo studies. Curr. Biol. CB *29*, R1110–R1118.

Delude, C., Moussu, S., Joubès, J., Ingram, G., and Domergue, F. (2016). Plant Surface Lipids and Epidermis Development. Subcell. Biochem. *86*, 287–313.

Delwiche, C.F., and Cooper, E.D. (2015). The Evolutionary Origin of a Terrestrial Flora. Curr. Biol. *25*, R899–R910.

Denay, G., Creff, A., Moussu, S., Wagnon, P., Thévenin, J., Gérentes, M.-F., Chambrier, P., Dubreucq, B., and Ingram, G. (2014). Endosperm breakdown in Arabidopsis requires heterodimers of the basic helix-loop-helix proteins ZHOUPI and INDUCER OF CBP EXPRESSION 1. Dev. Camb. Engl. *141*, 1222–1227.

Deng, X.W., Caspar, T., and Quail, P.H. (1991). cop1: a regulatory locus involved in light-controlled development and gene expression in Arabidopsis. Genes Dev. *5*, 1172–1182.

Depège-Fargeix, N., Javelle, M., Chambrier, P., Frangne, N., Gerentes, D., Perez, P., Rogowsky, P.M., and Vernoud, V. (2011). Functional characterization of the HD-ZIP IV transcription factor OCL1 from maize. J. Exp. Bot. *62*, 293–305.

Deshmukh, A.P., Simpson, A.J., and Hatcher, P.G. (2003). Evidence for cross-linking in tomato cutin using HR-MAS NMR spectroscopy. Phytochemistry *64*, 1163–1170.

Dimakos, V., Singh, T., and Taylor, M.S. (2016). Boronic acid/Brønsted acid co-catalyst systems for the synthesis of 2H-chromenes from phenols and α,β-unsaturated carbonyls. Org. Biomol. Chem. *14*, 6703–6711.

DiMichele, W.A., Phillips, T.L., and Pfefferkorn, H.W. (2006). Paleoecology of Late Paleozoic pteridosperms from tropical Euramerica [1]. J. Torrey Bot. Soc. *133*, 83–118.

Ding, Y., Li, H., Zhang, X., Xie, Q., Gong, Z., and Yang, S. (2015). OST1 kinase modulates freezing tolerance by enhancing ICE1 stability in Arabidopsis. Dev. Cell *32*, 278–289.

Doblas, V.G., Smakowska-Luzan, E., Fujita, S., Alassimone, J., Barberon, M., Madalinski, M., Belkhadir, Y., and Geldner, N. (2017). Root diffusion barrier control by a vasculature-derived peptide binding to the SGN3 receptor. Science *355*, 280–284.

Doll, N.M., Just, J., Brunaud, V., Caïus, J., Grimault, A., Depège-Fargeix, N., Esteban, E., Pasha, A., Provart, N.J., Ingram, G.C., et al. (2020a). Transcriptomics at Maize Embryo/Endosperm Interfaces Identifies a Transcriptionally Distinct Endosperm Subdomain Adjacent to the Embryo Scutellum. Plant Cell *32*, 833–852.

Doll, N.M., Bovio, S., Gaiti, A., Marsollier, A.-C., Chamot, S., Moussu, S., Widiez, T., and Ingram, G. (2020b). The Endosperm-Derived Embryo Sheath Is an Anti-adhesive Structure that Facilitates Cotyledon Emergence during Germination in Arabidopsis. Curr. Biol. CB *30*, 909-915.e4.

Doll, N.M., Royek, S., Fujita, S., Okuda, S., Chamot, S., Stintzi, A., Widiez, T., Hothorn, M., Schaller, A., Geldner, N., et al. (2020c). A two-way molecular dialogue between embryo and endosperm is required for seed development. Science *367*, 431–435.

Domínguez, E., España, L., López-Casado, G., Cuartero, J., and Heredia, A. (2009). Biomechanics of isolated tomato (Solanum lycopersicum) fruit cuticles during ripening: the role of flavonoids. Funct. Plant Biol. FPB *36*, 613–620.

Domínguez, E., Heredia-Guerrero, J.A., Benítez, J.J., and Heredia, A. (2010). Self-assembly of supramolecular lipid nanoparticles in the formation of plant biopolyester cutin. Mol. Biosyst. *6*, 948–950.

Dong, C.-H., Agarwal, M., Zhang, Y., Xie, Q., and Zhu, J.-K. (2006). The negative regulator of plant cold responses, HOS1, is a RING E3 ligase that mediates the ubiquitination and degradation of ICE1. Proc. Natl. Acad. Sci. U. S. A. *103*, 8281–8286.

Dou, M., Zhang, Y., Yang, S., and Feng, X. (2018). Identification of ZHOUPI Orthologs in Rice Involved in Endosperm Development and Cuticle Formation. Front. Plant Sci. *9*.

Doyle, J.A. (2006). Seed ferns and the origin of angiosperms. J. Torrey Bot. Soc. *133*, 169–209.

Dragota, S., and Riederer, M. (2007). Epicuticular Wax Crystals of Wollemia nobilis: Morphology and Chemical Composition. Ann. Bot. *100*, 225–231.

Dresselhaus, T., Sprunck, S., and Wessel, G.M. (2016). Fertilization Mechanisms in Flowering Plants. Curr. Biol. *26*, R125–R139.

Duckett, J.G., and Pressel, S. (2020). Of mosses and vascular plants. Nat. Plants *6*, 184–185.

Duckett, J.G., Pressel, S., P'ng, K.M.Y., and Renzaglia, K.S. (2009). Exploding a myth: the capsule dehiscence mechanism and the function of pseudostomata in Sphagnum. New Phytol. *183*, 1053–1063.

Duckett, J.G., Ligrone, R., Renzaglia, K.S., and Pressel, S. (2014). Pegged and smooth rhizoids in complex thalloid liverworts (Marchantiopsida): structure, function and evolution. Bot. J. Linn. Soc. *174*, 68–92.

Dumas, C., and Rogowsky, P. (2008). Fertilization and early seed formation. C. R. Biol. *331*, 715–725.

Dutta, S., Bradford, K.J., and Nevins, D.J. (1997). Endo-[beta]-Mannanase Activity Present in Cell Wall Extracts of Lettuce Endosperm prior to Radicle Emergence. Plant Physiol. *113*, 155–161.

Eigenbrode, S.D., and Jetter, R. (2002). Attachment to Plant Surface Waxes by an Insect Predator1. Integr. Comp. Biol. *42*, 1091–1099.

Elejalde-Palmett, C., Martinez San Segundo, I., Garroum, I., Charrier, L., De Bellis, D., Mucciolo, A., Guerault, A., Liu, J., Zeisler-Diehl, V., Aharoni, A., et al. (2021). ABCG transporters export cutin precursors for the formation of the plant cuticle. Curr. Biol. *31*, 2111-2123.e9.

Endress, P.K. (2011). Angiosperm ovules: diversity, development, evolution. Ann. Bot. *107*, 1465–1489.

Fabre, G., Garroum, I., Mazurek, S., Daraspe, J., Mucciolo, A., Sankar, M., Humbel, B.M., and Nawrath, C. (2016). The ABCG transporter PEC1/ABCG32 is required for the formation of the developing leaf cuticle in Arabidopsis. New Phytol. *209*, 192–201.

Fawke, S., Torode, T.A., Gogleva, A., Fich, E.A., Sørensen, I., Yunusov, T., Rose, J.K.C., and Schornack, S. (2019). Glycerol-3-phosphate acyltransferase 6 controls filamentous pathogen interactions and cell wall properties of the tomato and Nicotiana benthamiana leaf epidermis. New Phytol. *223*, 1547–1559.

Fedi, F., O'Neill, C.M., Menard, G., Trick, M., Dechirico, S., Corbineau, F., Bailly, C., Eastmond, P.J., and Penfield, S. (2017). Awake1, an ABC-Type Transporter, Reveals an Essential Role for Suberin in the Control of Seed Dormancy. Plant Physiol. *174*, 276–283.

Fendrych, M., Van Hautegem, T., Van Durme, M., Olvera-Carrillo, Y., Huysmans, M., Karimi, M., Lippens, S., Guérin, C.J., Krebs, M., Schumacher, K., et al. (2014). Programmed cell death controlled by ANAC033/SOMBRERO determines root cap organ size in Arabidopsis. Curr. Biol. CB *24*, 931–940.

Feng, F., and Song, R. (2018). O11 is multi-functional regulator in maize endosperm. Plant Signal. Behav. *13*, e1451709.

Feng, F., Qi, W., Lv, Y., Yan, S., Xu, L., Yang, W., Yuan, Y., Chen, Y., Zhao, H., and Song, R. (2018). OPAQUE11 Is a Central Hub of the Regulatory Network for Maize Endosperm Development and Nutrient Metabolism. Plant Cell *30*, 375–396.

Fernández, V., Guzmán, P., Peirce, C.A.E., McBeath, T.M., Khayet, M., and McLaughlin, M.J. (2014). Effect of wheat phosphorus status on leaf surface properties and permeability to foliar-applied phosphorus. Plant Soil *384*, 7–20.

Fernández, V., Guzmán-Delgado, P., Graça, J., Santos, S., and Gil, L. (2016). Cuticle Structure in Relation to Chemical Composition: Re-assessing the Prevailing Model. Front. Plant Sci. *7*.

Fich, E.A., Segerson, N.A., and Rose, J.K.C. (2016). The Plant Polyester Cutin: Biosynthesis, Structure, and Biological Roles. Annu. Rev. Plant Biol. *67*, 207–233.

Figueiredo, D.D., and Köhler, C. (2018). Auxin: a molecular trigger of seed development. Genes Dev. *32*, 479–490.

Fourquin, C., Beauzamy, L., Chamot, S., Creff, A., Goodrich, J., Boudaoud, A., and Ingram, G. (2016). Mechanical stress mediated by both endosperm softening and embryo growth underlies endosperm elimination in Arabidopsis seeds. Dev. Camb. Engl. *143*, 3300–3305.

Francoz, E., Ranocha, P., Pernot, C., Le Ru, A., Pacquit, V., Dunand, C., and Burlat, V. (2016). Complementarity of medium-throughput in situ RNA hybridization and tissue-specific transcriptomics: case study of Arabidopsis seed development kinetics. Sci. Rep. *6*, 24644.

Frangedakis, E., Waller, M., Nishiyama, T., Tsukaya, H., Xu, X., Yue, Y., Tjahjadi, M., Gunadi, A., Van Eck, J., Li, F.-W., et al. (2021). An Agrobacterium-mediated stable transformation technique for the hornwort model Anthoceros agrestis. New Phytol.

Franke, R., and Schreiber, L. (2007). Suberin — a biopolyester forming apoplastic plant interfaces. Curr. Opin. Plant Biol. *10*, 252–259.

Friedman, W.E. (1990). Double Fertilization in Ephedra, a Nonflowering Seed Plant: Its Bearing on the Origin of Angiosperms. Science *247*, 951–954.

Friedman, W.E. (1992). Evidence of a Pre-Angiosperm Origin of Endosperm: Implications for the Evolution of Flowering Plants. Science *255*, 336–339.

Friedman, W.E. (2013). One Genome, Two Ontogenies. Science *339*, 1045–1046.

Friedman, W.E., and Bachelier, J.B. (2013). Seed development in Trimenia (Trimeniaceae) and its bearing on the evolution of embryo-nourishing strategies in early flowering plant lineages. Am. J. Bot. *100*, 906–915.

Friedman, W.E., and Ryerson, K.C. (2009). Reconstructing the ancestral female gametophyte of angiosperms: Insights from Amborella and other ancient lineages of flowering plants. Am. J. Bot. *96*, 129–143.

Friis, E.M., Pedersen, K.R., and Crane, P.R. (2006). Cretaceous angiosperm flowers: Innovation and evolution in plant reproduction. Palaeogeogr. Palaeoclimatol. Palaeoecol. *232*, 251–293.

Fujita, S., De Bellis, D., Edel, K.H., Köster, P., Andersen, T.G., Schmid-Siegert, E., Dénervaud Tendon, V., Pfister, A., Marhavý , P., Ursache, R., et al. (2020). SCHENGEN receptor module drives localized ROS production and lignification in plant roots. EMBO J. *39*, e103894.

Fukuda, H., and Ohashi-Ito, K. (2019). Vascular tissue development in plants. Curr. Top. Dev. Biol. *131*, 141–160.

Fulda, M., Schnurr, J., Abbadi, A., Heinz, E., and Browse, J. (2004). Peroxisomal Acyl-CoA Synthetase Activity Is Essential for Seedling Development in Arabidopsis thaliana. Plant Cell *16*, 394–405.

Fursova, O.V., Pogorelko, G.V., and Tarasov, V.A. (2009). Identification of ICE2, a gene involved in cold acclimation which determines freezing tolerance in Arabidopsis thaliana. Gene *429*, 98–103.

Garcia, D., Fitz Gerald, J.N., and Berger, F. (2005). Maternal control of integument cell elongation and zygotic control of endosperm growth are coordinated to determine seed size in Arabidopsis. Plant Cell *17*, 52–60.

Gasser, C.S., and Skinner, D.J. (2019). Chapter Fourteen - Development and evolution of the unique ovules of flowering plants. In Current Topics in Developmental Biology, U. Grossniklaus, ed. (Academic Press), pp. 373–399.

Gasser, C., Broadhvest, J., and Hauser, B. (1998). Genetic Analysis of Ovule Development. Annu. Rev. Plant Physiol. Plant Mol. Biol. *49*, 1–24.

Gerrienne, P., and Meyer-Berthaud, B. (2007). The proto-ovule Runcaria heinzelinii Stockmans 1968 emend. Gerrienne et al., 2004 (mid-Givetian, Belgium): Concept and epitypification. Rev. Palaeobot. Palynol. *145*, 321.

Gerrienne, P., Meyer-Berthaud, B., Fairon-Demaret, M., Streel, M., and Steemans, P. (2004). Runcaria, a Middle Devonian Seed Plant Precursor. Science *306*, 856–858.

Gidda, S.K., Shockey, J.M., Rothstein, S.J., Dyer, J.M., and Mullen, R.T. (2009). Arabidopsis thaliana GPAT8 and GPAT9 are localized to the ER and possess distinct ER retrieval signals: functional divergence of the dilysine ER retrieval motif in plant cells. Plant Physiol. Biochem. PPB *47*, 867–879.

Gilbert, R.D., Johnson, A.M., and Dean, R.A. (1996). Chemical signals responsible for appressorium formation in the rice blast fungusMagnaporthe grisea. Physiol. Mol. Plant Pathol. *48*, 335–346.

Girard, A.-L., Mounet, F., Lemaire-Chamley, M., Gaillard, C., Elmorjani, K., Vivancos, J., Runavot, J.-L., Quemener, B., Petit, J., Germain, V., et al. (2012). Tomato GDSL1 is required for cutin deposition in the fruit cuticle. Plant Cell *24*, 3119–3134.

Giuliano, G., Pichersky, E., Malik, V.S., Timko, M.P., Scolnik, P.A., and Cashmore, A.R. (1988). An evolutionarily conserved protein binding sequence upstream of a plant light-regulated gene. Proc. Natl. Acad. Sci. U. S. A. *85*, 7089–7093.

González-Coronel, J.M., Rodríguez-Alonso, G., and Guevara-García, Á.A. (2021). A phylogenetic study of the members of the MAPK and MEK families across Viridiplantae. PLoS ONE *16*, e0250584.

Gou, J.-Y., Yu, X.-H., and Liu, C.-J. (2009). A hydroxycinnamoyltransferase responsible for synthesizing suberin aromatics in Arabidopsis. Proc. Natl. Acad. Sci. *106*, 18855–18860.

Graça, J., and Lamosa, P. (2010). Linear and branched poly(omega-hydroxyacid) esters in plant cutins. J. Agric. Food Chem. *58*, 9666–9674.

Graça, J., Schreiber, L., Rodrigues, J., and Pereira, H. (2002). Glycerol and glyceryl esters of omega-hydroxyacids in cutins. Phytochemistry *61*, 205–215.

Graham, L.E., Cook, M.E., and Busse, J.S. (2000). The origin of plants: Body plan changes contributing to a major evolutionary radiation. Proc. Natl. Acad. Sci. *97*, 4535–4540.

Gray, J.E., Holroyd, G.H., van der Lee, F.M., Bahrami, A.R., Sijmons, P.C., Woodward, F.I., Schuch, W., and Hetherington, A.M. (2000). The HIC signalling pathway links CO2 perception to stomatal development. Nature *408*, 713–716.

Greenspan, P., Mayer, E.P., and Fowler, S.D. (1985). Nile red: a selective fluorescent stain for intracellular lipid droplets. J. Cell Biol. *100*, 965–973.

Greer, S., Wen, M., Bird, D., Wu, X., Samuels, L., Kunst, L., and Jetter, R. (2007). The cytochrome P450 enzyme CYP96A15 is the midchain alkane hydroxylase responsible for formation of secondary alcohols and ketones in stem cuticular wax of Arabidopsis. Plant Physiol. *145*, 653–667.

Grienenberger, E., Besseau, S., Geoffroy, P., Debayle, D., Heintz, D., Lapierre, C., Pollet, B., Heitz, T., and Legrand, M. (2009). A BAHD acyltransferase is expressed in the tapetum of Arabidopsis anthers and is involved in the synthesis of hydroxycinnamoyl spermidines. Plant J. Cell Mol. Biol. *58*, 246–259.

Grimault, A., Gendrot, G., Chamot, S., Widiez, T., Rabillé, H., Gérentes, M.-F., Creff, A., Thévenin, J., Dubreucq, B., Ingram, G.C., et al. (2015). ZmZHOUPI, an endosperm-specific basic helix–loop–helix transcription factor involved in maize seed development. Plant J. *84*, 574–586.

Guzmán, P., Fernández, V., Khayet, M., García, M.L., Fernández, A., and Gil, L. (2014). Ultrastructure of Plant Leaf Cuticles in relation to Sample Preparation as Observed by Transmission Electron Microscopy. Sci. World J. *2014*, 963921.

Guzmán-Delgado, P., Graça, J., Cabral, V., Gil, L., and Fernández, V. (2016). The presence of cutan limits the interpretation of cuticular chemistry and structure: Ficus elastica leaf as an example. Physiol. Plant. *157*, 205–220.

Guzman-Puyol, S., Benítez, J.J., Domínguez, E., Bayer, I.S., Cingolani, R., Athanassiou, A., Heredia, A., and Heredia-Guerrero, J.A. (2015). Pectin-Lipid Self-Assembly: Influence on the Formation of Polyhydroxy Fatty Acids Nanoparticles. PLOS ONE *10*, e0124639.

Haig, D., and Westoby, M. (1989). Parent-Specific Gene Expression and the Triploid Endosperm. Am. Nat. *134*, 147–155.

Hama, T., Seki, K., Ishibashi, A., Miyazaki, A., Kouchi, A., Watanabe, N., Shimoaka, T., and Hasegawa, T. (2019). Probing the Molecular Structure and Orientation of the Leaf Surface of Brassica oleracea L. by Polarization Modulation-Infrared Reflection-Absorption Spectroscopy. Plant Cell Physiol. *60*, 1567–1580.

Hao, Y., Zong, X., Ren, P., Qian, Y., and Fu, A. (2021). Basic Helix-Loop-Helix (bHLH) Transcription Factors Regulate a Wide Range of Functions in Arabidopsis. Int. J. Mol. Sci. *22*, 7152.

Harrar, Y., Bellec, Y., Bellini, C., and Faure, J.-D. (2003). Hormonal Control of Cell Proliferation Requires PASTICCINO Genes. Plant Physiol. *132*, 1217–1227.

Harris, B.J., Harrison, C.J., Hetherington, A.M., and Williams, T.A. (2020). Phylogenomic Evidence for the Monophyly of Bryophytes and the Reductive Evolution of Stomata. Curr. Biol. CB *30*, 2001-2012.e2.

Haslam, T.M., and Kunst, L. (2013). Extending the story of very-long-chain fatty acid elongation. Plant Sci. Int. J. Exp. Plant Biol. *210*, 93–107.

Heredia-Guerrero, J.A., Benítez, J.J., Domínguez, E., Bayer, I.S., Cingolani, R., Athanassiou, A., and Heredia, A. (2014). Infrared and Raman spectroscopic features of plant cuticles: a review. Front. Plant Sci. *5*, 305.

Hetherington, A.J., Berry, C.M., and Dolan, L. (2016). Networks of highly branched stigmarian rootlets developed on the first giant trees. Proc. Natl. Acad. Sci. U. S. A. *113*, 6695–6700.

Hofhuis, H., Moulton, D., Lessinnes, T., Routier-Kierzkowska, A.-L., Bomphrey, R.J., Mosca, G., Reinhardt, H., Sarchet, P., Gan, X., Tsiantis, M., et al. (2016). Morphomechanical Innovation Drives Explosive Seed Dispersal. Cell *166*, 222–233.

Holmes, M.G., and Keiller, D.R. (2002). Effects of pubescence and waxes on the reflectance of leaves in the ultraviolet and photosynthetic wavebands: a comparison of a range of species. Plant Cell Environ. *25*, 85–93.

Hong, S.K., Kitano, H., Satoh, H., and Nagato, Y. (1996). How is embryo size genetically regulated in rice? Development *122*, 2051–2058.

Honkanen, S., Thamm, A., Arteaga-Vazquez, M.A., and Dolan, L. (2018). Negative regulation of conserved RSL class I bHLH transcription factors evolved independently among land plants. ELife *7*, e38529.

Hooker, T.S., Millar, A.A., and Kunst, L. (2002). Significance of the expression of the CER6 condensing enzyme for cuticular wax production in Arabidopsis. Plant Physiol. *129*, 1568–1580.

Hopmans, J.W., and Bristow, K. (2002). Current Capabilities and Future Needs of Root Water and Nutrient Uptake Modeling. Adv. Agron. 77 104–175.

Hosmani, P.S., Kamiya, T., Danku, J., Naseer, S., Geldner, N., Guerinot, M.L., and Salt, D.E. (2013). Dirigent domain-containing protein is part of the machinery required for formation of the lignin-based Casparian strip in the root. Proc. Natl. Acad. Sci. U. S. A. *110*, 14498–14503.

ten Hove, C.A., Lu, K.-J., and Weijers, D. (2015). Building a plant: cell fate specification in the early Arabidopsis embryo. Development *142*, 420–430.

Hu, Y., Jiang, L., Wang, F., and Yu, D. (2013). Jasmonate regulates the inducer of cbf expression-C-repeat binding factor/DRE binding factor1 cascade and freezing tolerance in Arabidopsis. Plant Cell *25*, 2907–2924.

Hu, Y., Han, X., Yang, M., Zhang, M., Pan, J., and Yu, D. (2019). The Transcription Factor INDUCER OF CBF EXPRESSION1 Interacts with ABSCISIC ACID INSENSITIVE5 and DELLA Proteins to Fine-tune Abscisic Acid Signaling during Seed Germination in Arabidopsis. Plant Cell.

Humphreys, C.P., Franks, P.J., Rees, M., Bidartondo, M.I., Leake, J.R., and Beerling, D.J. (2010). Mutualistic mycorrhiza-like symbiosis in the most ancient group of land plants. Nat. Commun. *1*, 103.

Iglesias-Fernández, R., Rodríguez-Gacio, M.C., Barrero-Sicilia, C., Carbonero, P., and Matilla, A. (2011). Three endo-β-mannanase genes expressed in the micropylar endosperm and in the radicle influence germination of Arabidopsis thaliana seeds. Planta *233*, 25–36.

Iglesias-Fernández, R., Barrero-Sicilia, C., Carrillo-Barral, N., Oñate-Sánchez, L., and Carbonero, P. (2013). Arabidopsis thaliana bZIP44: a transcription factor affecting seed germination and expression of the mannanase-encoding gene AtMAN7. Plant J. *74*, 767–780.

Ingram, G.C. (2010). Family life at close quarters: communication and constraint in angiosperm seed development. Protoplasma *247*, 195–214.

Ingram, G.C. (2017). Dying to live: cell elimination as a developmental strategy in angiosperm seeds. J. Exp. Bot. *68*, 785–796.

Ingram, G., and Nawrath, C. (2017). The roles of the cuticle in plant development: organ adhesions and beyond. J. Exp. Bot. *68*, 5307–5321.

Ishizaki, K., Shimizu-Ueda, Y., Okada, S., Yamamoto, M., Fujisawa, M., Yamato, K.T., Fukuzawa, H., and Ohyama, K. (2002). Multicopy genes uniquely amplified in the Y chromosome-specific repeats of the liverwort Marchantia polymorpha. Nucleic Acids Res. *30*, 4675–4681.

Ishizaki, K., Chiyoda, S., Yamato, K.T., and Kohchi, T. (2008). Agrobacterium-Mediated Transformation of the Haploid Liverwort Marchantia polymorpha L., an Emerging Model for Plant Biology. Plant Cell Physiol. *49*, 1084–1091.

Ishizaki, K., Johzuka-Hisatomi, Y., Ishida, S., Iida, S., and Kohchi, T. (2013). Homologous recombination-mediated gene targeting in the liverwort Marchantia polymorpha L. Sci. Rep. *3*, 1532.

Ishizaki, K., Nishihama, R., Ueda, M., Inoue, K., Ishida, S., Nishimura, Y., Shikanai, T., and Kohchi, T. (2015). Development of Gateway Binary Vector Series with Four Different Selection Markers for the Liverwort Marchantia polymorpha. PloS One *10*, e0138876.

Jakobson, L., Lindgren, L.O., Verdier, G., Laanemets, K., Brosché, M., Beisson, F., and Kollist, H. (2016). BODYGUARD is required for the biosynthesis of cutin in Arabidopsis. New Phytol. *211*, 614–626.

Jang, G., and Dolan, L. (2011). Auxin promotes the transition from chloronema to caulonema in moss protonema by positively regulating PpRSL1and PpRSL2 in Physcomitrella patens. New Phytol. *192*, 319–327.

Javelle, M., Vernoud, V., Depège-Fargeix, N., Arnould, C., Oursel, D., Domergue, F., Sarda, X., and Rogowsky, P.M. (2010). Overexpression of the Epidermis-Specific Homeodomain-Leucine Zipper IV Transcription Factor OUTER CELL LAYER1 in Maize Identifies Target Genes Involved in Lipid Metabolism and Cuticle Biosynthesis. Plant Physiol. *154*, 273–286.

Javelle, M., Vernoud, V., Rogowsky, P.M., and Ingram, G.C. (2011). Epidermis: the formation and functions of a fundamental plant tissue. New Phytol. *189*, 17–39.

Jefferson, R.A., Kavanagh, T.A., and Bevan, M.W. (1987). GUS fusions: beta-glucuronidase as a sensitive and versatile gene fusion marker in higher plants. EMBO J. *6*, 3901–3907.

Jeffree, C.E. (2007). The Fine Structure of the Plant Cuticle. In Annual Plant Reviews Volume 23: Biology of the Plant Cuticle, (John Wiley & Sons, Ltd), pp. 11–125.

Jeffree, C.E., Baker, E.A., and Holloway, P.J. (1975). Ultrastructure and Recrystallization of Plant Epicuticular Waxes. New Phytol. *75*, 539–549.

Jenks, M.A., Tuttle, H.A., Eigenbrode, S.D., and Feldmann, K.A. (1995). Leaf Epicuticular Waxes of the Eceriferum Mutants in Arabidopsis. Plant Physiol. *108*, 369–377.

Jessen, D., Olbrich, A., Knüfer, J., Krüger, A., Hoppert, M., Polle, A., and Fulda, M. (2011). Combined activity of LACS1 and LACS4 is required for proper pollen coat formation in Arabidopsis. Plant J. Cell Mol. Biol. *68*, 715–726.

Jessen, D., Roth, C., Wiermer, M., and Fulda, M. (2015). Two activities of long-chain acyl-coenzyme A synthetase are involved in lipid trafficking between the endoplasmic reticulum and the plastid in Arabidopsis. Plant Physiol. *167*, 351–366.

Jetter, R., Kunst, L., and Samuels, A.L. (2006). Composition of Plant Cuticular Waxes. In Annual Plant Reviews Volume 23: Biology of the Plant Cuticle, (John Wiley & Sons, Ltd), pp. 145–181.

Jill Harrison, C. (2017). Development and genetics in the evolution of land plant body plans. Philos. Trans. R. Soc. B Biol. Sci. *372*, 20150490.

Jones, V.A.S., and Dolan, L. (2012). The evolution of root hairs and rhizoids. Ann. Bot. *110*, 205–212.

Joubès, J., Raffaele, S., Bourdenx, B., Garcia, C., Laroche-Traineau, J., Moreau, P., Domergue, F., and Lessire, R. (2008). The VLCFA elongase gene family in Arabidopsis

thaliana: phylogenetic analysis, 3D modelling and expression profiling. Plant Mol. Biol. *67*, 547–566.

Ju, Z., and Bramlage, W.J. (1999). 373 Phenolics and Lipid-soluble Antioxidants in Fruit Cuticle of Apples and Their Antioxidant Activities in Model Systems. HortScience *34*, 508B – 508.

Ju, S., Go, Y.S., Choi, H.J., Park, J.M., and Suh, M.C. (2017). DEWAX Transcription Factor Is Involved in Resistance to Botrytis cinerea in Arabidopsis thaliana and Camelina sativa. Front. Plant Sci. *8*, 1210.

Kader, J.-C. (1996). LIPID-TRANSFER PROTEINS IN PLANTS. Annu. Rev. Plant Physiol. Plant Mol. Biol. *47*, 627–654.

Kameriing, Z. (1897). Zur Biologie und Physiologie der Marchantiaceen. 70.

Kanaoka, M.M., Pillitteri, L.J., Fujii, H., Yoshida, Y., Bogenschutz, N.L., Takabayashi, J., Zhu, J.-K., and Torii, K.U. (2008). SCREAM/ICE1 and SCREAM2 specify three cell-state transitional steps leading to arabidopsis stomatal differentiation. Plant Cell *20*, 1775–1785.

Kannangara, R., Branigan, C., Liu, Y., Penfield, T., Rao, V., Mouille, G., Höfte, H., Pauly, M., Riechmann, J.L., and Broun, P. (2007). The Transcription Factor WIN1/SHN1 Regulates Cutin Biosynthesis in Arabidopsis thaliana. Plant Cell *19*, 1278–1294.

Karas, B., Murray, J., Gorzelak, M., Smith, A., Sato, S., Tabata, S., and Szczyglowski, K. (2005). Invasion of Lotus japonicus root hairless 1 by Mesorhizobium loti Involves the Nodulation Factor-Dependent Induction of Root Hairs. Plant Physiol. *137*, 1331–1344.

Karmann, J., Müller, B., and Hammes, U.Z. (2018). The long and winding road: transport pathways for amino acids in Arabidopsis seeds. Plant Reprod. *31*, 253–261.

Kato, H., Yasui, Y., and Ishizaki, K. (2020). Gemma cup and gemma development in Marchantia polymorpha. New Phytol. *228*, 459–465.

Kawashima, T., and Goldberg, R.B. (2010). The suspensor: not just suspending the embryo. Trends Plant Sci. *15*, 23–30.

Kenrick, P., and Crane, P.R. (1997). The origin and early evolution of plants on land. Nature *389*, 33–39.

Kenrick, P., and Strullu-Derrien, C. (2014). The origin and early evolution of roots. Plant Physiol. *166*, 570–580.

Kidokoro, S., Kim, J.-S., Ishikawa, T., Suzuki, T., Shinozaki, K., and Yamaguchi-Shinozaki, K. (2020). DREB1A/CBF3 Is Repressed by Transgene-Induced DNA Methylation in the Arabidopsis ice1-1 Mutant[OPEN]. Plant Cell *32*, 1035–1048.

Kim, Y.S., Lee, M., Lee, J.-H., Lee, H.-J., and Park, C.-M. (2015). The unified ICE-CBF pathway provides a transcriptional feedback control of freezing tolerance during cold acclimation in Arabidopsis. Plant Mol. Biol. *89*, 187–201.

King, G.S. (1947). Some oil soluble dyes which stain suberized deposits in orange vesicles. Stain Technol. *22*, 145–147.

Knoche, M., Beyer, M., Peschel, S., Oparlakov, B., and Bukovac, M.J. (2004). Changes in strain and deposition of cuticle in developing sweet cherry fruit. Physiol. Plant. *120*, 667–677.

Kolattukudy, P.E. (1977). Lipid Polymers and Associated Phenols, Their Chemistry, Biosynthesis, and Role in Pathogenesis. In The Structure, Biosynthesis, and Degradation of Wood, F.A. Loewus, and V.C. Runeckles, eds. (Boston, MA: Springer US), pp. 185–246.

Kondou, Y., Nakazawa, M., Kawashima, M., Ichikawa, T., Yoshizumi, T., Suzuki, K., Ishikawa, A., Koshi, T., Matsui, R., Muto, S., et al. (2008). RETARDED GROWTH OF EMBRYO1, a new basic helix-loop-helix protein, expresses in endosperm to control embryo growth. Plant Physiol. *147*, 1924–1935.

Kong, L., Liu, Y., Zhi, P., Wang, X., Xu, B., Gong, Z., and Chang, C. (2020). Origins and Evolution of Cuticle Biosynthetic Machinery in Land Plants. Plant Physiol. *184*, 1998–2010.

Kościuczuk, E.M., Lisowski, P., Jarczak, J., Strzałkowska, N., Jóźwik, A., Horbańczuk, J., Krzyżewski, J., Zwierzchowski, L., and Bagnicka, E. (2012). Cathelicidins: family of antimicrobial peptides. A review. Mol. Biol. Rep. *39*, 10957–10970.

Kosma, D.K., Bourdenx, B., Bernard, A., Parsons, E.P., Lü, S., Joubès, J., and Jenks, M.A. (2009). The Impact of Water Deficiency on Leaf Cuticle Lipids of Arabidopsis. Plant Physiol. *151*, 1918–1929.

Krauss, P., Markstädter, C., and Riederer, M. (1997). Attenuation of UV radiation by plant cuticles from woody species. Plant Cell Environ. *20*, 1079–1085.

Kriegshauser, L., Knosp, S., Grienenberger, E., Tatsumi, K., Gütle, D.D., Sørensen, I., Herrgott, L., Zumsteg, J., Rose, J.K.C., Reski, R., et al. (2021). Function of the HYDROXYCINNAMOYL-CoA:SHIKIMATE HYDROXYCINNAMOYL TRANSFERASE is evolutionarily conserved in embryophytes. Plant Cell *33*, 1472–1491.

Kubo, M., Udagawa, M., Nishikubo, N., Horiguchi, G., Yamaguchi, M., Ito, J., Mimura, T., Fukuda, H., and Demura, T. (2005). Transcription switches for protoxylem and metaxylem vessel formation. Genes Dev. *19*, 1855–1860.

Kubota, A., Ishizaki, K., Hosaka, M., and Kohchi, T. (2013). Efficient Agrobacterium-mediated transformation of the liverwort Marchantia polymorpha using regenerating thalli. Biosci. Biotechnol. Biochem. *77*, 167–172.

Kunst, L., and Samuels, L. (2009). Plant cuticles shine: advances in wax biosynthesis and export. Curr. Opin. Plant Biol. *12*, 721–727.

Kurbidaeva, A., Ezhova, T., and Novokreshchenova, M. (2014). Arabidopsis thaliana ICE2 gene: phylogeny, structural evolution and functional diversification from ICE1. Plant Sci. Int. J. Exp. Plant Biol. *229*, 10–22.

Kurdyukov, S., Faust, A., Nawrath, C., Bär, S., Voisin, D., Efremova, N., Franke, R., Schreiber, L., Saedler, H., Métraux, J.-P., et al. (2006). The epidermis-specific extracellular BODYGUARD controls cuticle development and morphogenesis in Arabidopsis. Plant Cell *18*, 321–339.

Lafon-Placette, C. (2019). Endosperm genome dosage, hybrid seed failure, and parental imprinting: sexual selection as an alternative to parental conflict. Am. J. Bot. *107*.

Lafon-Placette, C., and Köhler, C. (2016). Endosperm-based postzygotic hybridization barriers: developmental mechanisms and evolutionary drivers. Mol. Ecol. *25*, 2620–2629.

Lambert, J.E., and Garber, P.A. (1998). Evolutionary and ecological implications of primate seed dispersal. Am. J. Primatol. *45*, 9–28.

Lang, Z., and Zhu, J. (2015). OST1 phosphorylates ICE1 to enhance plant cold tolerance. Sci. China Life Sci. *58*, 317–318.

Lange, B.M., Lapierre, C., and Sandermann, H. (1995). Elicitor-Induced Spruce Stress Lignin (Structural Similarity to Early Developmental Lignins). Plant Physiol. *108*, 1277–1287.

Łangowski, Ł., Stacey, N., and Østergaard, L. (2016). Diversification of fruit shape in the Brassicaceae family. Plant Reprod. *29*, 149–163.

Larsson, K.E., Kjellberg, J.M., Tjellström, H., and Sandelius, A.S. (2007). LysoPC acyltransferase/PC transacylase activities in plant plasma membrane and plasma membrane-associated endoplasmic reticulum. BMC Plant Biol. *7*, 64.

Lazaro, A., Valverde, F., Piñeiro, M., and Jarillo, J.A. (2012). The Arabidopsis E3 Ubiquitin Ligase HOS1 Negatively Regulates CONSTANS Abundance in the Photoperiodic Control of Flowering. Plant Cell *24*, 982–999.

Le, B.H., Cheng, C., Bui, A.Q., Wagmaister, J.A., Henry, K.F., Pelletier, J., Kwong, L., Belmonte, M., Kirkbride, R., Horvath, S., et al. (2010). Global analysis of gene activity during Arabidopsis seed development and identification of seed-specific transcription factors. Proc. Natl. Acad. Sci. *107*, 8063–8070.

Lee, J.H., Kim, J.J., Kim, S.H., Cho, H.J., Kim, J., and Ahn, J.H. (2012a). The E3 Ubiquitin Ligase HOS1 Regulates Low Ambient Temperature-Responsive Flowering in Arabidopsis thaliana. Plant Cell Physiol. *53*, 1802–1814.

Lee, J.-H., Jung, J.-H., and Park, C.-M. (2017). Light Inhibits COP1-Mediated Degradation of ICE Transcription Factors to Induce Stomatal Development in Arabidopsis. Plant Cell *29*, 2817–2830.

Lee, K.J.D., Dekkers, B.J.W., Steinbrecher, T., Walsh, C.T., Bacic, A., Bentsink, L., Leubner-Metzger, G., and Knox, J.P. (2012b). Distinct cell wall architectures in seed endosperms in representatives of the Brassicaceae and Solanaceae. Plant Physiol. *160*, 1551–1566.

Lee, K.J.D., Dekkers, B.J.W., Steinbrecher, T., Walsh, C.T., Bacic, A., Bentsink, L., Leubner-Metzger, G., and Knox, J.P. (2012c). Distinct cell wall architectures in seed endosperms in representatives of the Brassicaceae and Solanaceae. Plant Physiol. *160*, 1551–1566.

Lee, K.P., Piskurewicz, U., Turečková, V., Strnad, M., and Lopez-Molina, L. (2010). A seed coat bedding assay shows that RGL2-dependent release of abscisic acid by the endosperm controls embryo growth in Arabidopsis dormant seeds. Proc. Natl. Acad. Sci. *107*, 19108–19113.

Lee, S.B., Go, Y.S., Bae, H.-J., Park, J.H., Cho, S.H., Cho, H.J., Lee, D.S., Park, O.K., Hwang, I., and Suh, M.C. (2009). Disruption of glycosylphosphatidylinositol-anchored lipid transfer protein gene altered cuticular lipid composition, increased plastoglobules, and enhanced susceptibility to infection by the fungal pathogen Alternaria brassicicola. Plant Physiol. *150*, 42–54.

Lee, S.B., Yang, S.U., Pandey, G., Kim, M.-S., Hyoung, S., Choi, D., Shin, J.S., and Suh, M.C. (2020). Occurrence of land-plant-specific glycerol-3-phosphate acyltransferases is essential for cuticle formation and gametophore development in Physcomitrella patens. New Phytol. *225*, 2468–2483.

Lee, Y., Rubio, M.C., Alassimone, J., and Geldner, N. (2013). A mechanism for localized lignin deposition in the endodermis. Cell *153*, 402–412.

Lee, Y., Yoon, T.H., Lee, J., Jeon, S.Y., Lee, J.H., Lee, M.K., Chen, H., Yun, J., Oh, S.Y., Wen, X., et al. (2018). A Lignin Molecular Brace Controls Precision Processing of Cell Walls Critical for Surface Integrity in Arabidopsis. Cell *173*, 1468-1480.e9.

Lendzian, K.J., Nakajima, A., and Ziegler, H. (1986). Isolation of cuticular membranes from various conifer needles. Trees *1*.

Lewis, L.A., and McCourt, R.M. (2004). Green algae and the origin of land plants. Am. J. Bot. *91*, 1535–1556.

L'Haridon, F., Besson-Bard, A., Binda, M., Serrano, M., Abou-Mansour, E., Balet, F., Schoonbeek, H.-J., Hess, S., Mir, R., Léon, J., et al. (2011). A Permeable Cuticle Is Associated with the Release of Reactive Oxygen Species and Induction of Innate Immunity. PLOS Pathog. *7*, e1002148.

Li, J., and Berger, F. (2012). Endosperm: food for humankind and fodder for scientific discoveries. New Phytol. *195*, 290–305.

Li, F., Wu, X., Lam, P., Bird, D., Zheng, H., Samuels, L., Jetter, R., and Kunst, L. (2008). Identification of the Wax Ester Synthase/Acyl-Coenzyme A:Diacylglycerol Acyltransferase WSD1 Required for Stem Wax Ester Biosynthesis in Arabidopsis. Plant Physiol. *148*, 97–107.

Li, H., Ding, Y., Shi, Y., Zhang, X., Zhang, S., Gong, Z., and Yang, S. (2017). MPK3- and MPK6-Mediated ICE1 Phosphorylation Negatively Regulates ICE1 Stability and Freezing Tolerance in Arabidopsis. Dev. Cell *43*, 630-642.e4.

Li, Y., Beisson, F., Koo, A.J.K., Molina, I., Pollard, M., and Ohlrogge, J. (2007). Identification of acyltransferases required for cutin biosynthesis and production of cutin with suberin-like monomers. Proc. Natl. Acad. Sci. *104*, 18339–18344.

Li-Beisson, Y., Pollard, M., Sauveplane, V., Pinot, F., Ohlrogge, J., and Beisson, F. (2009). Nanoridges that characterize the surface morphology of flowers require the synthesis of cutin polyester. Proc. Natl. Acad. Sci. *106*, 22008–22013.

Li-Beisson, Y., Shorrosh, B., Beisson, F., Andersson, M.X., Arondel, V., Bates, P.D., Baud, S., Bird, D., DeBono, A., Durrett, T.P., et al. (2013). Acyl-Lipid Metabolism. Arab. Book *2013*.

Ligrone, R., Duckett, J.G., and Renzaglia, K.S. (1993). The Gametophyte-Sporophyte Junction in Land Plants. In Advances in Botanical Research, J.A. Callow, ed. (Academic Press), pp. 231–318.

Ligrone, R., Duckett, J.G., and Renzaglia, K.S. (2000). Conducting tissues and phyletic relationships of bryophytes. Philos. Trans. R. Soc. Lond. B. Biol. Sci. *355*, 795–813.

Lin, Q., Ohashi, Y., Kato, M., Tsuge, T., Gu, H., Qu, L.-J., and Aoyama, T. (2015). GLABRA2 Directly Suppresses Basic Helix-Loop-Helix Transcription Factor Genes with Diverse Functions in Root Hair Development. Plant Cell *27*, 2894–2906.

Linkies, A., Graeber, K., Knight, C., and Leubner-Metzger, G. (2010). The evolution of seeds. New Phytol. *186*, 817–831.

López-Casado, G., Matas, A.J., Domínguez, E., Cuartero, J., and Heredia, A. (2007). Biomechanics of isolated tomato (Solanum lycopersicum L.) fruit cuticles: the role of the cutin matrix and polysaccharides. J. Exp. Bot. *58*, 3875–3883.

Loubéry, S., De Giorgi, J., Utz-Pugin, A., Demonsais, L., and Lopez-Molina, L. (2018). A Maternally Deposited Endosperm Cuticle Contributes to the Physiological Defects of transparent testa Seeds1[OPEN]. Plant Physiol. *177*, 1218–1233.

Lu, J., and Magnani, E. (2018). Seed tissue and nutrient partitioning, a case for the nucellus. Plant Reprod. *31*, 309–317.

Lu, J., Le Hir, R., Gómez-Páez, D.-M., Coen, O., Péchoux, C., Jasinski, S., and Magnani, E. (2021). The nucellus: between cell elimination and sugar transport. Plant Physiol. *185*, 478–490.

Lu, P., Porat, R., Nadeau, J.A., and O'Neill, S.D. (1996). Identification of a meristem L1 layer-specific gene in Arabidopsis that is expressed during embryonic pattern formation and defines a new class of homeobox genes. Plant Cell *8*, 2155–2168.

Lü, S., Song, T., Kosma, D.K., Parsons, E.P., Rowland, O., and Jenks, M.A. (2009). Arabidopsis CER8 encodes LONG-CHAIN ACYL-COA SYNTHETASE 1 (LACS1) that has overlapping functions with LACS2 in plant wax and cutin synthesis. Plant J. Cell Mol. Biol. *59*, 553–564.

Lv, Z., Wang, S., Zhang, F., Chen, L., Hao, X., Pan, Q., Fu, X., Li, L., Sun, X., and Tang, K. (2016). Overexpression of a Novel NAC Domain-Containing Transcription Factor Gene (AaNAC1) Enhances the Content of Artemisinin and Increases Tolerance to Drought and Botrytis cinerea in Artemisia annua. Plant Cell Physiol. *57*, 1961–1971.

MacGregor, D.R., and Penfield, S. (2015). Exploring the pleiotropy of hos1. J. Exp. Bot. *66*, 1661–1671.

MacGregor, D.R., Gould, P., Foreman, J., Griffiths, J., Bird, S., Page, R., Stewart, K., Steel, G., Young, J., Paszkiewicz, K., et al. (2013). HIGH EXPRESSION OF OSMOTICALLY RESPONSIVE GENES1 Is Required for Circadian Periodicity through the Promotion of Nucleo-Cytoplasmic mRNA Export in Arabidopsis. Plant Cell *25*, 4391–4404.

Magnani, E. (2018). Seed Evolution, A "Simpler" Story. Trends Plant Sci. *23*, 654–656.

Manheim, B.S., Mulroy, T.W., Hogness, D.K., and Kerwin, J.L. (1979). Interspecific variation in leaf wax of Dudleya. Biochem. Syst. Ecol. *7*, 17–19.

Maruyama, D., Völz, R., Takeuchi, H., Mori, T., Igawa, T., Kurihara, D., Kawashima, T., Ueda, M., Ito, M., Umeda, M., et al. (2015). Rapid Elimination of the Persistent Synergid through a Cell Fusion Mechanism. Cell *161*, 907–918.

Mazurek, S., Garroum, I., Daraspe, J., De Bellis, D., Olsson, V., Mucciolo, A., Butenko, M.A., Humbel, B.M., and Nawrath, C. (2017). Connecting the Molecular Structure of Cutin to Ultrastructure and Physical Properties of the Cuticle in Petals of Arabidopsis. Plant Physiol. *173*, 1146–1163.

McConaha, M. (1941). Ventral Structures Effecting Capillarity in the Marchantiales. Am. J. Bot. *28*, 301–306.

McFarlane, H.E., Watanabe, Y., Gendre, D., Carruthers, K., Levesque-Tremblay, G., Haughn, G.W., Bhalerao, R.P., and Samuels, L. (2013). Cell wall polysaccharides are mislocalized to the Vacuole in echidna mutants. Plant Cell Physiol. *54*, 1867–1880.

McFarlane, H.E., Watanabe, Y., Yang, W., Huang, Y., Ohlrogge, J., and Samuels, A.L. (2014). Golgi- and trans-Golgi network-mediated vesicle trafficking is required for wax secretion from epidermal cells. Plant Physiol. *164*, 1250–1260.

Mckinney, D.E., Bortiatynski, J.M., Carson, D.M., Clifford, D.J., De Leeuw, J.W., and Hatcher, P.G. (1996). Tetramethylammonium hydroxide (TMAH) thermochemolysis of the aliphatic biopolymer cutan: insights into the chemical structure. Org. Geochem. *24*, 641–650.

Meinke, D., and Scholl, R. (2003). The preservation of plant genetic resources. Experiences with Arabidopsis. Plant Physiol. *133*, 1046–1050.

Menand, B., Yi, K., Jouannic, S., Hoffmann, L., Ryan, E., Linstead, P., Schaefer, D.G., and Dolan, L. (2007). An ancient mechanism controls the development of cells with a rooting function in land plants. Science *316*, 1477–1480.

Meyer, H.M., Teles, J., Formosa-Jordan, P., Refahi, Y., San-Bento, R., Ingram, G., Jönsson, H., Locke, J.C.W., and Roeder, A.H.K. (2017). Fluctuations of the transcription factor ATML1 generate the pattern of giant cells in the Arabidopsis sepal. ELife *6*, e19131.

Meyerowitz, E.M. (2001). Prehistory and history of Arabidopsis research. Plant Physiol. *125*, 15–19.

Millar, A.A., Clemens, S., Zachgo, S., Giblin, E.M., Taylor, D.C., and Kunst, L. (1999). CUT1, an Arabidopsis Gene Required for Cuticular Wax Biosynthesis and Pollen Fertility, Encodes a Very-Long-Chain Fatty Acid Condensing Enzyme. Plant Cell *11*, 825.

Mishler-Elmore, J.W., Zhou, Y., Sukul, A., Oblak, M., Tan, L., Faik, A., and Held, M.A. (2021). Extensins: Self-Assembly, Crosslinking, and the Role of Peroxidases. Front. Plant Sci. *12*, 664738.

Miura, K., and Ohta, M. (2010). SIZ1, a small ubiquitin-related modifier ligase, controls cold signaling through regulation of salicylic acid accumulation. J. Plant Physiol. *167*, 555–560.

Miura, K., Jin, J.B., Lee, J., Yoo, C.Y., Stirm, V., Miura, T., Ashworth, E.N., Bressan, R.A., Yun, D.-J., and Hasegawa, P.M. (2007). SIZ1-mediated sumoylation of ICE1 controls CBF3/DREB1A expression and freezing tolerance in Arabidopsis. Plant Cell *19*, 1403–1414.

Miura, K., Ohta, M., Nakazawa, M., Ono, M., and Hasegawa, P.M. (2011). ICE1 Ser403 is necessary for protein stabilization and regulation of cold signaling and tolerance. Plant J. Cell Mol. Biol. *67*, 269–279.

Mizuta, Y., and Higashiyama, T. (2018). Chemical signaling for pollen tube guidance at a glance. J. Cell Sci. *131*, jcs208447.

Möckli, N., Deplazes, A., Hassa, P.O., Zhang, Z., Peter, M., Hottiger, M.O., Stagljar, I., and Auerbach, D. (2007). Yeast split-ubiquitin-based cytosolic screening system to detect interactions between transcriptionally active proteins. BioTechniques *42*, 725–730.

von Mohl, H. (1842). Ueber die cuticula der gewächse,"in Linnaea. pp. 401–416.

von Mohl, H. (1847). Untersuchungen der Frage: bildet die cellulose die grundlage sammtlicher vegetabilischen membranen. Bot Zeit 5 497–505.

Molina, I., Bonaventure, G., Ohlrogge, J., and Pollard, M. (2006). The lipid polyester composition of Arabidopsis thaliana and Brassica napus seeds. Phytochemistry *67*, 2597–2610.

Molina, I., Ohlrogge, J.B., and Pollard, M. (2008). Deposition and localization of lipid polyester in developing seeds of Brassica napus and Arabidopsis thaliana. Plant J. *53*, 437–449.

Montgomery, S.A., Tanizawa, Y., Galik, B., Wang, N., Ito, T., Mochizuki, T., Akimcheva, S., Bowman, J.L., Cognat, V., Maréchal-Drouard, L., et al. (2020). Chromatin Organization in Early Land Plants Reveals an Ancestral Association between H3K27me3, Transposons, and Constitutive Heterochromatin. Curr. Biol. *30*, 573-588.e7.

Morley-Smith, E.R., Pike, M.J., Findlay, K., Köckenberger, W., Hill, L.M., Smith, A.M., and Rawsthorne, S. (2008). The Transport of Sugars to Developing Embryos Is Not via the Bulk Endosperm in Oilseed Rape Seeds. Plant Physiol. *147*, 2121–2130.

Motte, H., Vanneste, S., and Beeckman, T. (2019). Molecular and Environmental Regulation of Root Development. Annu. Rev. Plant Biol. *70*, 465–488.

Moussu, S., Doll, N.M., Chamot, S., Brocard, L., Creff, A., Fourquin, C., Widiez, T., Nimchuk, Z.L., and Ingram, G. (2017). ZHOUPI and KERBEROS Mediate Embryo/Endosperm Separation by Promoting the Formation of an Extracuticular Sheath at the Embryo Surface. Plant Cell *29*, 1642–1656.

Moyroud, E., Wenzel, T., Middleton, R., Rudall, P.J., Banks, H., Reed, A., Mellers, G., Killoran, P., Westwood, M.M., Steiner, U., et al. (2017). Disorder in convergent floral nanostructures enhances signalling to bees. Nature *550*, 469–474.

Mulroy, T.W. (1979). Spectral properties of heavily glaucous and non-glaucous leaves of a succulent rosette-plant. Oecologia *38*, 349–357.

Nakamura, M., Katsumata, H., Abe, M., Yabe, N., Komeda, Y., Yamamoto, K.T., and Takahashi, T. (2006). Characterization of the class IV homeodomain-Leucine Zipper gene family in Arabidopsis. Plant Physiol. *141*, 1363–1375.

Nakano, R.T., Matsushima, R., Ueda, H., Tamura, K., Shimada, T., Li, L., Hayashi, Y., Kondo, M., Nishimura, M., and Hara-Nishimura, I. (2009). GNOM-LIKE1/ERMO1 and SEC24a/ERMO2 Are Required for Maintenance of Endoplasmic Reticulum Morphology in Arabidopsis thaliana. Plant Cell *21*, 3672–3685.

Nakashima, K., Takasaki, H., Mizoi, J., Shinozaki, K., and Yamaguchi-Shinozaki, K. (2012). NAC transcription factors in plant abiotic stress responses. Biochim. Biophys. Acta *1819*, 97–103.

Nawrath, C., Schreiber, L., Franke, R.B., Geldner, N., Reina-Pinto, J.J., and Kunst, L. (2013). Apoplastic diffusion barriers in Arabidopsis. Arab. Book *11*, e0167.

Negin, B., Shachar, L., Meir, S., Ramirez, C.C., Horowitz, A.R., Jander, G., and Aharoni, A. (2021). Fatty Alcohols, a Minor Component of the Tree Tobacco Surface Wax, Reduce Insect Herbivory.

Nersissian, A.M., Immoos, C., Hill, M.G., Hart, P.J., Williams, G., Herrmann, R.G., and Valentine, J.S. (1998). Uclacyanins, stellacyanins, and plantacyanins are distinct subfamilies of phytocyanins: plant-specific mononuclear blue copper proteins. Protein Sci. Publ. Protein Soc. *7*, 1915–1929.

Niklas, K.J. (1997). The Evolutionary Biology of Plants (University of Chicago Press).

Niklas, K.J., Kutschera, U., Niklas, K.J., and Kutschera, U. (2009). The evolutionary development of plant body plans. Funct. Plant Biol. *36*, 682–695.

Nishida, I., Tasaka, Y., Shiraishi, H., and Murata, N. (1993). The gene and the RNA for the precursor to the plastid-located glycerol-3-phosphate acyltransferase of Arabidopsis thaliana. Plant Mol. Biol. *21*, 267–277.

Ogawa, E., Yamada, Y., Sezaki, N., Kosaka, S., Kondo, H., Kamata, N., Abe, M., Komeda, Y., and Takahashi, T. (2015). ATML1 and PDF2 Play a Redundant and Essential Role in Arabidopsis Embryo Development. Plant Cell Physiol. *56*, 1183–1192.

O'Hanlon, M.E. (2015). Germination of Spores and Early Stages in Development of Gametophyte of Marchantia polymorpha. Bot. Gaz.

Ohyama, K., Fukuzawa, H., Kohchi, T., Shirai, H., Sano, T., Sano, S., Umesono, K., Shiki, Y., Takeuchi, M., Chang, Z., et al. (1986). Chloroplast gene organization deduced from complete sequence of liverwort Marchantia polymorpha chloroplast DNA. Nature *322*, 572–574.

Okada, S., Fujisawa, M., Sone, T., Nakayama, S., Nishiyama, R., Takenaka, M., Yamaoka, S., Sakaida, M., Kono, K., Takahama, M., et al. (2000). Construction of male and female PAC genomic libraries suitable for identification of Y-chromosome-specific clones from the liverwort, Marchantia polymorpha. Plant J. *24*, 421–428.

Okuda, S., Fujita, S., Moretti, A., Hohmann, U., Doblas, V.G., Ma, Y., Pfister, A., Brandt, B., Geldner, N., and Hothorn, M. (2020). Molecular mechanism for the recognition of sequence-divergent CIF peptides by the plant receptor kinases GSO1/SGN3 and GSO2. Proc. Natl. Acad. Sci. U. S. A. *117*, 2693–2703.

Olsen, O.-A. (2001). ENDOSPERM DEVELOPMENT: Cellularization and Cell Fate Specification. Annu. Rev. Plant Physiol. Plant Mol. Biol. *52*, 233–267.

Olsen, O.-A. (2004). Nuclear endosperm development in cereals and Arabidopsis thaliana. Plant Cell *16 Suppl*, S214-227.

Olvera-Carrillo, Y., Van Bel, M., Van Hautegem, T., Fendrych, M., Huysmans, M., Simaskova, M., van Durme, M., Buscaill, P., Rivas, S., S. Coll, N., et al. (2015). A Conserved Core of Programmed Cell Death Indicator Genes Discriminates Developmentally and Environmentally Induced Programmed Cell Death in Plants. Plant Physiol. *169*, 2684–2699.

Opsahl-Ferstad, H.G., Le Deunff, E., Dumas, C., and Rogowsky, P.M. (1997). ZmEsr, a novel endosperm-specific gene expressed in a restricted region around the maize embryo. Plant J. Cell Mol. Biol. *12*, 235–246.

Orgell, W.H. (1955). The Isolation of Plant Cuticle with Pectic Enzymes. 12. Plant Physiol. *30*, 78–80.

Osborn, J.M., and Taylor, T.N. (1990). Morphological and Ultrastructural Studies of Plant Cuticular Membranes. I. Sun and Shade Leaves of Quercus velutina (Fagaceae). Bot. Gaz. *151*, 465–476.

Oshima, Y., and Mitsuda, N. (2013). The MIXTA-like Transcription factor MYB16 is a major regulator of cuticle formation in vegetative organs. Plant Signal. Behav. *8*, e26826.

Otegui, M.S., Capp, R., and Staehelin, L.A. (2002). Developing Seeds of Arabidopsis Store Different Minerals in Two Types of Vacuoles and in the Endoplasmic Reticulum. Plant Cell *14*, 1311–1327.

Panikashvili, D., Shi, J.X., Schreiber, L., and Aharoni, A. (2009). The Arabidopsis DCR Encoding a Soluble BAHD Acyltransferase Is Required for Cutin Polyester Formation and Seed Hydration Properties. Plant Physiol. *151*, 1773–1789.

Panikashvili, D., Shi, J.X., Bocobza, S., Franke, R.B., Schreiber, L., and Aharoni, A. (2010). The Arabidopsis DSO/ABCG11 transporter affects cutin metabolism in reproductive organs and suberin in roots. Mol. Plant *3*, 563–575.

Panikashvili, D., Shi, J.X., Schreiber, L., and Aharoni, A. (2011). The Arabidopsis ABCG13 transporter is required for flower cuticle secretion and patterning of the petal epidermis. New Phytol. *190*, 113–124.

Patwari, P., Salewski, V., Gutbrod, K., Kreszies, T., Dresen-Scholz, B., Peisker, H., Steiner, U., Meyer, A.J., Schreiber, L., and Dörmann, P. (2019). Surface wax esters contribute to drought tolerance in Arabidopsis. Plant J. *98*, 727–744.

Paul Knox, J., Peart, J., and Neill, S.J. (1995). Identification of novel cell surface epitopes using a leaf epidermal-strip assay system. Planta *196*, 266–270.

Penfield, S., Rylott, E.L., Gilday, A.D., Graham, S., Larson, T.R., and Graham, I.A. (2004). Reserve Mobilization in the Arabidopsis Endosperm Fuels Hypocotyl Elongation in the Dark, Is Independent of Abscisic Acid, and Requires PHOSPHOENOLPYRUVATE CARBOXYKINASE1. Plant Cell *16*, 2705–2718.

Peterson, K.M., Shyu, C., Burr, C.A., Horst, R.J., Kanaoka, M.M., Omae, M., Sato, Y., and Torii, K.U. (2013). Arabidopsis homeodomain-leucine zipper IV proteins promote stomatal development and ectopically induce stomata beyond the epidermis. Dev. Camb. Engl. *140*, 1924–1935.

Pfister, A., Barberon, M., Alassimone, J., Kalmbach, L., Lee, Y., Vermeer, J.E., Yamazaki, M., Li, G., Maurel, C., Takano, J., et al. (2014). A receptor-like kinase mutant with absent endodermal diffusion barrier displays selective nutrient homeostasis defects. ELife *3*, e03115.

Philippe, G., Gaillard, C., Petit, J., Geneix, N., Dalgalarrondo, M., Bres, C., Mauxion, J.-P., Franke, R., Rothan, C., Schreiber, L., et al. (2016). Ester Cross-Link Profiling of the Cutin Polymer of Wild-Type and Cutin Synthase Tomato Mutants Highlights Different Mechanisms of Polymerization1. Plant Physiol. *170*, 807–820.

Philippe, G., Sørensen, I., Jiao, C., Sun, X., Fei, Z., Domozych, D.S., and Rose, J.K. (2020). Cutin and suberin: assembly and origins of specialized lipidic cell wall scaffolds. Curr. Opin. Plant Biol. *55*, 11–20.

Pighin, J.A., Zheng, H., Balakshin, L.J., Goodman, I.P., Western, T.L., Jetter, R., Kunst, L., and Samuels, A.L. (2004). Plant cuticular lipid export requires an ABC transporter. Science *306*, 702–704.

Pires, N.D. (2014). Seed evolution: parental conflicts in a multi-generational household. Biomol. Concepts *5*, 71–86.

Pires, N., and Dolan, L. (2010). Origin and diversification of basic-helix-loop-helix proteins in plants. Mol. Biol. Evol. *27*, 862–874.

Pollard, M., Beisson, F., Li, Y., and Ohlrogge, J.B. (2008). Building lipid barriers: biosynthesis of cutin and suberin. Trends Plant Sci. *13*, 236–246.

Povilus, R.A., Diggle, P.K., and Friedman, W.E. (2018). Evidence for parent-of-origin effects and interparental conflict in seeds of an ancient flowering plant lineage. Proc. R. Soc. B Biol. Sci. *285*, 20172491.

Pressel, S., Ligrone, R., and Duckett, J.G. (2008). Cellular Differentiation in Moss Protonemata: A Morphological and Experimental Study. Ann. Bot. *102*, 227–245.

Pressel, S., Renzaglia, K.S., (Dicky) Clymo, R.S., and Duckett, J.G. (2018). Hornwort stomata do not respond actively to exogenous and environmental cues. Ann. Bot. *122*, 45–57.

Proust, H., Honkanen, S., Jones, V.A.S., Morieri, G., Prescott, H., Kelly, S., Ishizaki, K., Kohchi, T., and Dolan, L. (2016). RSL Class I Genes Controlled the Development of Epidermal Structures in the Common Ancestor of Land Plants. Curr. Biol. *26*, 93–99.

Pulsifer, I.P., Kluge, S., and Rowland, O. (2012). Arabidopsis LONG-CHAIN ACYL-COA SYNTHETASE 1 (LACS1), LACS2, and LACS3 facilitate fatty acid uptake in yeast. Plant Physiol. Biochem. *51*, 31–39.

Putarjunan, A., Ruble, J., Srivastava, A., Zhao, C., Rychel, A.L., Hofstetter, A.K., Tang, X., Zhu, J.-K., Tama, F., Zheng, N., et al. (2019). Bipartite anchoring of SCREAM enforces stomatal initiation by coupling MAP Kinases to SPEECHLESS. Nat. Plants *5*, 742–754.

Puttick, M.N., Morris, J.L., Williams, T.A., Cox, C.J., Edwards, D., Kenrick, P., Pressel, S., Wellman, C.H., Schneider, H., Pisani, D., et al. (2018). The Interrelationships of Land Plants and the Nature of the Ancestral Embryophyte. Curr. Biol. CB *28*, 733-745.e2.

Qu, L.-J., and Qin, G. (2014). Generation and Identification of Arabidopsis EMS Mutants. In Arabidopsis Protocols, J.J. Sanchez-Serrano, and J. Salinas, eds. (Totowa, NJ: Humana Press), pp. 225–239.

Raissig, M.T., Abrash, E., Bettadapur, A., Vogel, J.P., and Bergmann, D.C. (2016). Grasses use an alternatively wired bHLH transcription factor network to establish stomatal identity. Proc. Natl. Acad. Sci. U. S. A. *113*, 8326–8331.

Rautengarten, C., Ebert, B., Ouellet, M., Nafisi, M., Baidoo, E.E.K., Benke, P., Stranne, M., Mukhopadhyay, A., Keasling, J.D., Sakuragi, Y., et al. (2012). Arabidopsis Deficient in Cutin Ferulate encodes a transferase required for feruloylation of ω-hydroxy fatty acids in cutin polyester. Plant Physiol. *158*, 654–665.

Raven, J.A. (2002). Selection pressures on stomatal evolution. New Phytol. *153*, 371–386.

Ray, A.K., and Stark, R.E. (1998). Isolation and molecular structure of an oligomer produced enzymatically from the cuticle of lime fruit. Phytochemistry *48*, 1313–1320.

Reich, E., Schibli, A., Widmer, V., Jorns, R., Wolfram, E., and DeBatt, A. (2006). HPTLC Methods for Identification of Green Tea and Green Tea Extract. J. Liq. Chromatogr. Relat. Technol. *29*, 2141–2151.

Renault, H., Alber, A., Horst, N.A., Basilio Lopes, A., Fich, E.A., Kriegshauser, L., Wiedemann, G., Ullmann, P., Herrgott, L., Erhardt, M., et al. (2017). A phenol-enriched cuticle is ancestral to lignin evolution in land plants. Nat. Commun. *8*, 14713.

Rensing, S.A. (2016). (Why) Does Evolution Favour Embryogenesis? Trends Plant Sci. *21*, 562–573.

Rensing, S.A., Lang, D., Zimmer, A.D., Terry, A., Salamov, A., Shapiro, H., Nishiyama, T., Perroud, P.-F., Lindquist, E.A., Kamisugi, Y., et al. (2008). The Physcomitrella genome reveals evolutionary insights into the conquest of land by plants. Science *319*, 64–69.

Reyt, G., Chao, Z., Flis, P., Salas-González, I., Castrillo, G., Chao, D.-Y., and Salt, D.E. (2020). Uclacyanin Proteins Are Required for Lignified Nanodomain Formation within Casparian Strips. Curr. Biol. CB *30*, 4103-4111.e6.

Rich, M.K., and Delaux, P.-M. (2020). Plant Evolution: When Arabidopsis Is More Ancestral Than Marchantia. Curr. Biol. *30*, R642–R644.

Rojas-Murcia, N., Hématy, K., Lee, Y., Emonet, A., Ursache, R., Fujita, S., Bellis, D.D., and Geldner, N. (2020). High-order mutants reveal an essential requirement for peroxidases but not laccases in Casparian strip lignification. Proc. Natl. Acad. Sci. *117*, 29166–29177.

Rolletschek, H., Muszynska, A., and Borisjuk, L. (2021). The process of seed maturation is influenced by mechanical constraints. New Phytol. *229*, 19–23.

Roudier, F., Gissot, L., Beaudoin, F., Haslam, R., Michaelson, L., Marion, J., Molino, D., Lima, A., Bach, L., Morin, H., et al. (2010). Very-Long-Chain Fatty Acids Are Involved in Polar Auxin Transport and Developmental Patterning in Arabidopsis[W]. Plant Cell *22*, 364–375.

Rowland, O., Zheng, H., Hepworth, S.R., Lam, P., Jetter, R., and Kunst, L. (2006). CER4 Encodes an Alcohol-Forming Fatty Acyl-Coenzyme A Reductase Involved in Cuticular Wax Production in Arabidopsis. Plant Physiol. *142*, 866–877.

Růžička, K., Ursache, R., Hejátko, J., and Helariutta, Y. (2015). Xylem development – from the cradle to the grave. New Phytol. *207*, 519–535.

Sabelli, P.A., and Larkins, B.A. (2009). The Development of Endosperm in Grasses. Plant Physiol. *149*, 14–26.

Samuels, L., and McFarlane, H.E. (2012). Plant cell wall secretion and lipid traffic at membrane contact sites of the cell cortex. Protoplasma *249*, 19–23.

Samuels, L., Kunst, L., and Jetter, R. (2008). Sealing plant surfaces: cuticular wax formation by epidermal cells. Annu. Rev. Plant Biol. *59*, 683–707.

San-Bento, R., Farcot, E., Galletti, R., Creff, A., and Ingram, G. (2014). Epidermal identity is maintained by cell-cell communication via a universally active feedback loop in Arabidopsis thaliana. Plant J. Cell Mol. Biol. *77*, 46–58.

Sánchez-Montesino, R., Bouza-Morcillo, L., Marquez, J., Ghita, M., Duran-Nebreda, S., Gómez, L., Holdsworth, M.J., Bassel, G., and Oñate-Sánchez, L. (2019). A Regulatory Module Controlling GA-Mediated Endosperm Cell Expansion Is Critical for Seed Germination in Arabidopsis. Mol. Plant *12*, 71–85.

SARGANT, E. (1900). Recent Work on the Results of Fertilization in Angiosperms. Ann. Bot. *14*, 689–712.

Schaefer, D.G., and Zrÿ d, J.P. (1997). Efficient gene targeting in the moss Physcomitrela patens. Plant J. Cell Mol. Biol. *11*, 1195–1206.

Scheres, B., Benfey, P., and Dolan, L. (2002). Root Development. Arab. Book Am. Soc. Plant Biol. *1*, e0101.

Schmidt, H.W., and Schönherr, J. (1982). Development of plant cuticles: occurrence and role of non-ester bonds in cutin of Clivia miniata Reg. leaves. Planta *156*, 380–384.

Schönherr, J., and Ziegler, H. (1975). Hydrophobic cuticular ledges prevent water entering the air pores of liverwort thalli. Planta *124*, 51–60.

Schuster, A.-C., Burghardt, M., and Riederer, M. (2017). The ecophysiology of leaf cuticular transpiration: are cuticular water permeabilities adapted to ecological conditions? J. Exp. Bot. *68*, 5271–5279.

Seale, M., and Nakayama, N. (2020). From passive to informed: mechanical mechanisms of seed dispersal. New Phytol. *225*, 653–658.

Sechet, J., Frey, A., Effroy-Cuzzi, D., Berger, A., Perreau, F., Cueff, G., Charif, D., Rajjou, L., Mouille, G., North, H.M., et al. (2016). Xyloglucan Metabolism Differentially Impacts the Cell Wall Characteristics of the Endosperm and Embryo during Arabidopsis Seed Germination. Plant Physiol. *170*, 1367–1380.

Segado, P., Heredia-Guerrero, J.A., Heredia, A., and Domínguez, E. (2020). Cutinsomes and CUTIN SYNTHASE1 Function Sequentially in Tomato Fruit Cutin Deposition. Plant Physiol. *183*, 1622–1637.

Sela, D., Buxdorf, K., Shi, J.X., Feldmesser, E., Schreiber, L., Aharoni, A., and Levy, M. (2013). Overexpression of AtSHN1/WIN1 Provokes Unique Defense Responses. PLOS ONE *8*, e70146.

Serrano, M., Coluccia, F., Torres, M., L'Haridon, F., and Métraux, J.-P. (2014). The cuticle and plant defense to pathogens. Front. Plant Sci. *5*, 274.

Shepherd, T., Robertson, G.W., Griffiths, D., and Birch, A. (1999). Epicuticular wax composition in relation to aphid infestation and resistance in red raspberry (Rubus idaeus L.).

Shi, J.X., Malitsky, S., De Oliveira, S., Branigan, C., Franke, R.B., Schreiber, L., and Aharoni, A. (2011). SHINE transcription factors act redundantly to pattern the archetypal surface of Arabidopsis flower organs. PLoS Genet. *7*, e1001388.

Shi, Y.B., Li, Q., Damjanovski, S., Amano, T., and Ishizuya-Oka, A. (1998). Regulation of apoptosis during development: input from the extracellular matrix (review). Int. J. Mol. Med. *2*, 273–282.

Shigeyama, T., Watanabe, A., Tokuchi, K., Toh, S., Sakurai, N., Shibuya, N., and Kawakami, N. (2016). α-Xylosidase plays essential roles in xyloglucan remodelling, maintenance of cell wall integrity, and seed germination in Arabidopsis thaliana. J. Exp. Bot. *67*, 5615–5629.

Shimamura, M. (2016). Marchantia polymorpha : Taxonomy, Phylogeny and Morphology of a Model System. Plant Cell Physiol. *57*, 230–256.

Shockey, J.M., Fulda, M.S., and Browse, J.A. (2002). Arabidopsis Contains Nine Long-Chain Acyl-Coenzyme A Synthetase Genes That Participate in Fatty Acid and Glycerolipid Metabolism. Plant Physiol. *129*, 1710–1722.

Smallwood, M., Beven, A., Donovan, N., Neill, S. j., Peart, J., Roberts, K., and Knox, J. p. (1994). Localization of cell wall proteins in relation to the developmental anatomy of the carrot root apex. Plant J. *5*, 237–246.

Solovchenko, A., and Merzlyak, M. (2003). Optical properties and contribution of cuticle to UV protection in plants: Experiments with apple fruit. Photochem. Photobiol. Sci. Off. J. Eur. Photochem. Assoc. Eur. Soc. Photobiol. *2*, 861–866.

Soltis, D.E. (2021). Ancient seeds spill secrets about the evolution of flowering plants. Nature *594*, 185–186.

Somerville, C., and Koornneef, M. (2002). A fortunate choice: the history of Arabidopsis as a model plant. Nat. Rev. Genet. *3*, 883–889.

Sørensen, M.B., Mayer, U., Lukowitz, W., Robert, H., Chambrier, P., Jürgens, G., Somerville, C., Lepiniec, L., and Berger, F. (2002). Cellularisation in the endosperm of Arabidopsis thaliana is coupled to mitosis and shares multiple components with cytokinesis. Dev. Camb. Engl. *129*, 5567–5576.

Sosso, D., Luo, D., Li, Q.-B., Sasse, J., Yang, J., Gendrot, G., Suzuki, M., Koch, K.E., McCarty, D.R., Chourey, P.S., et al. (2015). Seed filling in domesticated maize and rice depends on SWEET-mediated hexose transport. Nat. Genet. *47*, 1489–1493.

Sreenivasulu, N., and Wobus, U. (2013). Seed-Development Programs: A Systems Biology–Based Comparison Between Dicots and Monocots. Annu. Rev. Plant Biol. *64*, 189–217.

Steemans, P., Hérissé, A.L., Melvin, J., Miller, M.A., Paris, F., Verniers, J., and Wellman, C.H. (2009). Origin and radiation of the earliest vascular land plants. Science *324*, 353.

Steinbrecher, T., and Leubner-Metzger, G. (2017). The biomechanics of seed germination. J. Exp. Bot. *68*, 765–783.

Stępiński, D., Kwiatkowska, M., Wojtczak, A., Domínguez, E., Heredia, A., and Popłońska, K. (2017). Cutinsomes as building-blocks of Arabidopsis thaliana embryo cuticle. Physiol. Plant. *161*, 560–567.

Strullu-Derrien, C., Selosse, M.-A., Kenrick, P., and Martin, F.M. (2018). The origin and evolution of mycorrhizal symbioses: from palaeomycology to phylogenomics. New Phytol. *220*, 1012–1030.

Sugano, S.S., Shirakawa, M., Takagi, J., Matsuda, Y., Shimada, T., Hara-Nishimura, I., and Kohchi, T. (2014). CRISPR/Cas9-mediated targeted mutagenesis in the liverwort Marchantia polymorpha L. Plant Cell Physiol. *55*, 475–481.

Sugano, S.S., Nishihama, R., Shirakawa, M., Takagi, J., Matsuda, Y., Ishida, S., Shimada, T., Hara-Nishimura, I., Osakabe, K., and Kohchi, T. (2018). Efficient CRISPR/Cas9-based genome editing and its application to conditional genetic analysis in Marchantia polymorpha. PloS One *13*, e0205117.

Szakiel, A., Pączkowski, C., Pensec, F., and Bertsch, C. (2012). Fruit cuticular waxes as a source of biologically active triterpenoids. Phytochem. Rev. *11*, 263–284.

Takada, S., Takada, N., and Yoshida, A. (2013). ATML1 promotes epidermal cell differentiation in Arabidopsis shoots. Dev. Camb. Engl. *140*, 1919–1923.

Takeda, S., Iwasaki, A., Matsumoto, N., Uemura, T., Tatematsu, K., and Okada, K. (2013). Physical interaction of floral organs controls petal morphogenesis in Arabidopsis. Plant Physiol. *161*, 1242–1250.

Takenaka, M., Yamaoka, S., Hanajiri, T., Shimizu-Ueda, Y., Yamato, K.T., Fukuzawa, H., and Ohyama, K. (2000). Direct transformation and plant regeneration of the haploid liverwort Marchantia polymorpha L. Transgenic Res. *9*, 179–185.

Tam, T.H.Y., Catarino, B., and Dolan, L. (2015). Conserved regulatory mechanism controls the development of cells with rooting functions in land plants. Proc. Natl. Acad. Sci. U. S. A. *112*, E3959-3968.

Tanaka, H., Onouchi, H., Kondo, M., Hara-Nishimura, I., Nishimura, M., Machida, C., and Machida, Y. (2001). A subtilisin-like serine protease is required for epidermal surface

Tanaka, T., Tanaka, H., Machida, C., Watanabe, M., and Machida, Y. (2004). A new method for rapid visualization of defects in leaf cuticle reveals five intrinsic patterns of surface defects in Arabidopsis. Plant J. *37*, 139–146.

Tarasov, V.A., Khadeeva, N.V., Mel'nik, V.A., Ezhova, T.A., and Shestakov, S.V. (2009). The Atlg12860 gene of Arabidopsis thaliana determines cathelicidin-like antimicrobial activity. Dokl. Biol. Sci. *427*, 332–334.

Tarén, N. (1958). Factors Regulating the Initial Development of Gemmae in Marchantia polymorpha. The Bryologist *61*, 191–204.

Taylor, E.L., and Taylor, T.N. (2009). Seed ferns from the late Paleozoic and Mesozioc: Any angiosperm ancestors lurking there? Am. J. Bot. *96*, 237–251.

Thamm, A., Saunders, T.E., and Dolan, L. (2020). MpFEW RHIZOIDS1 miRNA-Mediated Lateral Inhibition Controls Rhizoid Cell Patterning in Marchantia polymorpha. Curr. Biol. *30*, 1905-1915.e4.

The Arabidopsis Genome Initiative (2000). Analysis of the genome sequence of the flowering plant Arabidopsis thaliana. Nature *408*, 796–815.

Thomashow, M.F., and Torii, K.U. (2020). SCREAMing Twist on the Role of ICE1 in Freezing Tolerance[OPEN]. Plant Cell *32*, 816–819.

Tian, S., Fang, X., Wang, W., Yu, B., Cheng, X., Qiu, F., Mort, A.J., and Stark, R.E. (2008). Isolation and identification of oligomers from partial degradation of lime fruit cutin. J. Agric. Food Chem. *56*, 10318–10325.

Tranquet, O., Saulnier, L., Utille, J.-P., Ralph, J., and Guillon, F. (2009). Monoclonal antibodies to p-coumarate. Phytochemistry *70*, 1366–1373.

Tsuwamoto, R., Fukuoka, H., and Takahata, Y. (2008). GASSHO1 and GASSHO2 encoding a putative leucine-rich repeat transmembrane-type receptor kinase are essential for the normal development of the epidermal surface in Arabidopsis embryos. Plant J. Cell Mol. Biol. *54*, 30–42.

Vernoud, V., Laigle, G., Rozier, F., Meeley, R.B., Perez, P., and Rogowsky, P.M. (2009). The HD-ZIP IV transcription factor OCL4 is necessary for trichome patterning and anther development in maize. Plant J. *59*, 883–894.

Villarreal A, J.C., Crandall-Stotler, B.J., Hart, M.L., Long, D.G., and Forrest, L.L. (2016). Divergence times and the evolution of morphological complexity in an early land plant lineage (Marchantiopsida) with a slow molecular rate. New Phytol. *209*, 1734–1746.

Villena, J.F., Domínguez, E., Stewart, D., and Heredia, A. (1999). Characterization and biosynthesis of non-degradable polymers in plant cuticles. Planta *208*, 181–187.

Vishwanath, S.J., Delude, C., Domergue, F., and Rowland, O. (2015). Suberin: biosynthesis, regulation, and polymer assembly of a protective extracellular barrier. Plant Cell Rep. *34*, 573–586.

Voisin, D., Nawrath, C., Kurdyukov, S., Franke, R.B., Reina-Pinto, J.J., Efremova, N., Will, I., Schreiber, L., and Yephremov, A. (2009). Dissection of the Complex Phenotype in Cuticular Mutants of Arabidopsis Reveals a Role of SERRATE as a Mediator. PLOS Genet. *5*, e1000703.

Walton, T.J., and Kolattukudy, P.E. (1972). Determination of the structures of cutin monomers by a novel depolymerization procedure and combined gas chromatography and mass spectrometry. Biochemistry *11*, 1885–1897.

Weber, H., Borisjuk, L., Heim, U., Sauer, N., and Wobus, U. (1997). A role for sugar transporters during seed development: molecular characterization of a hexose and a sucrose carrier in fava bean seeds. Plant Cell *9*, 895–908.

Weber, H., Borisjuk, L., and Wobus, U. (2005). MOLECULAR PHYSIOLOGY OF LEGUME SEED DEVELOPMENT. Annu. Rev. Plant Biol. *56*, 253–279.

Wellesen, K., Durst, F., Pinot, F., Benveniste, I., Nettesheim, K., Wisman, E., Steiner-Lange, S., Saedler, H., and Yephremov, A. (2001). Functional analysis of the LACERATA gene of Arabidopsis provides evidence for different roles of fatty acid omega -hydroxylation in development. Proc. Natl. Acad. Sci. U. S. A. *98*, 9694–9699.

Weng, J.-K., and Chapple, C. (2010). The origin and evolution of lignin biosynthesis. New Phytol. *187*, 273–285.

Weng, H., Molina, I., Shockey, J., and Browse, J. (2010). Organ fusion and defective cuticle function in a lacs1lacs2 double mutant of Arabidopsis. Planta *231*, 1089–1100.

Wickett, N.J., Mirarab, S., Nguyen, N., Warnow, T., Carpenter, E., Matasci, N., Ayyampalayam, S., Barker, M.S., Burleigh, J.G., Gitzendanner, M.A., et al. (2014). Phylotranscriptomic analysis of the origin and early diversification of land plants. Proc. Natl. Acad. Sci. U. S. A. *111*, E4859–E4868.

Willis, K., and McElwain, J. (2014). The Evolution of Plants (OUP Oxford).

Wilts, B.D., Rudall, P.J., Moyroud, E., Gregory, T., Ogawa, Y., Vignolini, S., Steiner, U., and Glover, B.J. (2018). Ultrastructure and optics of the prism-like petal epidermal cells of Eschscholzia californica (California poppy). New Phytol. *219*, 1124–1133.

Wrzaczek, M., Brosché, M., Kollist, H., and Kangasjärvi, J. (2009). Arabidopsis GRI is involved in the regulation of cell death induced by extracellular ROS. Proc. Natl. Acad. Sci. *106*, 5412–5417.

Wu, R., Li, S., He, S., Waßmann, F., Yu, C., Qin, G., Schreiber, L., Qu, L.-J., and Gu, H. (2011). CFL1, a WW Domain Protein, Regulates Cuticle Development by Modulating the Function of HDG1, a Class IV Homeodomain Transcription Factor, in Rice and Arabidopsis. Plant Cell *23*, 3392–3411.

Xiao, F., Goodwin, S.M., Xiao, Y., Sun, Z., Baker, D., Tang, X., Jenks, M.A., and Zhou, J.-M. (2004). Arabidopsis CYP86A2 represses Pseudomonas syringae type III genes and is required for cuticle development. EMBO J. *23*, 2903–2913.

Xin, A., and Fry, S.C. (2021). Cutin:xyloglucan transacylase (CXT) activity covalently links cutin to a plant cell-wall polysaccharide. J. Plant Physiol. *262*, 153446.

Xing, Q., Creff, A., Waters, A., Tanaka, H., Goodrich, J., and Ingram, G.C. (2013). ZHOUPI controls embryonic cuticle formation via a signalling pathway involving the subtilisin protease ABNORMAL LEAF-SHAPE1 and the receptor kinases GASSHO1 and GASSHO2. Dev. Camb. Engl. *140*, 770–779.

Xu, B., Ohtani, M., Yamaguchi, M., Toyooka, K., Wakazaki, M., Sato, M., Kubo, M., Nakano, Y., Sano, R., Hiwatashi, Y., et al. (2014). Contribution of NAC Transcription Factors to Plant Adaptation to Land. Science *343*, 1505–1508.

Xu, B., Taylor, L., Pucker, B., Feng, T., Glover, B.J., and Brockington, S.F. (2021). The land plant-specific MIXTA-MYB lineage is implicated in the early evolution of the plant cuticle and the colonization of land. New Phytol. *229*, 2324–2338.

Xu, W., Fiume, E., Coen, O., Pechoux, C., Lepiniec, L., and Magnani, E. (2016). Endosperm and Nucellus Develop Antagonistically in Arabidopsis Seeds. Plant Cell *28*, 1343–1360.

Yamaguchi, M., Goué, N., Igarashi, H., Ohtani, M., Nakano, Y., Mortimer, J.C., Nishikubo, N., Kubo, M., Katayama, Y., Kakegawa, K., et al. (2010). VASCULAR-RELATED NAC-DOMAIN6 and VASCULAR-RELATED NAC-DOMAIN7 effectively induce transdifferentiation into xylem vessel elements under control of an induction system. Plant Physiol. *153*, 906–914.

Yan, A., Wu, M., Yan, L., Hu, R., Ali, I., and Gan, Y. (2014a). AtEXP2 Is Involved in Seed Germination and Abiotic Stress Response in Arabidopsis. PLOS ONE *9*, e85208.

Yan, D., Duermeyer, L., Leoveanu, C., and Nambara, E. (2014b). The Functions of the Endosperm During Seed Germination. Plant Cell Physiol. *55*, 1521–1533.

Yang, S., Johnston, N., Talideh, E., Mitchell, S., Jeffree, C., Goodrich, J., and Ingram, G. (2008). The endosperm-specific ZHOUPI gene of Arabidopsis thaliana regulates endosperm breakdown and embryonic epidermal development. Dev. Camb. Engl. *135*, 3501–3509.

Yang, W., Pollard, M., Li-Beisson, Y., Beisson, F., Feig, M., and Ohlrogge, J. (2010). A distinct type of glycerol-3-phosphate acyltransferase with sn-2 preference and phosphatase activity producing 2-monoacylglycerol. Proc. Natl. Acad. Sci. U. S. A. *107*, 12040–12045.

Yang, W., Simpson, J.P., Li-Beisson, Y., Beisson, F., Pollard, M., and Ohlrogge, J.B. (2012). A Land-Plant-Specific Glycerol-3-Phosphate Acyltransferase Family in Arabidopsis: Substrate Specificity, sn-2 Preference, and Evolution. Plant Physiol. *160*, 638–652.

Yashina, S., Gubin, S., Maksimovich, S., Yashina, A., Gakhova, E., and Gilichinsky, D. (2012). Regeneration of whole fertile plants from 30,000-y-old fruit tissue buried in Siberian permafrost. Proc. Natl. Acad. Sci. *109*, 4008–4013.

Yeats, T.H., and Rose, J.K.C. (2013). The formation and function of plant cuticles. Plant Physiol. *163*, 5–20.

Yeats, T.H., Martin, L.B.B., Viart, H.M.-F., Isaacson, T., He, Y., Zhao, L., Matas, A.J., Buda, G.J., Domozych, D.S., Clausen, M.H., et al. (2012). The identification of cutin synthase: formation of the plant polyester cutin. Nat. Chem. Biol. *8*, 609–611.

Yeats, T.H., Huang, W., Chatterjee, S., Viart, H.M.-F., Clausen, M.H., Stark, R.E., and Rose, J.K.C. (2014). Tomato Cutin Deficient 1 (CD1) and putative orthologs comprise an ancient family of cutin synthase-like (CUS) proteins that are conserved among land plants. Plant J. Cell Mol. Biol. *77*, 667–675.

Zachowski, A., Guerbette, F., Grosbois, M., Jolliot-Croquin, A., and Kader, J.C. (1998). Characterisation of acyl binding by a plant lipid-transfer protein. Eur. J. Biochem. *257*, 443–448.

Zhang, C., Teng, X.-D., Zheng, Q.-Q., Zhao, Y.-Y., Lu, J.-Y., Wang, Y., Guo, H., and Yang, Z.-N. (2018). Ethylene signaling is critical for synergid cell functional specification and pollen tube attraction. Plant J. Cell Mol. Biol. *96*, 176–187.

Zhang, Y., Chen, B., Xu, Z., Shi, Z., Chen, S., Huang, X., Chen, J., and Wang, X. (2014). Involvement of reactive oxygen species in endosperm cap weakening and embryo elongation growth during lettuce seed germination. J. Exp. Bot. *65*, 3189–3200.

Zhang, Y., Li, X., Yang, S., and Feng, X. (2017). Identification of ZOUPI Orthologs in Soybean Potentially Involved in Endosperm Breakdown and Embryogenic Development. Front. Plant Sci. *8*, 139.

Zhao, C., Wang, P., Si, T., Hsu, C.-C., Wang, L., Zayed, O., Yu, Z., Zhu, Y., Dong, J., Tao, W.A., et al. (2017). MAP Kinase Cascades Regulate the Cold Response by Modulating ICE1 Protein Stability. Dev. Cell *43*, 618-629.e5.

Zhao, L., Katavic, V., Li, F., Haughn, G.W., and Kunst, L. (2010). Insertional mutant analysis reveals that long-chain acyl-CoA synthetase 1 (LACS1), but not LACS8, functionally overlaps with LACS9 in Arabidopsis seed oil biosynthesis. Plant J. Cell Mol. Biol. *64*, 1048–1058.

Zhao, L., Haslam, T.M., Sonntag, A., Molina, I., and Kunst, L. (2019). Functional Overlap of Long-Chain Acyl-CoA Synthetases in Arabidopsis. Plant Cell Physiol. *60*, 1041–1054.

Zheng, H., Rowland, O., and Kunst, L. (2005). Disruptions of the Arabidopsis Enoyl-CoA Reductase Gene Reveal an Essential Role for Very-Long-Chain Fatty Acid Synthesis in Cell Expansion during Plant Morphogenesis. Plant Cell *17*, 1467–1481.

Zheng, Z., Xia, Q., Dauk, M., Shen, W., Selvaraj, G., and Zou, J. (2003). Arabidopsis AtGPAT1, a member of the membrane-bound glycerol-3-phosphate acyltransferase gene family, is essential for tapetum differentiation and male fertility. Plant Cell *15*, 1872–1887.

Zhong, R., Lee, C., and Ye, Z.-H. (2010). Global analysis of direct targets of secondary wall NAC master switches in Arabidopsis. Mol. Plant *3*, 1087–1103.

Zhu, Y., Yang, H., Mang, H.-G., and Hua, J. (2011). Induction of BAP1 by a moderate decrease in temperature is mediated by ICE1 in Arabidopsis. Plant Physiol. *155*, 580–588.

Ziv, C., Zhao, Z., Gao, Y.G., and Xia, Y. (2018). Multifunctional Roles of Plant Cuticle During Plant-Pathogen Interactions. Front. Plant Sci. *9*.

Annexe 1: Composition of Johnson's medium.

For 5 Litres of 1X modified Johnson's medium

Stock A	100 mL
Stock B	100 mL
Inositol (10mg/mL)	50 mL
Stock C	5 mL
Stock D	5 mL
$(NH_4)_2SO_4$	2 mL
$NH_4H_2PO_4$	3 mL
MES	2.665 g
Sucrose	50g
Sigma agar	1.4%

Adjust pH to 5.6 with 1M KOH and autoclave 120°C for 20min.

Stock solutions (for 1L each):

100X Stock A		Final concentration
KNO_3	30.3g	6mM
$MgSO_4$	6.15g	1mM

100X Stock B		Final concentration
$Ca(NO_3)_2$ $4H_2O$	47.2g	4mM

1000X Stock C		Final concentration
KCl	1.864g	25µM
H_3BO_4	0.773g	10µM
$MnSO_4$ $4H_20$	0.223g	1µM
$ZnSO_4$ $7H_20$	0.288G	1µM
$CuSO_4$ $5H_20$	0.0624g	0.25µM
$(NH_4)_6Mo_7O_{24}$ $4H_20$	0.309g	0.25µM

1000X Stock D		Final concentration
$FeSO_4$ $7H_20$	6.95g	25µM
Na_2EDTA	9.365g	25µM

$NH_4H_2PO_4$ (1mol/L)	5.75g for 50mL	0.6mM
$(NH_4)_2SO_4$ (1mol/L)	6.69g for 50mL	0.4mM